AIAA
R-093-2003

# Recommended Practice

# Calibration of Subsonic and Transonic Wind Tunnels

AIAA standards are copyrighted by the American Institute of Aeronautics and Astronautics (AIAA), 1801 Alexander Bell Drive, Reston, VA 20191-4344 USA. All rights reserved.

AIAA grants you a license as follows: The right to download an electronic file of this AIAA standard for temporary storage on one computer for purposes of viewing, and/or printing one copy of the AIAA standard for individual use. Neither the electronic file nor the hard copy print may be reproduced in any way. In addition, the electronic file may not be distributed elsewhere over computer networks or otherwise. The hard copy print may only be distributed to other employees for their internal use within your organization.

**AIAA**
**R-093-2003**

# Recommended Practice

# Calibration of Subsonic and Transonic Wind Tunnels

Sponsor

**American Institute of Aeronautics and Astronautics**

## Abstract

The calibration of a wind tunnel is a necessary, yet often neglected, process needed to ensure accurate and repeatable test data. In general, a wind tunnel calibration program encompasses many related topics—basic operating condition calibration, flow quality mapping, wall interference, and model blockage corrections are all topics that can be addressed as part of a tunnel calibration program. However, it is not practical to address all of these topics in a single document, so the scope of this recommended practice has been defined as the empty test section calibration of subsonic and transonic wind tunnels. This American Institute of Aeronautics and Astronautics (AIAA) Recommended Practice is intended to (1) provide an overview on the calibration of subsonic and transonic wind tunnels and (2) provide a basis for commonality within the wind tunnel community in the area of wind tunnel calibration. This document is a compilation of input from several wind tunnel operators and users that summarizes the best practices and recommendations from these experts.

Library of Congress Cataloging-in-Publication Data

Recommended practice : calibration of subsonic and transonic wind tunnels.
p. cm.
Includes bibliographical references and index.
ISBN 1-56347-661-4 (Hardcopy) -- ISBN 1-56347-662-2 (Electronic)
1. Wind tunnels--Calibration. 2. Aerodynamics--Research--Standards. 3. Wind tunnel models--Testing--Standards. I. American Institute of Aeronautics and Astronautics.

TL567.W5R435 2003
629.134'52--dc22

2003023502

Published by
**American Institute of Aeronautics and Astronautics**
**1801 Alexander Bell Drive, Reston VA 20191**

Copyright © 2003 American Institute of Aeronautics and Astronautics
All rights reserved.

No part of this publication may be reproduced in any form, in electronic retrieval system or otherwise, without prior written permission of the publisher.

Printed in the United States of America.

## Contents

Foreword ..... viii
1 Executive summary ..... 1
2 Introduction ..... 3
2.1 Background ..... 3
2.2 Definitions ..... 4
3 Wind tunnel calibration requirements and objectives ..... 5
3.1 Calibration basics ..... 5
3.2 Calibration goals ..... 7
3.3 Types of calibrations ..... 9
3.3.1 Full calibrations ..... 9
3.3.2 Check calibrations ..... 11
3.3.3 Axial static pressure distribution ..... 11
3.3.4 Integrated upflow calibration ..... 11
3.4 Calibration parameters ..... 11
3.5 Frequency of calibration ..... 12
3.6 Establishing statistical process control in the wind tunnel calibration ..... 13
3.6.1 Check standard ..... 14
3.6.2 Historical tracking ..... 14
3.6.3 Out-of-control variations ..... 15
4 Calibration and flow field measurements ..... 16
4.1 Steady-state pressure measurements ..... 17
4.1.1 Calibration measurements ..... 17
4.1.2 Mapping test section steady-pressure distributions ..... 18
4.1.3 Recommendations on data acquisition ..... 19
4.2 Axial static pressure distribution measurements ..... 20
4.2.1 Static pressure pipe ..... 20
4.2.2 Other stationary axial static pressure measurement devices ..... 23
4.2.3 Translating probes ..... 24
4.3 Flow-angularity measurements ..... 25
4.3.1 Integrated upflow measurement ..... 25
4.3.2 Pressure probes for flow-angle measurement ..... 26
4.3.3 Nonpressure probe systems ..... 28
4.4 Temperature measurements ..... 29
4.5 Humidity and dew point measurements ..... 29
4.5.1 Fog chamber unit ..... 30

4.5.2 Chilled mirror instruments ..... 30
4.5.3 Aluminum oxide sensors ..... 30
4.5.4 Silicon sensors ..... 31
5 Calibration test planning and execution ..... 32
5.1 Pretest preparation ..... 33
5.1.1 Planning and reporting ..... 33
5.1.2 Uncertainty analysis in the planning phase ..... 33
5.1.3 Online data analysis requirements ..... 34
5.2 Test preparation and execution ..... 36
5.3 Data analysis and data corrections ..... 39
5.4 Post-test activities ..... 40
5.4.1 Reporting of results ..... 40
5.4.2 Followup activities ..... 41
6 Examples of calibration procedures ..... 42
Annexes
A Nomenclature ..... 43
B Additional information on pressure probes used for flow-angle measurement ..... 51
C Calibration of NASA Glenn Research Center's 9- by 15-Foot Low-Speed Wind Tunnel ..... 55
C.1 Description of facility ..... 55
C.2 Calibration hardware ..... 57
C.2.1 Tunnel and test section instrumentation ..... 57
C.2.2 Calibration hardware and instrumentation ..... 58
C.2.3 Data acquisition systems ..... 63
C.3 Detailed calibration procedure ..... 63
C.4 Frequency and duration of full and check calibrations ..... 66
C.5 Data analysis ..... 66
C.5.1 Flow field data ..... 66
C.5.2 Turbulence measurements ..... 67
C.5.3 Boundary layer rake data ..... 68
C.5.4 Calibration curves for determining test section operating conditions ..... 69
C.6 Reporting of results ..... 73
D Lockheed Martin Low Speed Wind Tunnel ..... 75
D.1 Description of facility ..... 75
D.2 Test conditions ..... 76
D.3 Flow quality and calibration goals and requirements ..... 76
D.4 Tunnel and calibration instrumentation/hardware description ..... 77

D.5 Airstream calibration procedure ..... 78
D.6 Data reduction ..... 79
D.7 Frequency and duration of full and check calibrations ..... 80
D.8 Data acquisition system ..... 81
D.9 Data analysis and data corrections ..... 81
D.10 Flow quality information ..... 81
D.11 Reporting of results ..... 82
D.12 Recommendations for future calibrations ..... 82
E Calibration of the 11- by 11-Foot Transonic Wind Tunnel at the NASA Ames Research Center ..... 85
E.1 Overview of the facility calibration and flow quality surveys ..... 85
E.2 Facility description ..... 85
E.3 Facility tunnel conditions, hardware, and instrumentation ..... 86
E.3.1 Static and total pressure ..... 86
E.3.2 Tunnel total temperature ..... 88
E.3.3 Specific humidity ..... 88
E.4 Facility calibration goals ..... 88
E.5 Facility calibration installation and instrumentation ..... 88
E.5.1 Static pipe installation ..... 88
E.5.2 Static pipe instrumentation ..... 89
E.5.3 Flow uniformity installation ..... 90
E.5.4 Flow uniformity instrumentation ..... 91
E.6 Data acquisition ..... 91
E.6.1 Static pipe data acquisition ..... 92
E.6.2 Flow uniformity data acquisition ..... 92
E.7 Data reduction ..... 92
E.7.1 Calibration equations ..... 92
E.7.2 Flow uniformity equations ..... 93
E.7.2.1 Local A-plane and B-plane flow angle ..... 93
E.7.2.1 Total temperature ..... 94
E.7.2.3 Boundary layer ..... 94
E.7.3 Data reduction methods for the static pipe ..... 94
E.7.4 Data reduction methods for the flow uniformity ..... 95
E.8 Calibration results ..... 95
E.8.1 Factors affecting the static pipe calibration results ..... 95
E.8.1.1 Temporal variation of test section flow ..... 95
E.8.1.2 Effects of test section slots ..... 97

E.8.1.3 Mounting interference effects ..... 97
E.8.1.4 Tap error and pipe joint effects ..... 98
E.8.1.5 Instrumentation error effects ..... 99
E.8.2 Calibration results for the static pipe ..... 99
E.8.2.1 Mach number effects ..... 99
E.8.2.2 Reynolds number effects ..... 99
E.8.2.3 Centerline versus 33 in. below centerline ..... 101
E.8.3 Calibration results for the flow uniformity ..... 102
E.8.3.1 Flow angle ..... 102
E.8.3.2 Total pressure ..... 102
E.8.3.3 Total temperature ..... 103
E.8.3.4 Boundary layer ..... 104
F Maintenance calibration of the Veridian 8-Foot Transonic Wind Tunnel ..... 105
F.1 Description of facility ..... 105
F.1.1 Facility description ..... 105
F.1.2 Resident tunnel instrumentation ..... 106
F.1.3 Data acquisition systems ..... 107
F.2 Calibration hardware and instrumentation ..... 108
F.2.1 Static pipe ..... 108
F2.2 Instrumentation ..... 108
F.3 Maintenance calibration description ..... 109
F.3.1 Test section installation ..... 109
F.3.2 Test procedures ..... 112
F.4 Frequency and duration of full and check calibrations ..... 113
F.5 Data reduction and analyses ..... 114
G Mach number calibration of the Arnold Engineering Development Center PWT 16-ft Transonic Tunnel (16T) with the High-Angle Automated Sting (HAAS) test section ..... 121
G.1 Introduction ..... 121
G.2 Description of facility ..... 121
G.3 Calibration hardware ..... 121
G.4 Calibration instrumentation ..... 123
G.5 Test free-stream conditions ..... 123
G.6 Test procedures ..... 124
G.7 Data uncertainty ..... 124
G.8 Results and discussion ..... 124
G.8.1 Centerline Mach number distributions ..... 124

G.8.1.1 HAAS strut interference ..... 125
G.8.1.2 Test region ..... 126
G.8.1.3 Axial Mach number gradient ..... 126
G.8.2 Mach number calibration ..... 128
G.8.2.1 Baseline calibration ..... 128
G.8.2.2 Reynolds number effects ..... 128
G.8.3 Calibration application methodology ..... 128
H Bibliography of subsonic and transonic tunnel calibration reports ..... 131
References ..... 132

# Foreword

Wind tunnels are the primary source of test data for basic aerodynamic research and for the design and development of aircraft, aircraft components (including propulsion systems), launch vehicles and land vehicles. Since the 1960's, tens of thousands of wind tunnel test hours have usually been required to complete the development and evaluation of a new aircraft. Because of the advances in instrumentation and data systems that provide more accurate measurement of flow parameters and because of the increased sensitivity of aerodynamic and propulsion system performance to wind tunnel flow quality, the accurate calibration of wind tunnels has become progressively more important. Without detailed knowledge of the wind tunnel operating conditions and flow quality, it is impossible to provide reliable and accurate test data to support the needs of test customers.

In the past, there have been workshops and general meetings to discuss issues pertaining to wind tunnel calibration, but in general, no closure or final recommendations were produced from these exercises. To provide a means of closure on calibration issues, the AIAA Ground Testing Technical Committee (GTTC) formed a working group on wind tunnel calibration methodology. This working group was chartered to bring together wind tunnel calibration experts from various Government, industry, and university organizations to share information on calibration techniques and to ultimately make recommendations on preferred methods for wind tunnel calibration.

Because of the large variance in wind tunnel characteristics across facilities (e.g., Mach number range, size and type of facility, types of testing, model blockage effects, etc.), an exhaustive treatment of all pertinent calibration issues was not practical. Therefore, the working group focused on a subset of wind tunnels and test ranges. On the basis of discussions with wind tunnel users and operators from within the GTTC, the scope of the Wind Tunnel Calibration Methodology Working Group was limited to the empty test section calibration of subsonic and transonic wind tunnels. For this exercise, subsonic wind tunnels have a test section Mach number capability up to 0.5, and transonic tunnels up to 1.5. The working group decided to classify this document as a Recommended Practice because the variety of wind tunnels and types of testing conducted in each tunnel make it difficult to define standards that can be directly applied in all instances. Instead, general recommendations are made on hardware, methodologies, and philosophy such that each reader can determine the best calibration program for his or her situation. This document does not address such issues as wall interference, support interference, or model size. This is not to minimize the importance of these issues, since they must be addressed for each proposed wind tunnel test. However, many of these issues are covered in detail in other reference documents.

In order to facilitate the exchange of information between the member organizations and to build a database on wind tunnel calibrations, each organization wrote a summary report on their calibration procedures. The information in these summary reports became the building blocks for constructing this Recommended Practice.

The members of the GTTC Wind Tunnel Calibration Methodology Working Group were

| | |
|---|---|
| Allen Arrington, Chairman | QSS Group, Inc., at the NASA Glenn Research Center |
| Mark Perry, Vice-Chair | Lockheed Martin Corporation |
| Stephen Arnette | Sverdrup Technology |
| Alan Boone | NASA Ames Research Center |
| Colin Britcher | Old Dominion University |
| Tom Beutner | Air Force Research Lab |
| Andy Garrell | Veridian Engineering Division |

| | |
|---|---|
| James Hallissy | NASA Langley Research Center |
| Dennis Hergert | The Boeing Company |
| Bonnie Johnson | National Institute for Aviation Research |
| Mark Kammeyer | The Boeing Company |
| Mike Mills | Sverdrup Technology, AEDC Group |
| Mark Rennie | Aiolos Engineering Corp. |
| David Sanford | Micro Craft Technology |
| Lew Scherer | Northrop Grumman |
| Frank Steinle | Sverdrup Technology, AEDC Group |
| James Thain | National Research Council, Canada |

On the recommendation of the Wind Tunnel Calibration Working Group the following knowledgeable individuals reviewed the document and provided valuable critique:

| | |
|---|---|
| Max Amaya | NASA Ames Research Center |
| Cabot Broughton | National Research Council, Canada |
| Peter Brown | QSS Group, Inc., at the NASA Glenn Research Center |
| Joel Everhart | NASA Langley Research Center |
| Brian Geppart | University of Washington |
| Jose Gonsalez | QSS Group, Inc., at the NASA Glenn Research Center |
| Michael Hemsch | NASA Langley Research Center |
| Frank Jackson | Sverdrup Technology, AEDC Group |
| Frank Kmak | NASA Ames Research Center |
| Alan Linne | NASA Glenn Research Center |
| Kevin Mejia | The Boeing Company |
| Scott Meredith | Sverdrup Technology |
| Roman Paryz | Veridian |
| Fred Peitzman | Northrop Grumman |
| Juergen Quest | European Transonic Wind Tunnel |
| Mathew Rueger | The Boeing Company |
| David Spera | QSS Group, Inc., at the NASA Glenn Research Center |
| Peter Waudby-Smith | Aiolos Engineering |

This document was approved by the AIAA Ground Test Technical Committee (Mr. Allen Arrington, chairman) in January 2003.

The AIAA Standards Executive Council (Mr. Phil Cheney, chairman) approved the document in September 2003.

The AIAA Standards Procedures dictates that all approved Standards, Recommended Practices, and Guides are advisory only. Their use by anyone engaged in industry or trade is entirely voluntary. There is no agreement to adhere to any AIAA standards publication and no commitment to conform to or be guided by standards reports. In formulating, revising, and approving standards publications, the committees on standards will not consider patents that may apply to the subject matter. Prospective users of the publications are responsible for protecting themselves against liability for infringement of patents or copyright or both.

## Acknowledgments

The working group chair acknowledges the following significant contributions by nonworking group members: Max Amaya (NASA Ames Research Center) for providing a tunnel calibration example on the Ames 11- by 11-Foot Transonic Wind Tunnel (Annex E), and Nancy Amman (InDyne, Inc., at NASA Glenn) for her editorial review of the draft document and for her considerable aid in making a lot of pieces into one cohesive document.

## Dedication

The Wind Tunnel Calibration Working Group dedicates this document in memory of Frank Wright, formerly of the Boeing Company. Frank was not only an original member of the working group, but was also among those originally consulted on the formation of this group. Frank’s years of knowledge regarding wind tunnel testing and his insightful comments on topics relating to calibration were particularly important as the group began drafting this document.

# 1 Executive summary

The purposes of this document are (1) to provide an overview of the calibration of subsonic and transonic wind tunnels and (2) to provide a basis for commonality within the wind tunnel community in the area of wind tunnel calibration. Various standards have been developed over the years in the aeronautics industry, many of which pertain to ground testing. These standards have made it easier to share information and hardware, and have allowed the community to improve its overall effectiveness. This document, however, is not intended to set standards for wind tunnel calibration. Details of calibrating a wind tunnel vary from facility to facility according to the type of tests conducted, the operating envelope of the tunnel, and the physical constraints of the facility, which makes having a rigid definition of calibration procedures inappropriate. Instead, this document provides a set of recommended practices that the reader can use to develop a complete tunnel calibration program.

This document focuses on general calibration practices and principles that should be incorporated into the calibration of any tunnel. It provides recommendations on calibration hardware and instrumentation based on the current knowledge of the authors, along with a list of references that readers can use to develop detailed calibration schemes for their tunnels. Detailed examples have been included to provide insight into the current calibration activities at existing wind tunnel facilities. In addition, this document brings to light topics such as statistical quality control that have only recently been applied to tunnel calibration.

This guide strongly recommends that wind tunnel calibrations become a regular part of the operational cycle for any wind tunnel. A planned schedule of calibration tests should be created and executed to ensure that the wind tunnel is operating properly. Beyond this baseline requirement, planned calibration tests offer the advantage of constructing an extensive database describing the tunnel operation, which can be very useful in determining the cause of changes in a flow field. In short, wind tunnel calibrations should be thought of as a regularly scheduled maintenance activity or diagnostic test. Instead of a series of disconnected tests, the calibration activities should take the form of an ongoing test program.

Properly planned, recurring, and well-documented calibrations of a wind tunnel provide several benefits to the tunnel operator and end user.

- They ensure that the wind tunnel is operating as expected and are useful in identifying problems in the wind tunnel circuit.
- They provide potential customers with a documented assessment of the tunnel calibration and are essential in determining overall data quality.
- They provide data essential for interpretation and correction of test data.
- They provide archival documentation of tunnel operating conditions, so that modifications to the wind tunnel may be assessed for their impact on the operating conditions.
- They aid in establishing statistical process control on wind tunnel test data by providing a database of wind tunnel parameter variability.
- They aid in identifying data anomalies that are attributable to the wind tunnel itself, not to the variability in the calibration process.
- They may indicate, by comparison with previous calibrations, that portions of the wind tunnel circuit or instrumentation are in need of repair or recalibration.
- They facilitate tunnel-to-tunnel data comparisons.

Since calibration is considered a critical item in the health monitoring of a wind tunnel, this guide recommends that experienced personnel be assigned to the execution of calibration tasks. In instances where the calibration tests are perceived as routine, they are commonly used as training exercises for

less experienced personnel in the operation of the wind tunnel. Although training is important, it is also important that an experienced person lead the calibration activities. To maximize the value of a regular program of wind tunnel calibration, it is also important to maintain some level of personnel continuity over the course of the calibration program. A core group of personnel should be assigned to develop, execute, and report on the calibration test program with other personnel included as needed. Forming a team, as opposed to a single lead engineer, to be responsible for all aspects of the tunnel calibration program is the most desirable arrangement since the corporate knowledge can be passed between the team members. This cross training of personnel allows for continuity of calibration execution and task knowledge in the inevitable occurrence of personnel turnover.

Although this document is intended more for the practitioners who will conduct the tunnel calibration activities, it contains important points that managers in charge of wind tunnel operations should consider. The first of these points, which has been largely ignored over the years, is the strategic importance of a properly calibrated wind tunnel. A properly calibrated wind tunnel is required for timely, effective product development. Despite this fundamental point, wind tunnel managers often consider calibrations an option instead of a necessity. There have been instances of major wind tunnels operating for years between significant calibration activities. In the current environment of increased data accuracy requirements and reduced time available for tunnel tests, it is imperative that accurate and complete wind tunnel calibrations are established, maintained, and placed under process control. To not do so is to place at risk substantial investments in wind tunnel testing, which is unacceptable given the alternative of simply maintaining the wind tunnel calibration. In looking at the business case for regular wind tunnel calibration, the question should not be “Can we afford to?” but rather “Can we afford not to?” Regardless of which way the question is posed, the answer requires a valuation in terms that are understood economically by those in control of the investment. We believe that the operator of the wind tunnel should have a vested interest in taking the lead to establish such a valuation.

Some of the major items discussed in this Recommended Practice follow:

- The importance of detailed pretest planning and the use of uncertainty analysis in the planning phase
- The selection of calibration hardware and instrumentation that address the particular facility’s operating range and size, calibration history, and type of tests conducted
- The introduction of statistical process control as a means of tracking the wind tunnel calibration history and ensuring that the facility is operating within acceptable margins
- The frequency of calibration tests, both full or check calibrations, and how the timing of the calibration supports the process control philosophy
- The need for a consistent calibration team composition and the identification of a lead or project engineer
- The importance of documentation and the types of documentation required, ranging from engineering logs to formal test reports. The bottom line is that during a tunnel calibration, everything must be documented. It is then imperative that the results of the calibration and any related implications to the tunnel be quickly communicated to the facility staff and to the test customers
- A nomenclature list is included in Annex A to aid readers.

# 2 Introduction

## 2.1 Background

Wind tunnels play a critical role in the development of aircraft, launch vehicles, and land vehicles. Accurate predictions of vehicle and vehicle subsystem performance can be critical in determining whether a potential customer is willing to purchase the vehicle. Advances in instrumentation and data acquisition technology have improved data quality and greatly increased the quantity of measurements that can be made quickly and easily in a wind tunnel test. However, in some instances, the weak link in the data quality chain is a lack of sufficient detail or accuracy in information characterizing the tunnel flow field. Simply stated, the lack of a proper and current calibration can be the governing element of uncertainty in interpreting wind tunnel data. In analyzing and trying to understand data anomalies, the need for current wind tunnel calibration data is amplified further still. Given the aerospace community's concern with data quality, it is in the best interest of the wind tunnel operators to understand and maintain the calibrations of their facilities.

The resources required to calibrate a wind tunnel can be extensive, and since facilities are costly to run and commonly have full test schedules, it is often difficult to promote a proper calibration program as a requirement to maintaining a wind tunnel. However, the knowledge gained from these tests will help recover the cost of the calibrations in many ways. When viewed from an economic standpoint, the operators benefit if customers choose to employ the tunnel because of increased confidence, and the customers benefit if the improvement in data quality helps them to improve their designs. For instance, the current drag measurement goal for subsonic transport tests is one drag count (0.0001), so improving data quality may allow designers to trim a few more drag counts from their aircraft. This can increase payload and, therefore, revenues. Another benefit is that regular wind tunnel calibrations bring a facility under statistical control, which is a process of understanding the variations in the facility's systems and how these variations affect the data. Having the facility in statistical control allows a facility operator to differentiate between normal tunnel variations and true changes in tunnel characteristics. This increases facility availability and improves resource utilization in that no time or funds are wasted trying to fix perceived problems that are really just part of normal tunnel variability.

One goal of this document is to provide a better understanding of a wind tunnel calibration and make higher quality wind tunnel data possible by providing common calibration procedures. Specifically, this document provides guidelines on the empty test section calibration of subsonic and transonic wind tunnels. Another goal of this document is to emphasize the importance of establishing and maintaining wind tunnel calibration and of understanding why changes in a calibration occur. A true tunnel calibration is not only a calibration of specific tunnel parameters but also a comprehensive understanding of the test section flow quality. It is essential that a wind tunnel be calibrated completely and accurately and that this calibration can be maintained over the lifetime of the tunnel.

This document is intended for the use of wind tunnel operators, managers, and customers. In particular, it is meant as a teaching aid for engineers and technicians not familiar with wind tunnel calibration and as a refresher for those who have conducted calibration tests in the past but can benefit from information pertaining to current calibration practices. The methodology outlined in the document could also be used as the foundation for calibration procedures as part of quality assurance initiatives.

Extensive work has been done concerning wind tunnel calibration, as described in References 1 to 3. The most recent analysis of wind tunnel calibration hardware and methodology was done as part of the National Wind Tunnel Complex proposal (Reference 4). The purpose of this document is to provide guidelines on wind tunnel calibration procedures that, along with the existing body of work, will improve wind tunnel data quality. Adoption of the guidelines presented here could be the first step in moving toward international standards that would permit accurate investigation of tunnel-to-tunnel-to-flight test-bias issues. Other benefits of a common wind tunnel calibration methodology include:

- Better understanding of the impact of flow anomalies on test data
- Improved tunnel calibration documentation
- Better understanding and evaluation of Reynolds number effects
- Enhancement of facility-to-facility comparisons
- Increased understanding of procedures that allow users to improve their current methodology

## 2.2 Definitions

Calibration data include any measured flow field parameter that is used to either set or define the operating conditions in the test section, or is used for data corrections, or both. Wind tunnel calibration can be defined as the determination of the average value of various flow field parameters at a point or over some defined volume in all possible model locations within the test section. Flow field parameters in the test section that should be determined from a calibration include total, static, and dynamic pressures, total and static temperature, and airspeed and/or Mach number. The axial static pressure distribution, tunnel dew point or humidity, and the model integrated upflow and crossflow are also considered calibration parameters since they are required for data corrections. The calibration data are required information; that is, the tunnel cannot operate accurately without these data. The calibration data are used to define the test section operating conditions.

Flow quality information, on the other hand, is not used to directly correct test data, but can be helpful in troubleshooting anomalous data. Flow quality includes the spatial variations in all flow field parameters (the exception being the axial static pressure distribution, which is a calibration parameter), turbulence levels, boundary layer data, acoustic characteristics, and the transition Reynolds number.

It should be noted that these definitions of calibration and flow quality parameters are based primarily on aerodynamic testing for transport or fighter aircraft applications. Depending on the test objectives, some flow field parameters may have greater or lesser importance than others. Therefore, the calibration should be tailored to meet the needs of specific users. However, for the purposes of this document, the definitions given in this section will be used.

The empty test section calibration addressed in this document implies that there is no test hardware or other instrumentation installed in the test section other than that used for the calibration. The idea behind the empty test section calibration is to understand the operation of the tunnel without a test article installed. The definition of an empty test section will vary from tunnel to tunnel since some facilities include basic model support hardware as part of the empty test section. The point to remember is to be consistent in the definition of the empty test section for a specific tunnel and to repeat that same setup for all calibration testing.

# 3 Wind tunnel calibration requirements and objectives

In its simplest form, a wind tunnel calibration provides the actual test section operating conditions for a given tunnel configuration and input control parameters. This seems straightforward, but given the complexity of most large wind tunnels, their potentially extensive operating ranges, and the influence of the test section configuration on the flow field, the calibration of a wind tunnel quickly becomes a time- and labor-intensive effort.

## 3.1 Calibration basics

In order to know accurately or set operating conditions properly in the wind tunnel test section, one must first measure the test section flow field. Measurements of total pressure, differential pressure, static pressure, and total temperature are used to define the basic operation of the wind tunnel and to calculate the values of Mach number and Reynolds number. These measurements are made in the volume of the test section where test articles will be mounted during a tunnel test. The obvious problem is that these measurements cannot be made when a test article is installed. This is because the probes used to measure the flow conditions will cause disturbances that may alter the flow around the test article or, conversely, the test article flow field may influence the measurements made by the probes. The solution is to measure the airflow parameters in an empty test section (i.e., without the test article installed) and then to relate these test section values to measurements made at some other location in the tunnel, away from the influences of a test article. The locations of these remote measurements are usually referred to as the index or indicated measuring stations of the tunnel, whereas the measurement devices themselves are often called the facility instrumentation. Relating the indicated conditions to the actual flow conditions in the test section is the primary goal of a wind tunnel calibration. This basic relation between the facility instrumentation and the test section flow conditions is called the test section calibration.

For example, in some subsonic wind tunnels, the test section flow conditions are related to static pressures measured on either side of the contraction. As shown in Figure 1, the static pressures at the inlet and at the outlet to the contraction are measured using two sets of static pressure rings. During the calibration testing, the following test section calibration relationships are determined:

- A relationship between the test section dynamic pressure and the pressure drop across the contraction (the difference in the pressure sensed at the inlet and outlet of the contraction)
- A relationship between the test section static pressure and the static pressure measured at the outlet of the contraction, or a relationship between the test section total pressure and the static pressure measured at the inlet to the contraction.

During normal testing, these test section calibration relationships are used to determine the test section conditions from the measurements made with the static pressure rings.

This example illustrates the textbook use of facility instrumentation (static pressure rings in this case) to form the calibration relationships. As mentioned before, each wind tunnel is different, so the actual indicating instrumentation used may vary. For instance, rakes of pitot probes may be used to measure the settling chamber pressure, or small rakes mounted at the entrance of the test section, so that they cause minimal flow interference, may be used to measure both total and static pressure. In a transonic facility, total pressure and total temperature measured in the settling chamber and the pressure measured in a plenum chamber surrounding the test section may be used. In each case, the basic idea of relating the actual test section flow conditions to one or more remote indicating (facility) measurement station remains the same, regardless of the location and type of instrumentation selected.

Although this document focuses on the test section calibration and related aerodynamic measurements, there are also associated tasks that are part of the overall calibration measurement procedure that must be addressed:

(1) The relationship between the applied pressure at the sensors and the measured pressure (sensor and data system)

(2) The relationship between the test section conditions at the probes and the conditions at the reference sensors (test section calibration)

(3) The relationship between the test section conditions and those at the probes (probe calibration)

Implicit in item 2 is that the conditions at the probes match those at the sensors; however, this is not necessarily the case. Leaks in the pressure tubing between the probe and sensor will introduce errors and must be guarded against. Other probes, such as thermocouples, are integrated systems and avoid these types of errors, although care must be taken to assure that consistency in connections is maintained (end-to-end checks). Item 2 is described in this chapter. Item 3 is addressed in Section 4.1.1.

Item 1 is not addressed explicitly in this document, but it is a very important part of the overall test section calibration measurement procedure. Sensor calibration must be considered to be a fundamental part of the process. Sensor selection and sensor calibrations are a key to obtaining the required measurement uncertainty.

Note that the location of the facility instrumentation must be selected carefully to minimize any model-related effects on the reference measurements. The calibration effort will have little use if the reference values measured with an empty test section are different with a test article installed. If there is any question, then a sensitivity study of test article blockage on the facility instrumentation should be conducted prior to the calibration testing. If there is a problem, the location of the facility instrumentation should be changed accordingly.

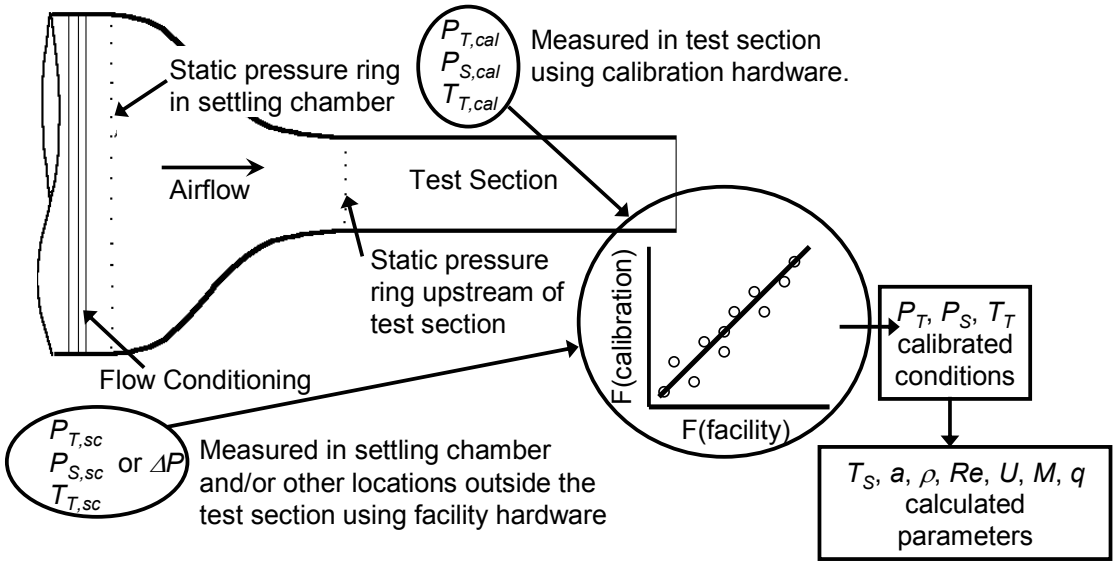



Figure 1 – Arrangement of measurements for monitoring operating conditions in a subsonic wind tunnel using a pair of static pressure rings.

Although the idea of relating the test section conditions to remote indicating measurements remains the basic concept of the calibration procedure, the complexity of the calibration is a function of the facility operating range, facility configurations, test configuration, and control input. Test section calibration relationships must be developed for the entire operating range of the facility, so a pressure tunnel will usually have a larger test matrix than an atmospheric tunnel with the same Mach number range. Likewise, a calibration must be developed for each test section configuration, including variable wall

porosity, model support configuration, and operating mode (open- or closed-loop operation). Another major consideration is whether there are specific customer test requirements and if the tunnel and calibration meet the needs of the customer as discussed in Section 3.2. The amount of calibration data required also depends on the type of calibration conducted, as described in Section 3.3.

## 3.2 Calibration goals

In order to establish meaningful wind tunnel calibration goals, it is first essential that the customer test objectives, especially allowable test data uncertainty, be fully understood. The type of tests conducted in a given facility and the objectives of these tests help determine the proper scope of the tunnel calibration and help determine priorities in completing an extensive calibration. Ideally, a tunnel calibration should cover in detail the entire operating range of the facility. However, because of constraints of time or other resources, it may be necessary to target specific operating regimes for detailed calibration and to collect less detailed data in the remaining operating envelope.

For example, a transonic wind tunnel may have a wide Mach number range, but the majority of its tests may be at subsonic transport cruise conditions. Therefore, the test section calibration for this facility may be tailored to provide detailed information for high-use conditions and less information at other conditions. The test section calibration still covers the entire operating range, but less time is devoted to those conditions not commonly requested by the customers. It is important to canvas tunnel customers to ensure that the calibration goals support their test objectives. The knowledge gained by fully understanding the present and future needs of the customers helps to determine the specific types of measurements required, the type of calibration that should be conducted, and the overall level of detail needed in the calibration. Each of these points is addressed further in subsequent sections.

In its simplest form, the product of a wind tunnel calibration is a set of relationships between test section and facility measurements for pressure and temperature. One common set of simple calibration curves for a subsonic tunnel is shown in Figure 2. In this example, the test section total pressure is related to the settling chamber pressure, the test section static pressure to the pressure measured at the contraction section exit, and the test section total temperature to the settling chamber temperature. These three curves are all that is needed to fully define the operating point of the wind tunnel, although other information is required to ensure data quality and for corrections to test parameters. Note that the example of Figure 2 is not the only set of test section calibration curves that can be used, but some combination of two pressure relationships using total, static, or dynamic pressure, along with total temperature, can be used.

The required accuracy for the test section calibration is determined from the customers' stated and rationalized accuracy requirements. The uncertainty can be estimated from pretest uncertainty analysis and from statistical analysis of repeat data sets. The wind tunnel calibration accuracy is just one part of the entire system that needs to be considered to meet a customer's test requirements. Other considerations include test instrumentation (transducers, balances, etc.) and the data-reduction system. Different portions of the tunnel's operating envelope may have different calibration accuracy requirements. Also, tunnels with wide operating ranges may require multiple sets of transducers of different spans or accuracies to provide the needed calibration accuracy.

The data requirements for the various types of test techniques (e.g., force and moment, loads, airframe integration, or propulsion) must be considered. These requirements can vary depending on how a customer uses the test results and on the customer's unique process of taking wind tunnel data and making full-scale predictions. For example, a force and moment test will require an understanding of the static pressure profile through the test section so that such things as buoyancy and wall interference effects can be accounted for. An important issue for propulsion testing is flow distortion at the inlet, including local variations in temperature, velocity, and flow angle. Potentially every customer could have different requirements.

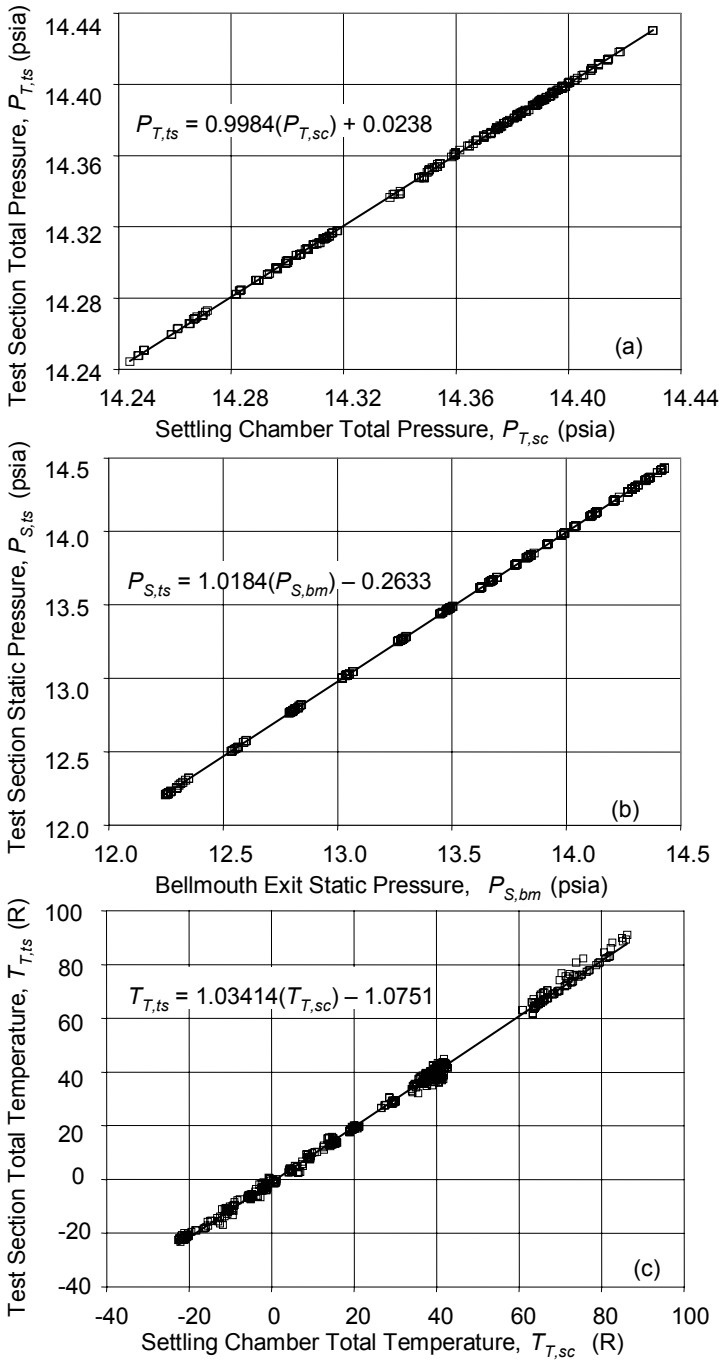



Figure 2 – Typical calibration curves for an atmospheric pressure subsonic wind tunnel. The graphs relate the parameters measured in the test section (*ts*) with the corresponding parameter measured upstream of the test section in the settling chamber (*sc*) or bellmouth (*bm*) area. The individual calibration curves are for (a) total pressure, (b) static pressure, and (c) total temperature.

In many cases, wind tunnel tests involve measuring increments between configurations (i.e., changes in measured parameters from one configuration to another), during which common uncertainty errors in the data of both configurations are assumed to cancel out. The key issues for incremental testing are within test reproducibility, consistency, and cycle time, whereas detailed knowledge of the test section flow quality is less important as long as the conditions are reproducible from test to test. Conversely, detailed

and accurate knowledge of local flow quality is of paramount importance for absolute data level testing if proper interpretation of the test data is to be performed, particularly when test programs use several different wind tunnel facilities, or when tunnel-to-tunnel comparisons are to be made.

Another consideration for the calibration is a determination of the stability of the tunnel operating point and the associated impact on measured and calculated parameters. Most tunnels exhibit some form of long period oscillation of the operating conditions. A detailed knowledge of these instabilities or fluctuations will aid in selecting the sampling period and data rates for testing.

The test section calibration of the tunnel will remain the same for any of the test types just mentioned, in that the basic operating parameters and conditions in the test section must be known for all test points. Understanding how a customer is going to use the tunnel will aid in developing a calibration test that will not only provide a meaningful calibration but aid in analyzing test data.

## 3.3 Types of calibrations

There are two basic types of test section calibrations: full calibrations and check calibrations; detailed descriptions of each calibration type are provided in the sections that follow, but in general, full calibrations provide very detailed measurements, whereas check calibrations are short tests that give a status of the health of the tunnel. It is important to realize that both full and check calibrations should be integrated into the overall calibration program for any wind tunnel. Both are needed to completely and effectively address all techniques for the tunnel calibration.

In addition to full and check calibrations, there are other calibration tests that are integral to the success of a tunnel calibration, including the measurement of the axial static pressure distribution and the determination of the integrated upflow. Both of these auxiliary calibrations are important for many aerodynamic tests. Each of these calibration types is described in this section. The details of how each is conducted, including a discussion of hardware and instrumentation and specific examples, are included in Sections 4.0, 5.0, and 6.0.

### 3.3.1 Full calibrations

A full test section calibration can be performed at a single point in the test section (point calibration), over a vertical planar region occupied by the model (planar calibration), or over the volume of the test section that a model will occupy (volume calibration). Each method has distinct advantages and disadvantages, which are discussed in the following paragraphs. In general, the procedure for each type of calibration is the same except that the number of survey points is different. The differences between the three types of test section calibrations are illustrated in Figure 3.

A point test section calibration relates flow conditions at the index measurement station to the flow conditions at a single point in the test section. For full-span models, the calibration point is typically at the point corresponding to the spanwise projection onto the test section centerline of the one-quarter mean aerodynamic chord (MAC) point; for a semispan model, the calibration point is typically at a spanwise location corresponding to the MAC but at an axial location corresponding to the wing quarter-chord. The advantage of a point calibration is that, of the three types of calibrations, it requires the least amount of time to perform. This means that a higher degree of attention and accuracy can be applied to a point calibration with minimal impact on the overall calibration schedule. The disadvantage is that a point calibration deals with flow information at only a single point in the test section and, therefore, does not capture the effect that flow variations within the test section may have on test results.

The planar test section calibration relates flow conditions at the index measurement station to test section flow conditions across a lateral plane. The test section plane selected for this calibration will typically correspond to a significant location on the test article in the test section. For example, depending on the type of testing conducted in the tunnel, the location of the plane could match the MAC point of a typical model or correspond to the position of the inlet of a propulsion simulator. The planar calibration requires more time to perform than the point calibration, but it provides information on flow parameter variations

around the test article. This information can be used to tailor the airstream corrections to a specific facility mounting system by averaging the conditions over the region occupied by the test article.

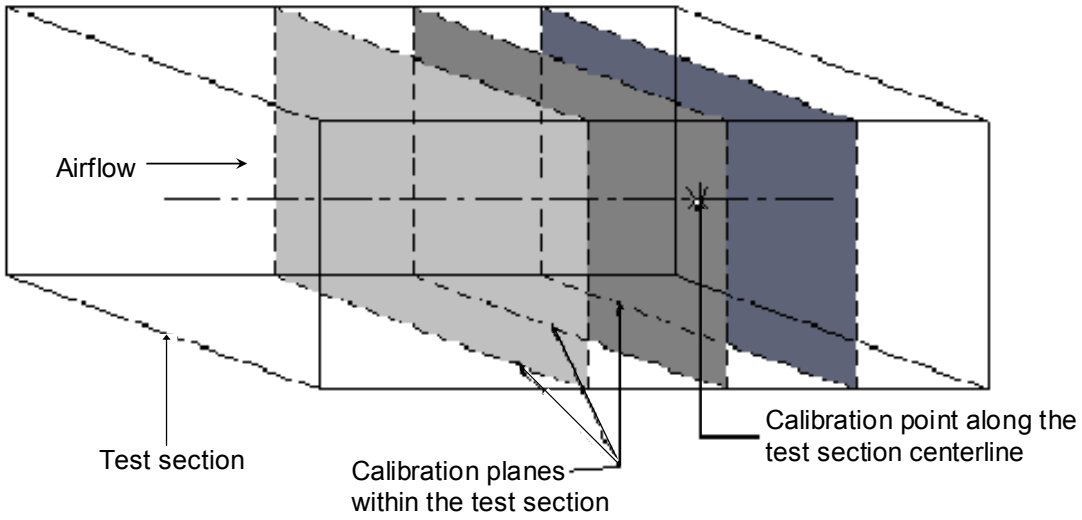



Figure 3 – Definitions of point, planar, and volume calibrations with respect to test section.

Probably the best way of performing a planar calibration is to combine a point calibration with a separate planar flow quality measurement. This method preserves the high accuracy of a point calibration while incorporating additional information on the variations of flow parameters throughout the calibration plane. Conducting a planar calibration in this manner will take longer than using a single piece of hardware to gather both calibration and flow quality data. If time constraints dictate that the calibration and flow quality data should be acquired simultaneously, then the calibration data could be based on a single measurement point or on an average of several points within the test plane. The averaging should take place only over the area occupied by the test article so that variations in areas not occupied by the test article do not skew the calibration averages.

A volume test section calibration consists of several planar surveys performed at various streamwise stations. It provides the most information about the test section calibration and flow quality, and consequently requires more time to perform than the other types of calibrations. This calibration type essentially allows for a complete mapping of the flow field within the test section volume. The additional information acquired can be used to determine flow conditions at any streamwise position of the model. For example, this information can be used to apply corrections to pitching moment caused by flow-angularity changes between the model reference center and the horizontal tail.

The volume calibration, like the planar, can be based on the simpler point calibration, with flow quality surveys added, or the calibration and flow quality data can be collected using the same hardware, with the same advantages and disadvantages as listed in the planar calibration.

On the basis of the information presented in this section, the recommended procedure is to base the primary test section parameters (total, static, pressure, and total temperature) on high-accuracy single-point measurements. The uniformity of this calibration data should be based on planar (or preferably volumetric) flow-quality measurements collected at operating conditions that bracket the test conditions. If the flow uniformity data show variations within the operating range such that the uniformity is a significant source of measurement uncertainty, then additional uniformity measurements are warranted.

### 3.3.2 Check calibrations

In addition to full calibration, a method to quickly check the tunnel test section calibration is recommended to minimize cost and tunnel time. From the statistical analysis and the historical calibration data, it is possible to identify calibration parameters that should be monitored more closely.

One way to monitor the flow and thus the need for a repeat calibration is to have a method to quickly check the flow parameters. An example might be a flow-angularity probe that is driven into the flow from a stored position. This system could make completely independent measurements of the tunnel speed and local flow angularity. In order to be utilized during a busy tunnel schedule, this device would need to be quickly and precisely inserted into the airstream. An uncertainty analysis should be performed on this check calibrator to ensure that the quality of the data satisfies the requirements.

Another approach would be to set up a standard calibration model that would be on standby for a quick installation into the tunnel to monitor selected parameters, such as test section upflow. This type of model is generally referred to as a check standard model. Any variation of the flow behavior in the tunnel is directly reflected by a change of the aerodynamic coefficients of the check standard model. The check standard model also provides for simultaneous checks of multiple tunnel parameters (such as tunnel flow angle determined from changes in the slope of the lift coefficient curve and turbulence level by monitoring the location of the boundary layer transition). The smallest deviations in an axial pressure gradient or flow angle can easily be detected. One or two shifts of tunnel time are a reasonable target for this type of check calibration.

### 3.3.3 Axial static pressure distribution

In addition to the basic test section calibration types discussed previously, it is also important to determine the axial static pressure distribution through the test section. This distribution is used to determine a buoyancy correction to drag and may also be used to determine the static pressure calibration of subsonic and transonic wind tunnels.

### 3.3.4 Integrated upflow calibration

The fundamental idea behind the integrated upflow measurement is that the lift force generated by a model with its zero-lift axis aligned with the test section longitudinal axis should ideally be zero. Any lift generated by the model in this orientation is the result of the integrated effect on the model of the test section upward flow angle. The integrated upflow measurement thus yields a correction to the effective angle of attack of a model, which is normally measured with respect to the test section longitudinal axis during testing.

## 3.4 Calibration parameters

During development of the baseline tunnel calibration, all measured tunnel parameters and flow quality need to be calibrated. The sensitivity of these calibrations to the tunnel or test section configuration needs to be established. For example, the changes in the calibration and flow qualities due to test section flow control doors, plenum evacuation or bleed, or model mounting systems will determine how accurately the flow-control devices need to be set. The calibration parameters, depending on the facility and its use, should include the following:

- **The tunnel total, static, and/or dynamic pressure related to the test section calibration point, plane, or volume.—**Which pressures are measured will vary between facilities; typically, two of these pressure values are measured directly, and the third is calculated. The tunnel static, total, and dynamic pressures are used to calculate Mach number, density, Reynolds number, and velocity (from which skin friction corrections are calculated). The dynamic pressure is used to calculate all force, moment, and pressure coefficients.

- **The tunnel total temperature source to the test section point or volume.—**This is used to calculate static temperature, speed of sound, density, velocity, and Reynolds number.

- **The integrated test section flow angularity in the volume occupied by typical models.—** This is used to correct the test model angle-of-attack as well as the lift and drag corrections for model mounts where the balance angle-of-attack changes with the model through the axis of rotation.

- **The longitudinal static pressure variation over the length of the test section occupied by typical model bodies.—**For semispan models, this would be along the floor or wall to which the body is mounted. The static pressure gradient is used to calculate a buoyancy drag correction.

- **Humidity or dew point.—**It is important to keep the humidity below a certain level to reduce the thermodynamic effect of water vapor-to-liquid transition on the local flow field (affecting the local Mach number and air density shocks).

In general, flow quality measurements and surveys are not covered by this document. However, some flow quality issues are important to specific facilities and test techniques. These can include

- **Longitudinal and lateral total and static pressure variations occupied by typical model wings, bodies, and horizontal tails throughout their angle-of-attack sweeps.—**This is used to calculate local Mach number variations.

- **Local flow angularity throughout the defined test volume.—**This is useful in understanding any apparent local wing twist or the flow field at the horizontal tail. Evaluation of the induced twist is important since it alters the span loading, resulting in a change in the induced drag. A stream angle correction done to correct the mean angle of attack will not compensate for this added effect.

- **Turbulence intensity throughout the volume occupied by typical models.—**This is useful in interpreting the boundary layer transition, separation, shock-boundary layer interaction, buffet onset, or skin friction drag test results.

- **Wall boundary layer thickness along the length of typical semispan model bodies.—**This is used in defining the semispan body standoff distance from the tunnel floor or wall.

- **Background acoustics in the test section.—**This information is used during aeroacoustic noise measurements to be able to identify the test section background noise in the test data. It is also needed for transition measurement.

- **Wall boundary conditions, including the effect of static pressure.—**This is useful in calculating tunnel wall interference effects.

Additional information concerning flow quality requirements is available in Reference 5.

## 3.5 Frequency of calibration

A comprehensive calibration is required for any new wind tunnel, or when modifications are made to the air path of an existing wind tunnel. The need for a full calibration in both of these instances is well recognized. However, once these commissioning or startup calibrations are completed, it is also necessary to recalibrate the wind tunnel on a regular basis to maintain the accuracy of the calibration and to ensure that the facility is operating as expected (i.e., is under statistical control as described in Section 3.6).

The accuracy of a wind-tunnel calibration can degrade over time, or become otherwise invalid, for a variety of reasons. For example, dirt buildup on flow-conditioning screens may cause a change in the test-section upflow over time. Similarly, outdoor temperature variations over the course of a day or a year may influence data quality in several ways and to a degree that intrudes upon the accuracy objectives of the facility. The difficulty in predicting sources and time scales of potential errors in a wind tunnel calibration means that the best way to maintain an accurate tunnel calibration is to establish a regular

recalibration program that spans all time scales. Specifically, repeat measurements should be performed during initial calibrations to define the short-term variability of the calibration. This exercise would also help to ensure that the facility starts up with a good baseline calibration. Recalibrations should also be completed on a long-term basis; as a minimum, we recommend semiannual or annual calibrations. The database of repeat calibrations is used to establish statistical process control for each calibration parameter, and it enables facility operators to understand the variability in their calibrations, and to eventually predict changes in the calibration. The principles of statistical process control are outlined in greater detail in Section 3.6.

## 3.6 Establishing statistical process control in the wind tunnel calibration

The concept and tools of statistical process control (SPC, References 6 to 10) have been used in various industries for decades, but their application to wind tunnel processes has not been widespread. Basically, SPC is used as a means of monitoring the reproducibility of a process. A process that is checked periodically with consistent results (within an acceptable range of limits) is considered to be “in control.” The implication is that a system that is in control will provide consistent results over time. For wind tunnel testing, where the measurement of multiple parameters is always required and where the test articles and test conditions are seldom the same for more than one or two tests, the application of statistical control concepts is more complicated than for simple measurement systems. This section describes a statistical process control approach to wind tunnel calibration.

Wind tunnel calibration is the foundation upon which data quality is built. Test results are nearly always a function of and are scaled (nondimensionalized) by the dynamic pressure parameter. The dynamic pressure, in turn, is derived from the facility calibration, which itself is the result of a measurement process and has inherent variation. That variation results not only from the measurement process but also from the presence of numerous other sources of variation within the facility. If the variation associated with the facility calibration is not known to be in a state of statistical control, credible statements about the uncertainty of the test conditions (and hence all data from the wind tunnel) cannot be made. For this reason, it is important that the wind tunnel calibration is maintained in a state of statistical control.

Many wind tunnels have operated for years under the premise that the tunnel calibration results represent a relation that is constant over time until overt changes are made to the facility itself. However, experience has indicated that this is not necessarily true. Repeat calibration tests conducted in a number of wind tunnels have shown that nominally identical tunnel calibration tests produce results with a significant and sometimes unacceptable level of variation. Generally, the variation derived from week-to-week or test-to-test run comparisons is significantly larger than the variation observed in back-to-back runs. Both the short-term and the long-term variation may be larger than expected from the instrumentation system alone, indicating that additional sources of variation exist in the process, the facility, or in other unaccounted factors. Possible sources of variation include tunnel control devices (slots, flaps, guide vanes, bleed valves, etc.); meteorological effects; thermal heating and cooling of the tunnel shell, airstream, or instrumentation; vibration; seal leaks; variability of human operators; procedural differences between operators or operational shifts; installation effects; dirt buildup on screens; and many others. The variation of tunnel calibration parameters over time that results from such variables has consistently been ignored by most of the wind tunnel testing community. However, with tighter customer data accuracy requirements, such variation is a factor that can no longer be safely ignored.

Achieving and maintaining a state of statistical control for the wind tunnel calibration process requires a continuing effort in three areas:

- A continuing series of check-standard calibration tests
- Historical tracking and analysis of both the variation and the mean values of critical parameters within the combined data sets from these tests
- Identification and elimination of causes for any “out of control” variation that is observed

### 3.6.1 Check Standard

The term “check standard” as used here refers to some standard test article that is held constant over time and is used for periodic verification of a measurement process. The objective of these check-standard calibration tests is to provide a continuing but limited set of repeated tunnel calibration data for assessing the stability of key flow parameters over time.

In order for multiple repeat entries to be practical, the check-standard tests must be designed to be of very short duration. They must be of limited scope, and the test hardware and instrumentation must be configured for rapid installation, setup, and removal. Since these tests are not intended to replace or necessarily even to mimic regular tunnel calibration tests, they may utilize different hardware, probes, or instrumentation than a regular calibration test. Subsonic and transonic wind tunnels, for example, might use a simple pitot-static probe mounted in the test section at a specific location where models are normally located. Facilities that conduct specialized types of testing may require other types of probes and instrumentation. It is not necessary that the check standard probe(s) give results identical to the primary calibration system. It is critical, however, that the test article utilized for the check-standard calibration, such as a pitot-static probe, remain unchanged over time, because any changes or alteration over time could introduce another source of variation into the test results. It is imperative, therefore, that probes and other similar instrumentation used for this testing be reserved solely for such tests and be treated with exceptional care to prevent damage or changes, such as surface scratches or damage to pressure orifices. Reference 11 gives an example of a check standard testing process applied to wind tunnel operation.

One complicating factor for efforts to establish and maintain statistical control in wind tunnel test processes is the large number of possible sources of variation that exist in a typical wind tunnel operation, even for relatively simple facilities. Because the objective is to capture and document the variation that exists in the testing process, it is important that the repeat testing associated with check-standard calibrations encompass all the normal sources of variation that may affect data in routine testing. This variation includes that which may result from the mechanical, electrical, meteorological, temporal, and/or human systems that are part of the wind tunnel environment. To accomplish this objective, the check-standard test must, to the extent possible, be scheduled and conducted in a manner that is similar to normal testing. Standard operating procedures for such elements as instrumentation, model setup, wind-off data points, and test condition sequencing should be used. The duration and sequence of test runs in the calibrations should be representative of the normal testing process. The tests should be operated across multiple shifts and with multiple crews (if that is the normal operation), and should be conducted at various seasons of the year. Even if consensus, belief, or previously obtained evidence indicates that such factors have not been significant sources of variation in the past, these factors are sources of variation that have the potential to cause the process to become out of control at any point in time. Data must, therefore, be acquired often enough and over a period of time long enough to capture whatever random and/or intermittent variation exists within the system.

### 3.6.2 Historical tracking

Another factor that makes establishing statistical control of a wind tunnel measurement process more complicated than some other processes is the fact that long-term repeatability (within-test and test-to-test) is generally different than short-term (back-to-back) repeatability and may be driven by different sources. The assessment of stability must specifically address these multiple levels of variation, and the short- and the longer-term variation must be examined independently. To address the short-term variation, back-to-back repeat data must be acquired. Each data set in the back-to-back series should represent an entire data set, with its own instrumentation zeros and tunnel start/stop sequence. In order to use simple statistical concepts, each group of back-to-back repeats must have the same number of runs. For most tunnel calibration data, the minimum recommended number of repeated data sets for such a group is three. Five would be significantly better, but cost concerns generally preclude such extensive testing. To address the longer-term variation, this group of short-term back-to-back repeats must also be repeated multiple times. These longer-term repeats can take the form of multiple short-term repeat

groups distributed throughout the duration of one test (within-test variation) or across separate test entries (test-to-test variation). Capturing the test-to-test variation is essential as it may well display the largest variations in the process, and that variation can only be captured by multiple test entries. Again, in order for the measured variation to represent the normal variation in the facility, both the short-term and the longer-term repeat testing must be conducted in a manner that will encompass all factors that might affect the data repeatability in normal testing.

Historical tracking and analysis of the variation and mean values are accomplished using the control chart concept developed by Walter Shewhart. In these control charts, the results from repeated tests are presented chronologically to track values of critical parameters over time. For wind tunnel testing, these charts generally should include the short-term data group means and their average over time, parameters that display the short-term and long-term variation, and control limits for each parameter. Control limits for these charts are estimates of the 3-sigma limit of variation based on the data acquired, and they indicate the range of variation that is normal for sampling from a stable process. If all data are randomly distributed about the means and lie within the control limits, the process is considered to be in statistical control, and the level of variation present is considered to be normal for the system under consideration. Even if the magnitude of the variation is considered by the facility to be unacceptable, improving it will probably be very difficult, time consuming, and expensive because there are likely to be no large individual causes of the variation. On the other hand, if some data fall outside the control limits or lie inside the limits but show evidence of nonrandom distribution, the process is deemed to be not in a state of statistical control. The occurrence of such “out-of-control” data is indicative that an “assignable cause” exists for the variation and that justification exists for expenditure of resources to identify and eliminate the cause.

### 3.6.3 Out-of-control variations

For the calibration process to be brought into statistical control, all assignable causes for out-of-control variation must be identified and eliminated. This can be a slow and painstaking effort, but is one that must be accomplished if credible estimates of data repeatability are to be made.

The existence of a state of statistical control can only be inferred from multiple repeated data sets, but there are no clear guidelines for how many data sets are required for a valid inference. Twenty to twenty-five test entries are satisfactory but are difficult to achieve in a reasonable span of time. Conducting 10 repeat check-standard tests with at least one repeat group per test (at each flow condition of interest) is about the minimum for a realistic inference of a state of statistical control. Even with multiple entries per year, acquiring such a data set will take significant calendar time. However, very useful information can be gained from analysis of data from only a few test entries, and that information is sufficient to begin the ongoing process of identifying and eliminating assignable causes of variation and thereby bringing the wind tunnel calibration process into statistical control and evaluating the process variation.

# 4 Calibration and flow field measurements

In the planning stage of a calibration program, choices must be made regarding the measurement technique, flow sensing probe(s), instrumentation, and mounting arrangement that will be used in each calibration test. These decisions are facilitated by a review of the goals and accuracy objectives of the test. Because of the wide variety of wind tunnels and types of tests conducted in these facilities, it is not practical for this document to identify standard hardware suitable for all calibration situations. Instead, several typical examples of calibration hardware will be presented. Detailed descriptions of the hardware devices, their design details, probe calibration procedures and the data corrections associated with each type may be found in References 2 and 12 to 16. Readers are encouraged to consult these references when selecting hardware to best meet the needs of their calibration program.

Many, if not all, of these probes require some sort of probe calibration before being used in a wind tunnel calibration. In some instances, a probe's calibration is a relatively simple determination of the probe's ability to measure a known pressure or temperature so that its recovery factor can be determined. Other calibrations, such as those for flow-angle probes, can be more costly and time consuming. In any case, the range of the probe calibration should match the actual operating conditions to be calibrated in the wind tunnel, to reduce or eliminate measurement errors such as Reynolds number effects. Also, because the probes frequently are quite delicate and can easily be bent, one must take care to preserve the integrity of both the probe and its supports or risk invalidating the probe calibration. A substantial amount of literature deals with probe design and calibration, such as in References 12 to 16 and in data published by commercial suppliers.

Instrumentation refers to the devices, such as pressure transducers and their supporting electronics systems, which are used to quantify the flow parameters sensed by the probes. Instrumentation is typically chosen on the basis of its availability and past performance history. In principle, any type of instrumentation may be used if it is shown to be adequate for the task. All instruments used in a wind tunnel calibration program should have up-to-date calibrations themselves. Preferably, the probes and instrumentation should have calibrations traceable to a recognized standards agency, such as the National Institute of Standards and Technology (NIST). The range of the probe calibration should be well matched to the operating conditions to be calibrated in the wind tunnel; this will maximize measurement accuracy and account for any possible Reynolds-number dependence of the probe calibration.

Mounting arrangements for calibration probes include a single probe, a single probe on a traversing mechanism, or a multiprobe rake. Each arrangement has advantages and disadvantages, and the mounting arrangement should be selected on the basis of the calibration objectives. In general, the most accurate mounting arrangement is the single probe; this is because a single-probe measurement usually involves more accurate instrumentation. Furthermore, aerodynamic interference effects from the mounting hardware are minimized, they are probably best known for the single-probe case, and they are usually already accounted for in the probe calibration. On the other hand, planar or volume calibrations can be performed much more quickly using a multiprobe rake, at the expense of decreased accuracy due to transducer/probe cross-calibration errors. The cost of using multiple measuring devices and related instrumentation can be mitigated by using a lower accuracy transducer. In addition, aerodynamic interference between the multiple probes on a rake, and due to the rake mounting structure, is also substantially greater than for the single-probe case; however, with proper rake design, a nearly constant aerodynamic interference can be attained at all measurement stations on a rake, and this may be acceptable if the objective of the test is to measure only variations of flow parameters over the survey area, as opposed to making highly accurate absolute measurements. Finally, in some cases, the intent of a calibration measurement is to capture the time-variation of test section flow parameters. On the other hand, some flow parameters, such as temperature, may vary so slowly that it is not feasible to obtain a steady-state measurement using a time-averaging technique. In these cases, a rake offers a substantial advantage over a single probe because it can acquire an instantaneous record of the flow field along its span. In general, a single probe on a traversing mechanism is a compromise between the

single probe and multiple-probe rake. Examples of typical mounting installations used in calibration testing are shown in Figures 4 and 5.

Although this document focuses on the more conventional and proven types of hardware and test procedures, the calibration team should be open to using other types of measurement platforms as the technology and opportunity permits. Examples are laser Doppler velocimetry (LDV) and particle imaging velocimetry (PIV), which could be used for checking the airspeed, turbulence intensity, and flow angle at discrete test section locations. There are several technical considerations such as seeding, alignment, optical access, and lighting that must be taken into account for these methods to be used in a given wind tunnel. As pressure- and/or temperature-sensitive paint (PSP/TSP) technologies mature, they may also be used to check tunnel calibration or flow quality parameters.

The following sections provide additional information on the most common measurements performed during a tunnel calibration, and options to consider for each measurement are presented. Because of the wide variety of wind tunnels and types of tests conducted, it is not practical to identify standard hardware suitable for all calibration situations. Instead, typical examples of calibration hardware are presented. More detailed descriptions of calibration hardware, design details, probe calibration procedures, and the data corrections associated with each type, can be found in References 17 to 19.

## 4.1 Steady-state pressure measurements

Of the types of measurements just listed, the one requiring the most attention to accuracy is the calibration of the pressure measurement systems. Pressure is the most basic and most important test section flow property to be characterized in the calibration testing. Pressure measurements are required for the analysis of essentially all test data acquired in the wind tunnel and, therefore, they have a significant impact on the quality of data acquired during production testing. Some examples of wind tunnel calibration parameters that are determined using pressure measurements include

- Calibration of the test section pressure measurement system (used to calculate facility Mach numbers and airspeed)
- Mapping of the total, static, and dynamic pressure distributions in the test section
- Boundary-layer measurements
- Wall surface pressures (e.g., blockage investigations)

### 4.1.1 Calibration measurements

Arguably, the best setup for a test section calibration is to use a single pitot-static probe with a calibration traceable to a recognized standards agency, such as NIST. An example of a single pitot-static probe used for test section calibration is shown in Figure 4. The probe was custom designed for its wind tunnel, but was cross calibrated with a second pitot-static probe that had a known calibration traceable to NIST. The cross calibration was performed by mounting both probes in the test section at the same time. Alternatively, the cross calibration could have been performed by mounting first one and then the other probe at the same location in the test section, and measuring the static and total pressures measured by each probe at the same test section dynamic pressures. Note that if the probe under test is mounted in its normal probe support during the cross calibration, then the calibration will automatically account for any additional flow interference contributed by the probe support.

As mentioned previously, the total and static pressure calibrations can also be performed using separate probes. Figure 5 shows a calibration probe, custom designed for static pressure measurements only. The complete probe installation, including support hardware, is arranged to minimize the overall aerodynamic interference at the probe static pressure taps.



Figure 4 – Single pitot-static probe used for test-section calibration (courtesy of Micro Craft Technology Inc.).




Figure 5 – Single probe with two-dimensional support, used for test-section static pressure calibration (courtesy of Boeing).

### 4.1.2 Mapping test section steady-pressure distributions

Global information on total and static pressure distributions in the test section is typically acquired as part of an assessment of test section flow quality. The data can also be used to calibrate the wind tunnel pressure-measurement system if a planar or volume calibration is preferred rather than the point calibration discussed previously.

The main objective of a test section pressure survey is to evaluate the spatial pressure variations within the test section flow. In this regard, absolute measurement accuracy is not essential, since it is still possible to deduce variations from pressure data with a constant or known aerodynamic interference error. Pressure variation measurements can, therefore, be performed using a multiprobe rake, especially

if the rake design is one that creates a consistent aerodynamic interference effect at all measurement stations. Given this, the best rake design is one with a two-dimensional support that spans the entire test section. An example of this type of rake is shown in Figure 6. Each probe on the rake shown in Figure 6 mounts a five-hole hemispherical tip for flow-angle measurements, with static taps located eight diameters downstream of the probe tip, and approximately 16 in. upstream of the rake body (i.e., 16 rake-thicknesses upstream). Using the rake, calibration data on the test section flow angle and on total and static pressure distributions can be acquired rapidly and simultaneously.

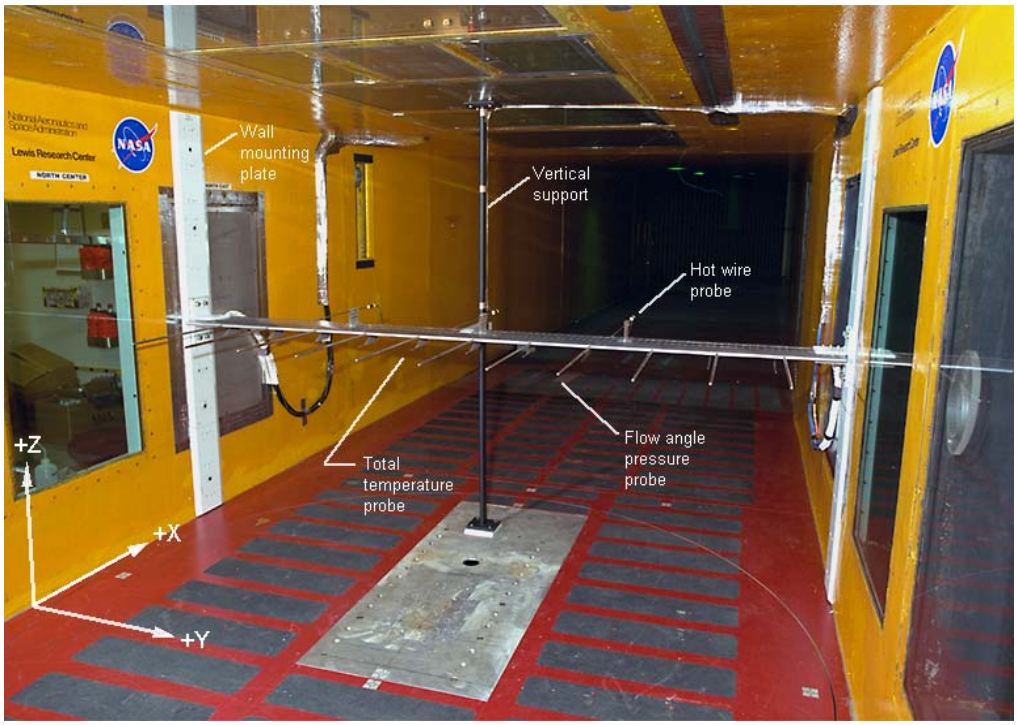



Figure 6 – Example of an instrumented rake used to collect calibration and flow quality data. Flow probes mounted on the rake include combination pressure probes, thermocouples, and thermal anemometry probes (courtesy NASA Glenn Research Center).

If significant three-dimensional flow effects are suspected, they can be estimated and corrected using computational methods. Satisfactory results can be obtained using routines such as an inviscid panel method, or even a simple source/sink potential-flow analysis.

Ideally, a survey of the test section pressure distribution should always be performed after any alterations to the wind tunnel circuit. In general, spatial variations of the total pressure distribution should be very small away from the wall boundary layers; if not, they may indicate upstream flow separations. Static pressure variations can result from several sources, including the state of upstream flow-conditioning elements (i.e., screens and honeycomb), a residual pressure field from the upstream contraction, or local effects such as imperfect techniques to account for boundary layer growth along the test section surface. In low disturbance tunnels, the causes for pressure variations can come from more obscure sources.

### 4.1.3 Recommendations on data acquisition

The data acquisition system should be well suited to the accuracy requirements of the wind tunnel calibration. The regular facility data acquisition system may be sufficiently accurate for calibration measurements; however, the calibration team must ensure this to be true through an uncertainty analysis. Other data acquisition options may be needed to achieve the required data quality. Because of the wide range of equipment available, it is not feasible to give a summary here of data acquisition options.

During production testing, most facilities now acquire pressure data using a pressure-scanning system that incorporates multiple transducers. These systems offer the advantage of speed. However, the accuracy of currently available pressure-scanning systems may not be sufficient for all calibration tests. The suitability of a pressure-measurement system should be evaluated using a pretest uncertainty analysis that considers transducer accuracy and range, analog-to-digital resolution, and the possibility of cross-calibration errors between multiple transducers.

If it is found that the test accuracy requirements cannot be met using a pressure-scanning system, then greater accuracy can be obtained using a single, high-accuracy transducer to sequentially measure all pressures in the data list. An argument against this approach is that, since the pressure data are not acquired simultaneously, the data become susceptible to errors introduced by temporal fluctuations of the mean test section dynamic pressure. This problem can be eliminated by continuously recording the test section reference pressure during the pressure scan so that the data can later be compensated for the temporal fluctuations. The only real disadvantage of this approach is that the total measurement time is substantially greater than that for a pressure-scanning system.

During the actual measurement of steady pressure data, standard data acquisition practices should be followed. As in any experimental measurement of steady-state parameters, the raw data should be filtered to avoid aliasing errors. For steady pressure measurements, the filtering is not necessarily electronic, since advantage can also be taken of the filtering effect of long pneumatic tubes. Ideally, some time should be set aside during the calibration program to characterize the facility dynamic-pressure fluctuations. During steady pressure measurements, the data-averaging time should be chosen to span the longest-period fluctuations.

## 4.2 Axial static pressure distribution measurements

One of the primary measurements in a wind tunnel calibration is the axial static pressure distribution. This information is used to determine corrections to aerodynamic force data acquired in the tunnel, but may also be used to determine the static pressure calibration for the test section.

Most tunnels have some level of axial static pressure nonuniformity resulting from an imperfect contraction or nozzle design, or from the influence of model support systems. The source of variations in the test section axial static pressure distribution depends on the type of wind tunnel. For an open jet wind tunnel, the test section static pressure varies rapidly near the nozzle and collector, and these effects may extend into the test region. For a solid wall wind tunnel, a residual axial static pressure gradient may exist if the test section wall divergence is insufficient to offset the blockage caused by boundary-layer growth on the test section walls. Pressure gradients are also induced close to any sources of suction or blowing, for example, near a suction plate for boundary-layer removal.

A nonuniform static pressure distribution along the test section axis induces a streamwise buoyancy force on a test article that is purely an artifact of the test section flow, resulting in an error in the measured drag. The measured axial static pressure distribution is used to determine a buoyancy correction, which is applied to correct drag data acquired in the tunnel. As drag divergence conditions are approached, a correction to the contribution of the rear part of the model to lift and pitching moment may also be required, because the Mach number is not the same for the rear of the model as for the reference condition.

There are two main methods of measuring the axial static pressure distribution: a static pipe or other stationary piece of hardware or a traversing static pressure probe, each method has its own distinct advantages and disadvantages.

### 4.2.1 Static pressure pipe

The static pipe is a constant-diameter pipe that is mounted in the test section with its length aligned with the flow. The pipe is tipped at its leading edge with a small angle cone or ogive. It is usually long enough to span the entire length of a wind tunnel's test section. A static pipe is commonly suspended in the

center of a test section, with the upstream end of the pipe secured by cables attached to mounting lugs located in the settling chamber or contraction. The downstream end is either mounted on a strut attached to the floor, or to the facility model support system. Figure 7 shows a typical static pipe mounted in a wind tunnel.

The static pipe has a large number of pressure orifices that are used to measure the static pressure at various locations along the pipe's length. The orifice spacing can vary along the length of the pipe, with orifices spaced more densely in regions of greater interest, for example, the main testing area of the test section. It is recommended that the location of each orifice have an angular offset (clocking) relative to the orifice immediately upstream so as not to be affected by orifice disturbances traveling downstream.

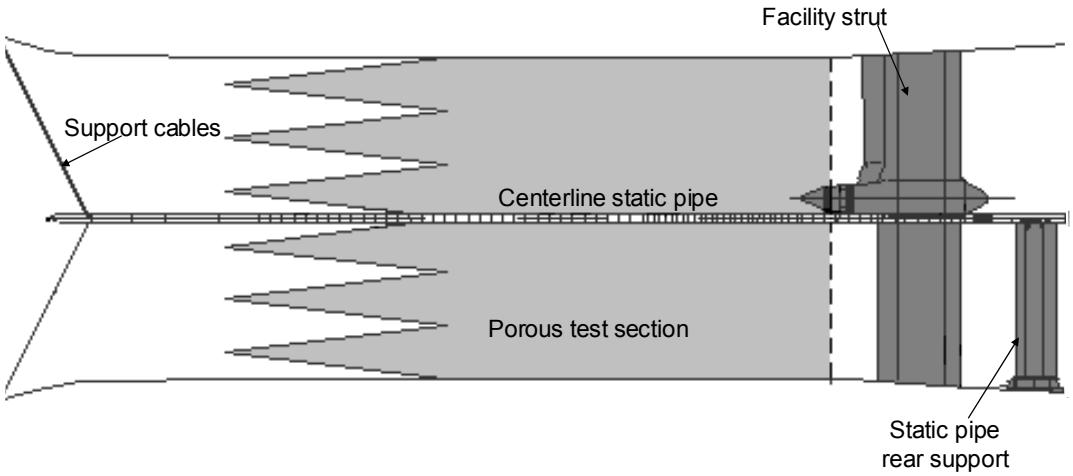



Figure 7 – Typical static pipe installation in a transonic wind tunnel. The static pipe is mounted vertically at the test section centerline, but offset laterally by 5 in. to account for the facility strut. This test configuration allows for the effects of the facility strut to be accounted for in the calibration.

The main advantage of the static pipe is that large amounts of data on the streamwise static pressure distribution can be acquired in a short amount of testing time. This is a great advantage for tunnels that must calibrate for numerous complex combinations of operational settings (drive system, plenum evacuation rates, and variable wall angles) and flow conditions (Mach number, Reynolds number). Effects on axial flow distributions can be quickly evaluated and optimized for various operating conditions of a tunnel. This particularly applies to variable density, transonic wind tunnels, where static pipes play an important calibration role.

Static pipe data are used to calibrate the tunnel reference static pressure (which often is located outside the test section in a plenum) to the test section centerline static pressure. The data from the centerline static pressure survey are usually averaged over a selected length of the test section, most commonly corresponding to the location and length of a particular wind tunnel model. This allows the calibration to be tailored to specific test section locations and/or lengths to match the needs of various classes of test articles or test types.

A static pipe is a means for measuring Mach number along the test section where the resulting data are then used to correct errors in Mach number and model drag. The pipe static pressures are usually converted to Mach numbers after being normalized by the tunnel total pressure. For transonic tunnels, it is necessary to not only have accurate test section Mach number measurement but also to have accurate measurements of local Mach number variations along the length of the test section. Test section Mach number gradients across a model lead to buoyant effects and errors in wave drag measurements. Buoyancy effects due to static pressure gradients over a wind tunnel model are determined from the static pipe data by integrating the empty-tunnel pressure distribution data over the model's surface and

removing the resultant force from the model's drag measurements. This is a concern for transonic wind tunnel users since much of the testing occurs in Mach number regimes where precise Mach number measurements are required; specifically, at $0.75 < M < 1.2$, where aircraft vehicles encounter drag rise, and at $1.0 < M < 1.6$, where wave drag effects become prominent. Vehicle drag becomes highly sensitive to Mach number and Mach number gradients in these speed regimes (i.e., small variations in Mach number cause large variations in drag).

As important as they are, static pipes do have disadvantages. Such a pipe is usually time consuming and cumbersome to install. Being supported only at its ends, a static pipe may sag along its length. Excessive sag may lead to errors in the pressure gradient measurements. In addition, a static pipe can be susceptible to vibration. The cables holding the pipe at the front end could induce artificial flow disturbances in the pressure field. Because of the streamwise length of a static pipe, boundary layer growth may become significant, influencing local streamlines and ultimately the measured pressure distribution. A transition band (boundary layer trip) can be included at the beginning of the cylindrical portion of the pipe to reduce the effects of boundary layer growth on the static pressure measurements. There is typically not enough room inside a static pipe to house the transducers measuring the pipe pressures, therefore, a hypodermic line must be run from each orifice, through the center of the pipe, and out the aft end to the transducers. These lines can be quite long, resulting in a low-frequency response for the measurement (i.e., pressure lags). Like all pressure-measuring devices, a static pipe is susceptible to orifice errors. Reference 2 provides a succinct discussion on orifice-induced static pressure errors, including many references. Finally, the location of the static pipe cannot be easily changed, making it impractical to use for planar surveys.

Reference 14 presents guidelines for designing and using a static pipe. For example, we recommend that the cross section of a static pipe not exceed 0.5-percent blockage of the test section, to minimize blockage-induced expansion effects. However, we believe that a test section with ventilated walls at subsonic conditions is not susceptible to this effect (another reason for the common use of a static pipe in transonic wind tunnels). At conditions greater than Mach 1.0 in a transonic tunnel, use of a static pipe that extends through the contraction region will affect the supersonic flow development. A correction derived from a computational fluid dynamics solution may be warranted. The nose and support cables of the pipe should be located well upstream of the test section and always in subsonic flow. This eliminates flow disturbances from a bow shock in front of the nose that would be present in supersonic flow. Subsonic flow at the nose assures that no transonic shocks pass over the pipe orifices, and it reduces the strength of the flow disturbances shedding off the cables. Cables near or within the test section should be swept back at an angle of approximately 30° to the centerline, and attachment points should be located behind the tunnel walls, if possible. The cables should be loaded with a large tensile force, and if appropriate, an upward moment should be applied at the downstream support to minimize sway and reduce sag, particularly in the midsection of the pipe where the area of highest importance usually resides. Pressure lag times associated with the long tube lengths of each static pipe orifice should be evaluated to define the data acquisition times during testing. References 20 to 22 have good discussions regarding pressure lags and calculating lag times.

A static pipe requires some basic attention to ensure a successful and meaningful calibration. The location of each pressure orifice relative to some known reference point on the static pipe should be inspected and documented. Because of the sheer number of pressure orifices, we recommend that all pressures be blown out and then a complete continuity and leak check be performed for every pressure on the pipe prior to installation in the tunnel. A record of the continuity and leak check results should be maintained throughout the process. In addition, all orifices must be inspected to ensure they are not damaged in any way and are free of debris.

When installed in a test section, the locations of the pipe orifices need to be correlated to some known reference in the test section. The pipe should undergo another continuity and leak check, once installed. The spatial position of the pipe should be measured and recorded. During the actual calibration, it is advisable to periodically check and record the pipe's sag. This can be accomplished quickly by measuring the pipe's local angle with a mechanical inclinometer placed at various locations along the top

of the pipe. In addition, the tensions on each of the pipe support cables should be recorded over the course of testing and retightened if found loose.

The selection of the transducers measuring the pipe pressures is extremely important. For subsonic applications, low-range transducers are needed because of the lower static pressure levels, whereas in a transonic wind tunnel a balance must be struck between accuracy and the coverage of a wider operating range. Often, the transducers measuring the static pipe pressures are less accurate than the tunnel reference static pressure transducer to which the pipe is calibrated. This of course is an undesirable condition. Unfortunately, due to the sheer number of static pressures being measured on a pipe, one is generally compelled to use electronically scanned transducers to measure many pressures at once and reduce the expense per measured orifice.

The difference between the centerline static pressure and the reference static pressure measured in the plenum surrounding the test section will usually be less than 1 percent. This difference can easily be overshadowed by the accuracy of the pipe transducers. An instrumentation shift due to temperature, which is probably one of the largest sources of error, can greatly affect the result of the calibration. One recommendation is to manifold pressure transducers, of similar accuracy and design as the reference pressure transducer, to one or two critical orifices on the pipe. These high-accuracy transducers would identify transducer shifts on the pipe and perhaps provide a means for correcting the data. To achieve accurate buoyancy corrections, Mach number gradients also need to be known accurately. Ultimately, desired accuracies must be identified and then instrumentation chosen appropriately through the application of the pretest uncertainty analysis.

#### 4.2.2 Other stationary axial static pressure measurement devices

Other hardware used to measure the axial static pressure distribution include static pressure rails, static pressure probes, and cone cylinders. Each of these pieces of hardware provides the static pressure distribution, but generally over a smaller portion of the test section.

A cone cylinder is a shortened version of the typical static pipe. Again, it provides only a local view of the axial static pressure distribution, but it is faster and easier to install in the test section than a static pipe. Figure 8 shows an example of a cone cylinder installed in a transonic wind tunnel. Cone cylinders can also be built in different sizes (diameters) to measure the effect of model blockage on the test section flow quality. Like the static pipe, cone cylinders can have multiple rows of static pressure taps, and the spacing of the taps can be designed according to the specific calibration needs of a tunnel.

A static pressure rail differs from a static pipe in that the rail is mounted directly to a test section surface, usually the floor, and therefore, does not measure the centerline static pressure distribution. The rail does provide an accurate indication of changes in static pressure through the test section along the surface on which it is mounted. However, a static rail does not account for vertical variations in static pressure. Measurements from static rails mounted on the floor, ceiling, and side walls could be averaged to obtain the centerline, but only if the variation is linear. Otherwise, a centerline measurement is needed. An advantage to the rail is that it mounts to the test section surface along its entire length, which makes it easier to install and align.

Another important consideration of the static rail mounted to the test section surface is the influence of the mounting on the resulting measurements. Any installation should be checked for influence of the attachments or supports. Also, the finish of the test section surface is very critical to flow quality and data quality (imperfections in the surfaces will generate disturbances that could affect test data). This is especially important for high Reynolds number tunnels, hence the test section surfaces should remain untouched.

Static pressure probes of various designs can also be used to provide a limited definition of the axial static pressure distribution. These probes can be mounted in the model support system. Because they are shorter probes, they provide only a very localized view of the axial static pressure variation in the test

section. However, their smaller size does make them much easier and faster to install and align. This makes this type of probe a good choice for check calibrations.

The measurement hardware devices described in this section are, by definition, shorter than the static pressure pipe, such that the nose may be in the test section during the calibration testing. If this is the case, then distribution of the wall pressures must be monitored for any disturbances from the nose of the hardware.

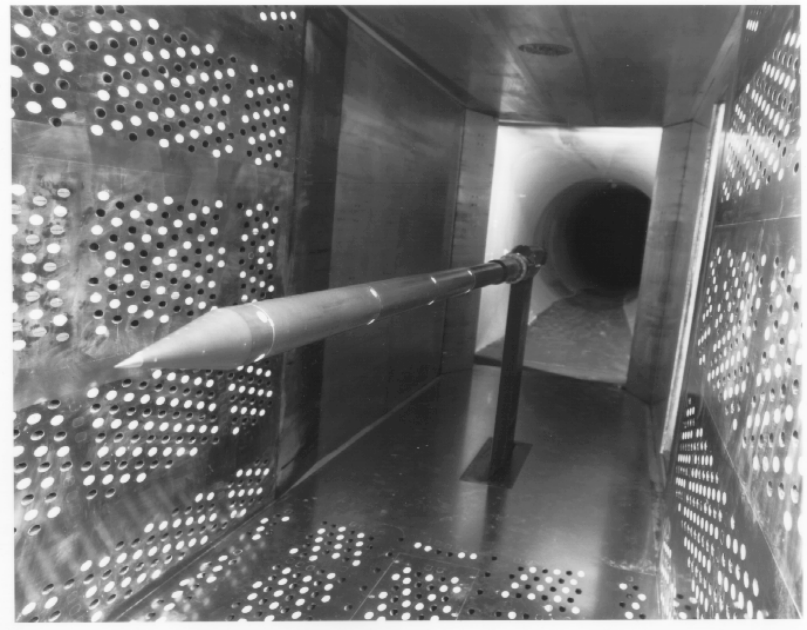


Figure 8 – A 4-in. diameter cone cylinder model installation in a transonic wind tunnel. This hardware is used to measure the static pressure distribution through the test section (courtesy of NASA Glenn).

### 4.2.3 Translating probes

Another common method of determining the test section axial-static pressure gradient is to measure the axial pressure distribution point-by-point with a single static pressure probe. In general, the single probe method offers the advantage of potentially higher accuracy than the static pipe method at the expense of longer data acquisition times. Since the measurement involves only a single probe, the method leads itself to better instrumentation such as an accurate and well-ranged pressure transducer and a high-quality calibrated probe. Another key advantage is that the orifice error is constant for all measurements. On the other hand, the axial pressure survey is constructed from data collected over some nontrivial period of time (as opposed to the near simultaneous collection of the axial pressure distribution obtained from a static pressure pipe). However, one can measure and correct for temporal variations of test section dynamic pressure by normalizing the static pressure data by some reference pressure. The real disadvantage of using a single probe is that substantially more test time may be required; however, this may be acceptable if a higher accuracy measurement of the axial pressure distribution is desired. There are also structural concerns that must be addressed particularly as the airspeed is increased. More robust equipment may be needed to ensure structural integrity and a stable measurement platform. Also, variation in the probe support interference can contribute to erroneous static pressure measurements, particularly near the aft end of the test section (i.e., due to changes in the blockage or profile of the support and/or translating hardware).

## 4.3 Flow-angularity measurements

Flow angularity is a critical parameter that has particular significance on the drag measurements—the aerodynamic force and moment test. Since aerodynamic forces respond to the integrated effect of flow-angle variations over the entire model, it makes the most sense if an evaluation of flow angularity takes the form of an average of spatial flow-angle variations in the vicinity of the model mounting location. The information obtained from this mapping of the test section flow angle can be used as an aid in test data analyses, such as correcting for changes in flow angle along the span of a model, or understanding flow distortions during an inlet test, or simply as a diagnostic tool for identifying and solving facility flow quality problems.

There are a variety of flow probes and measurement techniques that can be used to measure the local flow angle. Many of these are pressure probes that relate pressure differences to the flow angle through a calibration relationship. Other systems, such as thermal anemometry, optical techniques, and wind vane probes are also used, although these systems are not commonly used. Thermal anemometry and wind vanes are not as accurate as pressure probes, and optical techniques can be difficult to implement because of the lack of optical access and issues with seeding the flow fields.

### 4.3.1 Integrated upflow measurement

The method of measuring test section integrated upflow is similar to the procedure used for balance aerodynamic alignment during a normal model test (Reference 13). An important consideration of the integrated upflow measurement is that small errors in the orientation of the mounted model can also generate a lift force on the model that cannot be distinguished from an upflow effect. This problem is circumvented by testing the model both upright and inverted. The difference between the upright and inverted lift curves is related to mounting misalignment, whereas the offset of the mean lift curve from null lift at a $0^{o}$ angle of attack is related to the effect of the test section integrated upflow on the model.

The most accurate approach is to roll the model on the balance instead of rolling both the model and the balance. Error in longitudinal alignment of the balance looks exactly like stream angle and can't be separated from it. Rolling the model on the balance at least holds this error constant. On the other hand, rolling both the model and the balance together results in an inconsistent balance alignment error that results in an added bias error in the stream angle. With a consistent and accurate means of determining balance orientation, the procedure chosen would be of no consequence.

The integrated upflow measurement can be performed using either a dedicated check standard model or an actual test article. The check standard model has the advantage that the configuration is fixed; that is, the model is treated as dedicated calibration hardware and is not modified between uses. This ensures valid historical comparisons and tracking of changes in tunnel flow. The alternative of using an actual test model has the advantage of convenience. The inverted run can be performed at the beginning of a test, adding only a few hours of test time. Also, it is the truest measure of upflow for that model. The disadvantage is that it does not contribute to the historical flow-angularity database because the model configuration may change between tunnel entries.

The procedure for determining upflow for either a dedicated check standard model or an actual test model is identical. The model is installed inverted and aligned geometrically to zero yaw and pitch angles (it will be assumed at this point that model orientation devices such as inclinometers have been properly calibrated). The model is then tested over a limited angle-of-attack range, for example $\pm 5°$, at increments of $0.5°$. The sequence should always be such that the model sweeps from the most negative to the most positive angles to eliminate any hysteresis. This is repeated for each Mach number, dynamic pressure, or other parameters, as necessary. The model is then rolled upright, and the procedure is repeated. The stability axis lift coefficient is then plotted against angle of attack for the upright and inverted runs. The slopes of the upright and inverted curves should be identical. For upflow ($\Psi$), the inverted lift curve typically lies to the right of the upright lift curve. The "true" curve lies exactly half way between the two curves. An example is shown in Figure 9.

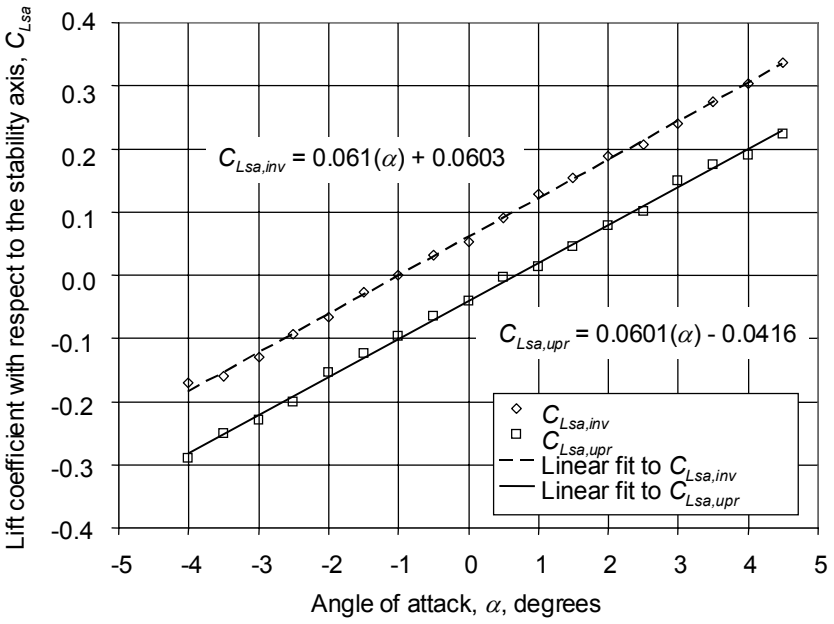



Figure 9 – Data from upright and inverted model runs used to determine integrated upwash.

In this example, the inverted curve lies to the left of the upright curve, indicating downflow (or negative upflow). The upflow is determined by calculating the zero-lift intercept for each curve, i.e., solving each of the curve-fit lines for $C_{Lsa} = 0$. The upflow is defined as one half the difference of the angles at zero lift:

$$\Psi = 0.5(\alpha_{CL0,\text{inv}} - \alpha_{CL0,\text{upr}})$$

For the example plot,

$$\alpha_{CL0,\text{inv}} = -0.9967 \quad \text{and} \quad \alpha_{CL0,\text{upr}} = 0.6922$$

and

$$\Psi = 0.5(-0.9967 - 0.6922) = -0.8445$$

This upflow term is added to the uncorrected upright angle of attack. To check for proper use of this term, applying this correction to upright and inverted curves (subtracting it from the inverted angle of attack and adding it to the upright angle of attack) should collapse them to a single curve.

To determine sidewash, the same procedure may be used while yawing the model over a limited range and plotting the stability axis side force coefficient as a function of yaw angle. If the model does not have sufficient side-force-generating surfaces or if the tunnel has no yaw capability, a slightly different approach may be necessary. It may be necessary to roll the model 90° (left wing up), “pitch” the model over a limited range, roll the model 180° (right wing up), and “pitch” the model over the same limited range. These “upright-inverted” runs may then be used to determine the sidewash terms.

### 4.3.2 Pressure probes for flow-angle measurement

Flow-angle pressure probes are designed so that the relative flow angle to the probe axis creates a pressure difference between opposing pressure ports on the probe. By measuring this pressure difference, the local flow angle can be determined from the probe calibration. A wide range of probe types are available, such as yawhead, claw, hemispherical head, and conical head probes, with the main differences between the probe types being principally differences in sensitivity and useful range. Very

high sensitivity flow-angle probes have been developed and proven in wind tunnel calibration and flow quality survey applications (Reference 17). Some probes, such as the hemispherical-head probe shown in
Figure 10, include additional pressure taps to allow simultaneous measurement of the local total and static pressure in addition to the local flow angle.

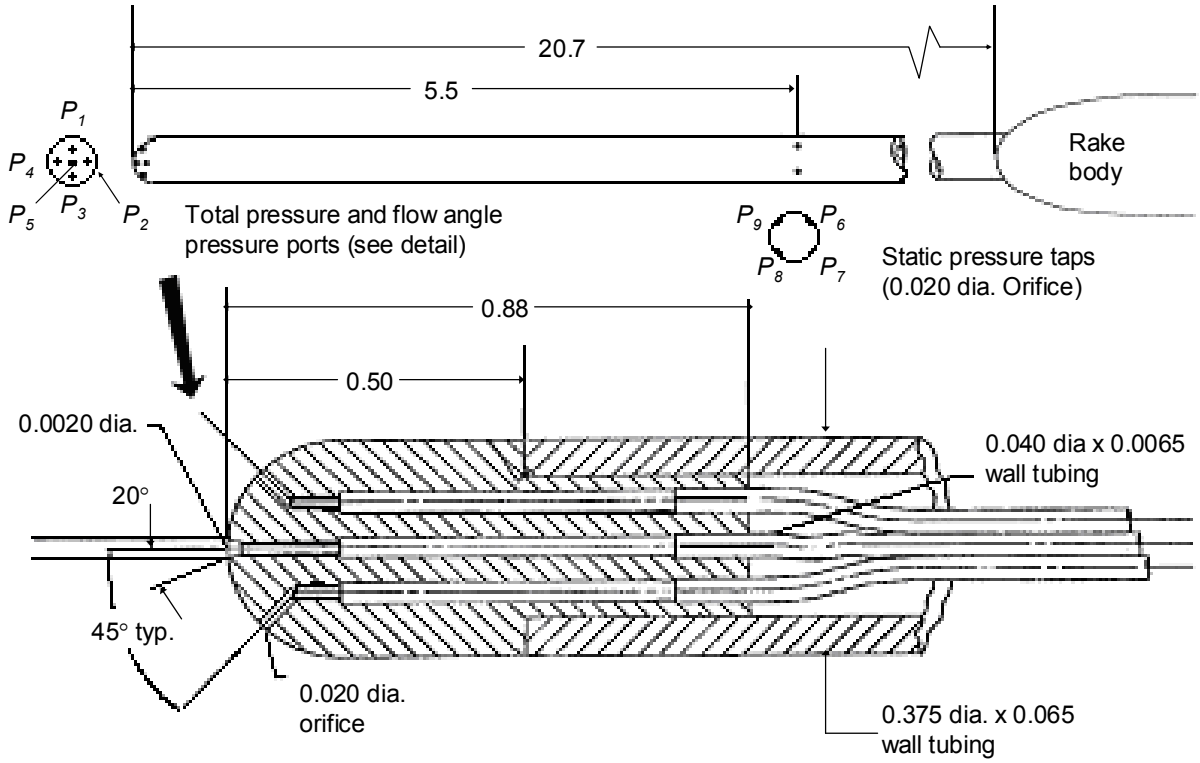



Figure 10 – Typical five-hole, hemispherical head flow-angularity probe layout. Dimensions given in inches.

Although the probes vary in design and complexity, each does require a calibration to relate the measured pressure differences to flow angle. These flow-angle probes use opposing pressure orifices (set 180° apart) to sense a pressure difference. Ideally, when the probe is perfectly aligned with the flow, the pressure difference is zero. Running the probe through a series of angles in a steady, consistent flow generates a calibration curve relating the pressure difference to the flow angle. Most of these probes have two sets of pressure orifices; one for sensing the pitch flow angle and a second for the yaw component. Separate calibration curves are required for each set of orifices used to sense flow angle. The probe calibration must also include corrections for both the measured total and static pressure.

There are several points that must be considered when making flow-angle measurements that affect the probe selection. Speed regime, environment, mounting, handling, calibration, and alignment are all key issues. For example, the sensitivity of typical flow-angle probes is probably well suited for sensing small angles at low speeds. Once a probe is calibrated, extreme caution must be exercised that the probe is not damaged because this could invalidate the probe calibration. Since many flow-angle probes are long and slender, it is quite easy to bend these probes during installation or configuration changes. Also, surface damage to the probe head will affect the calibration because any changes to the surface could change the pressure distribution over the orifices and, therefore, change the calibration. Therefore, tunnel cleanliness should be considered since any impact damage to the probe caused by even tiny debris in the airflow could change the probe calibration.

Alignment of the probe in the test section is critical. There are two schools of thought on alignment. The first is that the probe should be mounted and aligned to very tight tolerances to some reference planes in the tunnel (usually the test section centerline). This can be very tedious and time consuming, particularly if the probe support system cannot be easily adjusted to correct the misalignment. The process eliminates offsets that must be tracked and included in the calculation of the flow angle. The second method is to measure the misalignment of the probe from the reference planes, and then use these data to correct the measured flow angles. This method is generally faster in terms of hardware setup, but care must be taken in the use of the alignment data.

Annex B contains some additional information on the alignment and calibration of pressure probes used for flow-angle measurement. There is also a great deal of literature on the topic of wind tunnel flow-angularity measurement, such as References 12 to 16. In addition, Reference 18 discusses the calibration of a hemispherical-head probe for a transonic tunnel application, and Reference 19 describes a subsonic tunnel calibration application.

### 4.3.3 Nonpressure probe systems

As an alternative to the direct measurement of pressure, some probes measure the pressure effects on aerodynamic surfaces with force and stress transducers. An example of a nonpressure probe system for measuring flow angularity is the cruciform flow-angle probe. It consists of a 3-in.-span cruciform wing-body installed on a 0.16-in.-diameter, five-component force balance (see Figure 11). The probe body is a 0.375-in.-diameter ogive-cylinder, the wing chord is 2 in., and the overall length of the probe is 4.19 in. The leading edge of the wings has a 20° taper to a 0.064-in.-thick wing. The body is made of magnesium, which gives a model-balance natural frequency of about 180 Hz. A laser optical alignment device is used to align the probe longitudinal axis with the test section axis. The probe is typically mounted on a traversing strut mechanism to survey test section flow. The high natural frequency and very fast response of the force balance permit data acquisition in a continuous movement mode. Probe calibrations consist of pitch polars in both the upright and inverted positions for the upflow plane of the probe and at ±90° roll positions for the sidewash plane of the probe at each Mach number. Both planes of the probe are calibrated in the vertical plane of the wind tunnel so that the local flow angle (in the vertical plane) can be compared as a validation of the probe setup.

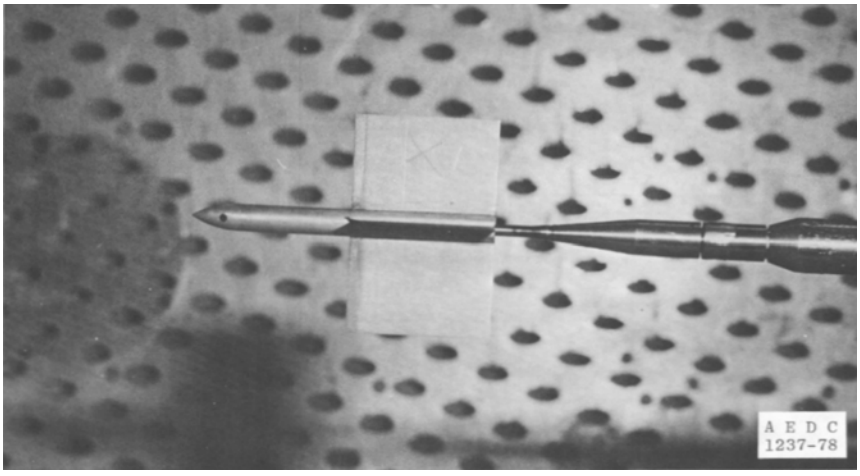



Figure 11 – Cruciform probe for flow-angle measurement (courtesy of Arnold Engineering Development Center).

## 4.4 Temperature measurements

Total temperature is the third parameter needed to set the test section operating conditions along with two pressure calibrations. Total temperature is usually measured with thermocouples, although other probe types, such as resistive temperature devices, can be used. A common arrangement is to relate test section total temperature measured by the calibration hardware to the total temperature in the settling chamber measured by the facility reference hardware (similar to the arrangement for pressure calibrations described in Section 3.1).

Total temperature probes should use aspirated heads to ensure the best recovery. Since air temperatures are relatively unaffected by interference effects, a rake of temperature probes can be used without significantly reducing accuracy. As with all rake installations, care must be taken to cross-calibrate the individual sensors. Also, it is imperative that an uncertainty analysis be done for temperature measurements because there are numerous error sources such as radiation, conduction, and lack of instrument calibration that can affect the quality of the data.

It may be possible to construct a grid of temperature sensors so that all the temperature uniformity data are acquired in a single test. In most cases, however, the rake of temperature sensors covers only a small portion of the test plane or test volume, so that the temperature uniformity must be measured using multiple passes of the rake. In these cases, temporal fluctuations of the mean tunnel temperature can appear as spatial temperature variations. One can compensate for this effect by mounting a reference temperature sensor at a fixed location in the test section for the duration of the temperature survey. Since this reference sensor reacts only to temporal variations of the mean test section temperature, the apparent spatial temperature variations can be removed from the data by subtracting the rake measurements from the temperature measured simultaneously by the reference sensor. Although it may be tempting to simply use the wind tunnel temperature probe as the reference temperature sensor, it is more accurate if the reference sensor is mounted in the test section flow and is of the same type as the temperature sensors used on the rake.

The most time-consuming part of measuring the test section temperature uniformity can be the time spent waiting for the tunnel to come to thermal equilibrium. By Reynolds analogy, it might be expected that the thermal boundary layer is the same thickness as the momentum boundary layer. However, the thermal boundary layer can be significantly larger than the momentum boundary layer, depending on the location of the heat exchanger in the wind tunnel circuit. (Unfortunately, screens and other flow-conditioning elements do not smooth out temperature variations.) The size of the thermal boundary layer should be monitored during the tunnel soak time, since the time required for the tunnel to achieve acceptable temperature uniformity is also an important performance parameter.

## 4.5 Humidity and dew point measurements

The presence of water in the airstream can have significant effects on wind tunnel test data, given the right conditions. If, as the air accelerates into the test section, there is sufficient moisture in the air and the stream static temperature drops below the dew point temperature, the moisture in the air will condense and form a fog in the test section. The resulting condensation can affect the local Mach number as well as other flow field parameters. In the subsonic regime, condensation will increase the Mach number and suppress the static pressure, whereas in supersonic flows, the reverse is true. More detailed accounts of these effects are found in References 2 and 14.

Reference 2 provides some indication of humidity limits for testing in the transonic regime. Observations in the AEDC 4T transonic wind tunnel indicate that force measurements are unaffected by humidity level until a fog is visible in the test section (water-vapor content of 0.002 lb/lb of air). Surface pressure measurement tests are more sensitive to humidity and should be conducted at humidity levels of 0.0015 lb of water/lb air, or lower.

These references also discuss approaches to solving the condensation problem, with the simplest, but sometimes most difficult, solution being to dry the tunnel circuit air to a very low dew point, say

–50 °F. Reference 14 points out that although a –50 °F dew point is still higher than the static temperatures that may be encountered in supersonic flows, the amount of water in the air at this dew point is very small and would have negligible effects even if it were to condense.

Humidity is considered a calibration parameter because it is used as a gauge of data quality, it is used to correct some test data, and it can be used in setting test section conditions (Reference 23). As such, it is important to accurately monitor the humidity level in the tunnel during both calibration and testing. Generally, the measured parameter is the dew point, and there are many instruments available for this application. Reference 24 describes testing done to evaluate several of these systems. A survey conducted as part of the research in Reference 24 showed that most wind tunnels were using chilled mirror moisture analyzers. However, up to three of these instruments were needed to ensure reliable data.

There are several key points to consider when making dew point measurements and selecting the instrumentation. They include measurement accuracy, instrument reliability and repeatability, and operational considerations. Some of the more common devices used to measure the humidity or dew point and their pros and cons are discussed in the following paragraphs.

### 4.5.1 Fog chamber unit

A fog chamber is usually an older, manually operated device for measuring dew point. The unit takes a sample of air from the tunnel and forces it into an observation chamber at a pressure above atmospheric. After the sample stabilizes, the operator rapidly exhausts most of the sample to the atmosphere, with a sudden expansion and simultaneous cooling of the gas that remains in the chamber. If the cooling is sufficient to bring the temperature of the gas down to or below the dew point, water vapor will condense in the form of a fine mist or fog that can be seen through a lighted observation window. From the pressure ratio recorded when the slightest fog is seen and the initial air temperature, the dew point is determined with a circular slide rule calculator. The typical accuracy of this type of system is ±5 °F, but errors of greater than 20 °F can occur at a dew point of –20 °F if the air sample contains insufficient dust particles to act as nuclei for the cloud droplets and/or if insufficient settling time is allowed before the sample is exhausted. Although the stabilization time required for these units is quoted as 10 to 15 sec, actual times of 2 to 3 min are often required. The units can also be very sensitive to differences in operator technique.

### 4.5.2 Chilled mirror instruments

As mentioned earlier, chilled mirror instruments are the most commonly used systems for measuring dew points in wind tunnels. Newer models have accuracies quoted as ±0.36 °F and operate over a very wide range of dew points. Typical ranges are –32 to 200 °F, –85 to 95 °F, and –100 to 167 °F. Some instruments use microprocessors to control and monitor the measurement and to compensate for changes that would affect accuracy, such as particulate buildup on the mirrors.

Although chilled mirror units do offer very good accuracy over a wide range of dew points, there are some concerns and limitations to be aware of. Typically, these units have slow response times and can take several minutes to stabilize. Contamination of the mirrors is also a significant concern, since any dust particle that comes in contact with the wetted mirror will remain on the mirror, trapping moisture and causing artificially high readings. However, with proper care and operation, chilled mirrors will provide reliable dew point data.

### 4.5.3 Aluminum oxide sensors

An example of this type of sensor contains an aluminum wire coated with a hygroscopic dielectric layer that is covered by a film of porous gold. The outer gold film and the inner aluminum core form the plates of a capacitor, which is excited with 60 Hz. Water vapor molecules, which enter the dielectric layer, are restricted because of the extremely small size of the pores, and they condense into liquid water. This high dielectric constant of water changes the capacitance of the sensor, which is measured by the analyzer. The instrument has a range of –112 to –4 °F with a specified accuracy of ±5.4 °F.

### 4.5.4 Silicon sensors

The sensing element in this type of dew-point measuring device consists of a moisture detector built on a low-mass silicon chip. A closed-loop temperature control eliminates ambient temperature error between –40 and 113 °F. The sensor operates satisfactorily between flow rates of 50 to 1500 $cm^3$/min or even in static conditions at an operating pressure from vacuum to 4000 psig. A “push-purge” feature heats the sensor to a high temperature to remove moisture and hydrocarbon vapor contaminants and allows online verification of instrumentation operation within 2 min. The sensor responds to a step change in moisture over an operating range from 64 to –76 °F in less than 1 min, with a sensitivity of 0.002 °F. The range of this unit is –76 to 32 °F with an accuracy of ±5.4 °F.

# 5 Calibration test planning and execution

A wind tunnel calibration is a test program, and it should be conducted with at least the same level of effort as any other wind tunnel test. As such, it is vital that sufficient time be provided for the upfront planning and preparation for the test, that ample time be given to collect and reduce the data during the tunnel entry, and that the calibration testing be documented fully. A good overview on conducting a wind tunnel test is provided in Reference 25.

During a wind tunnel calibration, it is extremely important to pay attention to details, to make careful, accurate measurements, to recheck measurements, to carefully record measurements, and to document everything. Great care must be exercised to obtain good, repeatable calibration data. The importance of an accurate wind tunnel calibration cannot be understated because errors in the calibration can produce erroneous data during future testing.

As the discussion in test planning and execution is developed in this section, there are several key items that must be considered and addressed. Some of these key points are listed here and must be remembered and applied throughout the calibration activity.

- It is essential that a standing group of personnel be consistently involved with the wind tunnel calibration program. One lead engineer should be identified as the primary point of contact for all calibration tasks. Having personnel permanently associated with the calibration provides the continuity needed to ensure accurate calibration data.
- Archive all data—don't throw anything away.
- If there are questions about the data, do not end the test until they are answered.
- Involve enough people to run the test and to concurrently re-reduce, plot, and analyze the data in an expedient manner.
- It is crucial that the location and orientation of each probe on a calibration rake (if used) be precisely known and recorded.
- The order of application of corrections should be the same during calibration and testing. For instance, if the dynamic pressure is not corrected for compressibility effects during the calibration, the data reduction employed during testing should correct for compressibility after the calibration is applied. Conversely, if the calibration is performed after compressibility corrections are applied, the data acquired during a given test should be corrected for compressibility before the calibrations are applied.
- It is difficult to detect all problems online because some postprocessing is required. It is, therefore, advisable to make repeat runs whenever possible and to perform offline processing as the test proceeds.
- A careful calibration engineer will perform replicates across tests and use control charts to monitor performance.
- Instrument zero-adjusts should be performed frequently to eliminate one source of data drift. However, care must be taken that calibration practices are not significantly different from normal testing procedures. If nonstandard procedures are used during calibration, the results will not reflect the normal level of variation that exists in the measurement process. To accurately reflect that variation, calibration testing should follow normal procedures as much as possible.

## 5.1 Pretest preparation

Pretest planning is essential, whether for a full calibration or a 1-day check calibration. We suggest that whatever pretest planning methods and documentation are used by an organization for a research test should also be applied to a calibration test. This planning is vital for several reasons. First, the level of data uncertainty must be determined in order to select proper instrumentation. Second, since wind tunnel testing can be expensive, it is important to optimize the calibration test matrix to get the most data in a prioritized order, in the most efficient manner possible. In addition, a detailed and well-documented test plan can be improved and reused over the course of a tunnel's calibration program.

### 5.1.1 Planning and reporting

An important first step in wind tunnel calibration is the test planning. The project engineer first needs to define the purpose, scope, and goals of the calibration. The overall measurement accuracy goals of the calibration program should be anchored to the future test requirements. The type of calibration (complete or check), facility status (recent modifications that would affect the flow field or systems upgrades that might impact data quality), and needs of upcoming test programs all influence the calibration test plan.

A prudent selection of the calibration hardware and instrumentation is crucial to a meaningful tunnel calibration. During the test-planning phase, a lead engineer should consider and define the required probe types, support hardware, traversing rigs, instrumentation, and instrumentation accuracies. The hardware and instrumentation plan must be sufficiently detailed to allow a project engineer to have the test section and tunnel adequately instrumented to accomplish the goals of the calibration.

As part of the planning phase, the lead engineer should issue a written pretest report outlining the test program. This report is important in that it serves as a centralized working guide for all wind tunnel personnel in setting up the test. This pretest report should provide an overview of the test program, including a statement of the calibration goals and objectives. It should include a list and description of all calibration hardware, instrumentation, setup procedures, positioning information, and references to drawings. This report should also describe the calibration test matrix, including test configurations, data reduction constants, data acquisition settings, and tunnel operating conditions. All instrumentation requirements, such as calibration requirements for all devices, must be clearly stated. Also included are any other special needs to complete the calibration, such as special instrumentation and photographic or flow visualization requirements.

The calibration test matrix should include repeat test points, which are essential to data quality. Ideally, repeat points should be taken during separate run sequences (that is, complete the first data set, perhaps a Mach number sweep, shut the tunnel down, restart, then repeat the sweep, or a portion thereof). If because of operational concerns or lack of time this is not practical (in some facilities, such as pressurized tunnels, the startup and shutdown sequences are very time intensive), then repeat points can be taken during the same run sequence, but the repeat points should be separated in time as much as practical. Setting a tunnel condition, then recording multiple data points back-to-back does not provide meaningful repeat points

Another important pretest document directed to the programming personnel describes all data collection and analysis software requirements. This computing requirements document should include, at a minimum, all required equations and algorithms, data output and format requirements, plotting requirements and special online computing requirements. The data analysis tools are discussed further in Section 5.1.3.

### 5.1.2 Uncertainty analysis in the planning phase

There are two general applications for uncertainty analysis. The first is a pretest analysis, where the best test techniques and instrumentation are identified, as discussed in this section. At this stage, a prediction is formulated to determine whether a given experiment will meet the requirements. In other words, it shows which measurements to make and how good they must be. The second use is the posttest, where

an analysis documents the uncertainty performance of the test and aids in the interpretation of the results (Section 5.4.1).

The standard reference for measurement uncertainty in wind tunnel testing is AIAA Standard S–071A–1999 (Reference 26). A supplemental document is AIAA Guide G–045–2003 (Reference 27), which provides additional information and examples to assist the experimentalist in performing an uncertainty analysis. The latest developments in the field of uncertainty analysis are contained in References 28 and 29. Reference 28 presents the current practice of the international metrology community, whereas Reference 29 harmonizes this approach with the engineering tradition in the United States. Reference 30 also is recommended as a general reference.

Uncertainties in any measurement technique can be classified as either bias or random uncertainties. A bias uncertainty is consistent from measurement to measurement and degrades the accuracy of each individual measurement and the average of a series of measurements to an equal extent. Averaging a large number of samples will not reduce the bias error of an instrument or measurement technique. By contrast, random uncertainties fluctuate from measurement to measurement and degrade the precision of individual measurements. When a series of measurements is averaged, the random error of the average is reduced in proportion to the square root of the number of samples in the series.

If identified and measured, bias errors sometimes may be reduced through calibration, provided the error is the same in the calibration procedure and the experiment. The use of redundant measurement techniques for the same quantity may be useful in discovering bias errors in the measurements. In addition, as part of the process of bringing a facility within statistical process control, the sources of random errors may be identified and addressed. Both random and bias errors should be considered and estimated as part of both the pretest planning and posttest analysis. This process may be useful in determining the appropriate measurement technique for a given measurement, and it is essential in order to assign a level of confidence to the measurement.

An uncertainty analysis can have the greatest impact when applied during the planning phase of a facility calibration. If a particular test technique has not been selected, a general uncertainty analysis can identify the best of competing methods. The lack of a detailed uncertainty tool should not preclude the preparation of a pretest analysis. Simplified equations and assumed uncertainties can be used to reveal which measurement errors are the uncertainty drivers. Approximate analytical solutions are often employed, coupled with spreadsheets or some other general-purpose tool. Numerical "jitter" programs can also be rapidly adapted for a general analysis. Again, the goal here is general: only overall uncertainties are considered. If a detailed error propagation tool already exists, one can simply combine all uncertainties into bias or precision. Reference 25 covers further details of the appropriate application of uncertainty analysis in the planning, execution, and reporting stages of an experiment.

Once the test technique has been chosen, a more detailed uncertainty analysis should be conducted to document the expected performance of the experiment. The purpose here is to show whether the objectives of the calibration can be realized, and if not, where improvements must be made. Any effort to increase detail by discriminating between bias and precision will be utilized again in posttest reporting. The pretest predictions should be performed using whatever information is available; for example, current specifications from standards laboratory calibrations or past experience with the same or similar instrumentation.

### 5.1.3 Online data analysis requirements

The standard tasks for every wind tunnel test include data acquisition, reduction, creation and maintenance of the database, data analysis, and archiving. For a wind tunnel calibration, all these tasks must be planned in great detail because each is vitally important to the success of the calibration. However, in the planning of these tasks, the greatest attention must be given to development of a fast, thorough, and versatile data analysis process. The work of the facility cannot proceed until calibration results are digested, verified, and then assimilated into the standard data-reduction programs.

There are three primary data analysis tasks to be addressed as part of any calibration. The first task is to perform a data quality check to verify the health and accuracy of sensors and instrumentation. Many of the data quality checking tasks are done in a calibration laboratory before and after the test entry or during the test setup. However, well-designed data quality analysis programs operating during the test can be invaluable for timely discovery of sensor and instrument problems. These data quality monitoring activities include pressure line continuity and leak checks, wind-off checking of tunnel pressures (the wind-off condition is the only time that the precise relationship of all tunnel pressures is known), range checking of many test measurements, and comparison of redundant test measurements.

The second task is the comparison of current calibration measurements to historical calibration data. This task is essential for verifying new calibration results. Example comparisons include plots of Mach number or dynamic pressure differences between calibrations, plots comparing test section centerline Mach number and statistical analysis of repeatability across calibration tests and within calibration tests. These first two data analysis tasks must be completed before the calibration apparatus is removed from the test section.

The final step is the analysis of data to determine new calibration constants for data reduction. Analysis programs must be prepared ahead of the test to carry out the averaging, smoothing, curve fitting, and statistical characterization of the calibration test data. Unless there were specific errors or bad practices used in previous calibrations, the procedures used to prepare calibration constants from prior calibration data should be reused. If the present calibration is simply a periodic calibration (i.e., if there are no physical differences in the facility or facility instrumentation between the current and prior calibrations), the new calibration data should be combined in some rational way with the historical calibration data. One suggestion is to combine the current calibration with the two most recent calibrations, giving equal weight to each calibration.

There are several commercially available analysis packages that fulfill all or most of the attributes in the following list. In addition, some organizations have developed proprietary analysis packages that allow them to handle their testing display and analysis requirements using custom software. The following is a software checklist to be used at the beginning of planning for a calibration test. It may be used to aid the selection of new analysis software or as a checklist to point out capabilities to be developed within a proprietary analysis package.

- Speed of presentation is essential, particularly for the first two tasks given. To avoid wasting calibration run time, alert messages and plots providing notification of sensor or instrumentation discrepancies should be available within a few seconds or minutes of the recording of a test point. Furthermore, the new data reduction constants and the statistical repeatability results should be available as soon as possible following the completion of the calibration test (a day or two at most).

- Though it probably should not be a surprise to an experienced test engineer, the sheer volume of information and the rate at which it accumulates during a test can be daunting. The only way of effectively managing this data mass is to have versatile tools available that rapidly summarize the data and report exceptions or problems rather than simply reporting the contents of the database.

- A capability for writing scripts, macros, or programming procedures is necessary so that plotting and analysis tasks can be automated to support the speed of presentation. In addition, this capability provides consistency to the plotting and analysis functions so that report plots will have a similar appearance and data analysis tasks can be duplicated from test to test.

- Connectivity to both current and previous calibration databases allows the comparison and cross plotting of test parameters. These comparisons can be much easier to perform if subsets of data can be extracted based not only on run number or point number but also conditionally on other database quantities, such as test conditions.

- Adaptability for troubleshooting purposes provides the ability to extract any calibration parameter contained within the calibration database. In addition, it is important to be able to look at the extracted item or items in many different ways, such as plotting, cross plotting, curve fitting, averaging, or determining the standard deviation or a correlation coefficient. The ability to extract this information from a spreadsheet, graphical user interface, or command line type interface makes troubleshooting a manageable task.

## 5.2 Test preparation and execution

Following the development of the calibration test plan, the preparation of the calibration hardware and software and the test facility required to successfully execute the plan can commence. Before the actual tunnel entry begins, it is wise to brief the facility staff on the objectives and significance of the test, the detailed test plan, and the need to carefully handle the hardware. These briefings become more important when calibration tests are conducted more frequently because they help prevent complacency that could lead to accidental damage of hardware or incorrect instrumentation setup. Caution must always be observed in handling the calibration hardware. The aim is to avoid any lengthy troubleshooting events, failures of critical calibration equipment, and acquisition of erroneous data during the actual test. The test preparation should include check procedures to verify the completeness of the work and the continuity and health of all instrumentation as well as the repeatability of the installation. These checklists should include ordered and detailed hardware installation instructions as well as detailed instructions for instrumentation checks and alignment and other hardware checks. There should also be check points for the engineer to inspect critical items.

Test preparation generally begins with bench calibration and checkout of all recording devices. Instrumentation devices are calibrated over their expected operating ranges. The lead engineer then scrutinizes all calibration results and uncertainty analyses for acceptance or replacement of instrumentation under the guidelines established during the test-planning phase.

Pressure transducers, strain-gauge balances, thermocouples, and other instrumentation will go through end-to-end checkouts. Most of the preinstallation hookup of instrumentation will involve plumbing the pressure taps to their respective recording devices. At this time, pressure key layouts become critically important for coordinating the routing of pressure lines to the data system. This ensures that the analysis software is receiving the proper input. Often there are large numbers of pressure lines confined in a small, restrictive area. The risk of pinching pressure tubes, creating leaks, or making mistakes in the plumbing of a tube can be high. Pressure tubes should be labeled with an identification number. Labeling is helpful both in plumbing and in troubleshooting. Ultimately, performing a complete continuity and leak check of every pressure on the calibration hardware will uncover any problems. A complete record of a continuity and leak check should always be constructed and maintained. This will allow the lead engineer to review the results of the check and decide whether to accept the results or call for repair.

Test preparation also requires thorough inspection of the calibration hardware. For example, the biggest source of pressure measurement error is usually orifice error. Therefore, the orifices should be made very carefully and then inspected with a magnifying glass before every test. Photographs of the orifices should be taken before each test and compared with records from previous tests. Slight nicks, dents, or protrusions in the orifice itself can make errors 10 times larger than necessary.

During test preparation, the lead engineer should review and finalize the run schedule for the calibration test. The run schedule should specify each operating condition at which the tunnel will be calibrated. This may include Mach number, Reynolds number, dynamic pressure, calibration hardware and test section configuration, and tunnel control settings. Also, if a dew point, temperature, or other type of sensitivity study is planned, these variables should also be specified. The layout of the run schedule should be clear and legible and should allow for easy logging of all critical items. The run schedule should always have some built-in contingency time because there will often be unexpected calibration findings that change the scope of the test plan or unexpected problems that cause delays in the run schedule. It is also

important that the run schedule have adequate repeats of the baseline calibration series, so that calibration uncertainties can be analyzed.

The test plan and run schedule should be constructed to consider the resident instrumentation and control systems used in the tunnel. The most common measures of tunnel conditions are total pressure, static pressure, and total temperature. Other resident tunnel instrumentation records the difference between the total and static pressure, the dew point, the tunnel circuit pressure rise, wall static pressure distributions, and/or adiabatic wall temperatures. Often, these instrumentation devices do not directly measure the free-stream condition within the test section flow core (the region where models are tested).

Most large wind tunnels, particularly transonic facilities, will have other control systems in addition to the main tunnel drive. The various operational settings and instrumentation from all these systems could be

- Main drive setting and total pressure increase to the test section (pressure rise)
- Auxiliary equipment speed or pressure (for an active plenum evacuation system)
- Diffuser reentry duct setting (if the nozzle geometry is variable and the system is an active system ducted back to the diffuser)
- Diffuser flap setting (for a semiactive system)
- Wall suction mass flow (if it can be measured directly, but more commonly is indicated indirectly through the other operational settings)
- Test section wall angle
- Nozzle contraction ratio (for a variable nozzle geometry)

It is possible to arrive at the same conditions in the test section with more than one combination of the control system settings. However, one combination may provide the most favorable test section Mach number distribution or flow quality, but may require a larger amount of electric power. There is then a tradeoff between flow uniformity and power requirements that could become a factor in defining operational settings for a tunnel calibration.

The final task of test preparation is installation into the tunnel, which requires a coordinated and focused effort by all personnel involved. The scope of a tunnel calibration tends to be greater than a typical model test program. Depending on the extent of the tunnel calibration, personnel might be working at several locations in the tunnel, behind bulkheads, in the auxiliary compressor leg, and elsewhere. Awkward calibration hardware is often involved (e.g., a static pipe). A checklist is essential during the installation process, and a written log of the entire event must be maintained.

The installation should encompass at a minimum the following steps:

- Configure the test section (install appropriate test section cart, test section wall arrangements, etc.).
- Install calibration hardware (follow installation drawings precisely).
- Wire in all recording devices and continuity check to ensure that they are responding.
- Perform a leak check on the pressure reference systems and calibration lines.
- Perform range and accuracy tests on the pressure data collection system and transducers.
- Leak and continuity check all calibration hardware pressure connections. These checks are essential to ensure quality data. Verifying that all instrumentation is actually connected correctly will aid in troubleshooting during and after the test.
- Set up the data acquisition system (i.e., amplifiers, filters, etc.).

- Thoroughly check the data reduction via a hand check (to avoid spending time during the actual calibration chasing down data-reduction problems when data analysis is underway).
- The position and alignment of the calibration hardware must be accurately measured and recorded for each tunnel run. These items include the spatial location of each probe if an instrumented rake is used, angular offsets in the pitch and yaw planes of any flow-angle probe or any other probe in which alignment might impact the results, such as static pipe droop or sag. Alignment of the calibration instrumentation may be performed using a variety of devices, including optical levels, transit theodolites, laser alignment tools, inclinometers, plumb bobs, scales, and others.
- Check and record test section wall alignments (particularly if they can be varied), diffuser reentry door settings, diffuser flap settings, and other settings.
- Inspect the test section to ensure that wall plates and optical access inserts are flat, flush, and sealed to avoid leaks and/or shock sources.
- Inspect the tunnel circuit for forgotten tools or open personnel access doors.
- The overall test setup should be documented in detail, including photographic records of the test installation.

The actual tunnel calibration entails executing the test plan and run schedule as efficiently and as thoughtfully as possible. For the majority of calibration testing, the tunnel would be operated as it would for a normal test. The exception to this is if the calibration involves investigating new operational procedures and control settings. The lead engineer would need to ensure that all tunnel personnel have the necessary operating charts and settings to accomplish their tasks, consistent with the test plan. Instrumentation error tolerances are outlined to convey to the operating crew what is acceptable and what is not acceptable when examining wind-off zeros.

Some form of temperature soak procedure should be followed before beginning the run schedule. In a tunnel calibration (and probably in all testing) it is most important to temperature-soak all test section calibration and resident instrumentation, the test section and plenum chamber wall surfaces, and the tunnel shell as thoroughly as possible. Online monitoring of temperatures for stabilization is always useful for indicating adequate temperature soak time, after which, hardware alignments should be remeasured and adjusted if necessary.

During wind-on testing, the test engineer should be verifying all tunnel control settings such as the position of movable test section walls and the motor speed of the auxiliary pumping system. All tunnel control settings must be recorded completely throughout the calibration. We recommend that multiple, steady-state data points be acquired over some period of time based on known cyclical variations in tunnel behavior. The actual time period used could vary from 10 or 20 sec to several minutes, depending on the facility. These data can then be averaged and statistically analyzed, which is particularly useful in identifying bad data. Long period variations in test section conditions can also be quantified.

Data should be reviewed while the test is being conducted. This is necessary to ensure that quality data are being recorded, that the tunnel is operating as expected, and that valuable test time is not being wasted. Data should be reduced and analyzed online or immediately after the run is completed. It is imperative that the test hardware not be removed or reconfigured until all questions concerning the data have been resolved.

It is essential that periodic alignment checks of the calibration hardware be performed and the results recorded. Immediately following the run, the hardware must be inspected for loose probes, obstructed instrumentation ports, or general damage. In addition, posttest alignment checks should be made to ensure that the hardware did not shift during the test. Instrumentation wind-off zeros should be checked frequently, particularly early in the test. The time interval between checks may be increased as confidence in the integrity of all instrumentation grows. Key instrumentation should be monitored online to

aid with quick identification of those sensors that are failing or are out of calibration. This will also allow for timely decisions concerning the test plan and run schedule.

Finally, the importance of keeping detailed logs and recording everything, cannot be stressed enough. The calibration of a tunnel is, in essence, a laboratory experiment leading to empirical relationships that correlate resident tunnel instrumentation and control settings to the test section free-stream conditions. If calibration records are incomplete, there is the risk of overlooking relationships or dependent variables important to the tunnel operation.

## 5.3 Data analysis and data corrections

Each mounting system/model combination occupies a certain region (point, plane, or volume) in the test section. Upon consideration of the model location and translation within the test section, the region is defined and the average flow parameters are determined for this region.

The calibration data should be reduced and plotted as cross-flow vectors, vorticity, total and static pressure contours, temperature contours, and Mach number contours as appropriate. If applicable, the calibration data should be plotted as nondimensional ratios. The plots should be examined carefully (particularly the total and static pressure contour plots) to determine if excessive instrumentation drift, bad data, or other problems went undetected online. A decision is then made to take actions such as voiding data, applying correction factors, or repeating the test run.

In addition to the previously described alignment and instrument error corrections, rake interference corrections may be determined. The tower to which the probes are mounted may not correspond well to the stem of a standard pitot-static tube; therefore, the standard correction for static pressure error may not be valid. The error (and the necessary correction) may be calculated using source-sink-modeling techniques. This also provides the opportunity to compute the tunnel blockage effects. Once the source strengths are known, the mounting system interference may be calculated at the probe tap locations. The correction is applied to the probe-derived dynamic pressure rather than the static pressure.

In the case of a static pipe, three corrections to the static pressures should be considered for significance and applied if necessary. First, orifice corrections (also known as tap errors) should be evaluated. The multiple data samples acquired for each test condition can be statistically evaluated on an orifice-by-orifice basis to uncover high precision errors (standard deviations) on a particular port. Sometimes, this can be due to an orifice error and if desired, the data from that orifice can be voided. In addition, orifice corrections can be derived from static pipe data if the static pipe data were acquired at two longitudinal positions or if the static pipe runs were performed upright and inverted. In these methods, two separate orifices on the pipe will have measured the static pressure in a particular location in the tunnel. The difference in the two measurements could possibly be caused by orifice error provided all precautions were taken in realigning the pipe and the errors in repeatability of tunnel conditions are not large enough to overshadow the orifice error itself. Trends from the pipe data need to be scrutinized and then an appropriate correction derived.

A second correction can account for any sag or bend in the pipe and would come in the form of a flow-angularity correction. First, it would require thorough documentation on the pipe sag during the test. A correction to the static pressures due to the measured flow angularity at each tap location may then be applied.

Finally, the third correction involves the error in the static pipe pressure distributions due to the boundary layer growth on the pipe. A correction may be approximated by accounting for the offset of the local streamline due to the boundary layer growth, equivalent to the boundary layer displacement thickness. In most cases, the correction can be ignored since the displacement thickness over the length of the pipe is relatively small in comparison to the pipe diameter.

It is necessary to develop algorithms that relate the resident tunnel instrumentation readings to the test section conditions because the resident instrumentation is not directly reading the test section conditions.

The most significant relationship used in transonic wind tunnel operation is that between the indicated Mach number (calculated using the indicated static and stagnation pressure) and the test section Mach number (measured by the calibration equipment). The resulting correction can take the form of a series of lookup tables, incremental corrections, or curvefits as functions of the indicated Mach number, Reynolds number, tunnel operational settings, and test section configuration. Similar relationships could be developed to correct the other resident instrumentation (i.e., stagnation pressure or stagnation temperature).

The final data analysis usually involves formulating corrections to be applied to model data. These corrections are meant to account for nonuniformities in the test section and to remove their effects from the model data. The most common corrections are buoyancy and flow angularity. A buoyancy correction accounts for the effects of Mach number gradients, which will induce a buoyancy-type force increment on the model. A flow-angularity correction accounts for flow curvature and misalignment of the incoming velocity vector that translates into a correction to model angle-of-attack and pitching moment.

## 5.4 Post-test activities

After all test and data analysis tasks have been completed, the last set of activities is to formally document the calibration test and to disseminate the information to all interested parties. It is suggested that formal written reports be generated to describe each calibration test conducted in a wind tunnel and that detailed documentation be maintained for the overall calibration program. It is also equally important to quickly make the facility staff and customers aware of the results of the calibration tests. These items are described more fully in the following section.

### 5.4.1 Reporting of results

It is recommended that two reports be prepared following a calibration. First, a short summary should be written within a few days of completion of the calibration. This report must include a test summary, the principal differences between the present calibration and past calibrations, a few summary plots, tables of new calibration constants, and a few installation photographs. The purpose of the summary report is to transmit necessary information to outside customers, managers, test engineering staff, and computer programmers so that testing operations can proceed in the facility.

The second report is a fully detailed calibration report having publication-quality plots, charts, and figures. The analysis software should be capable of generating all the plots, charts, and statistical analyses that are needed to generate these reports. This second, more formal report should describe, in detail, the calibration goals and objectives, hardware and methodology, data analysis procedures, and test results. There may be limitations on the type of distribution the report will have, based on the proprietary restrictions of a particular organization. However, even if the calibration information is intended solely for use within an organization, a written calibration report is still highly recommended to ensure that the correct data and pertinent facts are documented and communicated. In general, a formal general-distribution report should be written for each calibration test to guarantee that important aspects of the calibration are kept in a controlled document. This will ensure that the most important information is always accessible, even if engineering project files are lost or destroyed over time.

The guidance of References 26 and 27 should be followed for the reporting of experimental uncertainties. In general, the bias, precision, total uncertainty, and the method of combination should be reported for each experimental result. This is extremely important for the interpretation of the calibration results, particularly in regards to flow field uniformity. This point merits further discussion. Any variations larger than the measurement uncertainties must be attributed to either a neglected error source or to flow field nonuniformity. In the former case, the uncertainty analysis and data reduction processes need to be revisited to determine the source of error. The latter case has implications for production testing to be performed in the facility. Wind tunnel data reduction programs use the facility instrumentation combined with the facility calibration to compute one thermodynamic state for free-stream flow properties. This state is then used to normalize other test measurements into nondimensional coefficients. This process carries the implicit assumption that the free-stream properties are constant over the volume occupied by the test

article. The measured variations are conceptually a bias error in the free-stream properties that must be considered in addition to biases from the instrumentation.

The calibration report must consider the needs of future production tests in the facility. Future tests will use the calibration to obtain the free-stream reference thermodynamic state. The total uncertainties of the calibration experiment will become fossilized as bias on the reference state for production tests. In addition, any measured deviation from a uniform flow field introduces an additional (conceptual) bias for production tests. How this conceptual bias should be handled depends on the variations themselves and the needs of individual tests. For example, if the variation is predominantly in a gradient, standard buoyancy corrections may be all that is required. If, on the other hand, the variations were random, then an additional bias equal to the confidence interval of the free-stream properties computed over the model volume would be appropriate. This means that quantitative survey results, not just plots, must be included in the report.

These formal calibration reports, whether used internally or given unrestricted distribution, serve a very important role. They allow any customer of a facility to know exactly how the tunnel was calibrated, what type of uncertainties are inherent to the data, how the calibration may be used to enhance research test results, and what limitations there are in the use of the data.

### 5.4.2 Follow-up activities

In addition to formally documenting the calibration test and results in written reports, it is important that the calibration team directly relate the test results to both the facility staff and all research customers. The most important point to convey is what impact any changes in the calibration may have on recently completed test programs or how changes may affect facility operation. Even if there are no significant changes to the tunnel calibration, the facility staff and customers should still be notified, so that the reliability of the current tunnel calibration can be documented.

# 6 Examples of calibration procedures

Five case studies have been included in this guide to better illustrate the details involved in a complete calibration of a subsonic or transonic wind tunnel:

Annex C Calibration of NASA Glenn Research Center's 9- by 15-Foot Low-Speed Wind Tunnel

Annex D Lockheed Martin Low Speed Wind Tunnel

Annex E Calibration of the 11- by 11-Foot Transonic Wind Tunnel at the NASA Ames Research Center

Annex F Maintenance calibration of the Veridian 8-Foot Transonic Wind Tunnel

Annex G Mach number calibration of the Arnold Engineering Development Center PWT 16-ft Transonic Tunnel (16T) with the High-Angle Automated Sting (HAAS) test section

The focus of these examples is the methodology and hardware used in the tunnel calibrations, not the resulting calibration and flow quality data. Also, the examples provide insight as to why these tunnels are calibrated as they are (that is, what customer requirements were made that defined the calibration).

Although each of these organizations use different nomenclature, every effort has been made to be consistent throughout these examples (i.e., $P_T$ means total pressure throughout the document and in all of the annexes). This was done for clarity for the users. The nomenclature used by each organi-zation does vary slightly from that used in this document (for example, $P_o$, $P_0$, $P_t$, $P_T$, and $H$ were all used to designate total pressure), but a common set of nomenclature was developed for use in this recommended practice (see Annex A).

In addition to the five case studies included in the guide, a bibliography of reports on subsonic and transonic wind tunnel calibration tests is included in Annex H.

# Annex A—Nomenclature

Note that the nomenclature and symbols used in the calibration examples have been made consistent throughout this document (i.e., $P_T$ means total pressure throughout the document and in all the annexes). This was done for clarity for the users. The nomenclature used by each organization does vary slightly from that used in this document (for example, $P_o$, $P_0$, $P_t$, $P_T$, and $H$ were all used to designate total pressure), but a common set of nomenclature was developed for use in this recommended practice.

| | |
|---|---|
| $A_x$ | model cross-sectional area in the *y-z* plane, as a function of *TS* |
| $A_0$, $A_1$ | flow-angle probe calibration coefficients (linear model) |
| *a* | speed of sound |
| *b* | flow-angle probe calibration relation intercept |
| $C_D$ | drag coefficient |
| $C_{D,u}$ | uncorrected drag coefficient (Annex F) |
| $C_{Lsa}$ | lift coefficient relative to the stability axis |
| $C_{PS,\mathrm{cor}}$ | static pressure correction coefficient |
| $C_{PT,\mathrm{cor}}$ | total pressure correction coefficient |
| $C_0$ to $C_9$ | flow-angle probe calibration coefficients |
| *Cp* | pressure coefficient |
| $Cp_\alpha$ | pressure coefficient used in the flow-angle probe calibration (pitch) |
| $Cp_\beta$ | pressure coefficient used in the flow-angle probe calibration (yaw) |
| *c* | parameter used in the boundary layer thickness calculation |
| *dCp/dx* | pressure coefficient axial gradient |
| $d\overline{M}_{TS}/dx$ | Mach number gradient (Annex F) |
| *h* | value of *Z* at which the velocity ratio *u*/*U* becomes 1.0 |
| $K_{A1}$, $K_{A2}$, $K_{A3}$ | coefficients used in the pitch flow-angle correction equation (Annex D) |
| $K_{A5}$, $K_{A6}$, $K_{A7}$ | coefficients used in the yaw flow-angle correction equation (Annex D) |
| $K_{PT1}$, $K_{PT2}$, $K_{PT3}$ | coefficients used in the total pressure calibration (Annex D) |
| $K_{q1}$, $K_{q2}$, $K_{q3}$ | coefficients used in the dynamic pressure calibration (Annex D) |
| $K_{T,\mathrm{rec}}$ | probe total temperature recovery factor |
| $K_{\alpha 1}$ | five-hole cone probe pitch sensitivity determined from calibration |
| $K_{\alpha 2}$ | five-hole cone probe pitch offset determined from calibration |
| $K_{\beta 1}$ | five-hole cone probe yaw sensitivity determined from calibration |
| $K_{\beta 2}$ | five-hole cone probe yaw offset determined from calibration |
| $K_\phi$ | five-hole cone probe rotation factor |

| | |
|---|---|
| $L/D$ | ratio of honeycomb flow straightener cell length to cell diameter (Annex C) |
| $M$ | Mach number |
| $\bar{M}$ | average Mach number |
| $M_a$ | free-stream Mach number, calculated as the average of local Mach numbers over the test region |
| $M_{btm}$ | Mach number calculated from measurements along the bottom of the static pipe (Annex F) |
| $M_{cfs}$ | corrected free-stream Mach number (Annex F); |
| $M_i$ | local Mach number at an individual pressure orifice |
| $M_{\text{ind}}$ | Mach number for indicative airstream velocity in test section; indicated Mach number (Annex F) |
| $M_{\text{inf}}$ | free-stream Mach number determined from a surface fit (Akima spline) of the calibration data set (Annex G) |
| $M_{pc}$ | Mach number computed from $P_{S,pc}$ and $P_{T,sc}$ |
| $M_{\text{top}}$ | Mach number calculated for measurements along the top of the static pipe (Annex F) |
| $m$ | flow-angle probe calibration relationship slope |
| $n$ | number of data samples acquired per data point |
| $P$ | pressure |
| $P_{atm}$ | atmospheric pressure |
| $P_{\text{avg}}$ | average of flow-angle rpbe pressure $P_1$ through $P_4$ |
| $P_S$ | static pressure |
| $P_{S,btm}$ | pressure measured by ports along the bottom of the static pipe (Annex F) |
| $P_{S,pc}$ | static pressure measured in the test section plenum chamber |
| $P_{S,\text{cor}}$ | corrected test section static pressure at the model reference location |
| $P_{S,\text{ind}}$ | indicated static pressure based on the plenum pressure (Annex F) |
| $P_{S,\text{pipe}}$ | static pressure measured on the static pipe |
| $P_{S,\text{probe}}$ | static pressure measured by the flow-angle probe (Annex E) |
| $P_{S,\text{top}}$ | pressure measured by static ports along the top of the static pipe (Annex F) |
| $P_T$ | total pressure; tunnel stagnation pressure |
| $P_{T,\text{cor}}$ | corrected test section total pressure at the model reference location |
| $P_{T,\text{probe}}$ | total pressure measured by the flow-angle probe (Annex E) |
| $P_{T,sc}$ | total pressure measured in the settling chamber |
| $P_1$, $P_2$, $P_3$, $P_4$ | flow-angle probe pressures; $P_1$ and $P_3$—pitch-sensing taps on the five-hole cone probe, $P_2$ and $P_4$—yaw-sensing taps on the five-hole cone probe, Annexes B, C and E |

| | |
|---|---|
| $P_5$ | total pressure measured by the flow-angle probe (Annex C) |
| $P_6$, $P_7$, $P_8$, $P_9$ | static pressure measurements from the flow-angle probe (Annex C) |
| $PR_1$, $PR_2$ | reference pressures |
| $PR_{net}$ | net pressure rise in the tunnel (Annex F) |
| $q$ | dynamic pressure |
| $q_c$ | dynamic pressure computed from $P_{S,pc}$ and $M_c$ |
| $q_{probe}$ | dynamic pressure computed from $P_{S,probe}$ and $M_{probe}$ |
| $R$ | gas constant |
| Re | Reynolds number |
| $S_w$ | model reference area |
| $T_{DP}$ | dew point temperature |
| $T_R$ | temperature recovery factor |
| $T_{ref}$ | reference temperature |
| $T_S$ | static temperature |
| $T_T$ | total temperature |
| $T_{T,F}$ | tunnel total temperature measured upstream of contraction, °F (Annex E) |
| $T_{T,probe}$ | probe total temperature measured during the flow uniformity survey (Annex E) |
| $T_{T,Pcor}$ | corrected probe total temperature; corrected probe total temperature measured during the flow uniformity survey |
| $TI$ | turbulence intensity |
| $TS$ | tunnel station |
| $U$ | average airspeed; magnitude of velocity vector |
| $u$, $v$, $w$ | airspeed components in the axial, transverse, and vertical directions; mean velocity components in the axial, transverse, and vertical directions |
| $\bar{u}$, $\bar{v}$, $\bar{w}$ | mean velocity components in the axial, transverse, and vertical directions |
| $W_i$ | weighting factor based on tunnel station (Annex F) |
| $X$ | typical, or example, parameter |
| $\bar{X}$ | mean of parameter $X$ |
| $x$, $y$, $z$ | axial (streamwise), spanwise, and vertical coordinates, zero at the centerline of the flow passage, $z$ is positive for top, $y$ is positive for south. $x$ = 0 is defined at the start of the test section and is positive downstream |
| $Z$ | distance from test section surface |
| $Z_1$ | value of $Z$ associated with the boundary layer probe located nearest the tunnel surface |
| $\alpha$ | pitch flow angle; angle of attack |

| | |
|---|---|
| $\alpha_{CL0}$ | angle of attack at a lift coefficient of zero |
| $\alpha_f$ | flow angle of probe calibration flow stream in the pitch plane |
| $\alpha_h$ | angle of probe holder with respect to the centerline in the pitch direction |
| $\alpha_m$ | pitch flow angularity in the probe coordinate system (measured, uncorrected pitch flow angle, Annexes B and E) |
| $\alpha_o$ | offset angle of probe relative to probe holder in the pitch direction (Annex B) |
| $\alpha_{offset}$ | offset angle of probe in holder in the pitch direction (Annex B) |
| $\alpha_p$ | flow-angle probe bias angle in the pitch plane |
| $\alpha_t$ | true pitch flow angle (Annex B) |
| $\beta$ | yaw flow angle |
| $\beta_f$ | flow angle of probe calibration flow stream in the yaw plane |
| $\beta_h$ | angle of probe holder with regard to test section centerline in yaw direction |
| $\beta_m$ | yaw flow angularity in the probe coordinate system (measured, uncorrected yaw flow angle, Annex E) |
| $\beta_o$ | offset angle of probe relative to probe holder in the yaw direction (Annex B) |
| $\beta_{offset}$ | offset angle of probe in holder in the yaw direction (Annex B) |
| $\beta_p$ | flow-angle probe bias angle in the yaw plane |
| $\beta_t$ | true yaw flow angle (Annex B) |
| $\gamma$ | ratio of specific heats |
| $\Delta CD_{Buoy}$ | longitudinal buoyancy correction |
| $\Delta M$ | Mach number calibration parameter (Annex F), the difference between the free-stream Mach number calculated as the average of local Mach numbers in the test region ($M_a$) and the equivalent plenum chamber Mach number ($M_{pc}$) (Annex G) |
| $\Delta P$ | differential pressure; difference between total and static pressure |
| $\Delta P_\alpha$ | flow angle probe pressure differential for the pitch angle |
| $\Delta P_\beta$ | flow angle probe pressure differential for the yaw angle |
| $\Delta P_{ESP}$ | differential pressure measured between an electronically scanned pressure port and a fixed verification pressure used to monitor transducer zero shifts, psfd (Annex G) |
| $\Delta R$ | tunnel calibration parameter (Annex F) |
| $\Delta T$ | total temperature variation (Annex E) |
| $\Delta T_{DPS}$ | Delta temperature dew point system, temperature difference between the test section dew point temperature and the test section free-stream static temperature (Annex G) |
| $\Delta\alpha$ | angle of attack correction (annex D) |
| $\Delta\beta$ | angle of sideslip or yaw correction (annex D) |

| | |
|---|---|
| $\delta$ | boundary layer thickness |
| $\delta_1$ | boundary layer displacement thickness |
| $\delta_2$ | boundary layer momentum thickness |
| $\theta$ | test section wall angle, deg (positive when diverged) |
| $\rho$ | air density |
| $\sigma$ | standard deviation |
| $\phi$ | roll angle |
| $\psi$ | integrated upflow angle |

**Subscripts:**

| | |
|---|---|
| aft | measured by the aft rake |
| atm | atmospheric conditions; ambient atmosphere outside of tunnel |
| avg | average |
| *bm* | measured upstream of the TS in the contraction or bellmouth area |
| cal | parameter measured by the calibration instrumentation |
| *e* | condition at the edge of the boundary layer |
| *f* | calibration flow field |
| fac | parameter measured by the facility instrumentation |
| fit | parameter derived from a curve fit |
| *h* | at the probe holder |
| ind | indicated (Annex F) |
| inv | measurement or parameter with test article or flow angle probe in an inverted orientation (Annex B) |
| *j* | static port index along a static pipe (Annex F) |
| *L* | local condition within the boundary layer |
| *m* | measured parameter |
| *p* | piezometer |
| *pc* | parameter measured in the plenum chamber or based on the plenum chamber parameter |
| *sc* | parameter measured in settling chamber |
| *TS* | tunnel station |
| *ts* | test section or related to a parameter measured in the test section |
| *u, v, w* | related to the airspeed components in the axial, transverse, and vertical directions |

| | |
|---|---|
| *uc* | uncorrected for blockage or compressibility |
| upr | measurement or parameter with test article or flow angle probe in an upright orientation (Annex B) |
| var | variation (Annex E) |
| $\alpha$ | related to the pitch flow angle |
| $\beta$ | related to the yaw flow angle |

**Acronyms:**

| | |
|---|---|
| A/D | analog to digital |
| AEDC | Arnold Engineering Development Center |
| AIAA | American Institute of Aeronautics and Astronautics |
| BCD | binary-coded decimal |
| CTS | captive trajectory simulation (Annex F) |
| DRM | double-roll mechanism |
| DTC | digital temperature compensation |
| ESP | electronically scanned pressure |
| FSP | functional subsystem processor |
| GTTC | AIAA Ground Testing Technical Committee |
| HAAS | High-Angle Automated Sting |
| HF | hot-film probes |
| LDV | laser Doppler velocimetry |
| LSTS | Lockheed Martin low-speed test section |
| MAC | mean aerodynamic chord |
| MD | main drive (Annex F) |
| MUA | make-up air compressor system |
| NIST | National Institute of Standards and Technology |
| NWTC | National Wind Tunnel Complex |
| PCU | pressure calibrate unit |
| PES | plenum evacuation system (Annex F) |
| PIR | Preliminary Information Report |
| PIV | particle imaging velocimetry |
| PSI | Pressure Systems, Inc. |
| PSP | pressure-sensitive paint |

| | |
|---|---|
| PWT | Pressure Wind Tunnel |
| RTD | resistance temperature detector |
| SDS | standard data system |
| SMP | subsystem management processor |
| SMSS | sting model support system |
| SPC | statistical process control |
| STOVL | short takeoff and vertical landing |
| TMSS | turntable model support system |
| TRS | turbulence reduction system consisting of honeycomb and two screens |
| TS | tunnel station |
| TSP | temperature-sensitive paint |
| TWT | transonic wind tunnel |
| UPWT | Unitary Plan Wind Tunnel |
| V/STOL | vertical/short takeoff and landing |
| VTWT | Veridian Transonic Wind Tunnel |
| 16T | 16-ft Transonic Wind Tunnel at AEDC |
| 8×6 SWT | 8- by 6-Foot Supersonic Wind Tunnel at NASA Glenn |
| 9×15 LSWT | 9- by 15-Foot Low-Speed Wind Tunnel at NASA Glenn |

# Annex B—Additional information on pressure probes used for flow-angle measurement

Regardless of the type of probe used, it is necessary to relate the flow-angle measurements to a wind tunnel datum, typically the test section longitudinal axis. For example, the pitch flow-angle measurement can be broken down as follows:

$$\alpha_t = \alpha_m - \alpha_{\text{offset}}$$

where

$\alpha_t$ true pitch flow angle

$\alpha_m$ pitch flow angle measured by probe

$\alpha_{\text{offset}}$ angle of probe with respect to test-section longitudinal axis

Similar definitions are used for the yaw angle $\beta$.

The probe has a preferred mounting orientation so that the pitch flow angle $\alpha$ and the yaw flow angle $\beta$ components can be separated. In the simplest case, ports that are used to measure pitch angle are insensitive to probe yaw and vice versa. In Figure 10, ports $P_1$ and $P_3$ are used for pitch flow angle and ports $P_2$ and $P_4$ for yaw flow angle. Flow angle is related to the difference in pressure measured at the probe head: $P_3 - P_1$ for pitch is used for the example probe. This pressure difference is then normalized by another probe pressure or pressure difference, and the resulting pressure coefficient is used in the equation to relate the measured pressures to the flow angle through a calibration curve. For example, the pressure coefficient for pitch and yaw flow angles can be defined as

$$Cp_\alpha = \frac{P_3 - P_1}{q} \quad \text{and} \quad Cp_\beta = \frac{P_4 - P_2}{q}$$

Other definitions for the pressure coefficients can be used and are discussed in Reference 17.

Each flow-angle probe must be calibrated over the Mach number range of the facility because the characteristics of the probes are a function of the Mach number. The probe should be calibrated in the probe holder, since the probe holder may have an effect on the probe sensitivity. At each calibration point, the probe angle $\alpha$ is varied and the resulting $Cp_\alpha$ is measured (this is done similarly for $\beta$ and $Cp_\beta$). The location of the probe tip in the calibration facility flow field should not change while the probe angle is adjusted. This assures that any angle in the calibration flow field is constant for all points. At a given Mach number, the pressure coefficient for pitch or yaw angle will vary linearly with the flow angle over a given range of angles ($\pm 10°$ to $\pm 15°$, depending on the probe), so the relationships between the pressure coefficient and flow angle from the calibration are

$$Cp_\alpha = b_\alpha + m_\alpha \cdot \alpha \quad \text{and} \quad Cp_\beta = b_\beta + m_\beta \cdot \beta$$

where the coefficients $b$ and $m$ are determined during the probe calibration. Other mathematical models can be used, but those are more cumbersome and require more extensive calibrations (see Reference 18). The linear model used in this example is simple and works well for the wind tunnel application.

To properly quantify probe bias angle and calibration flow field angle, one must acquire calibration data for both probe upright and inverted orientations with respect to the probe mounting in the tunnel. So, for a probe that senses both pitch and yaw flow angles, the probe is calibrated at four roll angles: $\phi = 0°$ and $180°$ for the pitch angle and $90°$ and $270°$ for the yaw angle. Figure B.1 shows a typical calibration data

set for upright and inverted probe orientations for the pitch angle calibration and also provides definitions of the parameters used in this example.

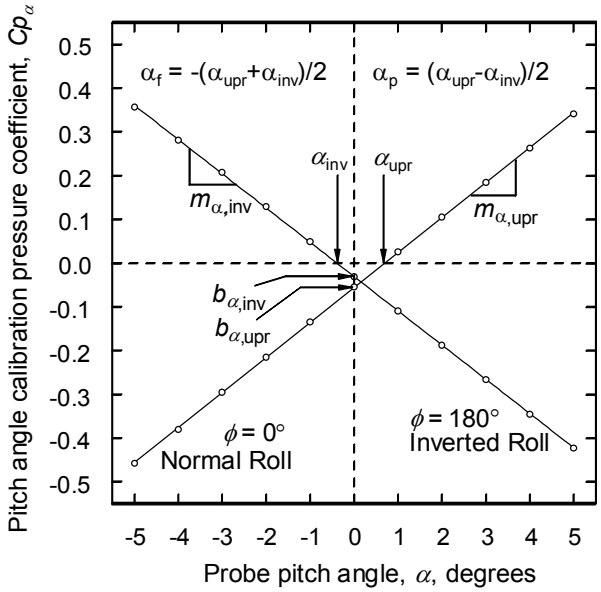



Figure B.1 – Typical $Cp_\alpha$ versus $\alpha$ data for normal (upright) and inverted roll orientations. Key nomenclature for the discrete linear model is defined.

From these calibration data and relationships, the equations for determining flow angles are derived:

$$\alpha_m = A_{0,\alpha} + A_{1,\alpha} Cp_\alpha \quad \text{and} \quad \beta_m = A_{0,\beta} + A_{1,\beta} Cp_\beta$$

where the slope term is

$$A_{1,\alpha} = \frac{2}{m_{\alpha,upr} - m_{\alpha,inv}} \quad \text{and} \quad A_{1,\beta} = \frac{2}{m_{\beta,upr} - m_{\beta,inv}}$$

The intercept term, $A_0$, is related to the probe angle axis (pitch or yaw) intercepts for the upright and inverted probe calibration curves—$\alpha_{upr}$ and $\alpha_{inv}$ or $\beta_{upr}$ and $\beta_{inv}$. For the pitch angle, the probe bias angle $\alpha_p$ and the calibration flow field angle $\alpha_f$ are calculated using

$$\alpha_p = \frac{\alpha_{upr} - \alpha_{inv}}{2} \quad \text{and} \quad \alpha_f = \frac{\alpha_{upr} + \alpha_{inv}}{2}$$

Similar equations are used for $\beta_p$ and $\beta_f$. The intercept term is then

$$A_{0,\alpha} = \alpha_p \quad \text{and} \quad A_{0,\beta} = \beta_p$$

This determination of the probe offset angles, $\alpha_{offset}$ and $\beta_{offset}$, is a difficult and time-consuming part of a wind tunnel flow-angle survey. In most cases, the probe offset angle measurement also has the most influence on the accuracy of the final results because a rudimentary determination of the offset angle can spoil the measurements made by a sophisticated probe.

In the interest of eventually determining the probe angles, the flow-angle probe is normally mounted in a probe holder. It is assumed that a method exists for measuring the angle of the probe holder with respect

to the test section centerline; however, there may still be an offset angle between the probe holder and the probe: that is,

$$\alpha_{\text{offset}} = \alpha_h + \alpha_o \quad \text{and} \quad \beta_{\text{offset}} = \beta_h + \beta_o$$

where

$\alpha_h$, $\beta_h$ angle of probe holder with respect to the tunnel centerline (in the pitch and yaw directions, respectively)

$\alpha_o$, $\beta_o$ offset angle of probe in the holder (in pitch and yaw directions, respectively)

The pitch angle of the probe holder $\alpha_h$ is usually measured using an inclinometer. The yaw angle $\beta_h$ is more difficult to measure. Some documented methods of measuring probe-holder yaw angle include using a theodolite aligned with the test-section longitudinal axis or attaching a laser to a probe holder that projects a beam onto a flow-conditioning screen in the settling chamber. Alternatively, a laser tracker has been used to measure three-dimensional coordinates of points on the probe holder and thereby determine the probe-holder pitch and yaw angles simultaneously. Wind speed is zero for all these methods of measuring yaw angles. Therefore, the probe holder must be sufficiently stiff so that the deflection under wind loads can be assumed to be negligible.

The offset angle accounts for the fact that, even if the flow is perfectly aligned with the probe holder, the flow-angle probe may still give a nonzero reading. The final equations for determining pitch and yaw flow angle are, respectively,

$$\alpha_t = A_{0,\alpha} + A_{1,\alpha}\text{Cp}_\alpha - \alpha_h - \alpha_o \quad \text{and} \quad \beta_t = A_{0,\beta} + A_{1,\beta}\text{Cp}_\beta - \beta_h - \beta_o$$

Even if the flow-angle probe is calibrated in its test mounting rig, the flow-angle measurements can still be influenced by flow interference effects if the flow interference varies over the test region. The best measurement setup to minimize aerodynamic interference effects uses a single probe with a two-dimensional support that spans the test section. Measurements made close to walls may still be influenced by interference effects. Since the empty test-section flow should be essentially free of separated or shear regions, these interference effects can be estimated and corrected using simple inviscid models, if necessary.

# Annex C—Calibration of NASA Glenn Research Center's 9- by 15-Foot Low-Speed Wind Tunnel

## C.1 Description of facility

NASA Glenn's 8- by 6-Foot Supersonic (8×6 SWT)/9- by 15-Foot Low-Speed Wind Tunnel (9×15 LSWT) complex is an atmospheric-pressure, continuous-flow propulsion wind tunnel; the facility layout is shown in Figure C.1. An elevation view of the 9×15 leg is shown in Figure C.2. The 8- by 6-ft test section is a porous wall type transonic test section with a Mach number range of 0.0 to 0.10 and 0.25 to 2.0. The 9- by 15-ft test section is located in the return leg of the 8- by 6-ft wind tunnel loop. This test section is of slotted wall construction, resulting in an 11-percent open area, and has a Mach number range of 0.0 to 0.2. Typical operating conditions for the facility are listed in Table C.1. Mach number (airspeed) is the controlled parameter; the pressure and temperature levels are dependent on the outside atmospheric conditions.

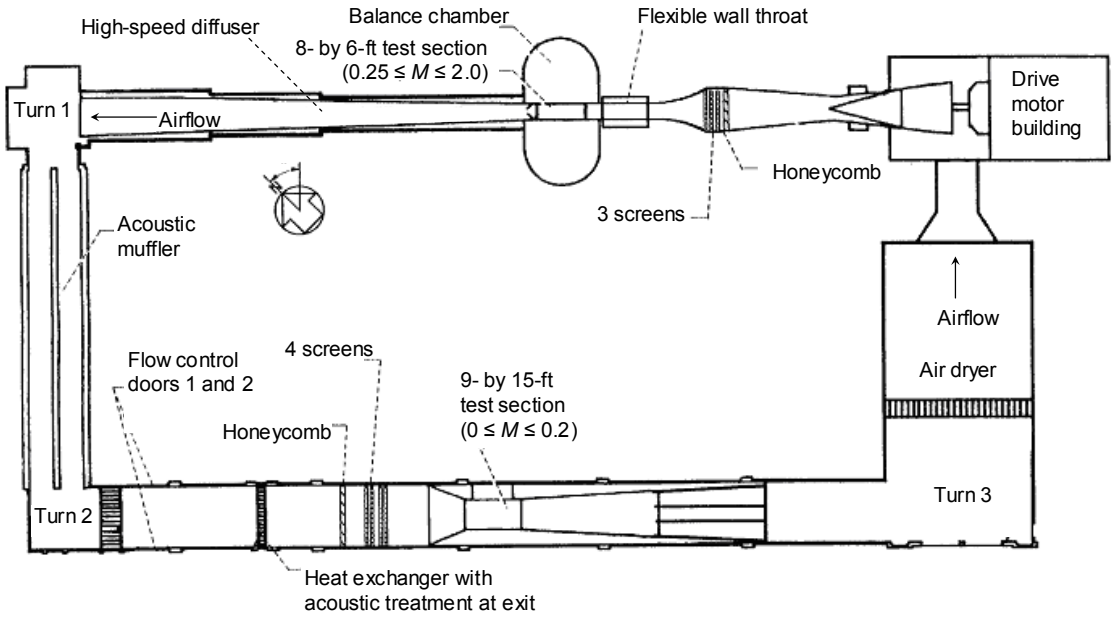



Figure C.1 – Plan view of the NASA Glenn 8-by 6-Foot Supersonic and 9- by 15-Foot Low Speed Wind Tunnel complex.

For standard operation, the airflow is driven through the facility by a seven-stage axial compressor (18-ft inlet diameter) that is powered by three 29 000-hp electric motors. Originally, the Mach number in the 9- by 15-ft test section was controlled by bleeding air via flow control doors 1 and 2 (Figures C.1 and C.2). Upgrades to the controls of the drive system now allow it to be operated using only one of the three electric motors, therefore allowing the compressor to operate at lower rotational speeds. Mach number is now set by adjusting the compressor speed and number of drive motors used (one drive motor is used to Mach 0.14; three motors are used above Mach 0.14). Very low-speed conditions are set by drawing air through the test section using the airblowers located in the facility air dryer. The 9- by 15-ft test section is 28.6 ft long. The walls of the test section diverge 0.25°; the floor and ceiling do not diverge. The walls, floor, and ceiling are equipped with removable acoustic panels. The acoustic treatment begins 4-in. downstream of the test section inlet (test section station 4) and extends for 27.5 ft. The acoustic panels reduce the inside height and width of the test section by about 4.0 in.

Tunnel flow quality improvements were made to the facility in 1992. The improvements that affected the 9- by 15-ft test section were the installation of flow conditioning devices in the settling chamber upstream of the test section, installation of acoustic treatment on the downstream face of the facility heat exchanger

(cooler), and the addition of diffuser fairings downstream of the test section. The flow conditioning devices installed in the settling chamber include a honeycomb flow straightener (ratio of cell length to cell diameter, *L*/*D* = 16) and four 10-mesh turbulence-reduction screens.

Reference 31 contains a more detailed description of the 9- by 15-ft wind tunnel facility. Information on the tunnel design and initial calibration is contained in Reference 32. Calibration and flow quality data for the facility prior to the flow quality improvements are documented in References 33 and 34. Reference 35 documents the calibration testing following the flow quality improvements, and Reference 36 summarizes the effectiveness of the flow quality improvements.

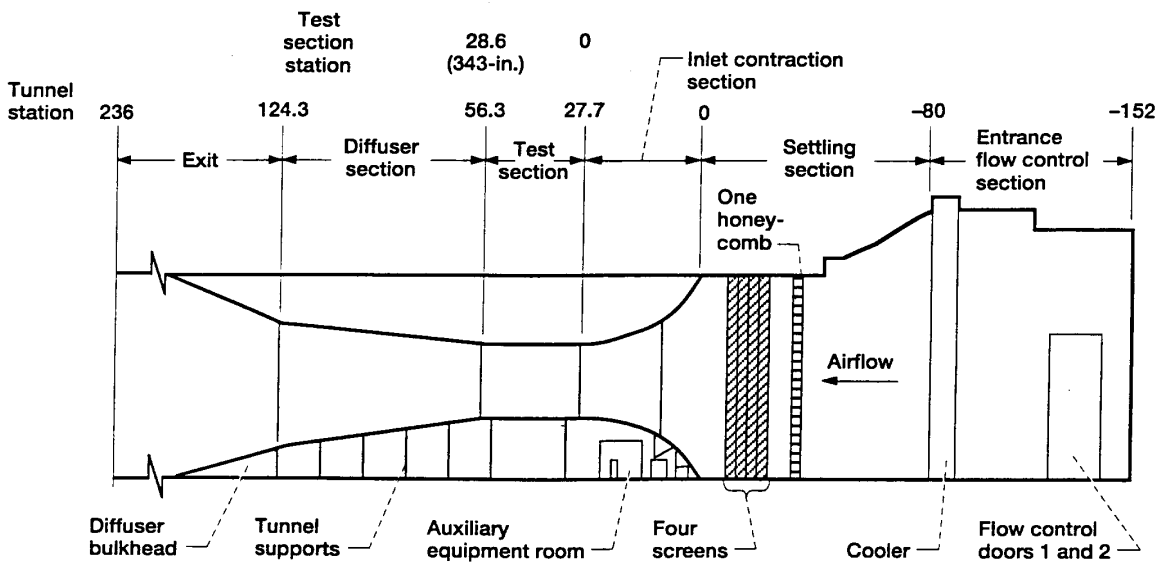



Figure C.2 – Elevation view of the 9x15 LSWT leg of the 8x6 SWT/9x15 LSWT complex. (All station numbers are in feet).

Table C.1 — Test section conditions in Glenn's 9- by 15-Foot Low-Speed Wind Tunnel

| Total pressure,[a] psia | Static pressure, [a] psia | Mach number | Total temperature, °R | Mach number uncertainty | Flow-angle uncertainty, deg |
|---|---|---|---|---|---|
| 14.681 | 14.152 | 0.229 | 543.3 | 0.0006 | 0.036 |
| 14.657 | 14.168 | .221 | 542.9 | .0006 | .039 |
| 14.627 | 14.227 | .199 | 543.3 | .0007 | .048 |
| 14.598 | 14.275 | .179 | 543.1 | .0008 | .059 |
| 14.575 | 14.315 | .161 | 542.0 | .0009 | .074 |
| 14.563 | 14.336 | .150 | 541.0 | .0009 | .087 |
| 14.554 | 14.354 | .141 | 540.0 | .0010 | .097 |
| 14.535 | 14.391 | .119 | 537.1 | .0012 | .137 |
| 14.519 | 14.414 | .102 | 535.6 | .0014 | .192 |
| 14.503 | 14.438 | .081 | 534.0 | .0017 | .314 |
| 14.493 | 14.456 | .061 | 534.3 | .0023 | .544 |
| 14.487 | 14.463 | .049 | 534.3 | .0028 | .812 |
| 14.483 | 14.483 | 0.0 | 528.4 | ------- | ------- |

[a]Uncertainty in pressure measurements, 0.0087 psia.

## C.2 Calibration hardware

Figure C.3 shows the elevation of the 9- by 15-ft test section and the measurement locations used during a full test section calibration (calibration and flow quality surveys). All the measurement hardware depicted in Figure C.3 is described in subsequent sections.

There are several reasons why particular calibration rakes, instrumentation, and procedures were selected for use in the 9×15 LSWT:

- **Historical**.—Hardware was selected as described in part to match older calibration and flow quality test equipment used in the facility. This was done to allow for more direct comparison between old and new data. Improvements were made to the newer hardware, in part from lessons learned from earlier tests, so there is a possibility that some differences in the data between old and new tests could be due, in part, to hardware changes. In the case of the 9×15 LSWT, the 15-ft survey rake described in this annex was based on an earlier 15-ft rake in terms of the number and distribution of the pressure probes. The newer rake has a lighter yet more rigid construction and improved instrumentation as well as increased measurement capabilities (flow-angle and temperature measurements were added).

- **Operational**.—Full calibrations are conducted every 5 to 8 years or following any significant modification to the facility flow path. Check calibrations are conducted at least annually. The calibration and flow quality hardware are hardy enough to survive multiple test entries over a period of years and still provide accurate data. The hardware also is easy to install and move during a flow quality survey test or check calibration.

- **Calibration goals**.—The majority of testing in NASA Glenn Research Center's wind tunnels is of an aeropropulsion nature, and often times involves inlet testing, hot gas ingestion, short takeoff vertical landing (STOVL) aircraft configurations, and fan propulsion system simulators. These types of tests often require detailed knowledge of the entire test section flow field, so the calibration programs include flow quality surveys. The data collected and the subsequent data reports include detailed information on the flow quality throughout the test section.

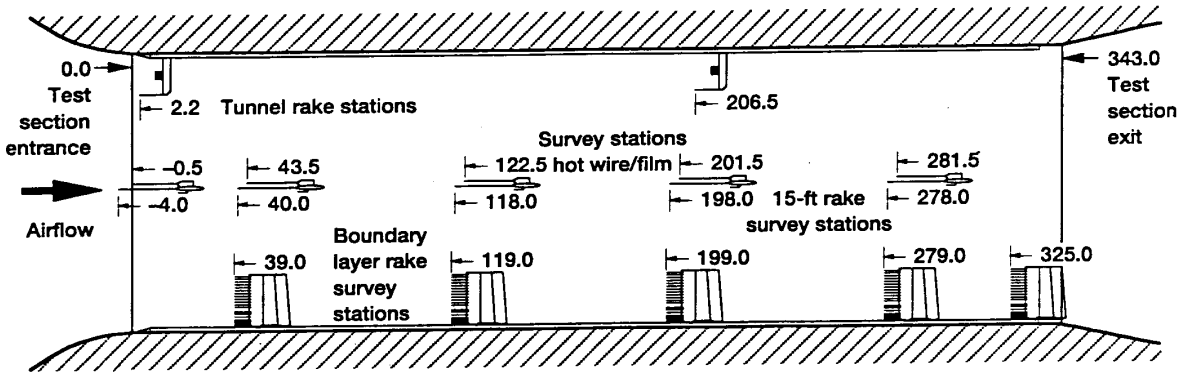



Figure C.3 – Elevation view of the 9x15 LSWT test section showing the location of tunnel and boundary layer survey rake instrumentation and axial flow-field surveys. (Test section stations are in inches.)

### C.2.1 Tunnel and test section instrumentation

The following facility instrumentation is used during the calibration: Two ceiling-mounted test section rakes are used to measure the standard test section operating conditions. Each rake is composed of one pitot-static probe and four thermocouples (type K). The pitot-static probe extends 12.25 in. from the test section ceiling. Figure C.3 gives the locations of these rakes in the test section. The total pressure is sensed using absolute pressure transducers with an accuracy of ±0.0015 psia; the difference between the total and static pressure is measured by delta pressure transducers with a ±0.0001-psid accuracy.

The following tunnel control settings are recorded during the calibration tests: compressor speed, number of drive motors or airblowers in use, and flow control door positions.

### C.2.2 Calibration hardware and instrumentation

The primary calibration hardware used in the 9×15 LSWT is the 15-ft survey rake. A typical installation of this rake is shown in Figure C.4, and the instrumentation layout is shown in Figure C.5. The instrumentation mounted on the rake includes 20 flow-angularity probes, 15 thermocouples, and 3 hot wire/film anemometry probes (one-, two-, or three-component probes are used). The flow-angularity probe spacing on the rake is not centered about the rake centerline so that a more detailed mapping of the flow field can be obtained at the location in the test section where many research test articles are positioned (the test articles are offset from the test section centerline to allow more room for the article to be tested at high incidence angles). The 15-ft rake can be mounted "inverted" (flipped end for end) so that the more tightly spaced probes are positioned at the opposite side of the test section to provide detailed flow field data for any test article that might be mounted in that area. The survey rake is supported at both ends by bolting the rake to wall-mounted support plates. These support plates are 106 in. high and have a rake-mounting bolt pattern such that the rake can be positioned vertically every 6 in. above or below the test section centerline. Additional support at the centerline of the rake is provided by a set of two cables that tie the rake to the tunnel floor and ceiling. The main body of the rake is in the form of a box composed of four 1-in. channel sections (2024–T3511 aluminum) that are riveted together in pairs to form two I-beams; these beams are connected by aluminum cover plates that form the upper and lower surfaces of the rake body. Leading and trailing edge fairings (6061–T6 aluminum) were added to the main structure to provide the aerodynamic contours. The rake is constructed in three sections of approximately 5 ft in order to better control the overall straightness of the rake. It is assembled prior to installation of the instrumentation. The overall length (span) of the rake is 176-in. (14-ft, 8-in.).

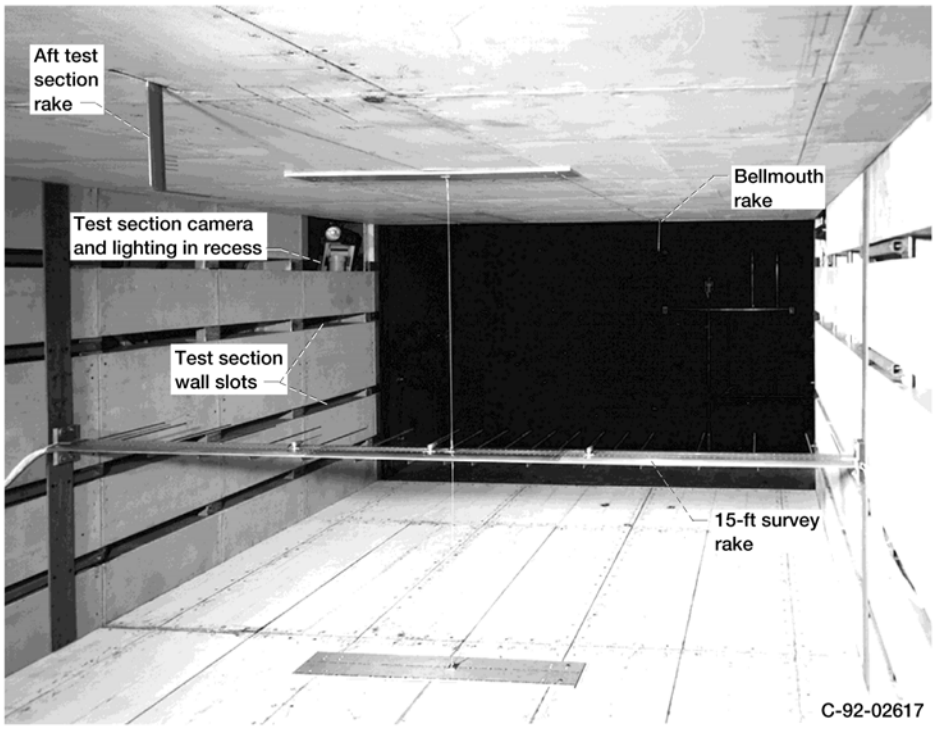



Figure C.4 – Typical installation of the 15-foot survey rake in the 9x15 LSWT test section.

The flow-angle probes are five-hole hemispherical head probes that allow the resolution of two flow-angle components—pitch and yaw. These probes were calibrated for a Mach number range of 0.05 to 0.20 (the Mach number range of the 9- by 15-ft test section is 0.00 to 0.20) by General Dynamics, Convair Division,

in San Diego, California (a facility now operated by Micro Craft). Total pressure is sensed by a port at the center of the probe tip. Four independent static pressure measurements are made using taps on the probe body; these four measurements are then averaged to indicate the static pressure at each probe. These probes extend 21.5-in. ahead of the leading edge of the rake.

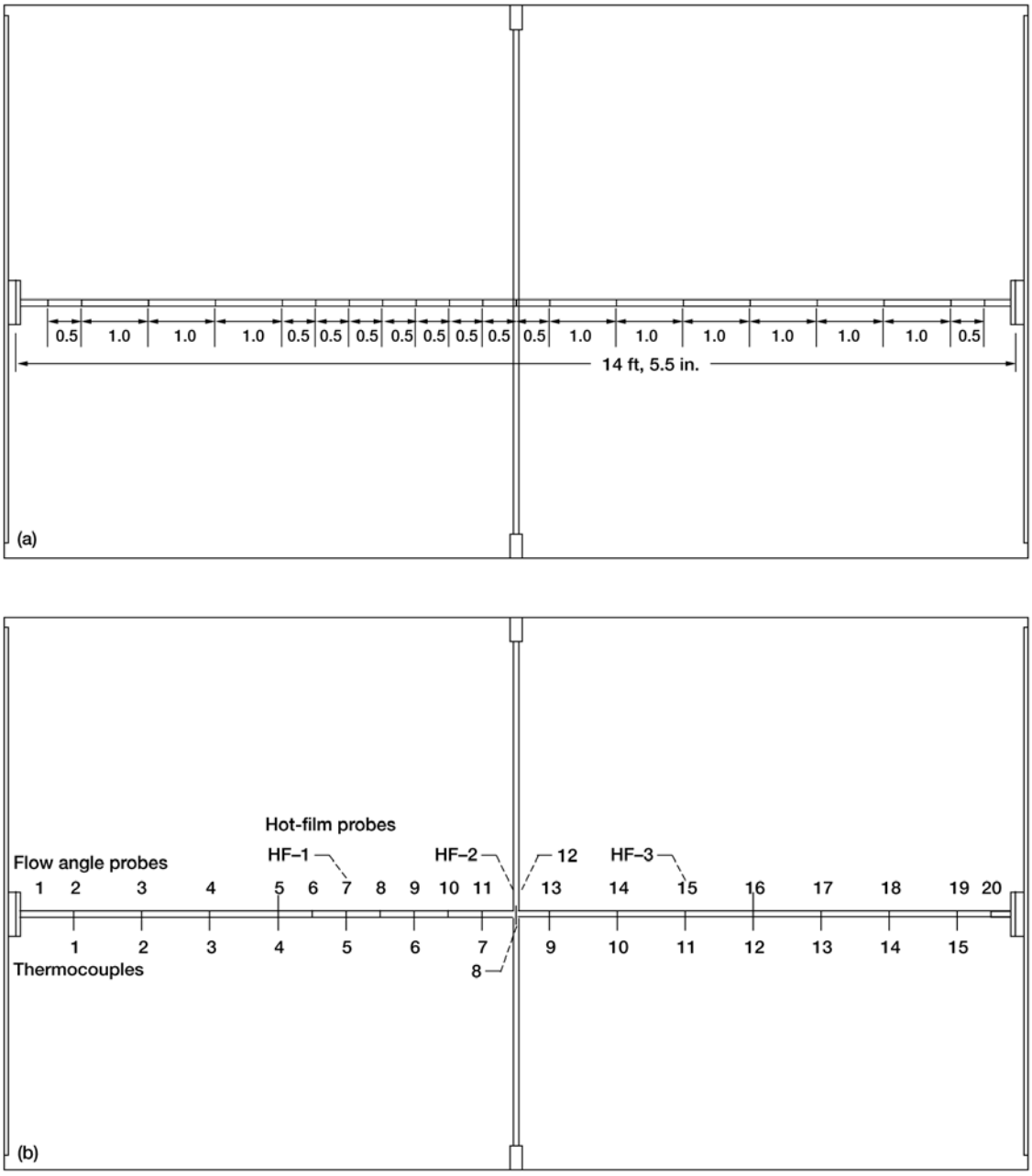



Figure C.5 – Instrumentation layout of the 15-foot survey rake. (a) Showing spacing between flow-angle probes. (All dimensions are in feet.) (b) Showing flow-angle probes, thermal anemometry probes, and thermocouple positions.

The misalignment of the flow-angle probes mounted on the array is measured following installation in the test section. Prior to the first run, the flow-angle probe pitch and yaw alignment offsets are measured using a mechanical inspection arm. The baseline rake pitch and yaw angles are measured using a digital inclinometer and tape measure. For each rake height change, the rake pitch and yaw angles are

measured and compared with the baseline values. The differences from the baseline values are used to correct the measured flow angles for rake misalignment.

Aspirated thermocouples with chromel-alumel (type K) sensing elements are used. The thermocouples are mounted to the bottom surface of the survey rake, with the heads of the thermocouples about even with the rake leading edge. Three hot wire/film anemometry probes are mounted to the upper surface of the 15-ft rake. The following probes are used during this entry:

(1) **Single-component probes.**—0.002-in.-diameter platinum film and 0.00015-in.-diameter tungsten wire end-flow probes. These probes are oriented with the sensing element in the vertical direction (i.e., perpendicular to the plane of the test section floor) and the horizontal direction.

(2) **Two-component probes.**—0.002-in.-diameter platinum film X end-flow probes. Tests are conducted with these probes oriented in both the vertical and horizontal planes.

(3) **Three-component probes.**—0.002-in.-diameter platinum film triple end-flow probes.

The lengths of the hot wire/film probe supports are such that the sensing elements are 3.6-in. downstream of the flow-angularity probe tips for the single and X probes and 5.1-in. downstream for the triple probes. The centerline of each hot wire/film probe support is 1.56-in. above the centerline of the flow-angularity probes. To eliminate vibration, the hot wire/film probe supports are tied to adjacent flow-angularity probe shafts by means of aluminum brackets. The brackets measure 3.0 by 1.0 by 0.5 in., have hemicylindrical leading edges, and are mounted such that the bracket leading edges are 13.7-in. downstream of the flow-angularity probe tips. The outside diameters of the hot wire/film probe supports and the flow-angularity probes are 0.180 and 0.375 in., respectively. The horizontal coordinates for the probes are –36.0, –2.0, 36.0 in. with respect to the tunnel centerline.

Before hot wire/film probes were used in the 9×15 LSWT, they were calibrated with a 1.5-in.-diameter free jet located in Glenn's Engine Research Building. The free jet is equipped with a barometer used to measure atmospheric pressure (static pressure at the jet exit) and a 1-psid differential pressure transducer measuring the difference between the jet static pressure and the jet plenum stagnation pressure. At nominal test section Mach numbers of 0.05, 0.10, 0.15, and 0.20, the calibration jet velocity uncertainties are ±3.0, ±1.6, ±1.2, and ±1.0 ft/sec, respectively. The uncertainty in the manual probe actuation system for pitch and yaw calibration is ±0.3°. After the hot wires/films were calibrated, additional data were obtained to determine repeatability. If the data were taken immediately after the calibration, repeatability for all probes was ±1.0 ft/sec for the mean velocity and ±0.7° in the pitch and yaw flow angle. If the probe/anemometer had to be disassembled and then reassembled and reset with the appropriate operating resistances, the repeatability was ±2.5 ft/sec for the mean velocity, and ±1.5° in pitch and yaw. Because the system is disassembled to transfer it from the calibration facility to the wind tunnel and then reassembled, the latter set of repeatability values apply to the wind tunnel calibration data. It should be noted that the same three 60-ft cables and the same three anemometer/signal conditioners are used during the calibration. During the test section data acquisition, 9 different 80-ft cables are used and there are 12 different anemometer/signal conditioner units available for use (3 of which are used in the calibration). This is important in explaining the data accuracy of the hot film/wire systems.

All the pressure and thermocouple instrumentation lines are housed inside the trailing-edge fairing. Some of the for hot wire/film coaxial cables are secured external to the rake trailing edge fairing.

A floor mounted, vertical rake has been designed and built for check calibrations. This quick-check rake can accommodate up to six pressure or temperature probes in the main structure in addition to thermal anemometry probes mounted from the side of the rake body. The standard probe setup for the quick-check rake is one each total pressure, static pressure and flow-angle probe, three total temperature probes and one thermal anemometry probe. The probes are calibrated in the Engine Research Building prior to the 9×15 test entry. Figure C.6 shows a typical installation of the quick-check rake. This rake can be installed, tested, and removed in one operational day and, therefore, can quickly and efficiently check the facility calibration at any time. The quick-check rake is tested at station 198 along the test section

centerline and at station 119 along the south turntable centerline (location of the inlet of most fan simulator models).

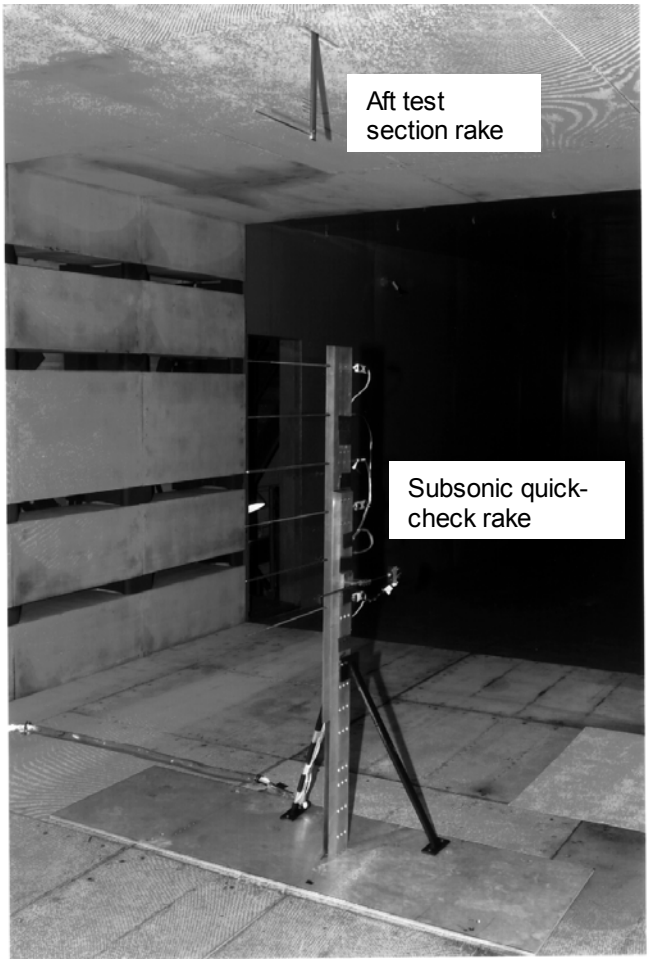



Figure C.6 – Installation of the quick-check rake in the 9x15 LSWT test section. Instrumentation mounted on the rake includes three thermocouples, a pitot-static probe, a static pressure probe, a five-hole hemispherical head flow-angle probe, and a thermal anemometry probe. The small rake mounted from the test section ceiling is the aft tunnel rake.

The traversing microphone system is used to survey the axial total and static pressure and total temperature distributions through the test section. This system is made up of a track system mounted to the test section floor and is remotely controlled. The track system is faired in to reduce aerodynamic and acoustic disturbances. A three-probe microphone stand outfitted with a pitot-static probe, static pressure probe, and total temperature probe is mounted on the track system and can be positioned anywhere along the track to provide data at a point.

Boundary layer surveys in the 9- by 15-ft test section are carried out using eight boundary layer rakes. A typical boundary layer rake used in these surveys is shown in Figure C.7; a typical test configuration is shown in Figure C.8. Each rake had 25 total pressure probes spaced so that a tight pressure distribution can be obtained near the test section surface. Six 10-24 countersunk socket head cap screws are used to fasten each boundary layer rake base plate to a 3/16-in.-thick aluminum plate. The same fasteners used to mount the acoustic boxes to the tunnel structure are used to mount the boundary layer rake/plate assemblies. Each 3/16-in.-thick aluminum plate has a 30° leading-edge bevel.

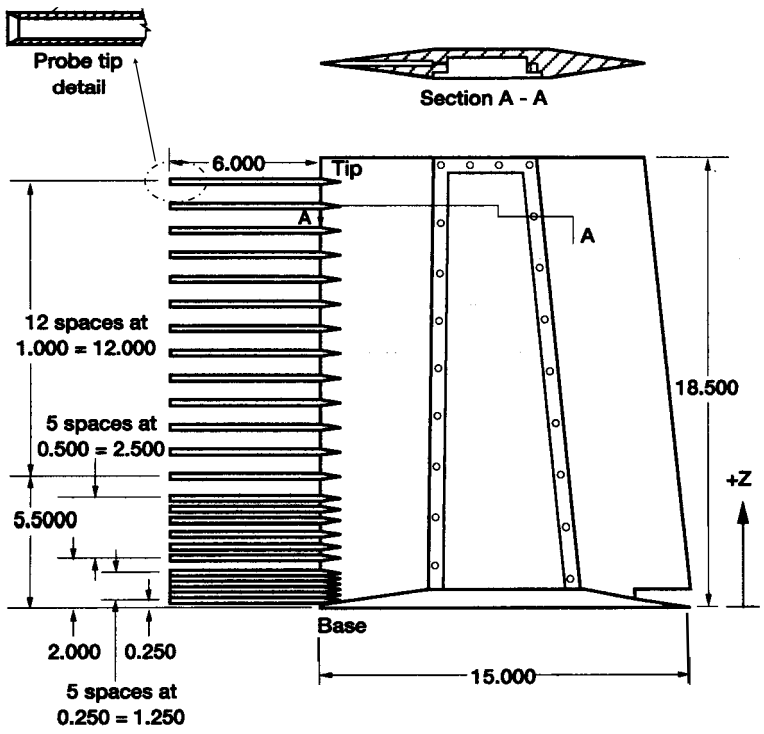



Figure C.7 – Typical boundary layer rake details, layout, and dimensions. (All dimensions are in inches.)

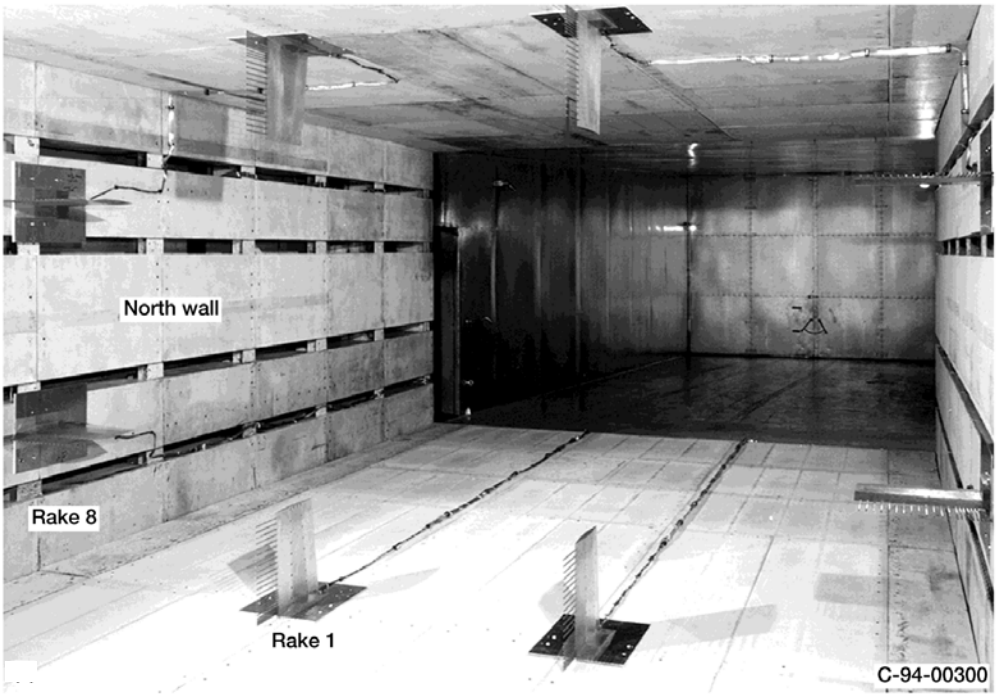



Figure C.8 – Typical installation of eight boundary layer rakes in the 9x15 LSWT test section.

### C.2.3 Data acquisition systems

The standard tunnel data system is used for all calibration testing. Steady-state pressure data are acquired with an electronically scanned pressure (ESP) system. The ESP system uses plug-in modules, each containing 32 individual transducers that can be addressed and scanned at a rate of 10 000 ports/sec. All ESP transducers can be calibrated online automatically every 20 min or at the discretion of the test engineer. For the calibration, a pneumatic valve is operated in each module to allow three pressures that are measured with precision digital quartz transducers to be applied. Throughout the test section calibration program, the ESP transducers are calibrated at each Mach number setting. For these tests, ±5 psid modules are used.

Real-time data acquisition and display are provided by Escort Alpha, the standard data system used in the large test facilities at Glenn. This system accommodates the ESP input, plus all steady-state analog and digital signals used, including survey rake and tunnel facility thermocouples and pertinent tunnel control parameters such as compressor speed, shock door positions, and positions of flow control doors 1 and 2. The Escort Alpha facility microcomputer acquires these data, converts them to engineering units, executes performance calculations, checks limits on selected channels, and displays the information in alphanumeric and graphical form with a 1-sec update rate. For this test, each collected data reading is the average of 20 scans (20 sec) of data.

The Escort system displays all measured data online in both graphical and alphanumeric formats (either default or user defined) at 1-sec update rates. In general, the tunnel controls, tunnel rake data, and calibration hardware data are monitored online during each test run. Any of the online displays can be printed for permanent record, but this is usually done only for troubleshooting purposes. There are also several data dump options that can print all measured and calculated data; these are also usually used only for troubleshooting.

Commercially available constant-temperature anemometers are used during hot wire/film measurements. Each anemometer has its own signal conditioner for low-pass filtering, direct-current (dc) offsetting, and amplifying. A commercially available, 16-channel, 12-bit analog-to-digital (A/D) converter with an input range of ±5 V is used to digitize the signal-conditioned anemometer bridge voltages. A commercially available personal computer with commercially available software is used to control the data acquisition process and to store the digitized data on computer hard disk. The data are later transferred to floppy disk media for permanent storage.

Signal-conditioner gains are typically set at 10 and 6 for the hot wire and hot film probes, respectively. Signal conditioner dc offsets are typically set at 2 and 3 V for the hot wire and hot film probes, respectively. These settings permit the anemometer output bridge voltages to stay within the ±5-V range of the A/D converter. Typical bridge output voltages vary between 3.0 and 3.4 V for the hot film and 1.65 and 1.85 V for the hot wire over the Mach numbers tested. Both the hot wire and hot film bridge voltages are low-pass filtered at 500 Hz. The A/D converter is configured to record all unsteady bridge voltages at a sampling rate of 2000 Hz. In addition, it is configured to record a minimum of 16 384 data points (8.192 sec worth of data) for every data record cycle. Typical frequency responses of the sensors are 40 and 2.5 kHz for the hot wire and the hot film, respectively. These approximate frequency responses are measured using a standard anemometer square wave test at a test section Mach number of about 0.15. The relatively low frequency responses of the probes result from the 100-ft cables that connect the probes to the anemometer equipment.

## C.3 Detailed calibration procedure

Figure C.3 shows the survey planes and measurement locations in the test section. There are five flow field (15-ft rake) survey stations. The survey station is defined as the distance from the test section inlet (test section station 0) to the tip of the flow-angularity probes. At each flow field survey station, data are collected with the 15-ft rake at 13 vertical positions (centerline and ±6, ±12, ±18, ±24, ±30, and ±36 in. from the centerline). At each position, data are taken at Mach numbers of 0.05, 0.10, 0.15, and 0.20. In addition, for the rake at the vertical centerline at station 198, a tighter Mach number schedule

was used to provide the facility calibration curve data. At this position, data are taken at Mach numbers of 0.05, 0.06, 0.08, 0.10, 0.12, 0.14, 0.15, 0.16, 0.18, 0.20, 0.22, and 0.23. A summary of the measurements made during calibration and flow survey testing is given in Table C.2. The test matrices for the calibration and flow field surveys are given in Table C.3.

Table C.2 — Summary of measurements made for a typical calibration test

| Source | Measurement | Number of measurements | Location |
|---|---|---|---|
| Facility instrumentation | Bellmouth total pressure | 1 | Test section inlet |
| | Bellmouth total temperature | 4 | Test section inlet |
| | Aft test section total pressure | 1 | Near model test plane in test section |
| | Aft test section total temperature | 4 | Near model test plane in test section |
| 15-ft survey rake instrumentation | Spanwise distributions of | | |
| | Total pressure | 20 | Axial surveys at stations –4, 40, 118, 198, and 278; 13 vertical heights at each station |
| | Static pressure | 20 | |
| | Total temperature | 15 | |
| | Flow-angle probe pressure | 20 | |
| | Turbulence levels | 3 | Axial surveys at stations –4, 40, 118, 198, and 278; 13 vertical heights at each station |
| Quick-check rake | Point measurements of | | |
| | Total pressure | 1 | The rake can be mounted at several locations in the test section |
| | Static pressure | 2 | |
| | Total temperature | 1 | |
| Boundary layer rakes | Total pressure profiles | 25/rake | Eight rakes are used, two per test section surface |

The first test run is at station 198, with the rake at the vertical centerline. Prior to the first run, the flow-angularity probe alignment offsets are measured using an optical transit, and the baseline rake pitch and yaw angles are measured using a digital inclinometer and a tape measure. For each rake height or station position change, the rake pitch and yaw angles are measured and compared with the baseline values. The differences from the baseline values are used to correct the measured flow angles for rake misalignment. Several rake positions are repeated at station 198 so that various hot wire/film probes can be used. The rake is also run in the “inverted” configuration at station 198 to support a test where the test article is mounted on the south side of the test section. After all calibration and flow field data points are completed at station 198, flow field surveys are made at stations 278, 118, 40, and –4.

As has been previously described, there are three hot wire/film probe supports mounted on the 15-ft rake. Coaxial cables (80-ft long) are used to connect the hot wire/film sensors to the anemometers. The probe shafts are mounted rigidly to the 15-ft rake structure via aluminum mounting blocks and to adjacent flow-angularity probe shafts via the aluminum brackets described previously. The yaw offsets measured for the 15-ft rake are assumed for the probe supports, and pitch offsets were measured with the same digital inclinometer used with the 15-ft rake. The uncertainty in the hot film/wire probe support alignment with respect to the test section centerline is $\pm 0.5°$, even with the pitch and yaw offsets; this was primarily due to the misalignment introduced by the aluminum mounting blocks and the aluminum stabilizing brackets.

Before every day of testing, hot wire/film resistances and cable resistances are measured and properly accounted for in the data acquisition process. In addition, the operating resistances (overheat ratios) for the specific probes in use are dialed into the anemometer units. Frequency response is also checked for the sensors. Hot films typically had frequency responses around 2 kHz, and hot wires typically have frequency responses around 50 kHz. These low-frequency responses are a result of the long cable lengths. Between test runs and during 15-ft rake position changes, the hot wire/film sensors are removed to prevent accidental breakage.

Table C.3 — Sample test matrices for a full aerothermal calibration and a calibration and flow quality check

[The letters in the blocks show where rake surveys are to be conducted and the Mach number schedule for that position.]

(a) Matrix for a full aerothermal calibration and flow quality survey.

| Rake station | 15-ft Rake vertical position | | | | | | | | | | | | |
|---|---|---|---|---|---|---|---|---|---|---|---|---|---|
| | –36 | –30 | –24 | –18 | –12 | –6 | CL | 6 | 12 | 18 | 24 | 30 | 36 |
| 198 | --- | --- | --- | --- | --- | --- | A | --- | --- | --- | --- | --- | --- |
| 198 | B | B | B | B | B | B | A | B | B | B | B | B | B |
| 278 | B | B | B | B | B | B | A | B | B | B | B | B | B |
| 118 | B | B | B | B | B | B | A | B | B | B | B | B | B |
| 40 | B | B | B | B | B | B | A | B | B | B | B | B | B |
| –4 | B | B | B | B | B | B | A | B | B | B | B | B | B |

| | |
|---|---|
| Traverse | Axial pressure distributions along the centerline; Mach schedule A |
| Boundary layer rakes | Eight rakes at stations 40, 119, 199, 278, and 325 (each station is a separate run); Mach schedule A |

(b) Matrix for a calibration and flow quality check.

| Rake station | 15-ft Rake vertical position | | | | | | | | | | | | |
|---|---|---|---|---|---|---|---|---|---|---|---|---|---|
| | –36 | –30 | –24 | –18 | –12 | –6 | [a]CL | 6 | 12 | 18 | 24 | 30 | 36 |
| 198 | --- | --- | --- | --- | --- | --- | A | --- | --- | --- | --- | --- | --- |
| 198 | B | B | B | B | B | B | B | B | B | B | B | B | B |
| 198 | B | --- | B | --- | B | --- | B | --- | B | --- | B | --- | B |
| 198 | --- | --- | --- | --- | --- | --- | B | --- | --- | --- | B | --- | --- |
| 278 | --- | --- | --- | --- | --- | --- | A | --- | --- | --- | --- | --- | --- |
| 118 | --- | --- | --- | --- | --- | --- | A | --- | --- | --- | --- | --- | --- |
| 40 | --- | --- | --- | --- | --- | --- | A | --- | --- | --- | --- | --- | --- |
| –4 | --- | --- | --- | --- | --- | --- | A | --- | --- | --- | --- | --- | --- |

(c) Matrix for a check calibration using the quick-check rake.

| Rake position | Mach number schedule |
|---|---|
| Station 198, tunnel centerline | A |
| Station 198, tunnel centerline | [b]A |
| Station 119, turntable centerline | A |

(d) Mach number schedules.

| Schedule type | Operation | Mach numbers/number of blowers |
|---|---|---|
| A | Three motors | Mach 0.10, 0.12, 0.14, 0.15, 0.16, 0.18, and 0.20 |
| | One motor | Mach 0.05, 0.06, 0.08, 0.10, 0.12, and 0.14 |
| | Air dryer air blower | Eight blowers to some minimum number of blowers |
| B | Three motors | Mach 0.10, 0.15, and 0.20 |
| | One motor | Mach 0.05, 0.10, and 0.14 |

[a]Centerline.
[b]Repeat test.

The data acquisition philosophy is to attempt to capture the turbulent velocity waveform. For this reason, data are nominally taken at a sampling rate of 20 or 50 kHz. For these sampling rates, low pass filters are set at 10 and 20 kHz, respectively. In addition, some data are obtained at a sampling rate of 0.5 kHz (0.2-kHz low-pass filtering) in an attempt to quantify low-frequency fluctuations in the test section mean

velocity. At every nominal tunnel Mach number, 20 480 data points are recorded and signal conditioner gains and dc offsets are adjusted to optimize use of the A/D converter input range. Nominal values of gain are 10 or 20 and nominal values of dc offset are 2 or 3 V depending on the 9×15 LSWT velocity.

Figure C.3 also shows the five boundary layer rake survey stations (39, 119, 199, 279, and 325). Eight boundary layer rakes are used at each station. Two rakes are mounted on each test section surface as shown in Figure C.7. At each station, data are taken at Mach numbers of 0.05, 0.06, 0.08, 0.10, 0.12, 0.14, 0.15, 0.16, 0.18, 0.20, 0.22, and 0.23. The test matrix for the boundary layer rake surveys is given in Table C.3. The eight rakes are mounted at the same station for each tunnel run, and then moved forward in the test section for each successive run, until all five stations are surveyed.

All the aerothermal wind tunnel calibration tasks are performed by the same team of engineers (in fact, the same engineering personnel conduct the calibrations in all four of the large tunnels at Glenn). Having the same personnel conduct all the calibration tasks provides the needed consistency required in a tunnel calibration program.

## C.4 Frequency and duration of full and check calibrations

Full tunnel calibration can be completed in 4 to 6 weeks. Calibration and flow quality checks using the 15-ft rake at station 198 on the tunnel centerline can be completed in 3 to 4 days, whereas a check calibration using the quick-check rake can be completed in 1 day (two-shift operation). At present, full calibrations are scheduled for every 5 to 8 years, or as needed pending modifications to the facility, flow quality checks are scheduled for every 2 to 3 years, and quick-check calibrations are scheduled two to three times per year. Also, program-specific calibrations can be conducted to provide a research customer with calibration or flow quality data required for a particular test program.

## C.5 Data analysis

The data reduction and analysis for each measurement set and for the creation of the test section calibration curves are described in the following sections.

### C.5.1 Flow field data

The following measured flow field data are collected using the 15-ft survey rake:

$P_T$ total pressure (20-point survey distribution)

$P_S$ static pressure (20-point survey distribution)

$T_T$ total temperature (15-point survey distribution)

$P_1$, $P_2$, $P_3$, $P_4$ flow-angularity pressures (20-point survey distribution)

So that the flow field data can be reviewed, ratios are formed of the flow field parameters sensed by the 15-ft survey rake instrumentation and the corresponding variables from the aft test section rake. Normalizing the parameters in this manner eliminates the run-to-run variations in atmospheric conditions so that the data can be more readily compared. The following equations are used to calculate needed flow field data.

The Mach number is determined using the ratio of the static to total pressure and the isentropic perfect gas equation (equation (44) from Reference 37, using $\gamma$ = 1.4):

$$M = \sqrt{5\left(\left(\frac{P_S}{P_T}\right)^{-0.2857} - 1\right)}$$

Velocity is determined using the definition of Mach number, $M = U/a$, where $a$ is the speed of sound ($a = (\gamma R T_S)^{0.5}$). The static temperature $T_S$ is calculated using the following relation (equation (43) from Reference 37)

$$T_S = \frac{T_T}{1 + 0.2M^2}$$

The local velocity is then determined using

$$U = M \cdot a$$

For the calculations where pressures and temperatures are used together, allowances are made for the difference in number and position of flow-angle probes to thermocouples. The Mach number associated with the flow-angle probe closest to each thermocouple is used to compute the static temperature. In the calculation for velocity, either the adjacent flow-angle probe/thermocouple pairs or the average of the two thermocouples on either side of a flow-angle probe are used as appropriate (depending on the local probe geometry).

Two components of flow angle are also measured by the five-hole hemispherical-head flow-angularity probes on the survey rake. As the name implies, the head of each probe has five pressure orifices. The center port ($P_5$) senses the total pressure, $P_T$. Ports $P_1$ and $P_3$ are used in determining the pitch flow angle, and $P_2$ and $P_4$ are used for the yaw flow angle. The difference in pressure measured by a pair of opposing ports is related to the flow angle through an extensive probe calibration. The probe calibration is based on the relationship between the probe attitude (flow angle) and two pressure ratios, $Cp_\alpha$ and $Cp_\beta$. The pressure ratios are defined as

$$Cp_\alpha = \frac{P_3 - P_1}{P_T - P_{avg}} \quad \text{and} \quad Cp_\beta = \frac{P_4 - P_2}{P_T - P_{avg}}$$

where $P_{avg} = 0.25(P_1 + P_2 + P_3 + P_4)$. The flow angle is related to these pressure ratios through a calibration equation; for the pitch angle $\alpha$, the relationship is

$$\alpha = C_0 + C_1 Cp_\alpha + C_2 Cp_\beta + C_3 Cp_\alpha^2 + C_4 Cp_\beta^2 + C_5 Cp_\alpha Cp_\beta + C_6 Cp_\alpha^3 + C_7 Cp_\beta^3 + C_8 Cp_\alpha^2 Cp + C_9 Cp_\alpha Cp_\beta^2$$

A similar equation is used for the yaw flow angle $\beta$. Details on correcting the flow-angle data for rake and probe misalignment are described in Reference 36.

The resulting pressure ratios, temperature ratio, Mach number, and flow-angle data are next plotted both as surface plots (or vector plots for the flow-angle data), to see the overall flow field profiles at each test section station, and as $x$-$y$ plots for specific locations in the test section, to get very detailed information in the flow field at critical stations in the test section. See References 34 and 35 for examples of these data plots. Review of the entire flow field is needed in the creation of the test section calibration curves, as described in Section C.5.4.

### C.5.2 Turbulence measurements

Hot wires and films are used to measure the velocity fluctuations in the 9- by 15-ft test section due to the passage of turbulent eddies or structures. As was previously mentioned, the hot wire and film probes were calibrated to establish the relationship between flow velocity and anemometer bridge voltage. In addition, two- and three-component probes were calibrated over a range of pitch and yaw angles.

Data reduction for all probes begins by converting the recorded fluctuating anemometer voltages into fluctuating velocities. For single-sensor probes, the calibration curve provides a direct relationship between the anemometer voltage and the axial velocity $u$. For multisensor probes, the sensor voltages and calibration curve information are used in a system of equations that is solved for the axial velocity $u$ and either one or two transverse velocity components, $v$ or $w$, depending on the probe type. The

transverse velocity component sensed by a two-component probe depends on the rotation of the sensing plane. During velocity component construction, anemometer voltages are corrected for differences in stagnation temperature between the calibration environment and the actual test environment. Velocities are corrected for differences in static pressure between the calibration environment and the actual test environment. Details of this anemometer-voltage to velocity-component transformation process can be found in Reference 38. Once the fluctuating velocity data are generated, statistical analysis is carried out on these velocity data. Because of the gaps in time introduced by the data acquisition process, statistics are calculated on segments of 1024 data points. The results from the different segments are averaged to arrive at results for the entire data set. Of primary interest are the mean velocity components, the magnitude of the velocity vector, the standard deviations of the velocity components, and the turbulence intensities of the velocity components. Definitions of these quantities follow:

$$\bar{u} = (1/n)\sum_{1}^{n} u \qquad \bar{v} = (1/n)\sum_{1}^{n} v \qquad \bar{w} = (1/n)\sum_{1}^{n} w/n$$

$$U = \left[\bar{u}^2 + \bar{v}^2 + \bar{w}^2\right]^{1/2}$$

$$\sigma_u = \left[(1/n)\sum_{1}^{n} u^2 - \bar{u}^2\right]^{1/2} \qquad \sigma_v = \left[(1/n)\sum_{1}^{n} v^2 - \bar{v}^2\right]^{1/2} \qquad \sigma_w = \left[(1/n)\sum_{1}^{n} w^2 - \bar{w}^2\right]^{1/2}$$

$$TI_u = \sigma_u / U \cdot 100 \text{ percent} \qquad TI_v = \sigma_v / U \cdot 100 \text{ percent} \qquad TI_w = \sigma_w / U \cdot 100 \text{ percent}$$

The frequency content of the velocity signals is also of interest. Power spectra are computed for the individual velocity signals so that dominant frequencies can be identified. Reference 38 explains the methods used to compute these power spectra.

### C.5.3 Boundary layer rake data

The boundary layer rakes measure total pressure profiles in the boundary layer. So that the Mach number profiles can be calculated, the static pressure measured at the aft-tunnel rake is assumed to be constant for all boundary layer rakes. This is assumed regardless of the axial station and rake position. For computing the boundary layer velocity profile, a constant speed of sound is assumed for all rakes regardless of the axial station and rake position. The speed of sound used is that computed using the static temperature at the aft-tunnel rake. The velocity profiles are then normalized with the boundary layer rake tip velocity. This forces the velocity ratio at the boundary layer rake tip to be 1.0. Once the boundary layer data are in velocity ratio form, a cubic spline is fit through the experimental data to generate interpolated spline points. A search algorithm is used with the experimental and spline data to determine the distance from the test section surface $Z$ at which the velocity ratio is equal to 0.990. Linear interpolation is used to further interpolate between spline data. This value of $Z$ is the boundary layer thickness. In equation form, the boundary layer thickness can be written as

$$\delta = Z\big|_{(u/U)=0.99}$$

Before displacement thickness and momentum thickness can be computed, the boundary layer velocity profiles have to be extrapolated down to the wall, or to $Z$ = 0.0. This is carried out using a power law function of the form

$$\frac{u}{U} = \left(\frac{Z}{\delta}\right)^{1/c}$$

The following equation is used to compute the value of $c$ for every boundary layer velocity profile:

$$c = \log_e \frac{Z_1}{\delta} \Big/ \log_e \left(\frac{u}{U}\right)_1$$

where $Z_1$ is the Z value for the boundary layer rake pitot probe nearest the wall and $(u/U)_1$ is the velocity ratio for the pitot probe nearest the wall.

Numerical integration using the extrapolated power law data and the interpolated spline data is used to calculate the boundary layer displacement thickness $\delta_1$ and the boundary layer momentum thickness $\delta_2$.

$$\delta_1 = \int_{Z=0}^{h} [1 - (u/U)]dZ$$

$$\delta_2 = \int_{Z=0}^{h} (u/U)[1 - (u/U)]dZ$$

The upper limit of integration *h* is the lowest value of *Z* at which the velocity ratio *u*/*U* becomes 1.0.

### C.5.4 Calibration curves for determining test section operating conditions

Calibration curves are developed from 15-ft rake data, and measurements are made simultaneously by the two tunnel rakes mounted from the test section ceiling. The basic approach for the 9×15 LSWT calibration curves is to relate the parameters measured by the aft test section rake to a point in the test section via a set of simple relationships. The calibration point is along the test section centerline at station 198. Flow field data from the entire test section volume are used to relate the conditions at the calibration point to any other location in the test section.

The aft test section rake is selected as the primary piece of facility hardware in the calibration process and in setting test section conditions during a research test. However, in tests where the model location or size interferes with the aft rake measurements, the bellmouth rake is used. Linear relationships for total pressure, total temperature, and Mach number allow measurements made by the bellmouth test section rake to be converted to aft test section rake measurements. Figure C.9 shows the relationships between the bellmouth and aft test section rakes. When this set of curves is used, the static pressure at the aft rake is calculated from the total pressure and Mach number using equation (44) from Reference 37:

$$P_{S,\text{aft}} = P_{T,\text{aft}} \left(1 + \frac{M_{\text{aft}}^2}{5}\right)^{-3.5}$$

Whether the aft test section rake measurements are used directly or the bellmouth rake data are used to create aft rake measurements, the next step is to relate the aft rake measurements to the parameters measured at the calibration point by the 15-ft survey rake. Ratios of the calibration point to the aft rake pressures are plotted as a function of the aft rake differential pressure (the difference between the total and static pressure measured by the aft rake). These curves are shown in Figure C.10. The calibration point total pressure is determined from the following equation from Figure C.10:

$$P_{T,ts} = P_{T,\text{aft}} \left[-0.00034008(P_{T,bm} - P_{S,bm}) + 1.0\right]$$

The flow field analysis described in Section C.5.1 shows that the total pressure is constant throughout the test section volume; therefore, the total pressure calculated at the calibration point is valid at any point in the test section.

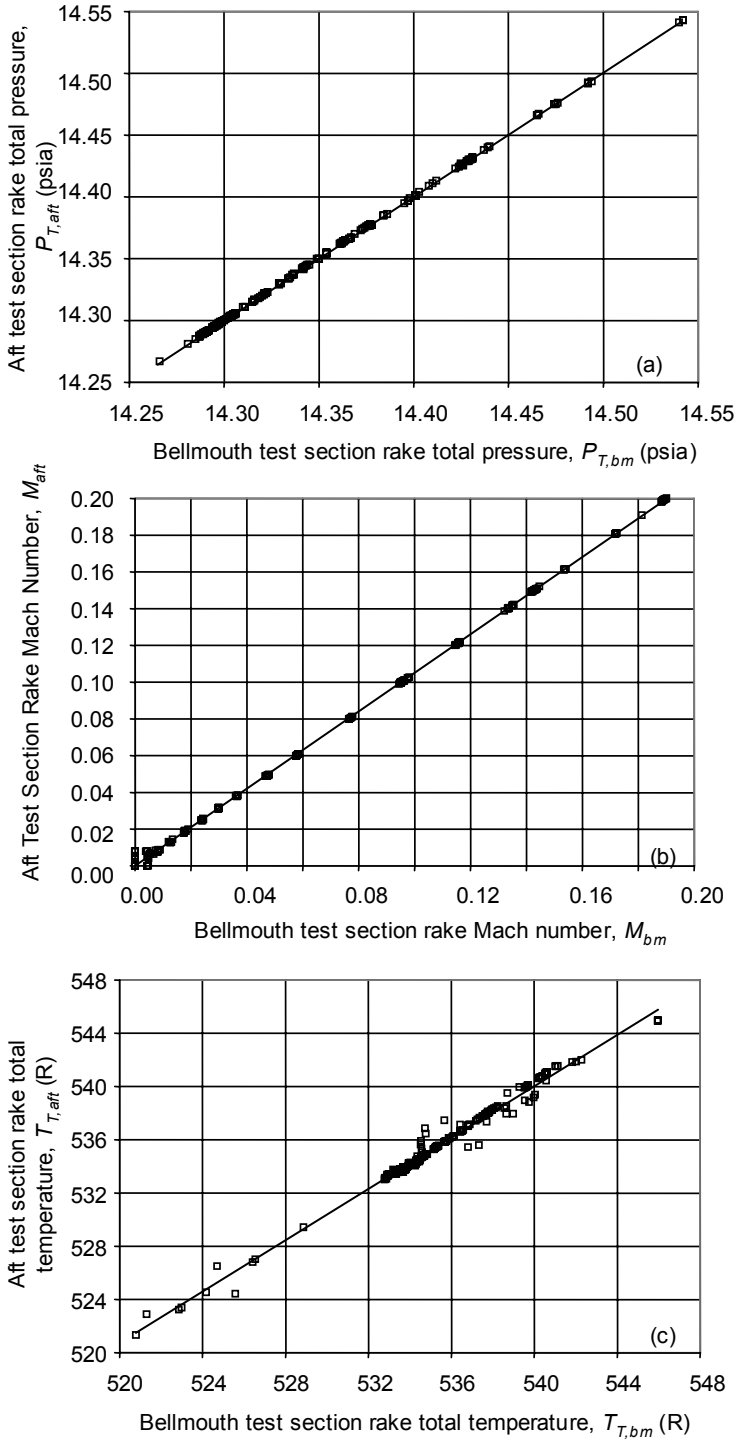



Figure C.9 – Curves used to relate parameters sensed by the bellmouth test section rake to the aft test section rake. (a) Total pressure; $P_{T,aft}$ = (1.00359280)$P_{T,bm}$ – 0.05119429. (b) Mach number; $M_{aft}$ = (1.04965287)$M_{bm}$. (c) Total temperature; $T_{T,aft}$ = (0.96399774)$T_{T,bm}$ + 19.45672803.

Static pressure at the calibration point is determined with this equation:

$$P_{S,ts} = P_{S,\text{aft}}\left[0.00048864(P_{T,bm} - P_{S,bm}) + 1.0\right]$$

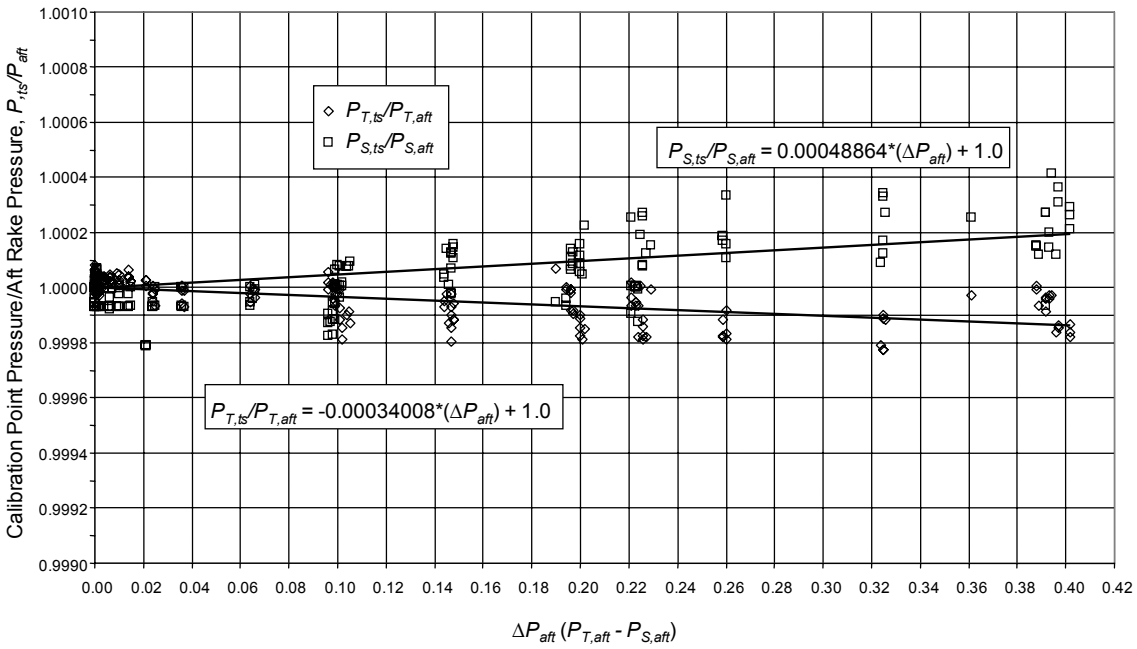



Figure C.10 – Calibration curves for determining total and static pressure at the calibration point from measurements made by the aft test section rake.

This flow field analysis (Section C.5.1) indicates that the static pressure is constant within a plane in the test section but that there is an axial variation through the test section. Figure C.11 shows a composite of data collected using the traversing system at various Mach numbers. Mach number is used for the axial correction instead of static pressure since the Mach number data collapses to a single trend line. The Mach number ratio at any axial station is determined from the equation of the trend line given in Figure C.11; the test section Mach number is calculated from this ratio and the aft test section Mach number:

$$M_{ts} = \left(\frac{M_{ts}}{M_{\text{aft}}}\right) M_{\text{aft}}$$

The test section static pressure is calculated from the corrected Mach number and the total pressure:

$$P_{S,ts} = P_{T,ts}\left(1 + \frac{M_{ts}^2}{5}\right)^{-3.5}$$

The total temperature at the calibration point is determined as a function of the aft test section rake total temperature and Mach number, as shown in Figure C.12. The ratio of calibration point to aft rake total temperature is calculated from the trend line equation. The calibration point total pressure is then calculated from this ratio using the known aft rake total temperature. There is no axial variation in total temperature for a given point within a plane. There is, however, a spanwise temperature gradient across the test section related to the heat exchanged upstream of the test section. The magnitude of the gradient is Mach number dependent. The following equation is used to correct the total temperature for spanwise variation:

$$T_{T,ts} = 24 M_{\text{aft}}^2 \left(\frac{y}{80}\right) + T_{T,ts}$$

The calibration curves and equations just described are used to determine the total and static pressure and total temperature at any point in the test section. Once the value of these parameters is known, all other flow field variables (Mach number, airspeed, static temperature, Reynolds number, etc.) can be calculated.

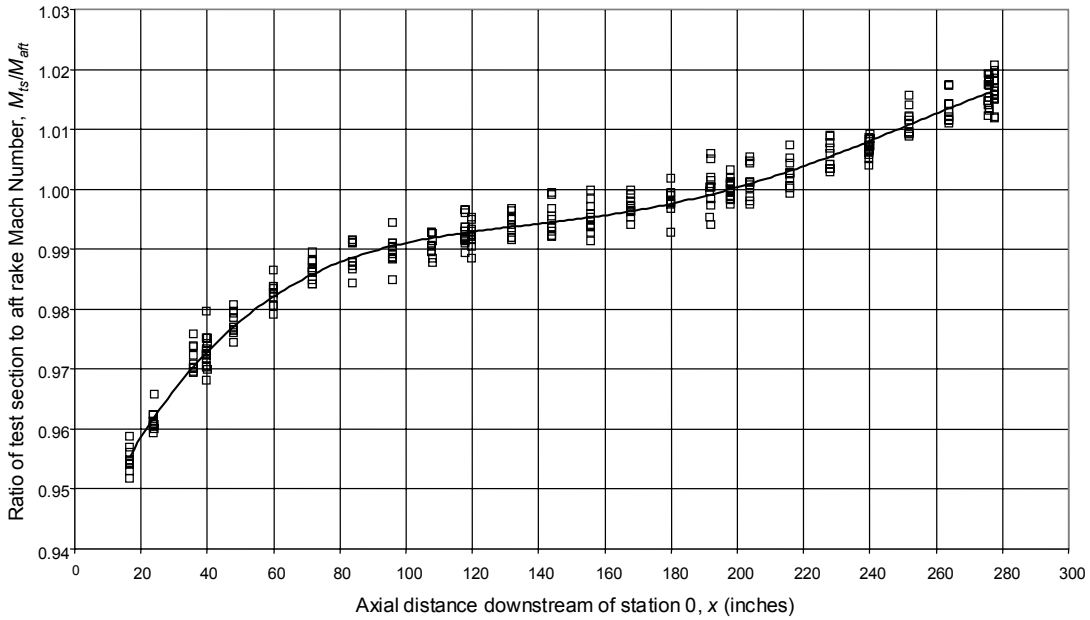



Figure C.11 – Axial correction for centerline Mach number. This curve is used to correct the static pressure for axial variations through the test section; $M_{ts}/M_{aft} = -5.10278352\text{x}10^{-11}\ x^4 + 3.97958514\text{x}10^{-8}\ x^3 - 1.05813978\text{x}10^{-5}\ x^2 + 1.24664169\text{x}10^{-3}\ x + 9.3749769\text{x}10^{-1}$.

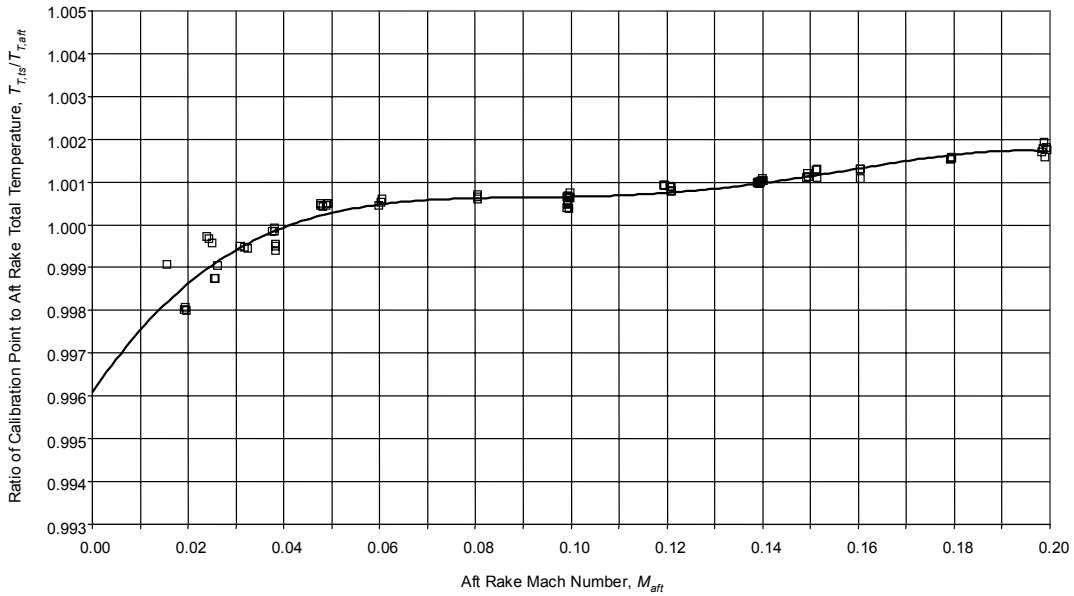



Figure C.12 – Calibration relationship used to determine total temperature at the calibration point from aft test section rake conditions; $T_{T,ts}/T_{T,aft} = -26.24504434\ M_{aft}^4 + 13.11555442\ M_{aft}^3 - 1.17355402\ M_{aft}^2 + 0.16827833\ M_{aft} + 0.99606985$.

## C.6 Reporting of results

All calibration and flow quality tests performed in Glenn's wind tunnels are documented in formal NASA reports. The formal NASA reports have an unlimited (unclassified) distribution, and are, therefore, available to anyone who wishes to see the report. As the cycle time to publishing the formal NASA report can be fairly lengthy (up to a year in the case of a large report), the test information is made available in the form of a Preliminary Information Report (PIR), which is an internal report for use at Glenn. The PIR is simply the final rough draft of the formal report after it has been through the review cycle as it is submitted to the editorial department for final publication. The PIRs are available to Glenn personnel and research customers.

The reports written to describe the calibration and flow quality tests are purposely very detailed and are generally long. Detailed descriptions of the hardware, instrumentation, procedures, data analysis, and test results, including extensive tabular and graphical data listings, are included in the reports. In doing this, there is a permanent record of the test and results.

# Annex D—Lockheed Martin Low Speed Wind Tunnel

## D.1 Description of facility

The Lockheed Martin Low Speed Wind Tunnel is a horizontal, atmospheric pressure, single-return-circuit, closed-throat system having an overall circuit centerline length of 780.5 ft. Figure D.1 shows the general arrangement of the wind tunnel. The facility has two large test sections in tandem. The test section dimensions and flow characteristics are summarized in the Table D.1. The first nozzle, of 3.4:1 contraction ratio, delivers air from the turbulence-settling chamber to the larger of the two test sections. This test section, designed for testing airplane models in the vertical/short takeoff and landing (V/STOL) flight regime, is designated as the V/STOL test section. The air then flows through a second nozzle, of 2.06:1 contraction ratio, into the smaller test section. This latter test section, designed for testing aircraft models in the normal horizontal low-speed flight regime, is designated as the low-speed test section. However, each test section has wide-ranging applications to nonaerospace test subjects as well.

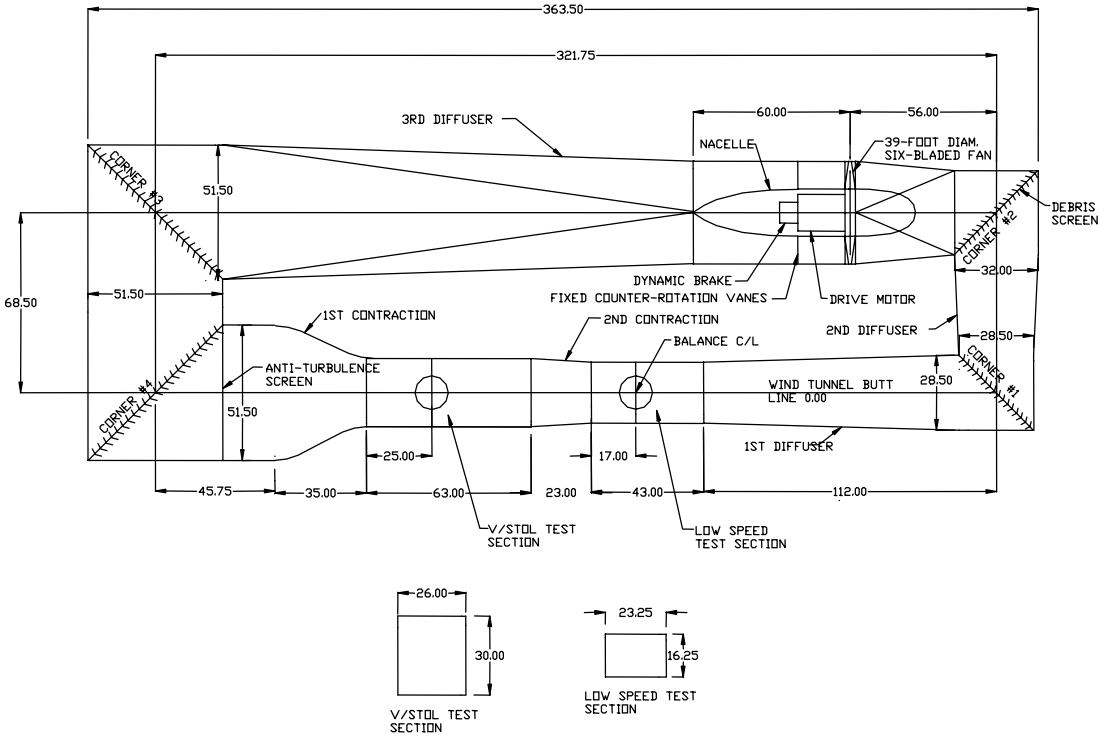



Figure D.1 – General arrangement, Lockheed Martin Low Speed Wind Tunnel (plan view). All dimensions given in feet unless marked otherwise.

The wind tunnel circuit structure, with the exception of the two test sections, is constructed of structural steel beams and steel plate. It is cooled, when necessary, by spraying water on the outside surfaces at a rate of approximately 7000 gal/min. The water is recovered in a concrete catch basin beneath the tunnel and recirculated. The wind tunnel stagnation temperature is maintained below 120 °F and usually below 90 °F to protect the wooden fan blades and to maintain reasonable working conditions in the test sections.

Both test sections are formed of welded steel framing overlaid with wood planking and a plywood lining. The V/STOL test section is 26 ft wide, 30 ft high, and 63 ft long, whereas the low-speed test section is 23.25 ft wide, 16.25 ft high, and 43 ft long. The roof and floor of each test section are parallel, whereas the sidewalls diverge slightly to account for boundary layer growth. There are no corner fillets in either test section. Each test section has full-height, adjustable breather slots at the downstream ends of the sidewalls to vent the test section in use to atmospheric pressure.

The wind tunnel is equipped to support testing of V/STOL or conventional low-speed aerospace models. Industrial models, architectural models, parachutes, dish antennas, trains, and automobiles can also be tested in the facility. Variable-frequency electrical power and a high-pressure air supply system are available to power simulated propulsion systems in the models or to satisfy other test requirements. Six-component aerodynamic forces and moments are measured on strut-mounted models by an external balance located below each test section or, when sting mounted, by an internal strain gauge balance. The balance output signals and the other channels of digital and analog signals are automatically recorded by an online data acquisition system.

Table D.1 — Summary of test section dimensions and speed ranges

| | Test section | |
|---|---|---|
| | **V/STOL** | **Low speed** |
| Size | | |
| Width, ft (m) | 26.0 | 23.25 |
| Height, ft (m) | 30.0 | 16.25 |
| Length, ft (m) | 63.0 | 43.00 |
| Velocity range | | |
| ft/sec | 20 to 150 | 40 to 300 |
| mph | 14 to 100 | 28 to 200 |
| kn | 12 to 90 | 24 to 180 |
| Dynamic pressure, $lb/ft^2$ | | 2 to 105 |

## D.2 Test conditions

Calibrations of the airflow in each test section have been performed over a region extending 9 ft upstream and downstream of the balance center and 9 ft to each side of the balance center (the balance centers coincide laterally and vertically with the center of their respective test sections). Throughout the calibration region, and within a height of 7 ft above and below the balance center, the dynamic pressure variation is less than 0.5 percent in the low-speed test section and less than 0.75 percent in the V/STOL test section. This variation holds for the entire operational range of dynamic pressure.

Static pressure in the low-speed test section is approximately 5 percent of the dynamic pressure below atmospheric pressure. The static pressure gradient at a height of 3 ft above the test section floor is approximately –0.00054 *Cp*/ft. At the center of the test section, it is approximately –0.00033 *Cp*/ft.

## D.3 Flow quality and calibration goals and requirements

Several wind tunnel customers were surveyed to determine the required accuracy for certain measured or calculated parameters. The results are summarized in Table D.2. One customer stated that, in addition to the accuracies listed, they prefer to test in facilities with turbulence intensities of less than 0.4 percent for force-type testing and less than 0.15 percent for inlet testing.

The end product of a test section calibration is a set of equations that define the angles of attack and yaw and the dynamic and total pressures as functions of the piezometer differential pressure. There are several sets of these equations, each of which is the average over a specific region of the test section. Prior to model installation, the region that the model will occupy is defined and this, in turn, dictates which region-specific calibrations are to be applied. The forms of these equations follow:

*Dynamic pressure, uncorrected for blockage or compressibility:*

$$q_{uc} = K_{q1}q_{ucp} + K_{q2}q_{ucp}^2 + K_{q3}q_{ucp}^3$$

where $q_{ucp}$ is the piezometer differential pressure, described in the following section.

*Total pressure:*

$$P_T = P_{S,sc} + P_{\text{atm}} + K_{PT1}q_{uc} + K_{PT2}q_{uc}^2 + K_{PT3}q_{uc}^3$$

where $P_{S,sc}$ is the settling chamber static pressure and $P_{\text{atm}}$ is the atmospheric pressure.

*Correction to the angles of attack and yaw:*

$$\Delta\alpha = K_{A1} + K_{A2}q_{uc} + K_{A3}q_{uc}2$$

$$\Delta\beta = K_{A5} + K_{A6}q_{uc} + K_{A7}q_{uc}2$$

where $\Delta\alpha$ and $\Delta\beta$ are additive corrections.

Table D.2 — Summary of required accuracy for each test section flow parameter

| Parameter | Required accuracy |
|---|---|
| $q$ | ±0.5 percent |
| $M$ | ±0.005 |
| $P_T$ | ±4.0 psf |
| $\alpha$ | ±0.05° |
| $\beta$ | ±0.05° |
| $dC_p/dx$ | ±0.00005 |
| $T_T$ | ±1.0 °F |
| $C_D$ | ±0.0005 |

[a] 0.3 psf at $M$ = 0.2.

## D.4 Tunnel and calibration instrumentation/hardware description

Test section dynamic pressure is set using piezometer rings located in the settling chamber and at the entrance to each test section. There are two piezometer rings at the entrance to the low-speed test section: an eight-hole "aircraft" and a two-hole "automotive" piezometer. One can configure the aircraft ring by selectively eliminating pressure taps (through the use of valves) to minimize model interference on the measured differential piezometer pressure. The automotive piezometer is designed to minimize the model-to-piezometer interference of automobile models. A differential pressure transducer is connected between the settling chamber and the appropriate test section piezometer, and its output is acquired by the data acquisition system. A list of tunnel instrumentation used for measuring nominal tunnel conditions and for airstream calibrations is provided in Table D.3.

In order to reduce instrumentation calibration errors, system calibrations (also known as end-to-end calibrations) are used on tunnel instrumentation. The instruments used to perform the system calibration are calibrated by the calibration laboratory because these instruments must be held to a higher degree of accuracy.

Table D.3 – List of instrumentation used for measuring tunnel conditions during an airstream calibration of the Lockheed Martin Low Speed Wind Tunnel

| Measurement | Manufacturer | Model | Typical calibration range | Lockheed calibration procedure |
|---|---|---|---|---|
| LSTS[a] dynamic pressure 1 | MKS Baratron | 398HD–00100 | 0 to 20 in. $H_2O$ | 6583C |
| LSTS[a] dynamic pressure 2 | MKS Baratron | 398HD–00100 | 0 to 20 in. $H_2O$ | 6583C |
| Total pressure | MKS Baratron | 398HD–00100 | 0 to 20 in. $H_2O$ | 6583C |
| Atmospheric pressure | Setra | 270 | 28 to 30 in. Hg | 6584 |
| Static temperature | Omega | 44018 | 34 to 120 °F | 9015C |
| Total temperature | Rosemont | 101 | 34 to 120 °F | 9015C |
| Five-hole probe | Lockheed | 07–LS01–5000–700 | ±5° | |
| ZOC-module | Scanivalve | | ±10 in. $H_20$ | In situ with calibrator |
| Inclinometer | Hilger & Watts | Model B | OC0026 | ±90° |

[a]Low-speed test section.

## D.5 Airstream calibration procedure

During airstream calibrations, a rake of seven five-hole, hemispherical-tip probes is installed in the test section as shown in Figure D.2. The probes measure 1.66 in. in diameter and 60 in. in length, with four circumferential static orifices, eight diameters behind the probe tip. The tower supporting the probes has a main member with a 3 in. diameter and has 1-in.-diameter stiffening members. The rake is connected to a 10-in.-of-water Scanivalve ZOC module (Scanivalve, Bath, U.K.). Probe pitch angles are measured with an inclinometer, and probe yaw angles are measured with plumb bobs and scales in relation to the tunnel centerlines. The resulting measurement accuracies are estimated to be ±0.03° in both pitch and yaw.




Figure D.2 – Airstream calibration rake installed in the Lockheed Martin Low Speed Wind Tunnel.

The procedure follows:

(1) The rake is installed with probes initially inverted, positioned with the static orifices within 1 in. of the desired lateral and longitudinal position.

(2) The rake is aligned vertically to within 0.5° in both the pitch and roll planes using an inclinometer on the 3-in. vertical member.

(3) The tunnel dynamic pressure is brought up to 75 lb/ft$^2$ and then returned to zero to set any nonelastic deflections. During the first run of the day, the tunnel is run for 10 min to eliminate any thermal stratification present in the tunnel. New wind-off zeroes and the final, prerun angle settings are recorded before restarting.

(4) Inverted runs are performed at 12.5, 20.0, 30.0, 40.0, 50.0, 60.0, and 75.0 lb/ft$^2$. Three data points are recorded at each dynamic pressure.

(5) The postrun yaw angle of each probe is accurately measured and recorded using plumb bobs off the side of the probe related to a reference line on the floor. This is done in such a way as not to deflect the probe sideways: the weight of the plumb bob is supported only with a downward pull on the string.

(6) The postrun pitch angle of each probe is measured using an inclinometer placed near the base of each probe. Standardized locations near the base of the probe are used so as to eliminate probe deflections.

(7) The probes are then rolled upright.

(8) Upright calibration runs are then performed at 12.5, 20.0, 30.0, 40.0, 50.0, 60.0, and 75.0 lb/ft$^2$.

(9) The yaw and pitch angles of each probe are measured, recorded, and plotted. They are also compared run-to-run; the absolute angles will change, but the relative angles of the probes should be consistent. If not, the problem should be investigated and corrected immediately.

(10) Instrument errors in pitch and yaw are determined from the upright-inverted runs. The differential pressure measurements are converted to angles (bottom minus top for pitch $\Delta P_\alpha$, left minus right for yaw $\Delta P_\beta$). With this sign convention, corrections are added for probe setting error and instrument error. The instrument error corrections for pitch and yaw angle are input to the software.

(11) The rake is moved to the next position, and steps 2, 3, 5, 6, 8, and 9 are repeated until all desired locations have been surveyed.

Historically, surveys have been conducted at $x$ = 0, ±9 ft, and $y$ = 0, ±3, ±6, and ±9 ft. The distance $x$ is positive downstream of the turntable lateral centerline and $y$ is positive to the right (looking upstream) of the longitudinal centerline. The resulting airstream calibrations are applicable to all but sting-mounted models. Surveys for sting-mounted models are normally conducted with the sting support system installed (to obtain sting field-effects at the model location) and are, therefore, beyond the scope of this discussion.

## D.6 Data reduction

Measured parameters include the total, static, and dynamic pressure at each probe location. The flow angularity in pitch and yaw are determined from the five-hole probe data as described in step 10 of the procedure. Online reduction provides fully corrected pressure data, but the angularity data must be corrected for probe setting errors and aerodynamic instrument errors. Setting errors, as previously mentioned, are measured at the end of each run. Aerodynamic corrections require setting error-corrected upright and inverted data to become available. Offline data reduction provides fully corrected data. Online data, however, allow very important data monitoring to be made, and previous experience has demonstrated the need for online data to be scrutinized.

The static pressure gradient may be derived from the rake-measured static pressure readings at various $x$-stations; however, the preferred method is to use a "static pipe." The static pipe, Figure D.3, measures 3 in. in diameter, is approximately 25 ft long, and has three circumferential static orifices at 12-in. intervals

between 2.5 and 22.5 ft from the tip. The static pressure gradient is generally determined along the tunnel centerline for aircraft testing, and 3 ft above the floor for automotive testing.

The data are reduced using various routines that construct calibration sheets for each region of the tunnel. Once these steps have been completed, cross-flow vector, vorticity, and pressure contour plots are constructed for each region using PVWAVE (Visual Numerics, Boulder, CO), a commercially available graphics and data analysis tool. The plots produced by this routine are examined carefully (particularly the total pressure contour plots) to determine if there was excessive instrumentation drift, bad data, or other problems that went undetected online. A decision is then made to void data, apply correction factors, or take other corrective action.




Figure D.3 – Static pipe installed in Lockheed Martin Low Speed Wind Tunnel.

## D.7 Frequency and duration of full and check calibrations

There is no established schedule for airstream calibrations. They are performed on an "as-needed" basis, typically: (1) following modifications that would alter the airflow in the test section (such as changes to the turning vane angle settings) or (2) prior to testing unique model/installation combinations for which a valid airstream calibration does not exist, for example, the location of a model in the test section. Airstream calibrations have been performed, on average, every 3 years.

The piezometers in both the test section and settling chamber are leak-checked semiannually, and empty-test-section calibrations of the ceiling and sidewall static pressure orifices are performed periodically. Furthermore, upright-inverted runs on aircraft models are performed to determine the basic flow angularity. It is assumed that the previous airstream calibration is valid if (1) the piezometer is not found to be leaking, (2) the empty-test-section ceiling and sidewall static pressure calibration repeats the results of previous calibrations, and (3) the upright-inverted runs produce the flow-angularity values that were predicted.

## D.8 Data acquisition system

The data acquisition system at the Lockheed Martin Low Speed Wind Tunnel is an evolving system. It is updated to stay as current as possible with computer technology, instrumentation sensors, and data acquisition methods. The computer systems currently in use consist of PC-based and Compaq-Alpha-based servers and workstations (Hewlett-Packard Company, Palo Alto, CA). All computer programs are written in Fortran on the Alpha systems and in C on the PCs. The Alpha systems utilize Compaq's VMS operating system, and the PCs utilize DOS and Windows.

Data from the wind tunnel instrumentation are input to the data system computers through analog-to-digital converters, read directly as binary-coded decimal (BCD), or measured by frequency counters. Converters are connected to the data system through a Neff Model 620 (Neff Instrument Corporation, Monrovia, CA) with integral signal conditioning and amplification for 128 data channels. The Neff accepts signals between –1.0 and 1.0 V full scale or between –10.0 and 10.0 V full scale, depending on the amplifier cards installed for each four-channel input set. The Neff filters the signals through a 10-Hz low-pass filter to ensure that steady-state voltages are measured. A 10-Hz filter has been found to respond quickly enough to capture the low-frequency data while effectively blocking out high-frequency noise, such as 60-cycle electrical signals.

Six Neff data channels are used to measure three basic wind tunnel airflow parameters and three reference pressures. Any of the remaining analog data channels may be used for reading pressure transducer, thermocouple, strain gauge, or other voltage-signal sources.

The system has been designed to provide both a near-real-time mode for setting and monitoring test conditions and a steady-state recording mode for storing and reducing data that become the test database. The system is automated with system health and data integrity monitoring provided. Model geometric angle, positioning system location, and test section free-stream test conditions are set and controlled by the data system.

## D.9 Data analysis and data corrections

Each mounting system/model combination occupies a certain "region" in the test section. Upon consideration of the model location and translation within the test section, the region is defined and the average flow parameters are determined for this region.

For the required small angle ranges, the calibration of the probe angularity orifices was found to be linear with no pitch/yaw cross-coupling when originally calibrated. Furthermore, there was no significant difference in pitch and yaw calibrations between probes. Therefore, constant calibrations of 0.077 $\Delta P_\alpha$ per degree of pitch and 0.080 $\Delta P_\beta$ per degree of yaw are used throughout. Following the conversion of $\Delta P_\alpha$ and $\Delta P_\beta$ to angles in this manner, corrections for probe setting and instrument error are applied.

In addition to the previously described alignment and instrument error corrections, rake interference corrections are determined. The tower to which the probes are mounted does not correspond well to the stem of a standard pitot-static tube; therefore, the standard correction for static pressure error cannot be used. The error (and the necessary correction) is calculated using source-sink modeling techniques. This also provides the opportunity to compute the tunnel blockage effects. Over the 15 to 75 psf range of dynamic pressure, the main tubular member of the tower changes from subcritical to supercritical flow; therefore, the source strength for its wake is calculated for drag coefficients of 1.2 and 0.3, respectively. Reference 39 reports these drag coefficients for a cylinder and shows them varying smoothly with Reynolds number; therefore, a smooth function is used for the calculations over the range of interest. The correction is applied to the probe-derived dynamic pressure rather than the static pressure.

## D.10 Flow quality information

There are two aspects to the results of an airstream calibration. The first is concerned with defining the quality of the airstream in terms of deviations from the mean. The second is concerned with quantifying the mean conditions for use when testing models in the tunnel. During previous airstream calibrations, it was determined that total, dynamic, and static pressures typically remain within 0.3 percent of the mean for a 2-sec sample time. The root mean square deviation from the mean for pitch and yaw are 0.08° and 0.09°, respectively. Data from previous airstream calibrations demonstrated that a 2-sec sample time is sufficient to accommodate short period fluctuations, but it is probably insufficient for long-term fluctuations. The long-term fluctuations are related to the time required for the flow to travel around the circuit, which, for example, is 32 sec at 50 mph, 16 sec at 100 mph, and 8 sec at 200 mph. It was decided to acquire four repeat data points at each condition rather than increase the sample time.

Figure D.4 shows the average flow angularity in the form of cross-flow vectors. Note that this vector plot is from a previous calibration that is no longer valid and is included only for illustration purposes. Figure D.5 shows the nondimensionalized vorticity distribution. Figures D.6 to D.8 show contours of deviation (percent) from the mean of the total, dynamic, and static pressure, respectively. The means are for the center three rows of probes (i.e., the center tunnel airplane model region) and are for a nominal dynamic pressure of 60 psf.

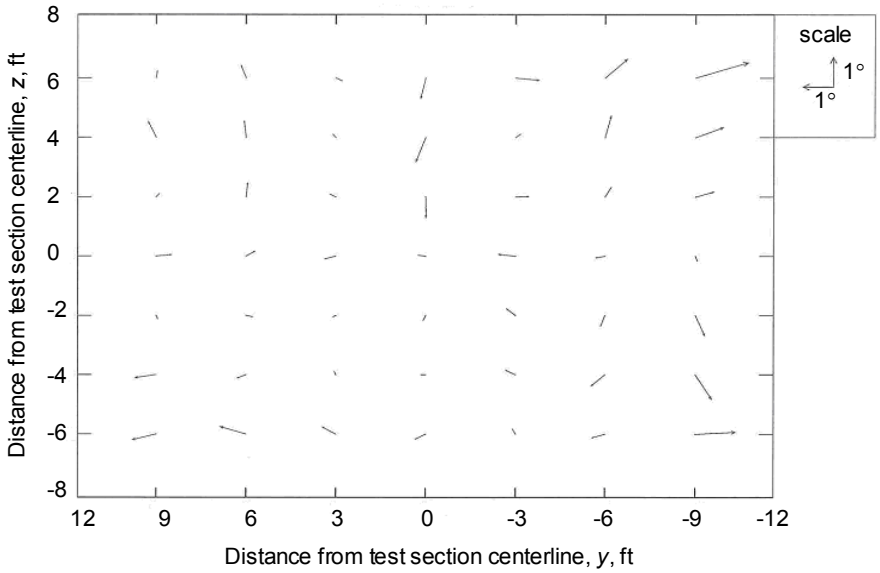



Figure D.4 – Sample cross-flow plot of airstream calibration vectors at $q$ = 60 psf in the Lockheed Martin Low Speed Wind Tunnel.

## D.11 Reporting of results

At the conclusion of an airstream calibration and associated data analysis, an internal communication is prepared and copies circulated to wind tunnel staff, up to the department manager level. This document includes an introduction, background, and descriptions of the experimental method, data reduction, data corrections, results, and discussion. If the calibration is in support of a specific test, that particular customer receives a copy of the document. The document is also commonly included in a data-reduction verification (hand-check case) package that is supplied to all aircraft customers and other customers upon request.

## D.12 Recommendations for future calibrations

For future airstream calibrations, we recommend that provisions be made to allow real-time pitch angle measurement on the rake body as well as on each probe to detect any dynamic-pressure-dependent deflections of the rig. Faster region-specific calibrations could be performed if the rake bar were mounted horizontally, because most of the regions are horizontal rectangles. Software should be modified so that measurements can be made prior to the run to produce fully corrected data online. Software should also be modified to allow online comparison to airplane region values (or other expected values). After the run, the measurements should be verified.

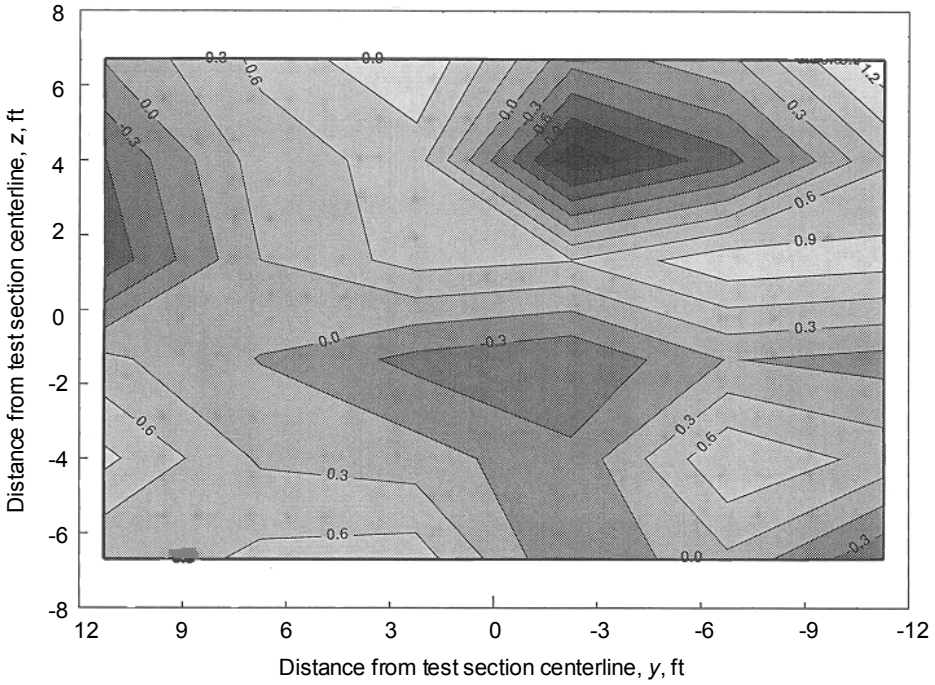



Figure D.5 – Sample test section vorticity distribution plot at $q$ = 60 psf in the Lockheed Martin Low Speed Wind Tunnel.

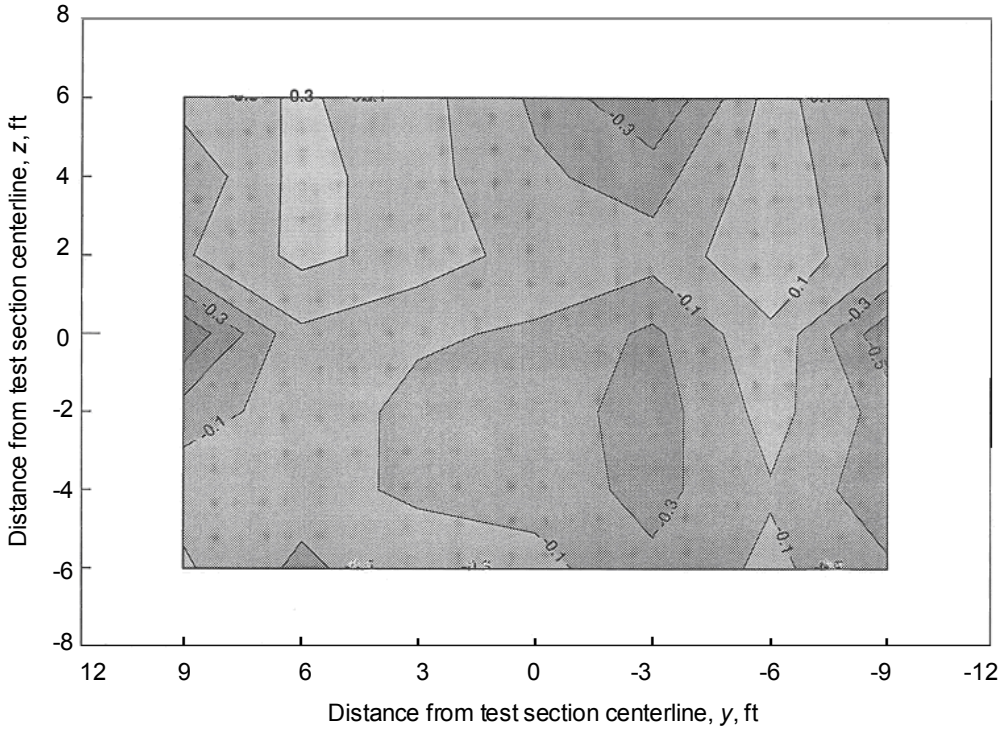



Figure D.6 – Sample plot of total pressure deviation (percent from airplane region mean) at $q$ = 60 psf in the Lockheed Martin Low Speed Wind Tunnel.

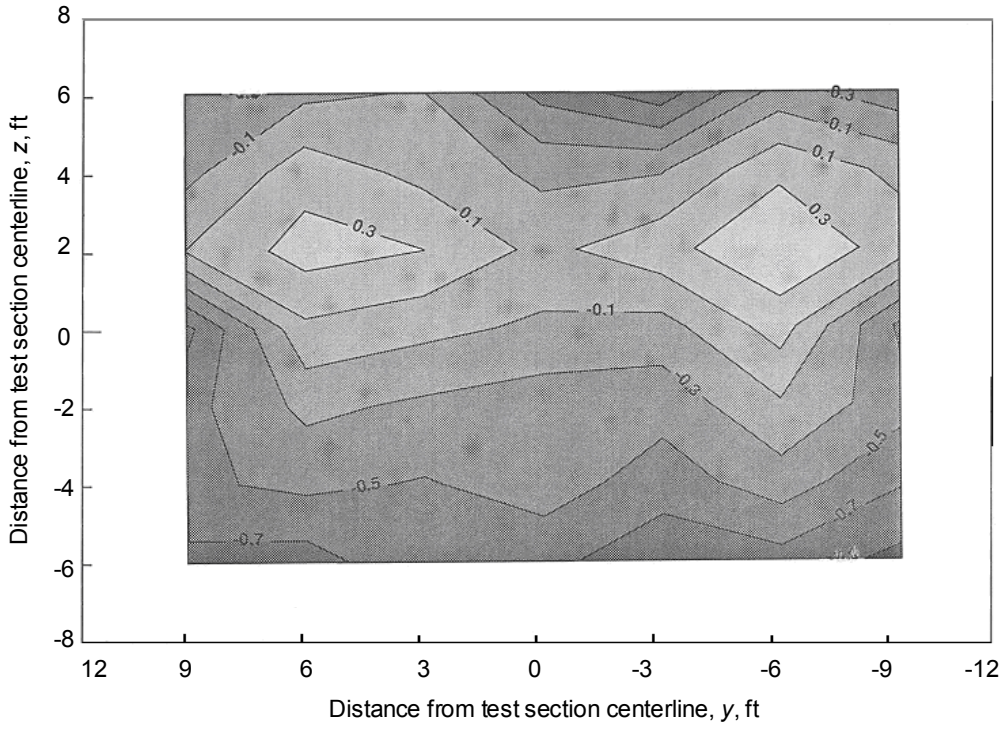



Figure D.7 – Sample plot of dynamic pressure deviation (percent from airplane region mean) at $q$ = 60 psf in the Lockheed Martin Low Speed Wind Tunnel.

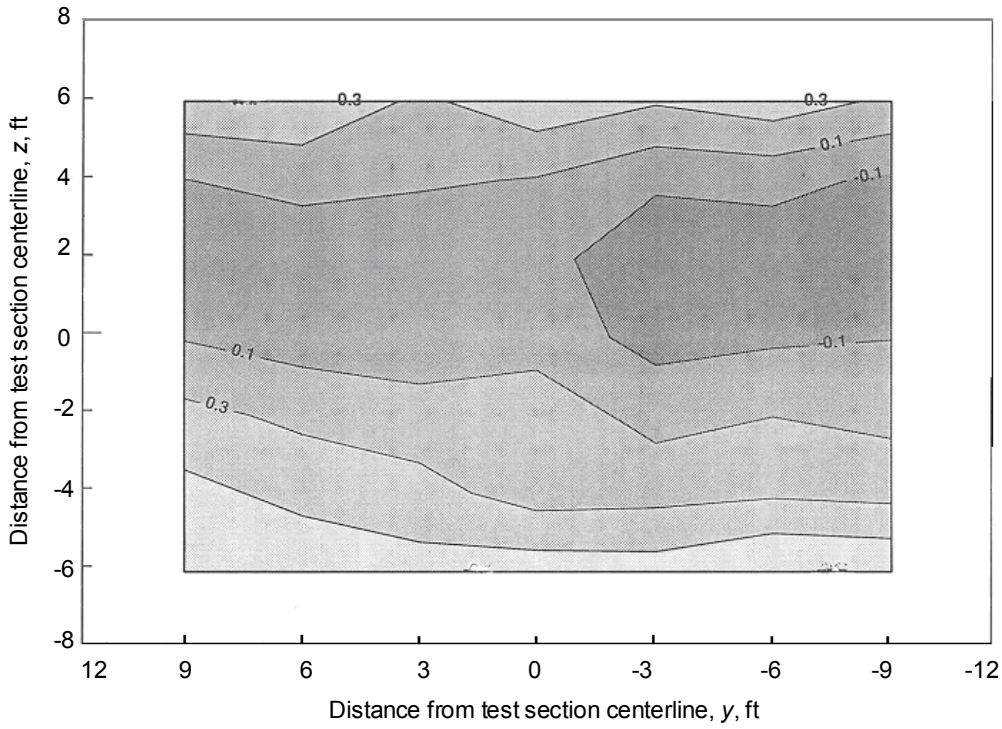



Figure D.8 – Sample plot of static pressure deviation (percent from airplane region mean) at $q$ = 60 psf in the Lockheed Martin Low Speed Wind Tunnel.

# Annex E—Calibration of the 11- by 11-Foot Transonic Wind Tunnel at the NASA Ames Research Center

## E.1 Overview of the facility calibration and flow quality surveys

The comprehensive calibration and flow quality surveys of the 11- by 11-Foot Transonic Wind Tunnel (TWT) include a static pipe calibration, a flow uniformity survey, a turbulence and acoustics survey, and an LB–425 calibration model test. The purpose of each test follows:

- Static pipe calibration—This survey measures the static pressure distribution through the nozzle and test section. The pipe consists of 444 static pressure taps distributed along the 60-ft pipe length at various spacing intervals. Static pressure calibration tables are generated for full-span and semispan test section configurations, and data are used to generate clear tunnel buoyancy corrections for model loads.

- Flow uniformity survey—This survey measures the uniformity of the total pressure, flow angularity, and temperature as well as boundary layer characteristics for full-span and semispan test section configurations. Data are used to create total pressure correction tables. Five-hole cone probe results are useful for evaluating flow anomalies in the test section and flow-angularity characteristics for semispan models. For full-span models, flow-angle corrections to the data are generally determined by testing models in the upright and inverted attitudes.

- Turbulence and acoustics survey—This survey measures the three components of the nondimensional fluctuating mass-flux or “turbulence level” using hot-wire anemometry and noise or “acoustic level” using differential dynamic pressure transducers. Turbulence levels can be an important factor in testing laminar flow airfoils where high levels of free-stream turbulence can cause premature transition of the airfoil boundary layer. Acoustic measurements are used to support weapons bay testing by providing background noise measurements for the test section.

- LB–435 calibration model test—This survey measures the integrated effects of test section flow quality on an actual transport airplane model, tracks flow angularity, and evaluates data repeatability along with test techniques and processes. This model has been tested many times in the 11- by 11-Foot TWT.

This annex discusses the static pipe calibration and flow uniformity survey following the modernization of the 11- by 11-Foot TWT (References 40 and 41). The primary goal of these two tests was to prepare the calibration tables for the 11- by 11-Foot TWT. These tables supply the information that allows the computation of the test Mach number, dynamic pressure, and model buoyancy for the particular mounting location of a test article in the test section. The tables provide the relationship between the facility's institutional total and static pressure measurement and the total and static pressure measurement at the reference point of the model.

Data for the static pipe calibration and flow uniformity survey are acquired for both full-span and semispan test section configurations. For the full-span configuration, all the test section baffled wall slots are open, allowing air exchange between the test section and the plenum. For the semispan configuration, the floor baffles are removed and replaced with solid fillers to provide a solid reflection plane.

The turbulence and acoustics survey conducted after the modernization is reported in Reference 42.

## E.2 Facility description

The Unitary Plan Wind Tunnel (UPWT) consists of three tunnel legs and an auxiliaries facility: the 11- by 11-ft transonic wind tunnel, the 9- by 7-ft supersonic wind tunnel, and the 8- by 7-ft supersonic wind tunnel (Figure E.1). The two supersonic legs share a common 11-stage axial-flow compressor and aftercooler drive leg, and they use diversion valves at the ends of the common leg. A three-stage axial-

flow compressor drives the 11- by 11-ft leg. A common drive motor system can be coupled to either the 3-stage or 11-stage compressor. One tunnel can therefore be run while test articles are being installed in or removed from the other two.

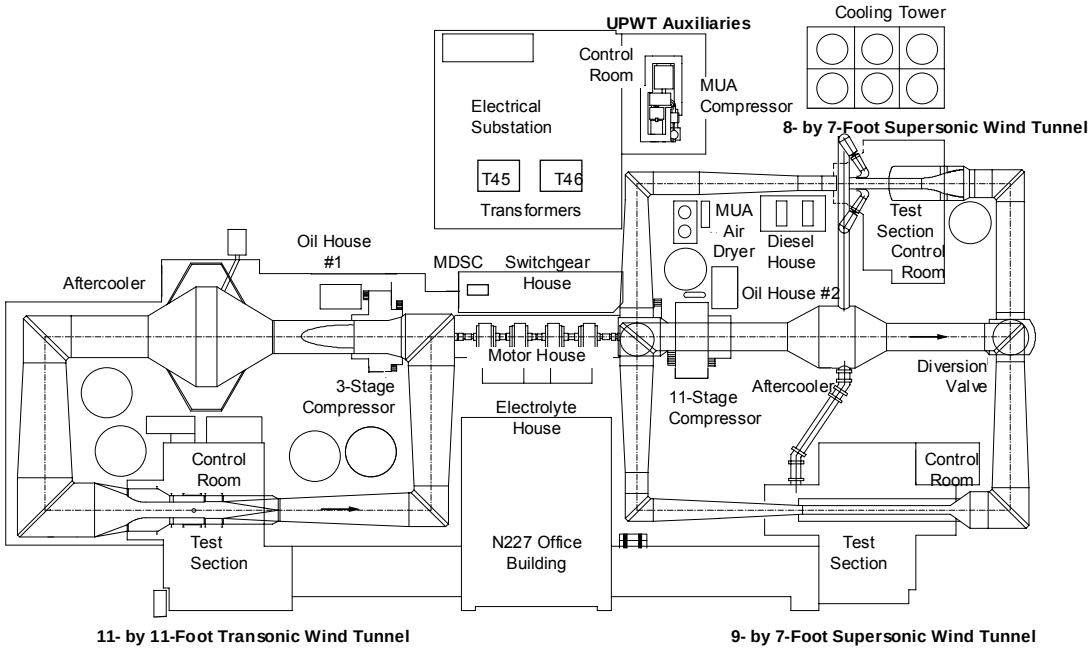



Figure E.1 – Unitary Plan Wind Tunnel (UPWT) at the NASA Ames Research Center.

The 11- by 11-ft transonic leg is a closed-circuit, variable-pressure, continuous operation wind tunnel (Figure E.2). Subsonic Mach number control involves setting the compressor drive speed to one of 10 setpoints and using variable-camber inlet guide vanes for fine Mach number control. Supersonic Mach number control involves setting the flexible wall nozzle to achieve the proper area ratio in addition to setting the compressor drive speed and the inlet guide vanes. A tandem diffuser system with an annular diffuser followed by a wide-angle diffuser is upstream of a 70-ft-diameter aftercooler section in the drive leg. Flow-smoothing vanes are located in the tandem diffuser to improve flow uniformity entering the heat exchanger and temperature uniformity in the test section. The settling chamber upstream of the contraction is 38 ft in diameter. A turbulence reduction system (TRS) located in the settling chamber includes a 1-in.-cell-diameter, 20-in.-long honeycomb for flow straightening followed by two 0.041-in.-diameter-wire, 6-mesh screens for turbulence reduction. The contraction provides a transition from the circular cross section of the settling chamber to the square cross section of the test section. The contraction ratio is 9.4. The test section is 11- by 11-ft in cross section and 22 ft in length. Slots in all four walls run the full length of the test section. The slots contain baffles that provide a 6-percent porosity into the plenum chamber. Ejector flaps on all four walls at the exit of the test section can be set remotely to control the plenum flow bypassed from the test section. Flow exits the test section and enters a transition region back to the circular main diffuser. A plenum evacuation system (PES) provides an active method of removing air from the test section plenum by using the make-up air (MUA) compressor system of the auxiliaries facility.

## E.3 Facility tunnel conditions, hardware, and instrumentation

### E.3.1 Static and total pressure

The tunnel plenum static pressure $P_{S,pc}$ is sampled from eight tubes located within the plenum chamber surrounding the test section. The tube bundle is located streamwise at tunnel station (TS) 30, laterally at $y$ = 118 in. (52 in. outward from the test section wall), and vertically at $z$ = 0 in. (the tunnel centerline).

Two of the tubes supply the primary and backup $P_{S,pc}$ measurement used to compute Mach number in the data system. The tubes are connected to pressure transducers located in racks that are within a foot in elevation of the tunnel centerline.

The uncorrected tunnel total pressure $P_{T,sc}$ is sampled from three identical rakes located in the settling chamber just downstream of the turbulence reduction screens. Each rake has eight pitot probes, and each probe is manifolded to its counterpart on the other rakes and pneumatically connected and routed out of the tunnel. Two of these sources serve as the primary and backup $P_{T,sc}$ measurements used to determine Mach number in the data system. The probes are connected to pressure transducers located in racks that are within a foot in elevation of the tunnel centerline.

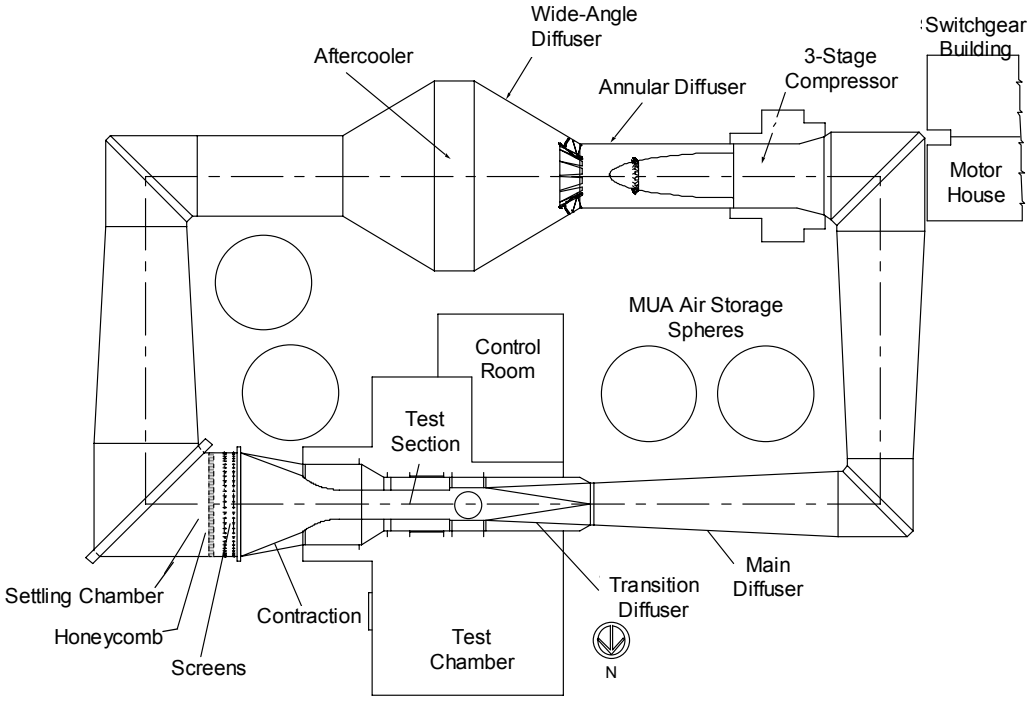



Figure E.2 – 11- by 11-Foot Transonic Wind Tunnel.

The additional $P_{S,pc}$ and $P_{T,sc}$ source probes are also routed out of the tunnel and are used as sources for the facility's control system measurements, as redundant sources for the data system, or as auxiliary sources for testing purposes (i.e., as test-dependent reference pressures or calibration pressures).

The $P_{S,pc}$ and $P_{T,sc}$ pressures used to determine the test section Mach number are measured with the facility's flow reference system. Two complete flow reference systems are used for all tests, a primary and a backup. Each system comprises four precision transducers with different sensing ranges. Two quartz transducers sense $P_{T,sc}$ and two special high-accuracy silicon transducers sense the pressure differential $P_{T,sc} - P_{S,pc}$. The absolute transducers sensing $P_{T,sc}$ have ranges of 15 and 45 psia and accuracy ratings of 0.01 percent of full scale. The transducers sensing the differential pressure $P_{T,sc} - P_{S,pc}$ have ranges of 10 and 30 psid and accuracy ratings of 0.02 percent of full scale. The transducers are transported to the NASA Ames Metrology lab on a fixed schedule and calibrated against NIST traceable standards. Built-in overpressurization features protect the low-range transducers from damage. Depending on the facility operating speed and pressure, software selects between the low or high range $P_{T,sc}$ and $P_{T,sc} - P_{S,pc}$ measurements to give the best Mach number accuracy. Uncertainty analysis of this system has determined that Mach number errors caused by flow reference system measuring errors are less than ±0.0005 for all operating conditions within the facility test envelope.

### E.3.2 Tunnel total temperature

The tunnel total temperature $T_{T,F}$ is measured using four resistance temperature detector (RTD) probes. The probes are located on the corner vanes upstream of the settling chamber and distributed on the face of the turning vanes in the core flow. The four temperature readings are averaged to obtain a temperature measurement representative of the flow cross section. The accuracy of these temperature probes is stated by the manufacturer to be ±2.0 °F.

### E.3.3 Specific humidity

A microprocessor-controlled humidity analyzer is used to measure the moisture content of the air within the tunnel circuit. The analyzer uses a chilled-mirror dew-point sensor and a pressure transducer to determine dew-point temperature, absolute pressure, and other psychometric variables. Data from a primary and backup analyzer are recorded to the data system in units of parts per million (ppm) by weight. The accuracy of the humidity measurement is ±50 ppm by weight.

The humidity measurements are used as indicators of when to increase the dry air exchange rate or, in some cases, when to cease testing to purge the humid tunnel air and replenish with dry air. For most tests, a limit of 500 ppm by weight is used to guide dry air exchange and purge decisions. Wind tunnel flow condition data are not corrected for tunnel humidity effects in the data system.

## E.4 Facility calibration goals

An outline of the static pipe test goals follows:

- Determine the test section static pressure calibration tables for semispan and full-span test section configurations.
- Determine the in-test data repeatability of the calibration factors.
- Establish time histories of institutional tunnel condition pressures at several selected Mach numbers.
- Determine the amplitude and frequency content (0.1 Hz < frequency < 10 Hz) of the $P_{S,pc}$ and $P_{T,sc}$ variation for its effect on test data accuracy.
- Determine a time correlation between pipe pressures and $P_{S,pc}$ to ascertain the effect of pneumatic tube lag and damping on calibration accuracy.

An outline of the flow uniformity test goals follows:

- Map the total pressure, total temperature, and flow-angle uniformity in the survey regions.
- Determine the test section total pressure calibration tables for full-span and semispan test section configurations.
- Measure the boundary layer profiles at three test section streamwise locations, and determine the displacement thickness and momentum thickness.

## E.5 Facility calibration installation and instrumentation

### E.5.1 Static pipe installation

The test installation of the static pipe is shown in Figure E.3. For this calibration, the 6-in.-diameter static pipe was mounted at two heights within the test section. The centerline height was used to determine calibration data for full-span model tests, whereas the position 33 in. below centerline was used to determine the tunnel calibration data for semispan model tests.

The pipe was suspended between a set of tensioning cables at the upstream end and the sting model support system (SMSS) at the downstream end. A hydraulic cylinder connected the static pipe to the SMSS through clevis/pin joints. The cylinder provided up to 10 000-lb tension to add stiffness and stability to the pipe.

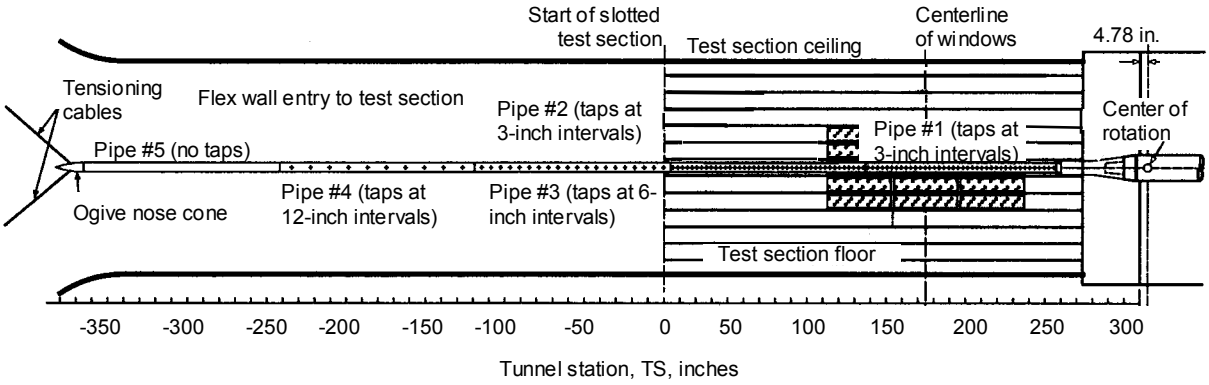



Figure E.3 – Static pipe installation in the 11- by 11-Foot Transonic Wind Tunnel.

The pipe is composed of five 10.25-ft-long segments that are connected end-to-end with Marmon Clamps. The clamps were hand fitted to provide an extremely smooth connection between pipe sections. The pipe sections were numbered one through five starting at the downstream end and progressing upstream. The first two pipe segments were instrumented with pressure taps at 3 in. intervals longitudinally along the pipe. At each axial station, four pressure taps were placed 90° from one another. In addition, each set of four taps was rotated about the pipe centerline by 15° from its upstream neighbors so that the downstream taps were not within the disturbance flow field of the upstream taps. Pipe 3 had pressure taps at 6-in. intervals, pipe 4 at 12-in. intervals, and pipe 5 was not instrumented. There were a total of 444 separate pressure taps on the four instrumented pipe segments. The first two segments extended through the length of the slotted test section and contained 324 of these taps.

### E.5.2 Static pipe instrumentation

Miniature electronically scanned pressure (ESP) instrumentation with digital temperature compensation (DTC) was used to measure the pressures associated with the calibration test ($P_{S,pipe}$) along the static pipe. With DTC, each of the pressure sensors in the ESP module is characterized for temperature dependence within the instrumentation firmware. As pressure data are acquired during tests, the temperature of each individual transducer is sensed and corrections are applied to the measurements to account for temperature-induced drift. This feature gives the system a remarkable degree of stability and accuracy and reduces the overall calibration requirements.

A stable monitor pressure was measured with both a transducer on each DTC ESP module, and a high-accuracy quartz transducer. The pressure-measuring accuracy, as indicated by the monitor pressure error, remained well within the manufacturer's specification for many hours of continuous testing. The largest single source of instrument error on previous calibrations using the older technology ESP units had been temperature drift on the transducers, which occurred at different rates and in opposite directions.

Modules populated with 5-psid transducers were used for most of the static pipe pressures that were located within the test section. Pressures extending into the nozzle section were measured with 15-psid transducers. Referring to Figure E.3, pressures upstream of TS –48 and downstream of TS 232 were measured with two 15-psid instruments, and all others were measured with six 5-psid units. The manufacturer's specification for accuracy on the transducers was 0.05 percent of the transducer's full scale rating. This translates to ±0.36 psf for the 5-psid modules and ±1.08 psf for the 15-psid units.

An uncertainty analysis undertaken during the test planning period revealed that the key to calibration accuracy was accurately measuring the pressure difference ($P_{S,pipe} - P_{S,pc}$). With this in mind, seven unused ports on each of the static pipe modules were pneumatically connected to the extra facility $P_{S,pc}$ pressure. The data were then reduced in a manner that removed the error associated with the module reference pressure transducer (so that it was not included in the overall error budget) by making it a "common mode," or "correlated," biasing error. The overall instrumentation uncertainty for measuring the pressure difference ($P_{S,pipe} - P_{S,pc}$) was nominally ±0.23 psf for the 5-psid modules and ±0.56 psf for the 15-psid units.

### E.5.3 Flow uniformity installation

Models mounted on the SMSS are generally positioned to locate the balance center in the range from TS 155 to TS 165. Semispan models are mounted on the turntable model support system (TMSS), which is situated on the floor at TS 106. The flow uniformity test surveyed the flow field near TS 165 and 106 using two hardware installations. A flow-angle probe and a total temperature probe were used to make local measurements of total pressure, flow angularity, and total temperature. In addition, boundary layer rakes were positioned at three streamwise locations to measure the boundary layer growth characteristics in the test section.

A planar survey at TS 165 was conducted using the MK XII traversing head survey apparatus, shown in Figure E.4. The MK XII consists of a 0°-sweep, 80.5-in.-span symmetric wing with a traversing head (mouse). The mouse supports both the flow angle and the total temperature probes and has a cavity for instrumentation. The temperature probe was mounted 2.5 in. above the flow-angle probe. The mouse, which was remotely controlled, was traversed laterally across the wing over a $y$ = ±30 in. range. The entire apparatus was supported by sting hardware mounted to the SMSS, allowing vertical translation of $z$ = ±36 in. Stress load limitations prevented the MK XII from being used at supersonic conditions, so it was replaced with a probe holder. This fixed the flow-angle probe position on the tunnel centerline ($y$ = 0 in.) and the temperature probe at $y$ = 3.5 in.

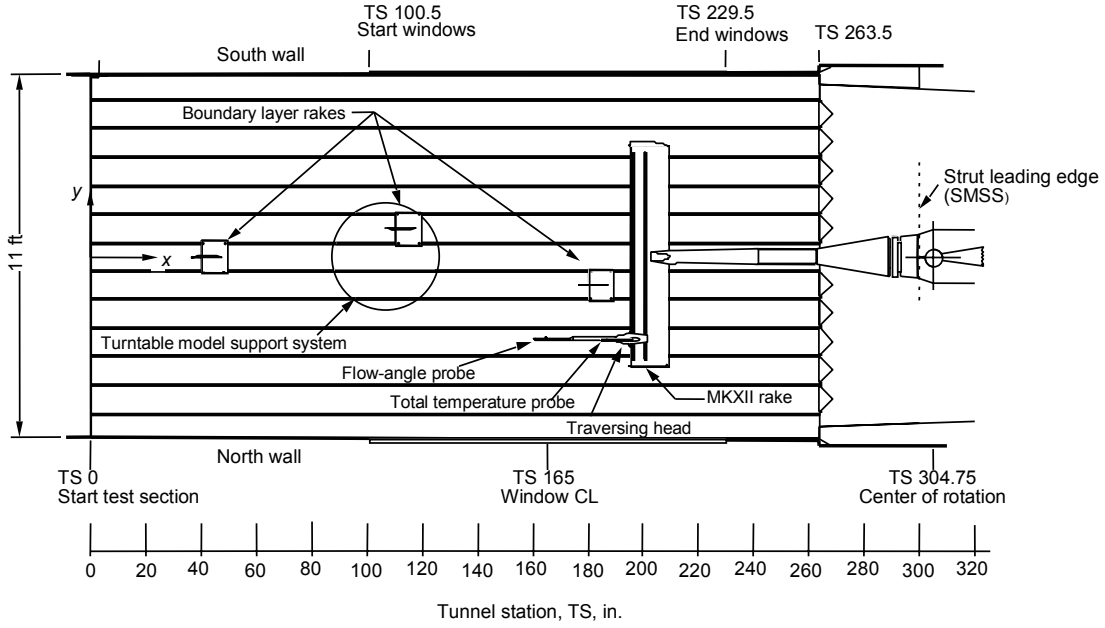



Figure E.4 – MK XII installation in the 11-by 11-Foot Transonic Wind Tunnel.

The same probe holder was used for a centerline survey at TS 106 over a vertical range of $z$ = –54 to 24 in. For this measurement, the floor slot baffles were removed and replaced with solid fillers to provide the reflection plane necessary for semispan model testing.

### E.5.4 Flow uniformity instrumentation

Flow-angularity and total pressure data were collected from a five-hole cone probe with holes arranged on a 40° conical nose and a set of static-sensing taps arranged on the aft body (Figure E.5). Pressure differences across the cone were measured using temperature-compensated, 1-psid pressure transducers. The manufacturer-quoted accuracies are 0.06 percent "best straight line" with ±0.025-percent of full scale/°F for thermal zero shift and ±0.01 percent of reading/°F for thermal sensitivity shift. The transducers were calibrated at the NASA Ames Metrology lab using equipment traceable to NIST standards. The probe total and static pressures were each plumbed to eight ports on a 15-psid, DTC ESP module.

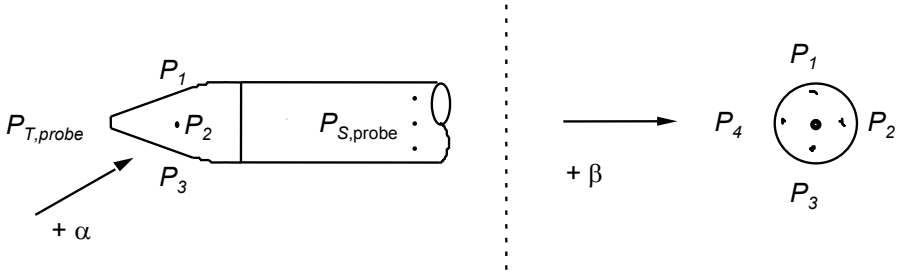



Figure E.5 – Five-hole cone probe.

Probe angle of attack was measured using a precision accelerometer. The accelerometer was placed in the traversing head for the MK XII installation and in the instrumentation cavity on the supersonic probe holder. Accelerometers were calibrated at the NASA Ames Metrology lab and re-zeroed in the test section against a standard with an accuracy of 0.005°. Probe sideslip angle was measured using the SMSS knuckle-sleeve device, which uses a pair of rotating bent arms called the knuckle and the sleeve to obtain taper angles in the pitch and yaw planes anywhere between ±15°. The angular offsets between the probe tip and the angle measurement devices were carefully measured and accounted for in the data reduction. The horizontal position of the probe along the *y*-axis was measured using an encoder, and the vertical position along the *z*-axis were measured using a string pot.

Test section total temperature $T_{T,\text{probe}}$ was measured with an RTD mounted in a shielded probe holder. The accuracy of this airflow probe was stated by the manufacturer to be ±2.0 °F.

Boundary layer characteristics were defined from measurements using three 10-in.-high rakes. Each rake was instrumented with twenty 0.04-in.-diameter pitot probes. The probes were plumbed to 15-psid transducers on DTC ESP modules. The boundary layer rakes were positioned on the test section floor with rake 1 at $x$ = 36 in., $y$ = 0 in.; rake 2 at $x$ = 106 in., $y$ = 10.4 in.; and rake 3 at $x$ = 176 in., $y$ = –10.4 in.

Redundant facility $P_{T,sc}$ and $P_{S,pc}$ pressures were measured using eight ports on the same DTC ESP modules used for the flow-angle probe pressures. As with the static pipe, these pressures were used in the data reduction to minimize the bias error associated with the ESP module reference pressure.

## E.6 Data acquisition

Steady-state data were acquired using the wind tunnel facility's standard data system (SDS). The SDS consists of a subsystem management processor (SMP), a number of functional subsystem processors (FSPs), and a large number of X-terminals that provide wind tunnel personnel with graphical user interfaces to the features of SDS. The SMP is an Enterprise 3500 server (Sun Microsystems, Santa Clara, CA) running the Solaris operating system. The SMP manages the overall data acquisition activity in a facility. Its tasks include coordinating the FSPs, interfacing with the automated tunnel condition and model attitude control systems, and providing a command and control interface for operations personnel. The SMP also provides visualization and analysis tools for both the real-time and near-time data streams. FSPs are Pentium-class PCs running LynxOS Real-Time UNIX (Lynx Real-Time Systems, Inc.). These

modular units are responsible for collecting data from particular types of sensors. The six FSP instrument categories are balance, surface pressure, digital, general purpose analog, tunnel condition/model attitude, and temperature. Each FSP was designed to perform instrument-specific data acquisition tasks for collecting the highest quality data at the sensor and instrument's maximum throughput. Sensor data were transmitted in parallel across a 100 Base-T Ethernet highway to the SMP, where they were averaged, converted to common engineering units, and further reduced to test-specific final results.

### E.6.1 Static pipe data acquisition

The static pipe test provided one set of calibration tables for sting-mounted models and a second set for turntable-mounted semispan models. The calibration tables for semispan testing were measured with the static pipe located 33 in. below the tunnel centerline, which more closely matches the model reference point of semispan models. Data were normally recorded in groups of six data points with a 30-sec delay programmed between data points. Several of the calibration test conditions were repeated up to five times over the duration of the test so that repeatability statistics could be extracted from the test database. All data were acquired using a 1-sec sampling period, which was determined to be optimum during an initial sampling study. The reference pressure used for the static pipe ESP modules was a steady "driven" or controlled pressure and was set to be within ±0.5 psi of the tunnel static pressure as the tunnel was set to the desired Mach number and total pressure. Pressures were allowed to settle for several minutes before data were taken at the new tunnel conditions.

### E.6.2 Flow uniformity data acquisition

Test section flow properties were measured at Mach numbers of 0.4, 0.6, 0.8, 0.85, 1.2, and 1.4 at total pressures of 2120, 3180, and 4600 psf. A sampling study was initially performed, and a 1-sec duration was chosen for data acquisition. A flow-angle probe calibration was performed at 3180 psf for subsonic Mach numbers and at 2120 psf for supersonic Mach numbers with the flow-angle probe on the centerline at TS 165. The calibration involved pitching the probe from –2° to 2° in 0.25° increments for four probe orientations, $\phi$ = 0°, 180°, 90°, and 270°. The MK XII survey apparatus was then installed, and the planar survey was conducted at TS 165. The mouse was traversed horizontally from $y$ = –30 to 30 in., in 6-in. increments. At each horizontal position, the survey apparatus was traversed from $z$ = –36 to 36 in., in 6-in. increments. After the survey was completed for a given tunnel conditions set point, the next calibration condition was set and the probe positioning was conducted in the reverse order. For the supersonic test conditions, the MK XII was replaced with the probe holder and a centerline survey was conducted from $z$ = –36 to 36 in., in 6-in. increments.

For evaluating the flow uniformity for the semispan model test, the centerline survey hardware was moved to TS 106 and the slot baffles were removed from the test section floor and replaced with solid fillers. The centerline survey was conducted from $z$ = –54 to 24 in., in 6-in. increments. Boundary layer rakes were initially installed in the test section for the survey at TS 165 but were removed when they interfered with the flow-angle measurements at the supersonic conditions.

## E.7 Data reduction

### E.7.1 Calibration equations

The static pipe and flow uniformity tests provide the calibration tables to correct the facility's institutional total and static pressure measurement to the true total and static pressure in the test section. The tables provide one correction factor for static pressure, $C_{PS,\mathrm{cor}}$, and a second factor for total pressure, $C_{PT,\mathrm{cor}}$. These factors are defined as follows:

$$C_{PS,\mathrm{cor}} = \left( \frac{P_{S,\mathrm{pipe}} - P_{S,c}}{q_c} \right) \tag{E.1}$$

and

$$C_{PT,\text{cor}} = \left( \frac{P_{T,\text{probe}} - P_{T,sc}}{q_c} \right) \tag{E.2}$$

Each of the calibration tables contains entries for 38 test section locations at 3-in. intervals, 15 Mach numbers, and 4 total pressures. When a data reduction program is set up for a test project, the streamwise location of the model reference point in the test section and the test type (full-span or semispan) are specified. A lookup table is then extracted from the calibration table, which includes correction factors at the 15 calibrated Mach numbers and 4 calibrated total pressures. During the test project, this table was used to obtain correction factors for $P_{T,sc}$ and $P_{S,pc}$. For intermediate points between the calibrated test conditions, linear interpolation was performed on both $P_{T,sc}$ and $M_c$ to arrive at the proper correction factors. Linear extrapolation was used to determine the correction factors for points outside the calibrated test conditions.

The correction factors were used to generate corrected test conditions as follows:

$$P_{S,ts} = P_{S,c} + C_{PS,\text{cor}}\left(q_c\right) \tag{E.3}$$

$$P_{S,ts} + P_{T,sc} + C_{PS,\text{cor}}\left(q_c\right) \tag{E.4}$$

The calibrated tunnel Mach number and dynamic pressure were then computed from $P_{S,ts}$ and $P_{T,ts}$ using standard compressible flow equations (Reference 43).

### E.7.2 Flow uniformity equations

#### E.7.2.1 Local *A*-plane and *B*-plane flow angles

Flow angularity in the 11- by 11-Foot TWT is referenced to the tunnel coordinate system whose origin is located at the start of the test section along the centerline (Figure E.4). The flow angle $\alpha$ is in the *A*-plane, which is the vertical plane defined by the *x*–*z* axis. The flow angle $\beta$ is in the *B*-plane, which is the horizontal plane defined by the *x*–*y* axis. The sign conventions for flow angularity are defined in Figure E.5. Positive $\alpha$ is flow coming up from the floor, positive $\beta$ is flow from the south wall to the north wall, or from the right to the left, pilots view.

The local flow angles in the *A*-plane and *B*-plane were defined by

$$\alpha_m = \left[ K_{\alpha 1}\left( \frac{P_3 - P_1}{q_{\text{probe}}} \right)^2 + K_{\alpha 2} \right] K_\phi \tag{E.5}$$

$$\beta_m = \left[ K_{\beta 1}\left( \frac{P_4 - P_2}{q_{\text{probe}}} \right) + K_{\beta 2} \right] K_\phi \tag{E.6}$$

The local flow angularity was then adjusted for the probe angle of attack and sideslip to give the flow-angularity properties in the tunnel coordinate system.

$$\alpha = \alpha_m - \alpha_{\text{offset}} \tag{E.7}$$

$$\beta = \beta_m - \beta_{\text{offset}} \tag{E.8}$$

#### E.7.2.2 Total temperature

Test section total temperature variation is an important indicator of transonic test section flow quality. A temperature recovery factor was computed to evaluate the probe performance,

$$K_{T,\text{rec}} = \left( \frac{T_{T,\text{probe}} - T_s}{T_T - T_s} \right) \tag{E.9}$$

The probe temperature was then corrected using the recovery factor,

$$T_{T,P\text{cor}} = T_{T,\text{probe}} \left[ \frac{10.2M^2}{1 + 0.2K_{T,\text{rec}} \left( M^2 \right)} \right] \tag{E.10}$$

#### E.7.2.3 Boundary layer

The boundary layer displacement thickness and momentum thickness were computed from the rake total pressures and the free-stream tunnel conditions using the following equations:

*Displacement thickness*

$$\delta_1 = \int_0^{\delta} \left( 1 - \frac{\rho_L u_L}{\rho_e u_e} \right) dy \tag{E.11}$$

*Momentum thickness*

$$\delta_2 = \int_0^{\delta} \frac{\rho_L u_L}{\rho_e u_e} \left( 1 - \frac{u_L}{u_e} \right) dy \tag{E.12}$$

The pressure data, the standard definition for Mach number, and a temperature profile that assumed an adiabatic wall boundary condition were used to determine the ratios of the local velocity to the edge velocity and the local density to the edge density.

*Ratio of the local velocity to that at the boundary layer edge*

$$\frac{u_L}{u_e} = \left( \frac{M_L}{M_e} \right) \sqrt{\frac{1.0 + 0.2T_R \left( M_e \right)^2}{1.0 + 0.2T_R \left( M_L \right)^2}} \tag{E.13}$$

where $T_R$ is the temperature recovery factor (0.986).

*Ratio of the local density to that at the boundary layer edge*

$$\frac{\rho_L}{\rho_e} = \left(\frac{T_{s,e}}{T_{s,L}}\right)\sqrt{\frac{1.0 + 0.2T_R\left(M_L\right)^2}{1.0 + 0.2T_R\left(M_e\right)^2}} \qquad \text{(E.14)}$$

### E.7.3 Data reduction methods for the static pipe

At any given axial position along the static pipe, the four measured pressures were averaged and converted to pressure coefficient form using Equation (E.1). The plotted symbols in Figure E.6 are the average of all of the data points that were acquired during the test period for the given test condition (Mach 0.95, $P_{T,sc}$ = 1.0 atm). For this particular test condition, each symbol is an average of 120 data points. The heavy solid line in Figure E.6 is a plot of a smoothing curve fit determined from the set of averaged data. A polynomial curve fit method was used for all calibration data from Mach 0.2 through 1.0. For supersonic test conditions, a "boxcar" smoothing algorithm was used because the pressure distributions did not fit the polynomial pattern. Weak tunnel- and static-pipe-generated shocks and expansions caused the more erratic pressure distributions that were measured at supersonic conditions. Curve fit results were used to generate both the tunnel control system tables for setting tunnel Mach number and Reynolds number and data-reduction system tables for computing Mach numbers and Reynolds numbers for test projects.

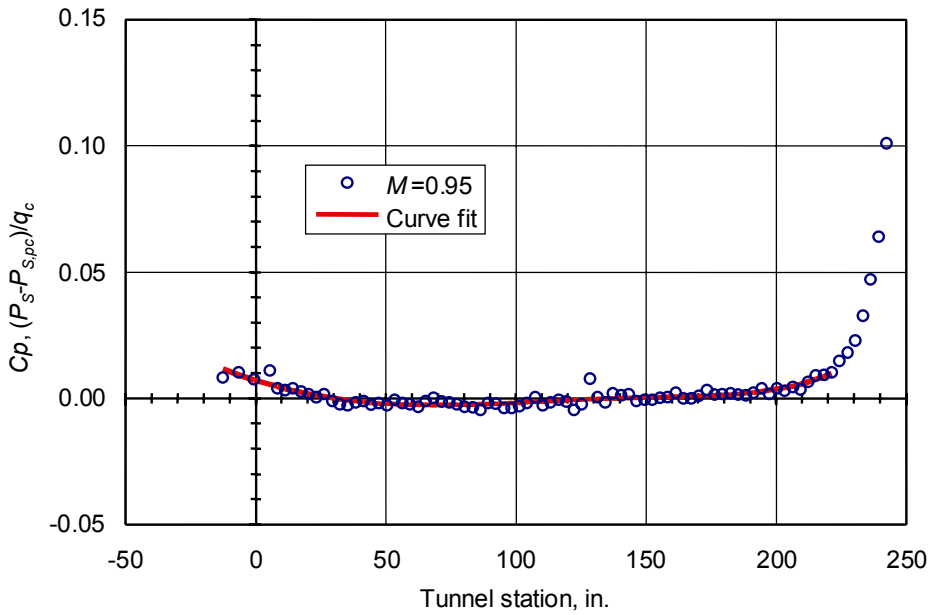



Figure E.6 – Average centerline *Cp* distribution and curve fit for $M$ = 0.95, $P_{T,sc}$ = 2125 psf. Sample duration is 1.0 second; number of data points, 120.

### E.7.4 Data reduction methods for flow uniformity

Established procedures were used for calibrating the five-hole cone probe in the test section for various Mach numbers at a tunnel total pressure of 3180 psf. These procedures involved pitching the probe at four roll orientations, $\phi$ = 0°, 180°, 90°, and 270°. Calibration constants derived from calibration runs were applied to the measured pressure data to compute the local flow-angularity properties of the tunnel using Equations (5) to (8). Data were then processed using commercially available data analysis software to produce flow-angle vector plots. An average recovery factor of 0.94 was determined from the temperature data and used to compute the corrected temperature in the test section for all runs.

## E.8 Calibration results

### E.8.1 Factors affecting the static pipe calibration results

#### E.8.1.1 Temporal variation of test section flow

The standard deviations of the pipe *Cp*'s at Mach 0.95 and $P_{T,sc}$ = 1 atm are presented in Figure E.7. The data points were recorded once per second for 120 sec. The odd shape shown in Figure E.7 with its minimum point near TS 230 and continuously varying standard deviation is caused by a combination of pneumatic lag in the pressure tubing of the pipe and a low-frequency, small-amplitude time variation of test section static pressure. The pressure-scanning modules were mounted in the instrumentation enclosure of the SMSS. The pressure tubing from the module to the port, therefore, increased in length from the ports at the downstream end of the pipe to the upstream end.

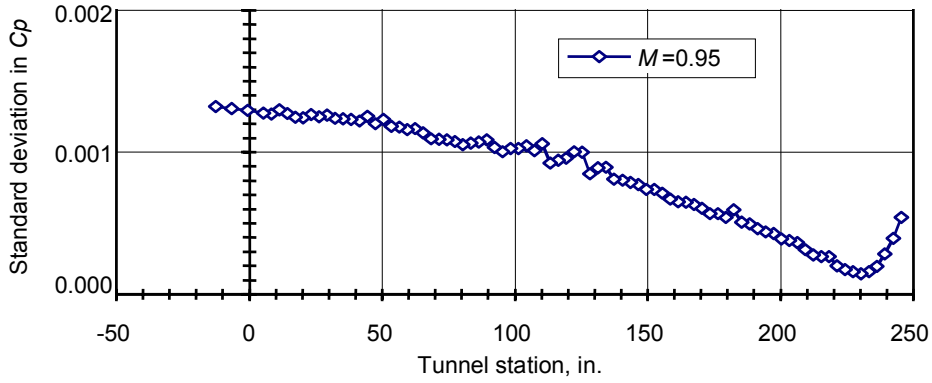



Figure E.7 – Standard deviation in the centerline *Cp* distribution at Mach = 0.95, $P_{T,sc}$=2125 psf. Sample duration, 1 sec; number of data points, 120.

A comparison of the time variation of the facility reference static pressure $P_{S,pc}$ and the measured static pipe pressure at TS 230 (the standard deviation minimum point in Figure E.7) is presented in Figure E.8. The normalized deviations of the two pressures are compared so that time correlation is clearly illustrated within a single figure. Both the phasing and standard deviation of the time variation of these two pressures are nearly identical. The correlation coefficient of the two pressures is indicated on the figure as 0.997. At this location on the static pipe, the pneumatic damping characteristic of the tubing is equal to the damping of the $P_{S,pc}$ pressure tubing. At TS 110, the pressure tubing connecting the static pipe port to the pressure scanning module is 120 in. longer than it is for the taps at TS 230. The comparison of the normalized deviation of the pipe pressure at this location is shown in Figure E.9. This figure shows that the pipe pressure at TS 110 is lagging in time and has a reduced standard deviation with respect to the $P_{S,pc}$ pressure. At TS 0, the pressure tubing connecting the static pipe port to the pressure scanning module is 230 in. longer than it is for the taps at TS 230. Figure E.10 shows that this pipe pressure lags more and shows a further reduced standard deviation with respect to $P_{S,pc}$. The effect of the combination of the tunnel time varying flow and the pneumatic tubing damping/lag differences results in added precision uncertainty averaging about ±0.001 to the measured static pipe pressure coefficients. Smoothing by curve fit and averaging of multiple data points negates most of the effects of this source of data inaccuracy.

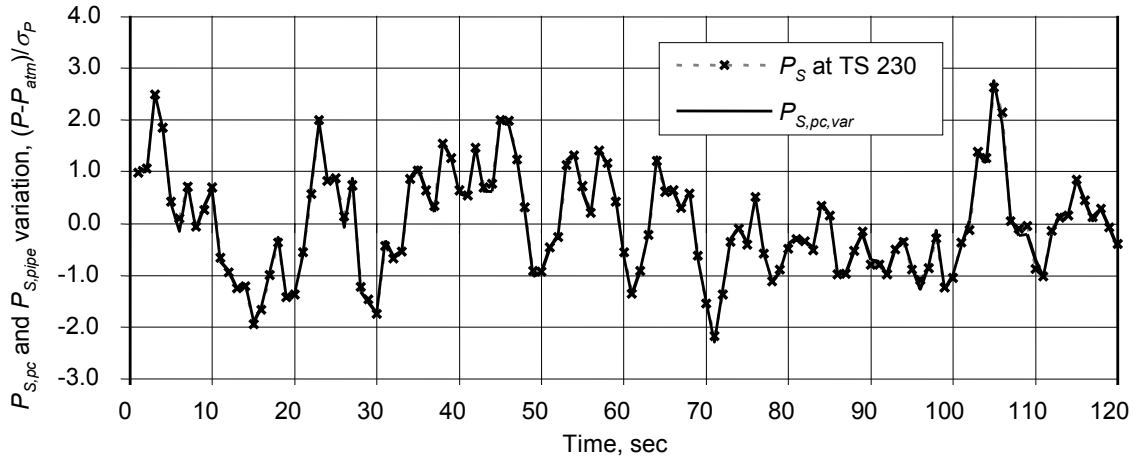



Figure E.8 – Temporal variation of test section pressure at tunnel station 230 for Mach = 0.951 and $P_{T,sc}$= 2125 psf. Sample duration, 1 sec; correlation coefficient, 0.9970; $P_{S,pc}$, 1187.7 psf; $\sigma_{P_{S,pc}}$, 1.29 psf; $P_{S,pipe,avg}$, 1204.97 psf; $\sigma_{P_{S,pipe}}$, 1.22 psf;.

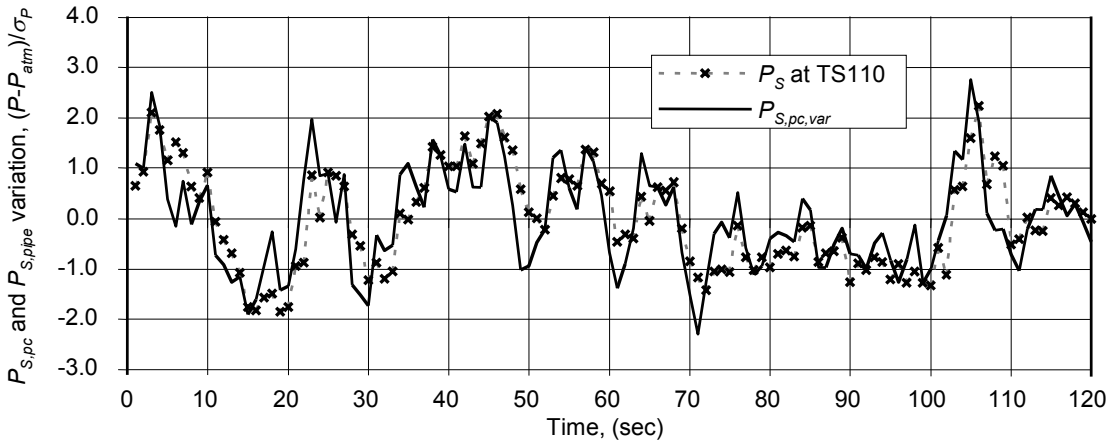



Figure E.9 – Temporal variation of test section pressure at tunnel station 110 for Mach = 0.951 and $P_{T,sc}$= 2125 psf. Sample duration, 1 sec; correlation coefficient, 0.799; $P_{S,pc}$, 1187.7 psf; $\sigma_{P_{S,pc}}$, 1.29 psf; $P_{S,pipe,avg}$, 1185.60 psf; $\sigma_{P_{S,pipe}}$, 0.84 psf;.

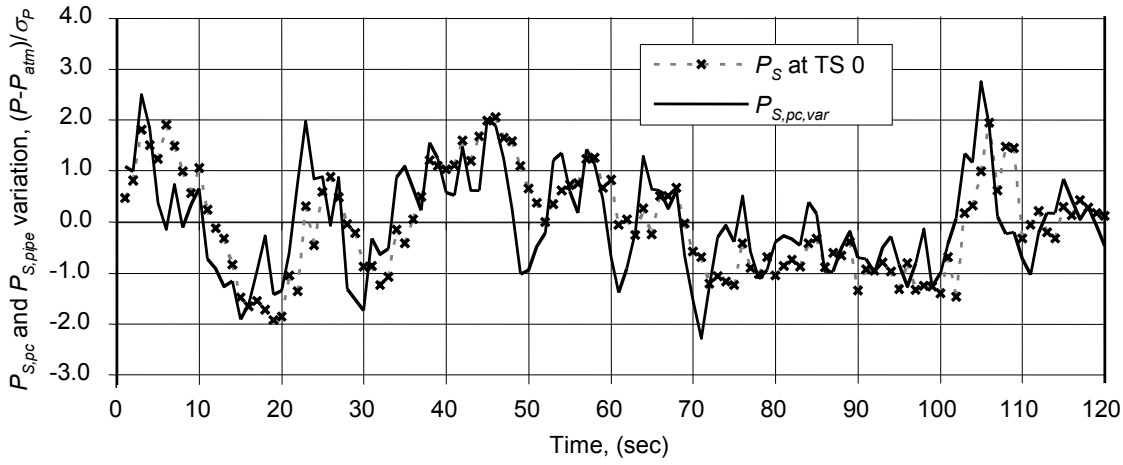



Figure E.10 – Temporal variation of test section pressure at tunnel station 0 for Mach = 0.951 and $P_{T,sc}$= 2125 psf. Sample duration, 1 sec; correlation coefficient, 0.656; $P_{S,pc}$, 1187.7 psf; $\sigma_{P_{S,pc}}$, 1.29 psf; $P_{S,pipe,avg}$, 1193.25 psf; $\sigma_{P_{S,pipe}}$, 0.72 psf;.

### E.8.1.2 Effects of test section slots

Curve fits for the semispan calibration for Mach 0.6 to 1.0 are shown in Figure E.11. The falling pressure gradient at the start of the test section is attributed to the relieving effects of the test section slots, which start at TS 0.

### E.8.1.3 Mounting interference effects

Referring again to Figure E.11, the rising pressure gradient near the downstream end of the test section is believed to be caused by interference effects from the static pipe hydraulic cylinder fairing and the 11-by 11-ft TWT SMSS, which feed forward into the test section. Since the shape and volume of the static pipe fairing is similar to the stings and adapters commonly used to support sting-mounted models, no additional Mach corrections are currently used to account for this mounting interference. This pressure distribution is used to compute a clear tunnel buoyancy correction that is applied to the measured model forces.

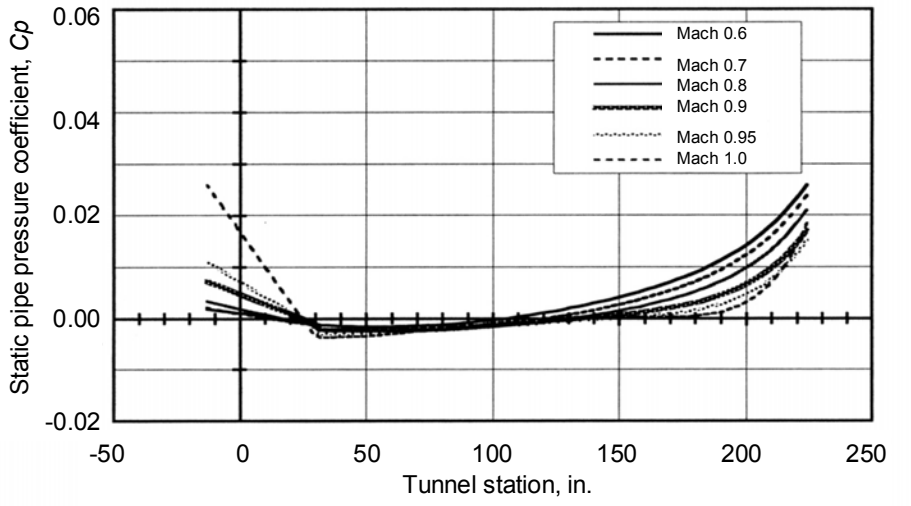



Figure E.11 – Effect of test section slots on centerline static pipe *Cp* distribution. $P_{T,sc}$ = 2127 psf.

### E.8.1.4 Tap error and pipe joint effects

The curve fit residuals ($Cp_m$ – $Cp_{fit}$) for the Mach range from 0.6 to 1.0 are shown in Figure E.12. The residuals are caused by tap error in the pipe pressure measurements. Tap error is a result of local imperfections at the tap or on the pipe surface in the neighborhood of the tap. It can be seen in Figure E.12 that the curve fit residuals are nearly identical for this range of test section Mach number, which infers that the residuals are an artifact of the pipe or pipe taps rather than of the flow in the tunnel. The static pipe is also used to calibrate the 12-Foot Pressure Wind Tunnel. Results from the 12-Foot Pressure Wind Tunnel facility calibration were compared with those seen in Figure E.12 and showed remarkably similar residuals. This suggests that tap error is the cause of the small-scale variation in measured pressure along the test section length and that it justifies the smoothing procedure used in the calibration data reduction. The large residuals shown near TS 5 and 125 coincide with the joints in the static pipe assembly between adjacent 10.25-ft pipe sections (see Figure E.3).

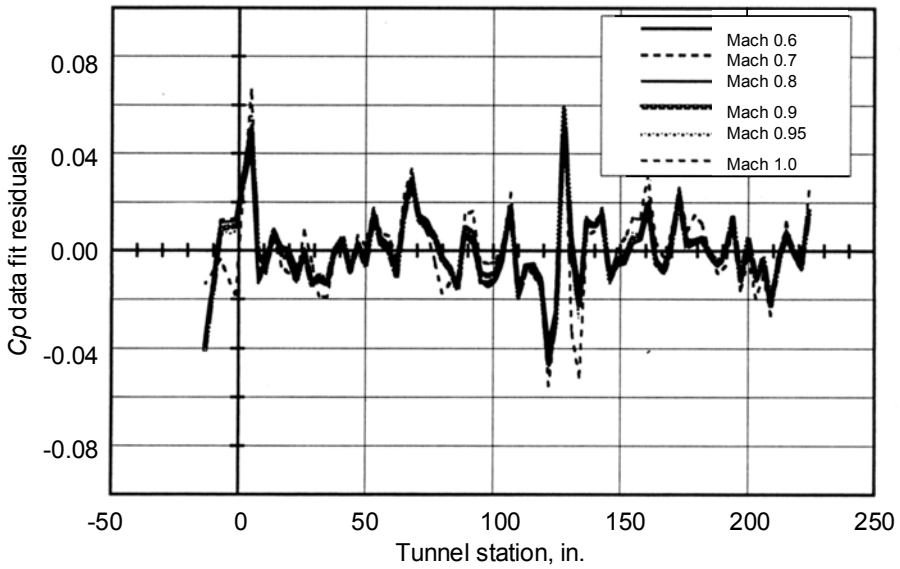



Figure E.12 – Tap error distribution along static pipe. $P_{T,sc}$ = 2127 psf.

### E.8.1.5 Instrumentation error effects

During the planning phases of the static pipe calibration, uncertainty analysis was used to guide choices of instrumentation, instrumentation hookup, and data-reduction procedures. Figure E.13 shows the results of these uncertainty analyses for the actual instrumentation, instrument hookup, and data reduction program that was used. The goal for the calibration was to limit the Mach errors due to the instrument error sources to ±0.001 for all test conditions within the test matrix. On the basis of the data checking and repeat data points that were recorded during the calibration, the instrumentation performed to the specifications claimed by the manufacturers.

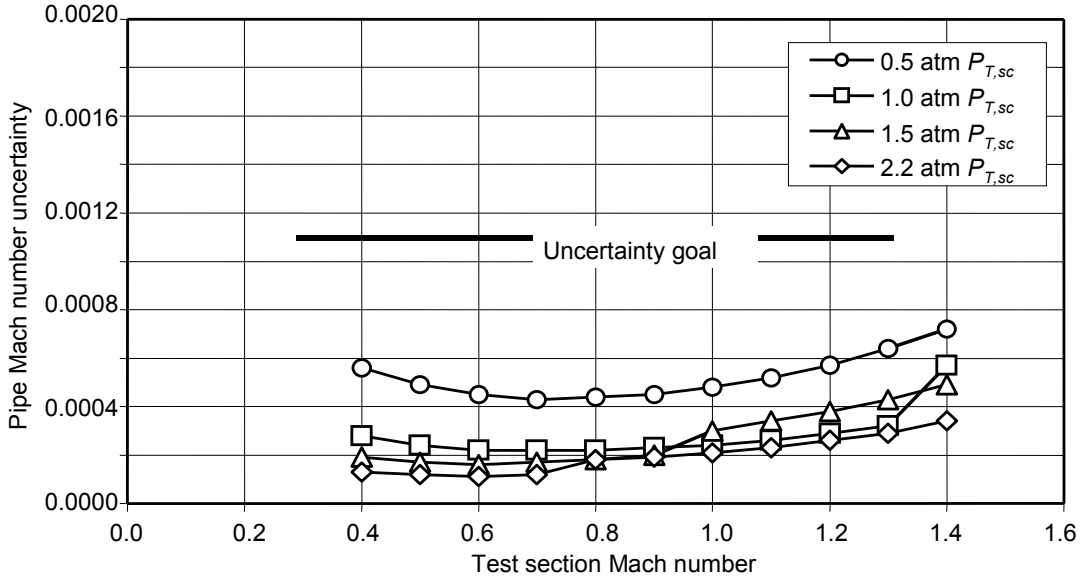



Figure E.13 – Uncertainty analysis predictions based in ±5 psid DTC pressure scanning modules and flow reference system.

### E.8.2 Calibration results for the static pipe

The following sections summarize the effects of the primary test variables.

#### E.8.2.1 Mach number effects

The effect of Mach variation on the test section *Cp* for subsonic and supersonic operation can be seen in Figures E.14 and E.15, respectively. Within these figures, the Mach number is varied while the facility total pressure is maintained at 1.0 atm. The most noticeable trends shown in Figure E.14 are the increase in the slot effect for increasing Mach number at TS 0 and the decrease in the "forward feeding" interference effect of the static pipe fairing and the sting model support for increasing Mach numbers. For supersonic Mach numbers (Figure E.15), the obvious change is a greater longitudinal variation of the *Cp* in comparison to subsonic values, especially in the forward half of the test section. These effects are attributable to the discontinuity in the wall boundary condition where the test section slots begin. Small mass additions through the slots produce diffuse tunnel shocks that originate in the first foot of the test section. A second obvious difference between the subsonic and supersonic *Cp* distributions is the absence of a pressure influence from the pipe hydraulic cylinder fairing and the SMSS at the downstream end of the static pipe. The supersonic test section flow effectively eliminates upstream propagation of the pressure disturbance arising from the fairing and support system.

#### E.8.2.2 Reynolds number effects

Subsonic and supersonic Reynolds number effects on the test section *Cp* distribution are summarized in Figures E.16 and E.17, respectively. The Mach number is fixed for the data contained within the figures, whereas the tunnel total pressure is varied through the setpoint values of 0.5, 1.0, 1.5, and 2.2 atm. In Figure E.16, a Mach number of 0.8 was chosen to illustrate the Reynolds number effects at subsonic test conditions. The effects shown are small but systematic. There appears to be a *Cp* increase that varies with tunnel total pressure. The most likely cause for this phenomenon is the change in test section boundary layer growth that occurs at the different Reynolds numbers. Boundary layer growth forces differing amounts of slot cross flow and consequent changes in the pressure differential between the plenum chamber and test section. Figure E.17 illustrates the Reynolds number effects for Mach 1.2. The most obvious difference between the supersonic and subsonic Reynolds number effects is the pressure disturbance that appears on the static pipe 20 to 70 in. downstream of the start of the test section slots.

The disturbance is believed to be caused by diffuse tunnel shocks that arise near the slot origin in response to the slight changes in slot mass flow.

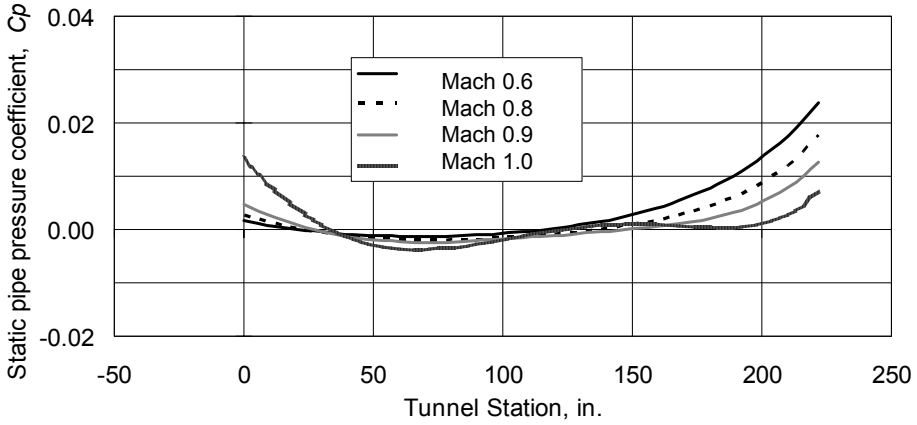



Figure E.14 – Subsonic Mach number effects on centerline *Cp* distribution at 1.0 atm .

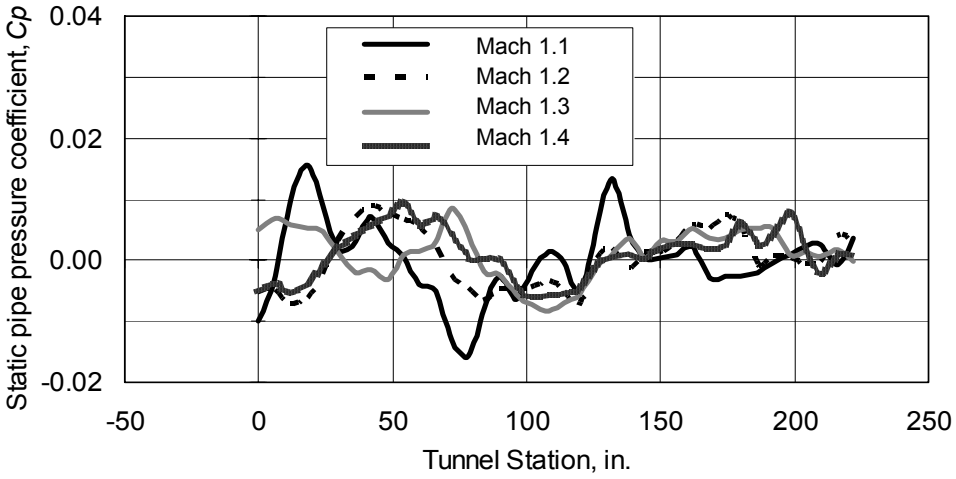



Figure E.15 – Supersonic Mach number effects on centerline *Cp* distribution at 1.0 atm .

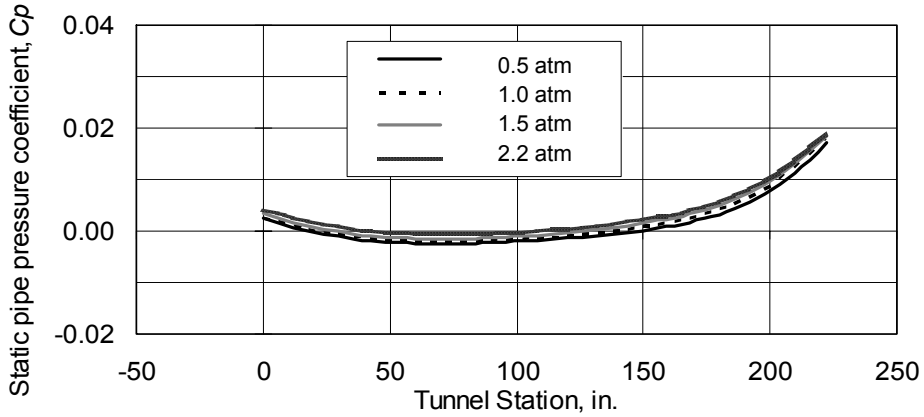



Figure E.16 – Reynolds numbers effects on centerline *Cp* distribution at subsonic Mach number settings (Mach = 0.8).

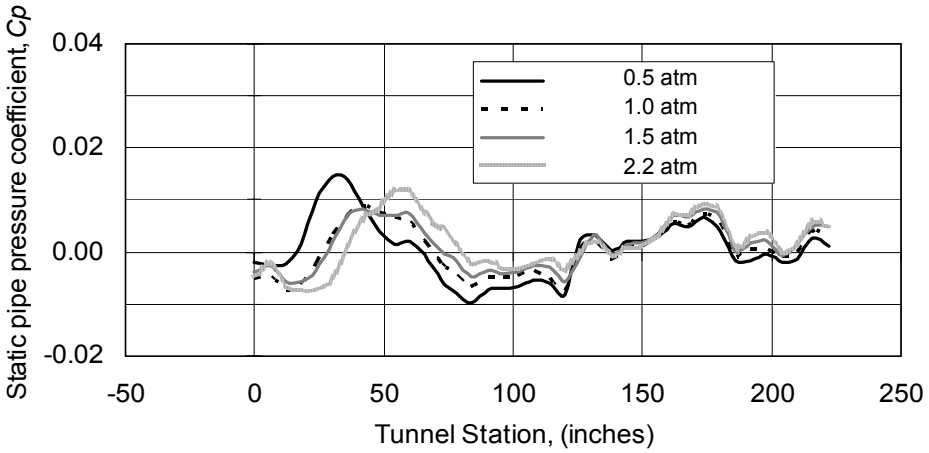



Figure E.17 – Reynolds numbers effects on centerline *Cp* distribution at supersonic Mach number settings (Mach = 1.2).

### E.8.2.3 Centerline versus 33 in. below centerline

The difference between the *Cp* distribution on the tunnel centerline and 33 in. below the centerline is shown for Mach 0.8 in Figure E.18. These differences are minor in the regions where most wind tunnel models are positioned: TS 106 for semispan models and TS 155 to 165 for full-span models.

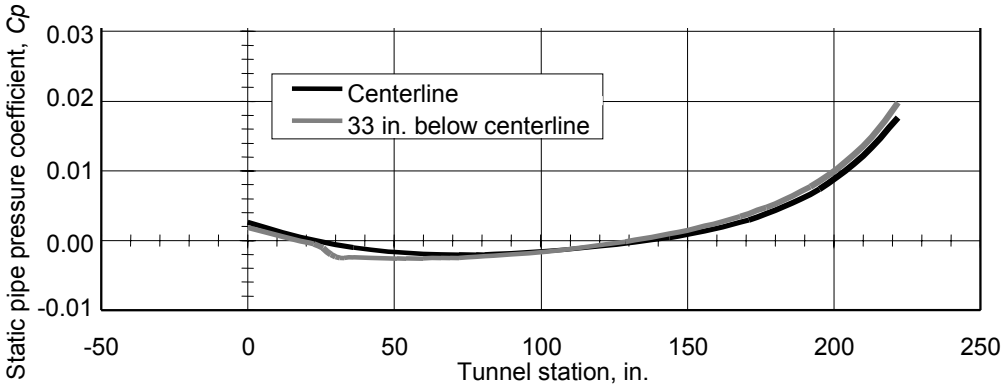



Figure E.18 – Effect of vertical height on centerline *Cp* distribution at 1 atm and Mach 0.80.

### E.8.3 Calibration results for flow uniformity

#### E.8.3.1 Flow angle

Flow-angularity results for Mach 0.8 and $P_{T,sc}$ = 3180 psf at TS 165 are presented in Figure E.19. For the planar survey, measurements were made over the range defined by $y$ = ±36 in. and $z$ = ±36 in. The vector plot shows very small flow angles especially in the core region where models are tested. Statistics for all the measurements in this plane yield an average and standard deviation of 0.08° and 0.044° for the *A*-plane flow angle and 0.04° and 0.061° for the *B*-plane flow angle. The slightly larger flow angles measured closest to the tunnel walls may be a result of the flow field being deflected by the survey apparatus itself. Premodernization flow-angle surveys measured large flow-angle gradients on the centerline within several feet of the test section floor. Values for $\alpha$ and $\beta$ were as much as 0.35° at $z$ = –26.4 in. Figure E.19 clearly shows that this anomaly is no longer present in the flow. The improvement in the test section flow angularity is attributed to the addition of the honeycomb in the settling chamber.

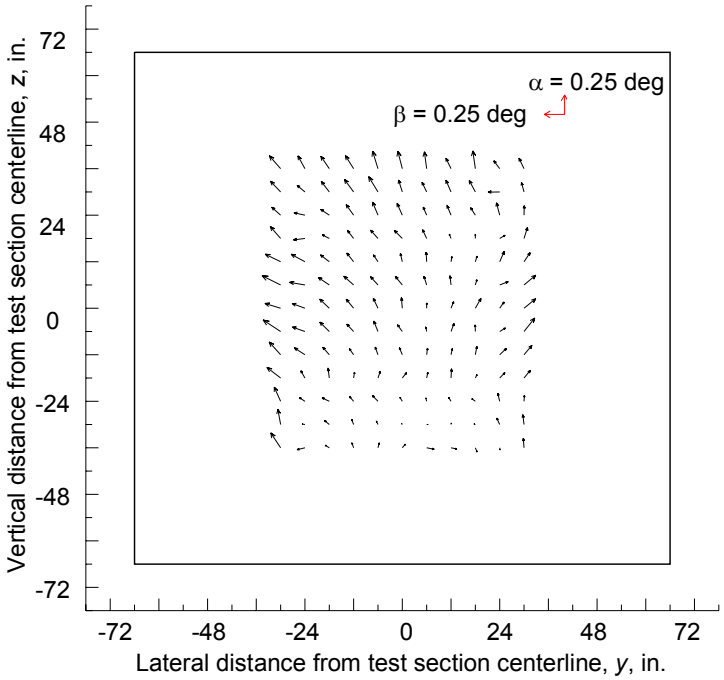



Figure E.19 – Flow angularity at tunnel station 160 at Mach 0.80; $P_{T,sc}$, 2119 psf; $T_{T,F}$, 80.7 °F. Average pitch angle = 0.08°; standard deviation of pitch angle = 0.044°. Average yaw angle = 0.04°; standard deviation of yaw angle = 0.061°.

#### E.8.3.2 Total pressure

The total pressure variation for Mach 0.85 and $P_{T,sc}$ = 2120 psf is presented using a contour plot of $C_{PT,\mathrm{cor}}$ (Figure E.20). The figure shows a small variation in the test section total pressure from that measured by the facility probes. Values for $C_{PT,\mathrm{cor}}$ are largest at the centerline and drop to zero near the test section walls. Measurements made in the test section prior to the addition of the TRS showed good agreement with those measured by the facility total pressure probes. At that time, facility total pressure was measured using probes located on the centerline, mounted off the turning vane set just upstream of the contraction. The variation in $P_T$ shown in Figure E.20 is a result of the introduction of the TRS. Pressure losses resulting from the honeycomb and screens are a function of the dynamic pressure entering the TRS, which varies across the radius. Pressure loss across the TRS is, therefore, nonuniform and largest at the centerline.

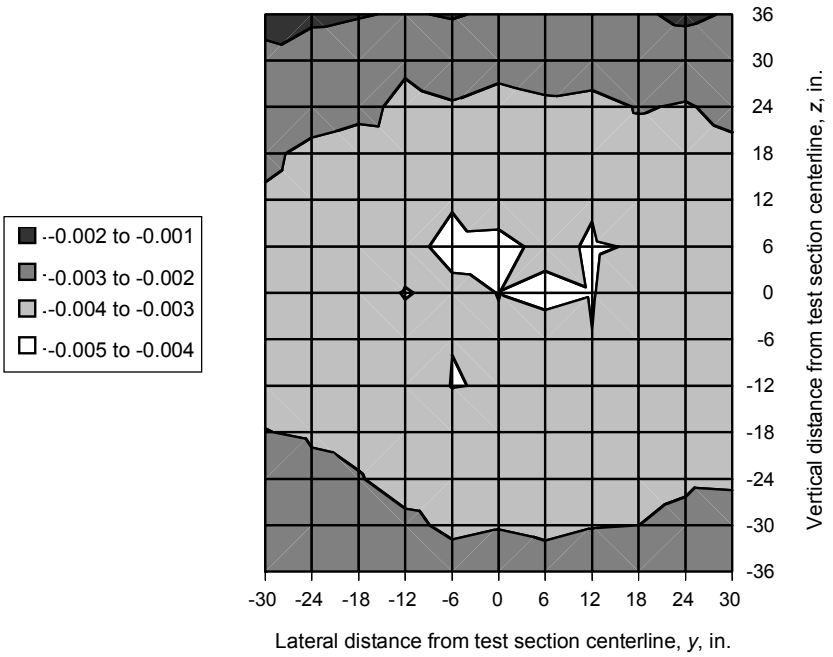



Figure E.20 – Total pressure correction coefficient ($P_T$=($P_{T,probe}$-$P_{T,sc}$)/$q$) contour at tunnel station 159.5. Mach 0.85; $P_{T,sc}$, 2120 psf.

### E.8.3.3 Total temperature

The total temperature variation for Mach 0.85 and $P_{T,sc}$ = 2120 psf is presented in Figure E.21 using a contour plot of $\Delta T$ = ($T_{T,\text{probe}}$ – $T_{T,F}$). The data show a slight increase in the total temperature above the centerline, but the levels measured are within 2 °F.

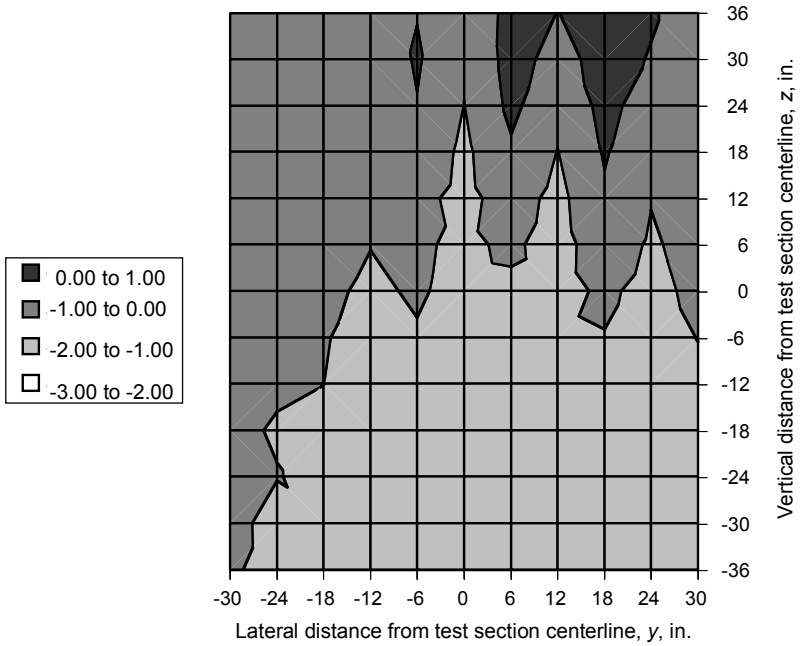



Figure E.21 – Total temperature contour ($\Delta T$=$T_{T,probe}$-$T_T$ °R) at tunnel station 185. Mach 0.85; $P_{T,sc}$, 2120 psf.

### E.8.3.4 Boundary layer

Boundary layer measurements are useful for determining the proper standoff height for semispan models. Figure E.22 and E.23 present the displacement thickness and momentum thickness for Mach 0.4 and 0.8 for $P_{T,sc}$ = 3180 psf from three sets of data. Data at TS 36 are for floor slots normal, which is influenced by flow exchange between the test section and the plenum. Data at TS 176 are with the floor sealed and give the upper bound for determining the proper standoff height for semispan models. Data at TS 106 are from a premodernization test with the floor slots sealed and are within the bound defined by the data at TS 176.

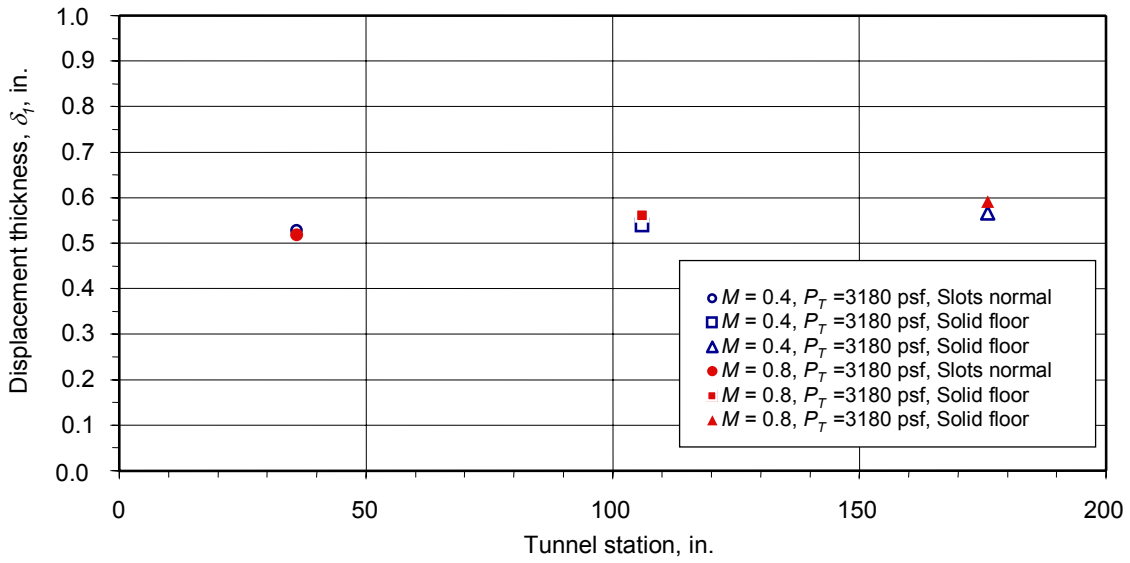



Figure E.22 – Boundary layer displacement thickness.

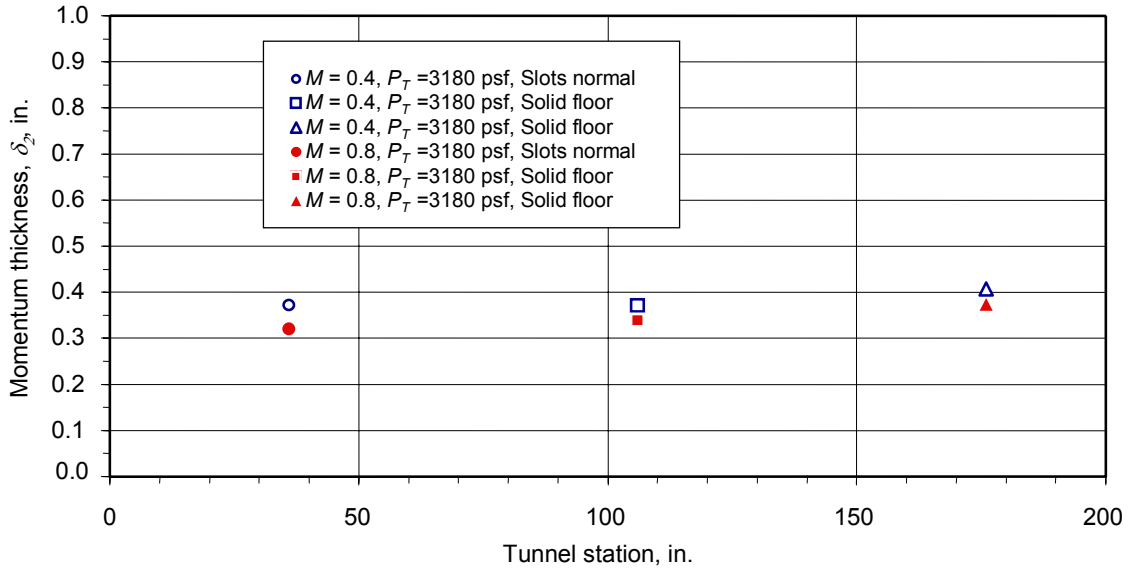



Figure E.23 – Boundary layer momentum thickness.

# Annex F—Maintenance calibration of the Veridian 8-Foot Transonic Wind Tunnel

## F.1 Description of facility

### F.1.1 Facility description

The Veridian Transonic Wind Tunnel (VTWT) is a closed-circuit tunnel with a test section dimension of 8 by 8 by 18.75 ft. (96 by 96 by 225 in.) and is represented in Figure F.1. The facility has a maximum clear tunnel Mach number of 1.35 and operates at various tunnel stagnation pressure from 0.10 to 3.25 atm, independent of Mach number. Figure F.2 is the operating range of the VTWT. Under conventional operations (the dark region of Figure F.2), the tunnel operates continuously at Reynolds numbers up to about 5 million per foot or a dynamic pressure of approximately 900 lb/ft², over most of the Mach number range. The VTWT also operates as a blowdown tunnel. In the blowdown mode (the light region of Figure F.2) and for limited test duration, higher Reynolds numbers up to 12.5 million/ft or a dynamic pressure of approximately 2200 lb/ft$^2$ can be achieved using the tunnel's ejector-augmentation system (Ref. 44).

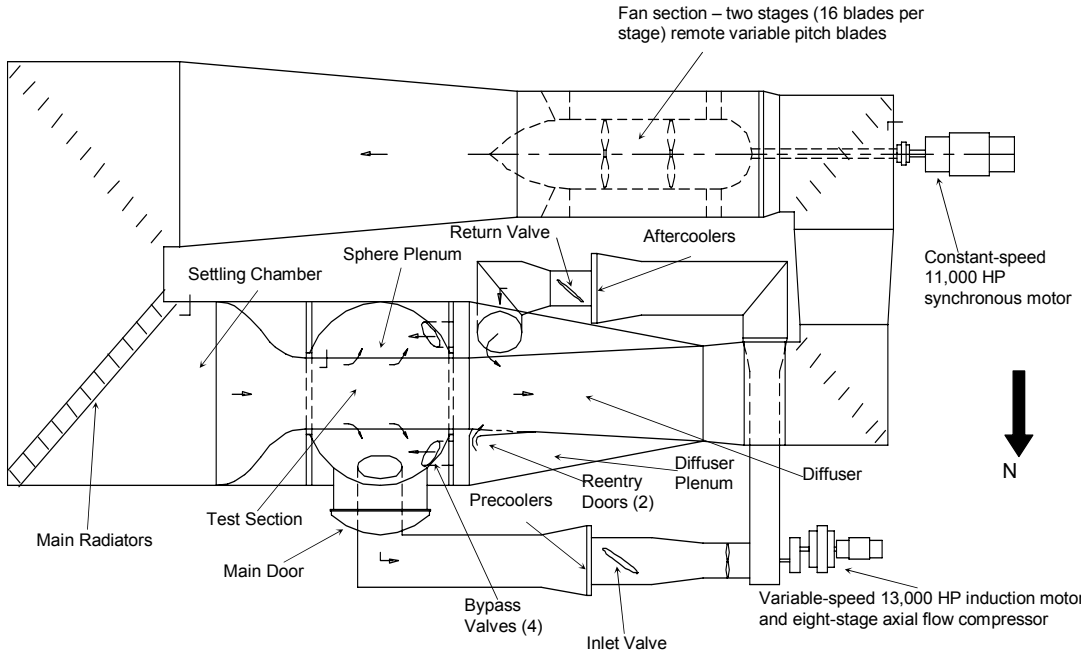



Figure F.1 – Plan view of the Veridian 8-Foot Transonic Wind Tunnel (VTWT). The VTWT utilizes an active plenum evacuation system in combination with the main drive to achieve transonic Mach numbers.

The VTWT main drive (MD) is an external, constant-speed 11 000-hp synchronous motor with a 1250-hp direct-current (dc) starting motor. The motor system drives a two-stage fan in the tunnel circuit. Each fan stage is outfitted with 16 cambered blades that are varied (synchronously) in pitch angle to set the Mach number.

The VTWT utilizes an actively controlled plenum evacuation system (PES) at Mach numbers greater than or equal to 0.60. The PES draws air through the four walls of the test section, which are uniformly perforated at a fixed 22.5-percent porosity, with perforations perpendicular to the wall boundaries. The test section sidewalls are movable and can be converged or diverged remotely up to ±1°. A secondary, variable-speed 13 000-hp induction motor, with a 1250-hp dc starting motor and an eight-stage, axial-flow compressor drives the PES. The secondary motor system evacuates a sphere plenum chamber surrounding the test section to initiate ventilation of the test section. This process promotes boundary layer removal and de-blocking of the test section for achieving transonic speeds. The PES and perforated

test section walls also work to attenuate any shock reflections off the test section walls, particularly important to low supersonic testing. Air removed by the PES is returned downstream of the test section into the tunnel diffuser section via a diffuser plenum and reentry passageways. Four butterfly valves located between the diffuser plenum and sphere plenum, allow a portion of the evacuated air to be bypassed back to the sphere. Throttling of these bypass valves allows fine control of the sphere plenum pressure, achieving steady and uniform control of the test section static pressure and Mach number. The bypass valves can be varied manually but are typically switched into the Mach Controller System for automatic control.

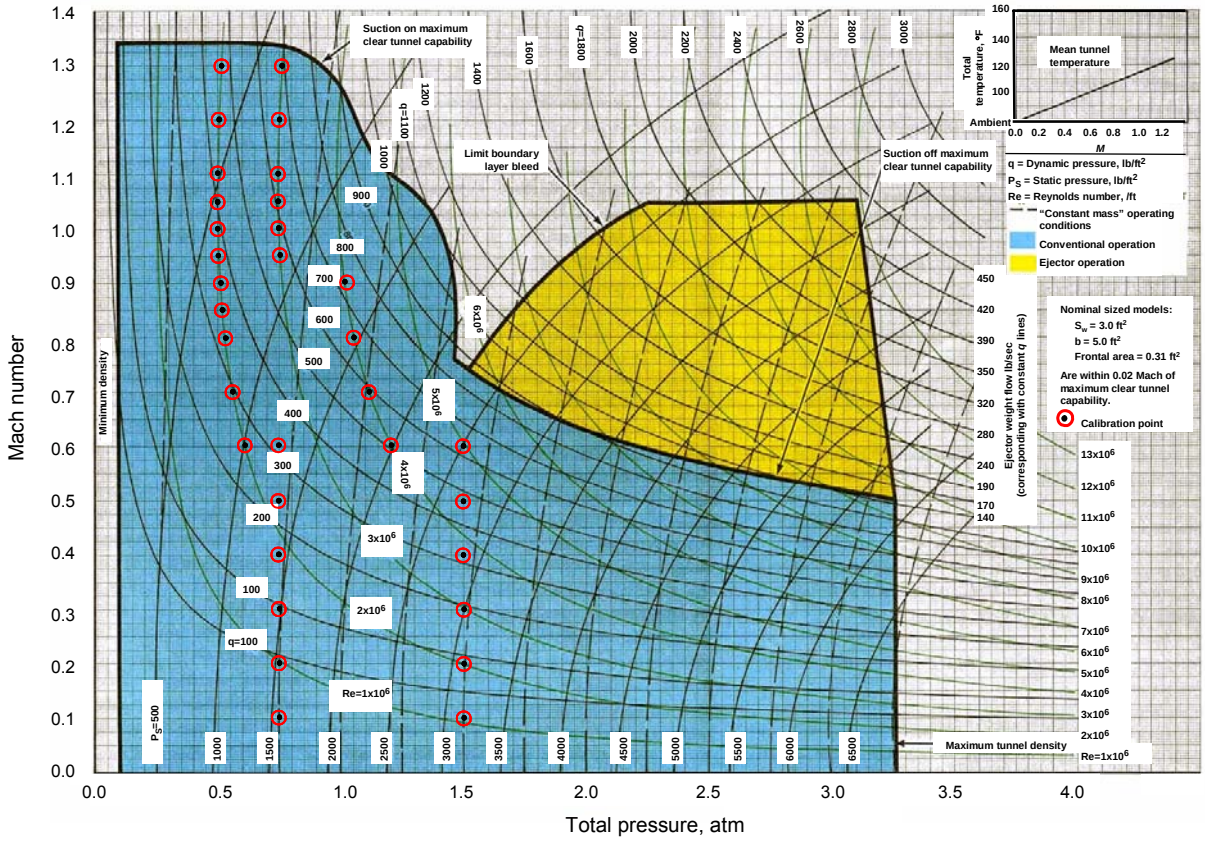



Figure F.2 – Operating envelope of the Veridian 8-Foot Transonic Wind Tunnel. Points indicated on figure correspond to conditions routinely checked in a maintenance calibration.

The main tunnel circuit is equipped with a collection of water-fed cooling coils located just upstream of the settling chamber. In addition, the secondary drive circuit has pre-cooler and after-cooler systems. The entire cooling system of the tunnel maintains the test section total temperature in a range of approximately 65 to 140 °F, over the entire Mach number range. The tunnel is also equipped with an air-drying system capable of maintaining absolute humidity levels below 0.0020 lbm of water/lbm of dry air, provided tunnel entries are kept to a minimum. The upstream and downstream ends of the VTWT test section are equipped with gate valves. By setting the variable-pitch blades of the MD system to a zero thrust condition and closing the gate valves, the sphere plenum can be brought to ambient condition, leaving the tunnel circuit at its test density and humidity, and allowing entrance into the test section for model work.

## F.1.2 Resident tunnel instrumentation

The VTWT has various, resident instrumentation to measure critical air stream conditions. There is a ceiling-mounted Pitot probe located 18.250 in. from the start of the test section, which measures stagnation pressure $P_T$. In addition, an indicated static pressure $P_{S,ind}$ is measured above the test section in the upstream part of the sphere plenum. Two Paroscientific Digiquartz Intelligent Transmitter absolute

pressure transducers (Model 1045A) (Paroscientific Inc., Redman, WA), with pressure ranges from 0 to 45 lb/in.$^2$, record $P_{S,ind}$ and $P_T$ (Ref. 47). The transducers are placed in an enclosure that is maintained at a positive 5-lb/in.$^2$ pressure above the tunnel total pressure to keep contaminants out. The enclosure and transducers are located above the test section. The manufacturer's accuracy on these transducers is ±0.01-percent full scale, or ±0.0045 lb/in.$^2$ The sensor integration time of the Paroscientific transducer can be adjusted to optimize resolution, noise, rejection, and sample rate (Ref. 48). The VTWT uses these transducers at a resolution of 0.005 lb/in.$^2$ The transducers are calibrated on a 6-month cycle using the VTWT's DH PG7601 High Accuracy Pressure Calibration System (DH Instruments, Phoenix, AZ) (accuracy at ±20 ppm). They are calibrated over the pressure range of 1.5 to 45 lb/in.$^2$ to encompass the operating range of the tunnel.

The measured $P_{S,ind}$ and $P_T$ define an indicated Mach number $M_{ind}$, which denotes the air stream velocity condition in the test section. Since this Mach number is based on sphere plenum pressure $P_{S,ind}$ and not the actual static pressure at a test article location in the test section, a calibration is required to establish a relationship between the indicated conditions and the actual test section conditions (to be discussed further in Section F.5).

A stagnation temperature $T_T$ is measured in the tunnel's settling chamber and is used to represent the stagnation temperature in the test section. The device for measuring $T_T$ is a system of three, Iron-Constantan (Type J) thermocouple probes located at the 3, 9, and 12 o'clock positions along the settling chamber wall. The three thermocouple-outputs are electrically connected to provide one averaged $T_T$ reading. The uncertainty of $T_T$ is estimated to be ±1 °F. Dew point DP is also measured in the settling chamber using an Edgetech DewPrime III hygrometer (Edgetech, Milford, MA) with chilled-mirror technology.

The combination of a variable pitch fan section and the active PES (Section F.1.1) enables the VTWT to operate at varying pressure rise for the same nominal test section Mach number. Varying pressure rise for a given Mach number will in effect vary the Mach number distribution in the test section. For a given Mach number, the pressure rise must be explicitly known to characterize the Mach number distribution in the test section. To measure pressure rise, two additional total head probes are located in the tunnel: one in the settling chamber and the other just upstream of the MD fan section, designated H1 and H4, respectively. H1 and H4 are plumbed to an Edwards Model 590 Barocel differential pressure transducer (Chell Instruments Ltd, Norfolk, U.K.). The Model 590 has a differential pressure range of 0 to 100 mbar (approximately 1.5 lb/in.²). The manufacturer's stated accuracy is ±0.15-percent full scale or ±0.0025 lb/in². The Barocel output is designated $PR_{NET}$ indicating the net pressure rise in the tunnel circuit.

### F.1.3 Data acquisition systems

A dual Athlon MP1900+ based PC (Advanced Micro Devices, Inc., Sunnyvale, CA) is the Central Acquisition Processor (CAP) of the VTWT's data acquisition system (DAS). CAP functions as the command and control center for nine networked, function-specific PCs, a Tustin Data System 2100 (AP Labs Tustin Electronics Division, San Diego, CA) and a Pressure System, Inc. (PSI) 8400 System (Pressure Systems, Inc., Hampton, VA, Ref. 49). CAP provides the operator interface, which includes: parameter setup, operator command entry, and data parameter displays. The data display windows are user configurable and can display data in either engineering units or raw form. Resident tunnel instrumentation (such as $P_{S,ind}$ and $P_T$) are interfaced to the CAP through their function-specific PCs.

Pressure data is acquired using PSI electronically scanned pressure (ESP) modules, which are interfaced through the PSI 8400 System. CAP controls the timing of data acquisition between the Tustin, the PSI 8400 systems and the PCs. Finally the CAP correlates this data (as well as that received from any auxiliary processors), and transmits the data via Fast Ethernet to the Data Reduction Computer and Server for data processing.

## F.2 Calibration hardware and instrumentation

### F.2.1 Static pipe

A typical static pipe is utilized for a maintenance calibration of the VTWT. Veridian's static pipe is 2.5-in. in diameter (less than 0.1-percent blockage) and approximately 29.5 ft long in its current configuration. The pipe sections are made from cold-drawn, 0.25-in. wall, mechanical steel tubing. Along the length of the pipe are 148 static pressure orifices drilled in 0.375-in.-diameter brass inserts that have been press fit and epoxied into the pipe. The orifices are located at the pipe stations listed in Table F.1. Pairs of orifices are at each pipe station, one orifice on the top and one on the bottom. The top and bottom ports run in line with each other. Steel tubing (Type 304 annealed, 0.0425-in. outer diameter, 0.00775-in. wall) run from each orifice, through the center of the pipe, and exit at the pipe's aft end. The length of each tube varies according to which pipe station the tube originates. For example, orifice 0 at pipe station 39.69 (~3.25 ft), has a tube length of about 26.75 ft, and orifice 73 at pipe station 314.85 (~26.25 ft), has a tube length approximately 23 ft shorter, at a length of 3.75 ft. Approximately 10 ft of plastic tubing (Strip-a-tube SAT/V/031/1 79–1 800 (Ono Industries, Inc., Ono, PA), 0.030-in. inner diameter) is attached to each tube.

Table F.1 — Static pipe orifice designations and locations

| Orifice | | Pipe station,[a] in. | Orifice | | Pipe station,[a] in. | Orifice | | Pipe station,[a] in. | Orifice | | Pipe station,[a] in. |
|---|---|---|---|---|---|---|---|---|---|---|---|
| Top | Bottom | | Top | Bottom | | Top | Bottom | | Top | Bottom | |
| [b]0 | [c]100 | 39.69 | 19 | 119 | 144.00 | 38 | 138 | 212.00 | 57 | 157 | 250.00 |
| 1 | 101 | 72.00 | 20 | 120 | 148.00 | 39 | 139 | 214.00 | 58 | 158 | 252.00 |
| 2 | 102 | 76.00 | 21 | 121 | 152.00 | 40 | 140 | 216.00 | 59 | 159 | 254.00 |
| 3 | 103 | 80.00 | 22 | 122 | 156.00 | 41 | 141 | 218.00 | 60 | 160 | 262.85 |
| 4 | 104 | 84.00 | 23 | 123 | 160.00 | 42 | 142 | 220.00 | 61 | 161 | 266.85 |
| 5 | 105 | 88.00 | 24 | 124 | 164.00 | 43 | 143 | 222.00 | 62 | 162 | 270.85 |
| 6 | 106 | 92.00 | 25 | 125 | 168.00 | 44 | 144 | 224.00 | 63 | 163 | 274.85 |
| 7 | 107 | 96.00 | 26 | 126 | 172.00 | 45 | 145 | 226.00 | 64 | 164 | 278.85 |
| 8 | 108 | 100.00 | 27 | 127 | 176.00 | 46 | 146 | 228.00 | 65 | 165 | 282.85 |
| 9 | 109 | 104.00 | 28 | 128 | 180.00 | 47 | 147 | 230.00 | 66 | 166 | 286.85 |
| 10 | 110 | 108.00 | 29 | 129 | 184.00 | 48 | 148 | 232.00 | 67 | 167 | 290.85 |
| 11 | 111 | 112.00 | 30 | 130 | 188.00 | 49 | 149 | 234.00 | 68 | 168 | 294.85 |
| 12 | 112 | 116.00 | 31 | 131 | 192.00 | 50 | 150 | 236.00 | 69 | 169 | 298.85 |
| 13 | 113 | 120.00 | 32 | 132 | 196.00 | 51 | 151 | 238.00 | 70 | 170 | 302.85 |
| 14 | 114 | 124.00 | 33 | 133 | 200.00 | 52 | 152 | 240.00 | 71 | 171 | 306.85 |
| 15 | 115 | 128.00 | 34 | 134 | 204.00 | 53 | 153 | 242.00 | 72 | 172 | 310.85 |
| 16 | 116 | 132.00 | 35 | 135 | 206.00 | 54 | 154 | 244.00 | 73 | 173 | 314.85 |
| 17 | 117 | 136.00 | 36 | 136 | 208.00 | 55 | 155 | 246.00 | --- | ---- | --------- |
| 18 | 118 | 140.00 | 37 | 137 | 210.00 | 56 | 156 | 248.00 | --- | ---- | --------- |

[a]The nose of the pipe is designated as pipe station 0.
[b]The orifice is actually on the right side of the pipe (pilot's view)
[c]The orifice is actually on the left side of the pipe (pilot's view)

### F.2.2 Instrumentation

The 148 static pressures of the static pipe are connected to four ±5 lb/in.$^2$ differential, 48-port ESP modules. The manufacturer's accuracy on the ESP modules is ±0.05-percent of full-scale or ±0.0025 lb/in.$^2$ The VTWT services these modules prior to the tunnel calibration per the VTWT service procedure. Any ports identified as having a leak exceeding the VTWT's accepted tolerance for a leak rate of 0.5 percent of the signal per minute are tagged as bad and not used. In addition, each port of each module

goes through a series of run side, calibration/checkout cycles to identify any unacceptable ports. Ports having large voltage offsets in comparison to the rest of the module are also not used.

Two Paroscientific Digiquartz Intelligent Transmitter absolute pressure transducers (Model 1045A), with pressure ranges from 0 to 45 lb/in.$^2$, are used in conjunction with the static pipe ESP modules. The Paroscientific transducers are placed in tandem (i.e., teed) with the module ports assigned to measure orifices 27 and 127. The intent of this arrangement is to have an independent pressure-measuring device to aid in the evaluation of the static pipe data. Both Paroscientific transducers are set to a resolution of 0.0005 lb/in.$^2$ The manufacturer's accuracy on these transducers is quoted at ±0.01-percent full scale, or ±0.0045 lb/in.$^2$ Having onboard thermal compensation, the Paroscientific transducers are more stable than the ESP modules currently in service at the VTWT.

The Paroscientific transducers are calibrated against the VTWT's DH PG7601 High Accuracy Pressure Calibration System (accuracy at ±20 ppm). They are calibrated over the pressure range of 1.5 to 15 lb/in.$^2$ to encompass all conditions that will be encountered when performing the test schedule. An initial calibration is performed on both Paroscientific transducers to determine new calibration coefficients for the reduced pressure range. Afterwards, three hysteresis calibrations are performed using the new coefficients, to quantify the precision of the Paroscientific transducers.

## F.3 Maintenance calibration cescription

### F.3.1 Test section installation

The test section floor of the VTWT is part of a rail-mounted cart that can be interchanged with other cart systems equipped with various test article support arrangements. The VTWT has four carts systems: the Reflection Plane cart, the Island Fairing cart, the Sting Cart (Ref. 45), and the Captive Trajectory Simulation cart (Ref. 46). The Sting Cart is the most commonly used cart in the VTWT. The Sting Cart is composed of a vertical strut and pitch (pod) mechanism upon which various combinations of angle adapter and roll mechanisms can be mounted. Performance, stability and control, static and dynamic pressure measurements, store carriage loads, inlet evaluation, and after-body loads testing are commonly performed on this cart.

In a maintenance calibration of the Sting Cart, two basic test section configurations are investigated: strut/pod only and strut/pod with double-roll mechanism (DRM), shown installed in Figures F.3 and F.4, respectively. The two configurations encompass most of the mounting arrangements utilized on the Sting Cart. In both installations, a 35° (total angle) nose cone (9.75 in. long) is installed on the front of the pod or DRM during the calibration.

The static pipe is mounted to the floor of the tunnel diffuser next to the cart's strut using its standard 48-in. static pipe riser, filler block, and spacer assembly. This setup positions the pipe nominally 5 in. to the right of the tunnel centerline and vertically on the centerline of the test section. A shim is placed in the forward section of the riser assembly, between the spacer and filler block, to minimize local pipe angles (i.e., sag) to within ±0.4°. The bolts holding the pipe and support assembly to the diffuser floor are torqued to 65 ft-lb. The upstream end of the pipe extends into the contraction section of the tunnel where three cables, attached to the tunnel shell, support the forward end of the pipe (Figure F.5). The cables incline to the air stream at an angle of 55° and attach at the pipe's 2, 6, and 10 o'clock positions (pilot's view), approximately 13 in. from the pipe's nose. The pipe support cables are loaded in tension to approximately 250 lb each. The pipe nose and upstream support cables are located in subsonic flow throughout the operating range of the tunnel.

The orifice positions (Table F.1) on the pipe are located relative to the test section or tunnel station (TS). A plumb bob is dropped down to the floor from an orifice on the pipe from which a measurement is taken, parallel to the center scribe line on the floor, to the cart leading edge known to be at TS 102.75. The start of the test section, which is the end of the contraction section, is designated TS 0.000.

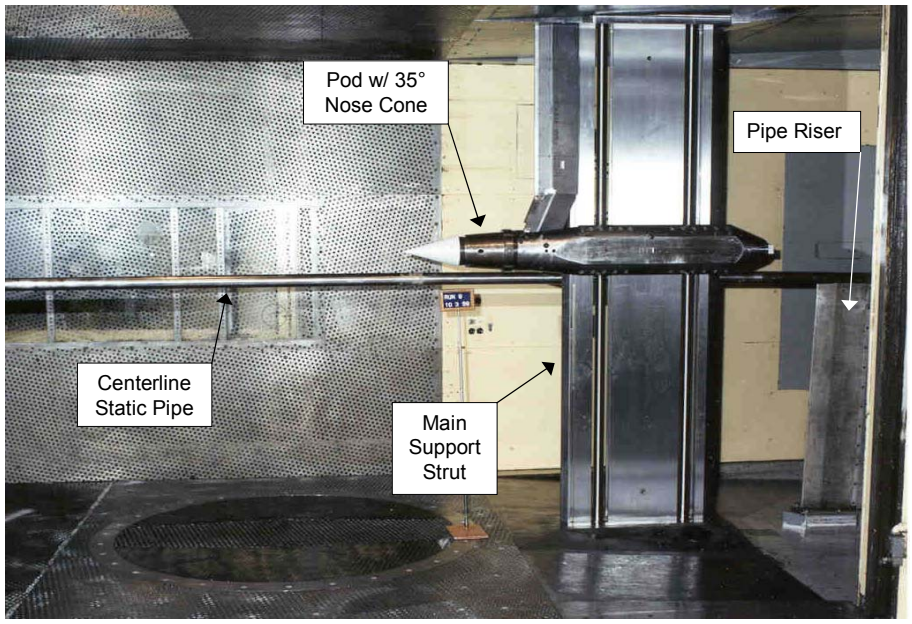



Figure F.3 – Baseline configuration of the VTWT test section with main support strut and pitch pod. The static pipe is located on the vertical centerline and 5 in. to the right of the strut.

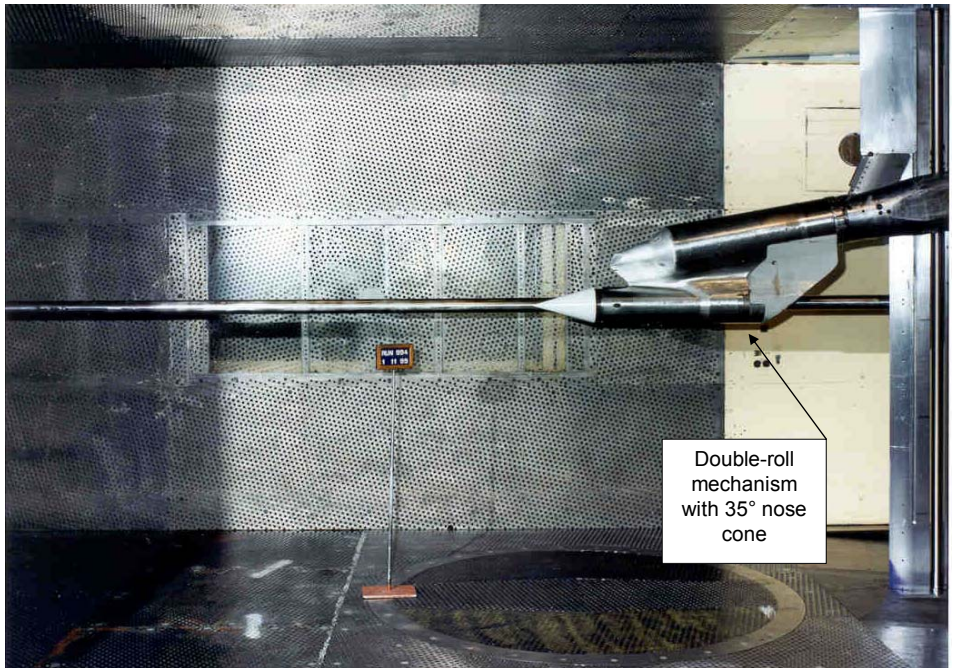



Figure F.4 – The VTWT test section with main support strut, pitch pod, and double-roll mechanism.

The primary source of error in the VTWT's ESP modules is temperature effects. Therefore, the static pipe ESP modules are housed in an environmental enclosure. The enclosure is a heavy foam box with a copper lining inside. Heating elements are glued to the copper liner, between the liner and the foam box walls, to provide temperature control inside the enclosure. The ESP modules are placed inside the box with all the tubing and cables exiting the box through a cutout hole. A resistance-temperature detector probe monitors the enclosure's temperature. As it turns out, the heating elements are rarely used

because the environmental enclosure, with ESPs in place, tends to stabilize on its own at a temperature of approximately 130 °F.

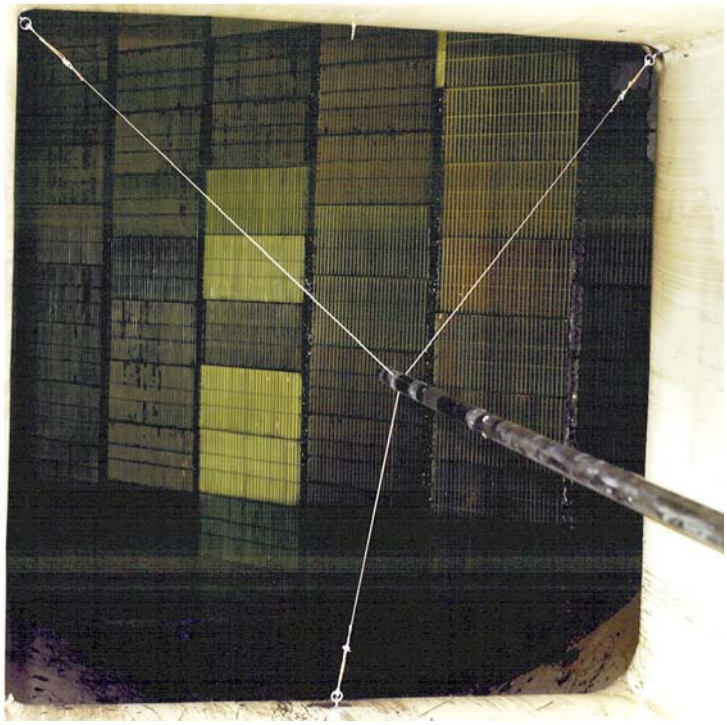


Figure F.5 – Upstream support cables of the static pipe. Cables are loaded to approximately 250 lb each. Static pipe nose and support cables remain in subsonic flow over the entire operating range of the tunnel.

Two Mansfield & Green Pneumatic Pressure Testers (Model 750 Type K) and dead weights provide known and fixed reference pressures for the differential ESP modules. The testers are contained inside a bell jar located in the VTWT Control Room and are designated as $PR_1$ and $PR_2$. Two Paroscientific transducers (Model 1045A, same model as the $P_{S,ind}$ and $P_T$ Paroscientifics) set at a resolution of 0.005 lb/in² measure and record both $PR_1$ and $PR_2$ (nominally equal to the dead weight plus the pressure in the bell jar). $PR_1$ is used as reference side pressure of the ESPs and is appropriately set for the static pipe pressure readings expected during the test section calibration. $PR_1$ is also plumbed to one read-side port on each of the ESP. In addition, $PR_2$, set 4 lb/in² above $PR_1$ is plumbed to each ESP. Together, $PR_1$ and $PR_2$ provide a health monitoring of the ESPs using the known $PR_1$ and $PR_2$ values and comparing them to the output reading of from the ESPs.

The surface of the static pipe is cleaned and buffed, and the orifice inserts are checked for smoothness. Orifices are also inspected for debris and are cleared if necessary. The test section walls and seams are visually inspected for misalignments, surface steps, and any other anomalies (a procedure followed prior to any wind-on activity). Any misalignments or steps are eliminated if possible. All orifices of the static pipe would have been blown out, plumbed, and leak and continuity checked prior to installation. After installation into the tunnel, the pipe orifices undergo a second leak and continuity check. In addition, the reference and calibration lines of the ESP modules are checked for leaks.

The entire tunnel circuit is inspected for any irregularity prior to the tunnel calibration. The movable sections of the test section's north and south walls are checked and verified that at 0° divergence/convergence they are indeed parallel. This is accomplished by measuring the distance from each wall to the tunnel's centerline scribe, at approximately 20-in. increments along each wall. The walls are considered parallel if measurements are within ±0.0625 in. The test section ceiling, south wall, and north wall are configured with their standard perforated Plexiglas windows. The test section floor is

perforated steel plate (no Plexiglas). Video cameras are set up in the ceiling and the north wall for remote viewing of the static pipe during the calibration.

## F.3.2 Test procedures

A maintenance calibration is performed along the operating conditions most commonly encountered in customer testing. Figure F.2 identifies these calibration points relative to the operating range of the VTWT. Calibration points are chosen starting at Mach 0.10 and ending at Mach 1.30. A finer Mach number spacing is used over the drag rise with 0.85, 0.95, and 1.05 added to the test schedule. The baseline Mach number series is performed at a Reynolds number equal to 2.0 million/ft for Mach numbers 0.60 to 1.30 and a stagnation pressure of 0.75 atm for Mach numbers from 0.10 to 0.60. Mach 0.60 is calibrated two ways: one time using the PES and another time without the PES. All Mach numbers less than 0.60 are performed without the PES. The baseline Mach number series is repeated three times throughout the course of the calibration. A second Mach number series is included in the calibration but at higher Reynolds numbers and stagnation pressures to quantify Reynolds number effects. It includes a Reynolds number equal to 4.0 million/ft for Mach numbers 0.60 to 0.90, a Reynolds number equal to 3.0 million/ft for Mach numbers 0.95 to 1.30, and a stagnation pressure of 1.50 atm for Mach numbers 0.10 to 0.60. In a maintenance calibration, tunnel settings, such as for MD blade angle (which sets pressure rise), wall angles and PES settings, follow the standard Mach dependent schedule for the Sting Cart and are utilized throughout the calibration. If this were a comprehensive test section calibration, the tunnel settings would be optimized for their effect on Mach number gradient and tunnel power usage, increasing the scope of the test schedule.

A specific data acquisition procedure is employed to address tunnel stabilization time and pressure lag. The lag time for the farthest orifice from the ESP modules, orifice 0 (at a tube length of 26.75 ft), to reach 99-percent equilibrium (Refs. 20 and 21) is conservatively on the order of 10 sec. The data acquisition procedure follows:

(1) Set the desired tunnel conditions.

(2) Once on condition, wait 15 sec to allow the tunnel and static pipe pressures to stabilize.

(3) Acquire 80 points of continuous scan data at 4 points/sec (sampling event of 20 sec).

(4) Go to the next condition.

In addition to the conditions that are automatically being acquired by the data acquisition computers, the MD blade angle $\beta$, bypass valve positions (four valves), MD ac motor amperes, MD dc motor amperes, and CD motor amperes are also logged throughout the calibration.

After the initial setup of the static pipe and during the actual wind tunnel calibration, the pipe's local angles are periodically measured and recorded using a Hilger & Watts 360° Clinometer (Hilger & Watts, Ltd., London, U.K.) placed at predefined locations along the top of the pipe. Experience with the setup has shown that the static pipe maintains its initial sag characteristics throughout a calibration (see Figure F.6). The spatial position of the pipe in the test section is also periodically recorded. Various length measurements are made from the test section floor and from the south wall, to the pipe's centerline. The tensions on each of the three pipe support cables are recorded over the course of testing. In addition, test section wall angles are checked throughout the test program.

During testing, the operation crew reviews pipe data online for any evidence of plugged pressure ports. This is accomplished by comparing the orifice readings to the pressure measurements from the resident tunnel instrumentation, when the tunnel is at the wind-off condition. At that condition, the static pipe pressures and resident tunnel pressures should all read the same. To facilitate the review process, the VTWT computer automatically calculates and reports the difference between ESP port readings and the tunnel $P_{S,ind}$ (static pressure). A plugged pressure port will appear as a large offset from the tunnel $P_{S,ind}$, indicating the presence of trapped air in the tube that is not at the current wind-off pressure.

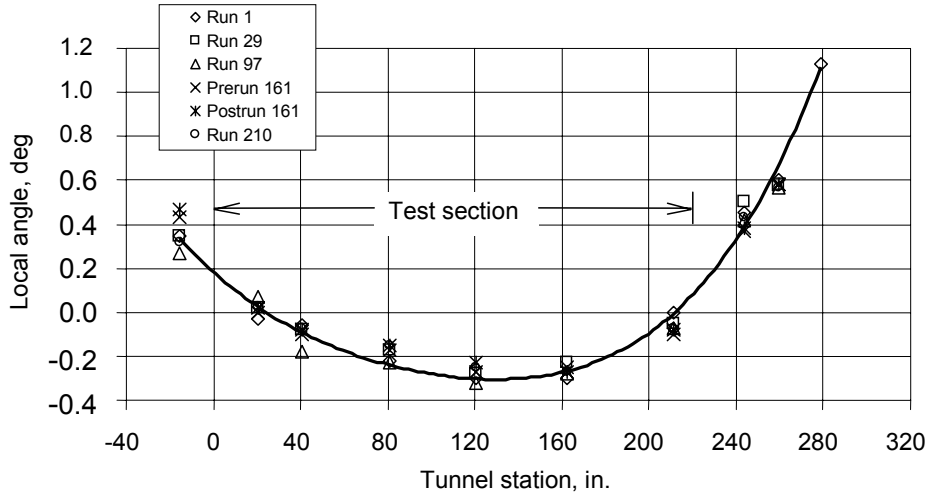



Figure F.6 – Local pitch angle of static pipe versus tunnel station. Pipe angle is held within ±0.50° across the test section and pipe orientation is maintained throughout testing.

Special procedures are followed to keep the tunnel circuit dry because the VTWT's tunnel isolation system (see Section F.1.1) cannot be used for entering the test section. The pipe's forward end extends beyond the east gate valve, rendering the valve unusable. The entire tunnel must be equalized to ambient conditions when entering the test section, thus compromising the dry environment of the tunnel. After extended periods with the tunnel circuit open to the ambient environment, the tunnel circuit is pumped down to approximately 1200 lb/ft$^2$ (~0.5 atm). It is then run at Mach 0.80 for approximately 15 min to thoroughly temperature soak the tunnel structure. Afterward, the tunnel is purged twice with farm air prior to continuing with the calibration. The goal is to reestablish an absolute humidity of 0.0020 lbm of water/lbm of dry air, which is typical for customer testing.

## F.4 Frequency and duration of full and check calibrations

Maintenance calibrations using the static pipe are now performed approximately every 3 to 5 years whereas in the past they were rarely done at all. Since maintenance calibrations use standard, pre-established operational settings they only takes approximately 7 days to complete, which includes installation and removal of the calibration equipment. A tunnel calibration requiring optimization of new tunnel settings such as PES settings and tunnel pressure rise involves a much more extensive run schedule and can take up to 2 weeks or more to complete.

Other methods of calibrating the test section less frequently employed because of their more intricate installations and run schedules include spatial mapping of the local flow angularity in the test section with a shuttlecock (force measuring) or flow probe (pressure measuring). They are typically performed only if a tunnel flow quality problem is suspected or if the tunnel has undergone a major renovation or a new support system is introduced.

Although not a check calibration per se, a generic model standard test is performed approximately once every year to check the repeatability and health of the tunnel through analysis of its aerodynamic data (e.g., $C_L$ vs. a, $C_L$ vs. $\underline{C}_D$, etc.) and integrated up-flow (i.e., flow angularity via upright vs. inverted testing). A typical model standard test lasts 5 days.

A number of peripheral measurements are acquired during a centerline static pipe calibration. They include floor and ceiling wall static pressures, aft test section total pressure, secondary compressor leg pressures, diffuser plenum pressures, and adiabatic wall temperatures. These instrumentation are left in place after removal of the static pipe and continuously monitored for evidence of the tunnel deviating from its calibration levels.

In all cases, the scope of a tunnel calibration is directly affected by the available time in a wind tunnel schedule and/or available funding.

## F.5 Data reduction and analyses

The following paragraphs describe the primary reduction algorithms and output variables utilized in reporting and analyzing the static pipe data. In a maintenance calibration, the significance of the static pipe data are to verify tunnel repeatability, reaffirm operation settings, and adjust calibration curves. The purpose of the calibration curves is threefold: (1) to correlate the indicated condition in the sphere plenum, where static pressure $P_{S,ind}$ is measured, to the condition in the test section where models are positioned, (2) to provide the longitudinal pressure distribution through the test section so that buoyancy corrections can be determined, and (3) to define the area in the test section, or "sweet spot," having the best Mach number uniformity, for model testing.

The 80 samples acquired in a calibration run (see Section F.3.2) are averaged for each instrumentation measurement. Standard deviations of the samples are also computed and reviewed for indications of unstable measurement conditions warranting repeating calibration runs or investigating the source of the instabilities. The average $\overline{X}$ and standard deviations $\sigma_x$ of the 80 data points are determined as follows:

$$\overline{X} = \frac{1}{n}\sum_{i=1}^{n} X_i$$

where $n$ = 80

and

$$\sigma_x = \sqrt{\frac{\sum_{i=1}^{n}(X_i - \overline{X})^2}{n-1}}$$

where $n$ = 80

Prior to reducing final calibration results, the pressure measurements are reviewed thoroughly for evidence of contaminated data. Plots like those shown in Figure F.7, pipe static pressure versus tunnel station, and Figure F.8, port standard deviation versus tunnel station, are reviewed The standard deviations of each pipe orifice are scanned particularly closely. A problem with an orifice, such as debris on or around the orifice, can sometimes be indicated by a deviation that is inordinately high in comparison to the rest of the pipe pressures. Regarding the actual pressures, a reading from a particular port on the pipe that continuously reads out of range from surrounding orifices and remains that way over the entire Mach number range can also indicate a bad pressure port.

Any static pipe pressures identified as being plugged or leaking before or during the calibration would have been subsequently blanked (i.e., substitutions are not made) from the data output prior to computation and analyses. If plugged or leaking pressures are involved in an average, the average is revised accordingly to exclude the bad pressure(s).

To correlate conditions in the test section to the conditions measured at the reference station, data reduction starts with the calculation of an indicated Mach number $M_{ind}$, using the plenum pressure $P_{S,ind}$ at the reference station (all equations assume a specific heat ratio of 1.4):

$$M_{ind} = \left[ 5\left( \frac{P_T}{P_{S,ind}} \right)^{2/7} - 5 \right]^{1/2}$$

The nature of the correlation between the indicated Mach number and the test section condition is expressed as the computed free-stream Mach number,

$$M_{cfs} = M_{ind} + \Delta M$$

where $\Delta M$ is a calibration variable that is derived from the static pipe measurements and is a function of the test conditions (e.g., Mach number and Reynolds number) and the operating settings of the tunnel (e.g., $\Delta R$, wall angle, and compressor speed). The following discussion explains how $\Delta M$ is determined.

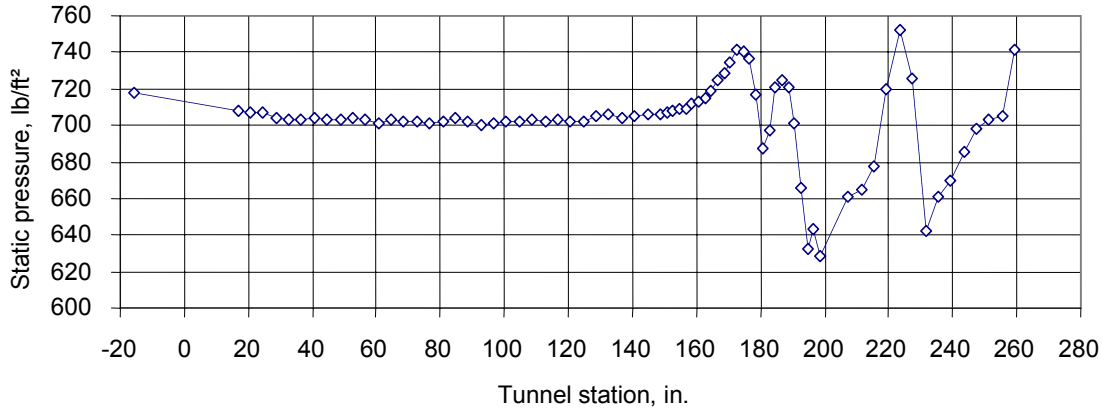



Figure F.7 – The static pressure distribution for M = 0.80, Re = 2.0 million/ft with the DRM installed. The DRM influence on the distribution can be seen starting at approximately TS 140 with a marked increase in static pressure and corresponding decrease in Mach number.

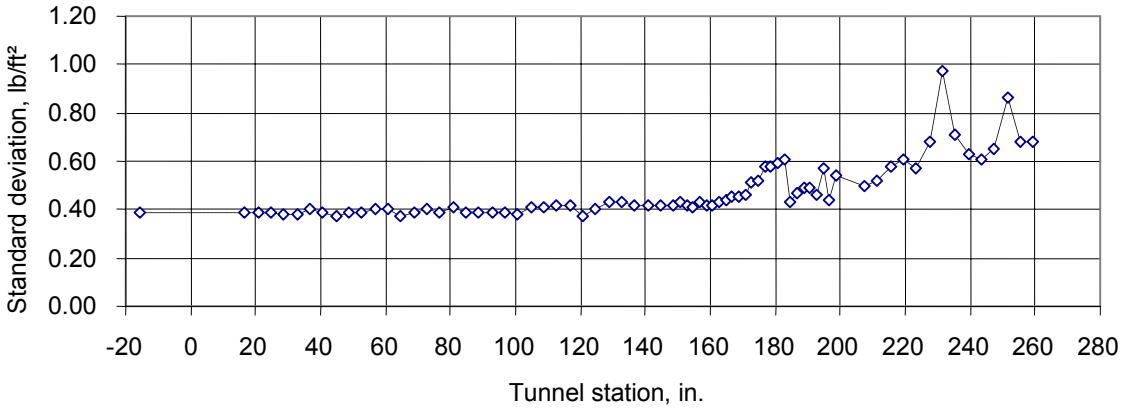



Figure F.8 – The standard deviation of measured static pressure versus tunnel station for M = 0.80, Re = 2.0 million/ft with the DRM installed. Pressure unsteadiness increases as the tunnel flow encounters the DRM and support strut/pod.

The conversion of static pipe data to Mach numbers assumes an isentropic expansion through the test section and uses the stagnation pressure $P_T$ and the static pressures measured along the static pipe. The Mach number is determined at each static pipe orifice along the top and bottom of the pipe. Along the top of the pipe, the measured pressures $P_{S,top}$ are used to calculate a Mach number $M_{top}$:

$$M_{top,j} = \left[ 5\left( \frac{P_T}{P_{S,top,j}} \right)^{2/7} 15 \right]^{1/2}$$

And similarly, the pressures measured at each orifice along the bottom of the pipe $P_{S,btm}$ are used to calculate a Mach number $M_{btm}$:

$$M_{btm,j} = \left[ 5\left( \frac{P_T}{P_{S,btm,j}} \right)^{2/7} 15 \right]^{1/2}$$

where $j$ = 100 to 173 from Table F.1

The tunnel stations for each pair of orifices would have been determined during the installation procedures (see Section F.3.1). Therefore, for each TS, an average Mach number $\overline{M}_{TS}$ and an incremental Mach number $\Delta M_{TS}$ are calculated:

$$\overline{M}_{TS} = \frac{1}{2}\left(M_{top} - M_{btm}\right)_{TS}$$

$$\Delta M_{TS} = \overline{M}_{TS} - M_{ind}$$

Finally, the calibration variable $\Delta M$ is calculated as a weighted average over a given $TS$ range.

$$\Delta M = \left( \sum_{i=1}^{n} W_i \Delta M_{TS} \right) \Big/ \left( \sum_{i=1}^{n} W_i \right)$$

where $W_i = TS_{i+1} - TS_i$.

Mach number gradients $d\overline{M}_{TS}/dx$ are also determined, using a linear curve fit of the static pipe Mach numbers over various $TS$ ranges. Together, $\Delta M$ and $d\overline{M}_{TS}/dx$ are plotted to reveal and summarize trends and to characterize Mach distribution intra-test repeatability and the effects from the DRM and Reynolds number.

Intra-test repeatability is shown in Figure F.9. $d\overline{M}_{TS}/dx$ shows excellent repeatability across the entire Mach number range of the CTS cart test section. The repeatability of $\Delta M$ was within a band of ±0.0002 for M < 0.60, increasing to approximately ±0.0015 for $M$ = 0.60 through 1.20. $M$ = 1.30 is the greatest variation at approximately ±0.0025.

Figure F.10 illustrates the effects of the DRM on the Mach number distribution of the in the test section and illustrates the importance of establishing calibration curves for differing model support systems. At $M \leq 1.0$, effects of the DRM can be seen in the Mach number gradient $d\overline{M}_{TS}/dx$ and $\Delta M$ over TS 90-135 and more substantially over TS 130-155. The DRM's effect increases the Mach number gradient in the test section at the subsonic numbers. At Supersonic Mach numbers, the presence of the DRM is not propagated forward, having no effect on $d\overline{M}_{TS}/dx$ and little to no effect on $\Delta M$ (variations are within the repeatability band established in Figure F.9).

Figure F.11 shows the effects of Reynolds number on the Mach number distribution. It indicates that Reynolds number effects are not significant over the specified $R$e range (2.0 x $10^6$ per foot and 3.0 and 4.0 x $10^6$ per foot for $M \geq 0.60$ and $P_T$ of 0.75 atmospheres to 1.5 atmospheres for $M < 0.60$). This finding is consistent with past calibrations of our Sting Cart.

Once $\Delta M$ is established for the various operational settings and test section configuration, test section conditions can be determined using the resident tunnel instrumentation measurements (see Section F.1.2) stagnation pressure $P_T$, indicated static pressure $P_{S,ind}$ (sphere plenum pressure), and stagnation temperature $T_T$. Recalling the equation for the indicated Mach number $M_{ind}$ and corrected free-stream Mach number $M_{cfs}$ given earlier:

$$M_{ind} = \left[ 5\left( \frac{P_T}{P_{S,ind}} \right)^{2/7} - 5 \right]^{1/2}$$

$$M_{cfs} = M_{ind} + \Delta M$$

For a customer test, $\Delta M$ would have been calculated over the *TS* range corresponding to the location of a wind tunnel model.

The following parameters can be calculated once $M_{cfs}$ is known:

Corrected free-stream static pressure in pounds per square foot,

$$P_S = P_T \left(1 + 0.2 M_{cfs}^2\right)^{-7/2}$$

Free-stream static temperature in degrees Rankine,

$$T_S = T_T \left(1 + 0.2 M_{cfs}^2\right)^{-1}$$

Free-stream dynamic pressure in pounds per square foot,

$$q = 0.7 P_S \left(M_{cfs}\right)^2$$

Free-stream Reynolds number $\times 10^{-6}$ in units of per foot,

$$\mathrm{Re} = 1.2322 P_S M_{cfs} \left[ \frac{T_S + 216}{T_S^2} \right]$$

Free-stream velocity in feet per second,

$$U = 49.01 M_{cfs} \left(T_S\right)^{1/2}$$

Free-stream density in slugs per cubic foot,

$$\rho = \frac{2q}{U^2}$$

The VTWT determines a longitudinal, wind-axis buoyancy correction from static pipe data to account for the effects of tunnel-induced, non-uniform static pressure (Mach number) distributions on the measured drag of the model. It is generally understood that a body located in a non-uniform static pressure field will experience a force in reaction to the pressure distribution acting over the body's surface. Therefore, non-uniform pressure distributions resulting from the test section design or resident support systems will induce incremental forces on the model that are not an element of the true aerodynamics of the vehicle. As is the case with tunnel flow angularity, a correction must be applied to the customer's data to account for the buoyant effects on the model from the tunnel's non-uniform static pressure distribution.

The pressure data from the static pipe are integrated over the model surface to determine the resultant net drag force acting on the model. The static pipe pressures at each tunnel station are converted to coefficient form using the free-stream static pressure $P_s$ and dynamic pressure $q$:

$$Cp_{TS} = \frac{P_{S,TS} - P_S}{q}$$

The pressure coefficients are then integrated over the model's outer surface and then normalized by the model reference area (usually the wing area). The general form of the longitudinal buoyancy equation $\Delta CD_{Bouy}$ is:

$$\Delta CD_{Bouy} = -\frac{1}{S_w}\int_{A_x} Cp_{TS}\, dA_x$$

where

$A_x$ model cross-sectional area in the *y-z* plane, as a function of *TS*

$S_w$ model reference area

The longitudinal buoyancy correction would then be added to the model's uncorrected drag coefficient,

$$C_D = C_{D,u} + \Delta CD_{bouy}$$

Final Mach number distributions are summarized as plots of static pipe Mach number $\overline{M}_{TS}$ versus tunnel station. Figure F.12 presents a sample. The Mach distributions and pressure (Mach number) steadiness shown in Figures F.8 form the basis for determining the "sweet spot" of the test section. Marked changes in either Mach distribution or steadiness would indicate the bounds of where models would ultimately be tested.

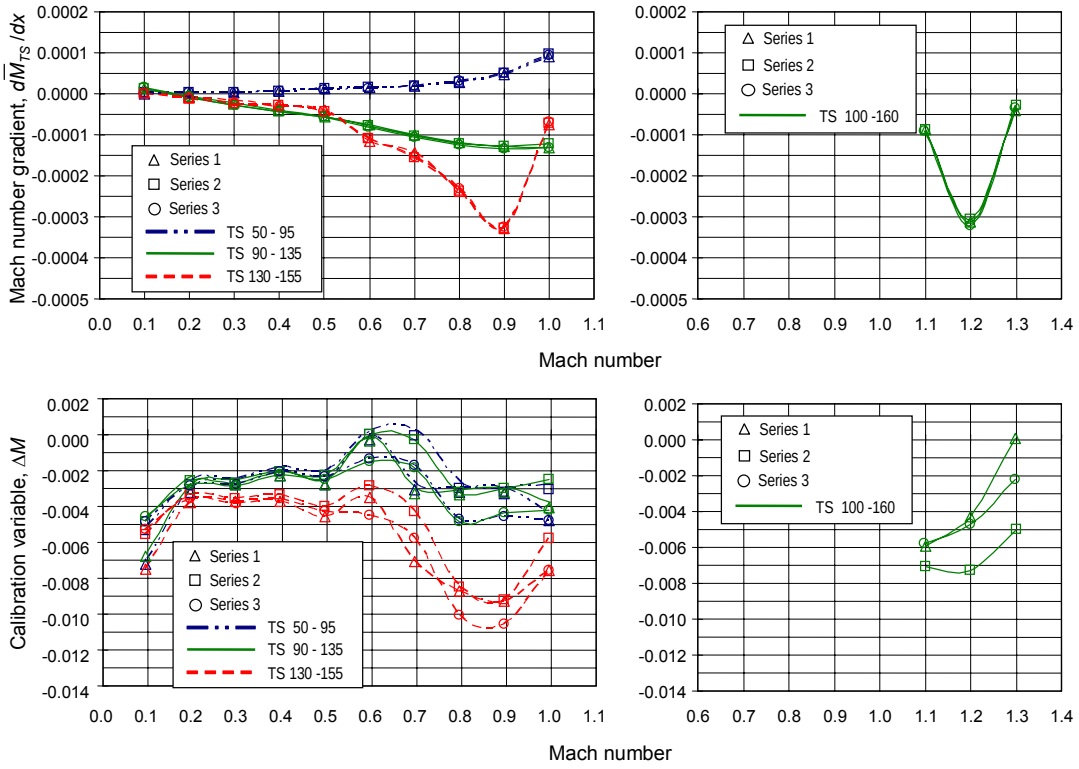



Figure F.9 – Intra-test repeatability of $d\overline{M}_{TS}/dx$ (gradient) and DM over the calibration Mach number schedule for key TS ranges.

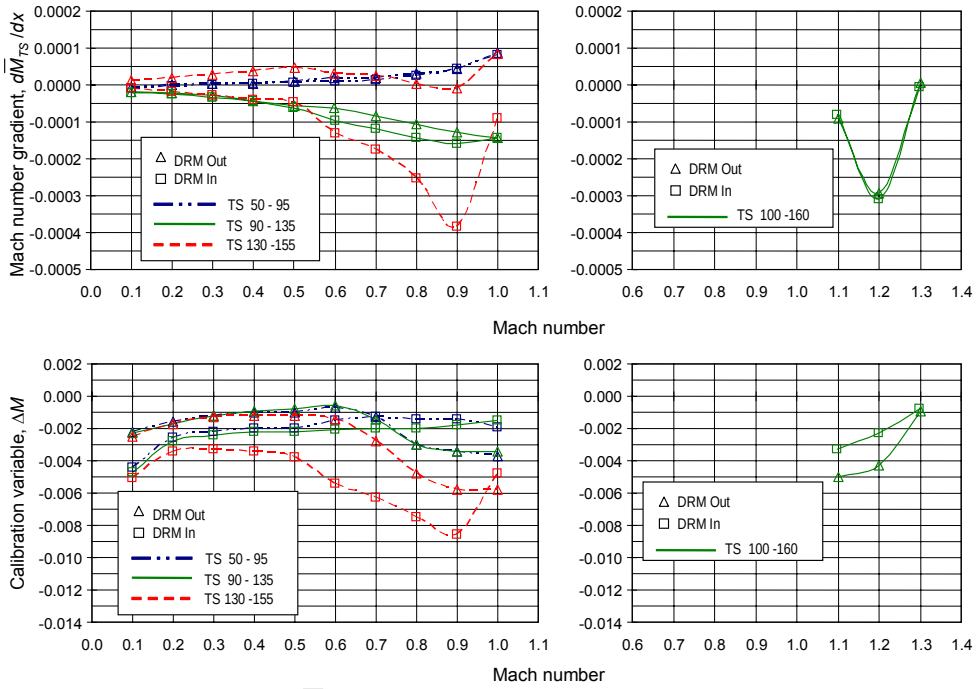



Figure F.10 – DRM effect on $d\overline{M}_{TS}/dx$ (gradient) and DM over the calibration Mach number schedule for key TS ranges (noted on the charts). The DRM has an obvious influence on Mach number distribution over TS 130 – 155.

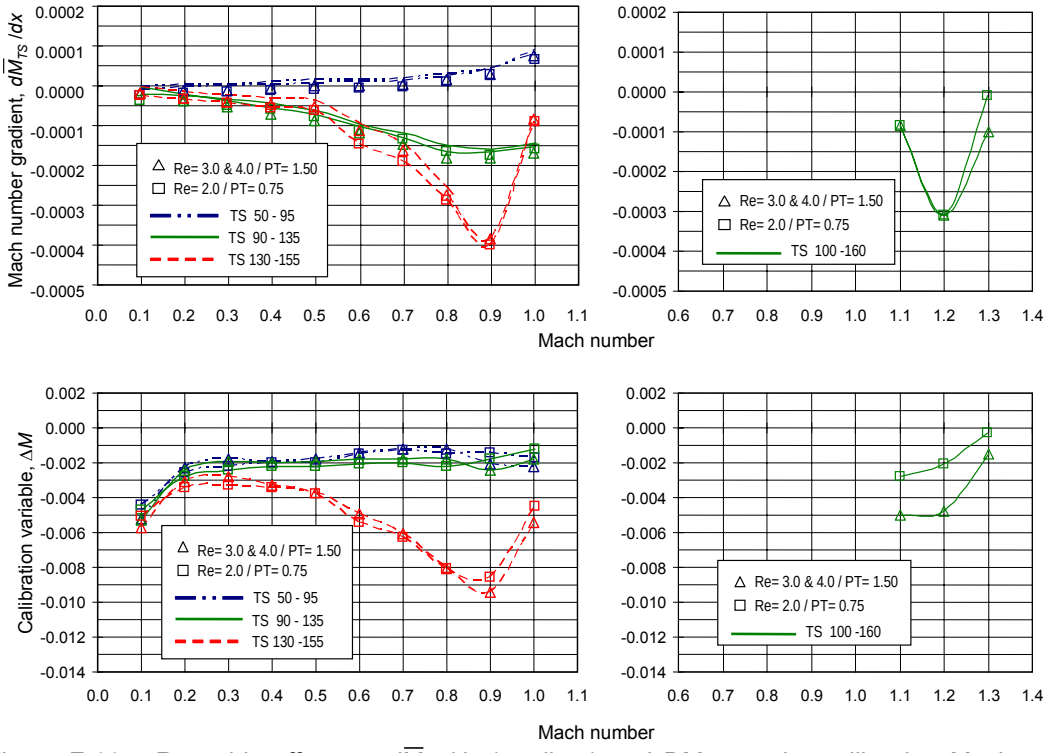



Figure F.11 – Reynolds effect on $d\overline{M}_{TS}/dx$ (gradient) and DM over the calibration Mach number schedule for key TS ranges (noted on the charts). Given the intra-test repeatability band (Figure F.9), Re effect on Mach number distribution is insignificant.

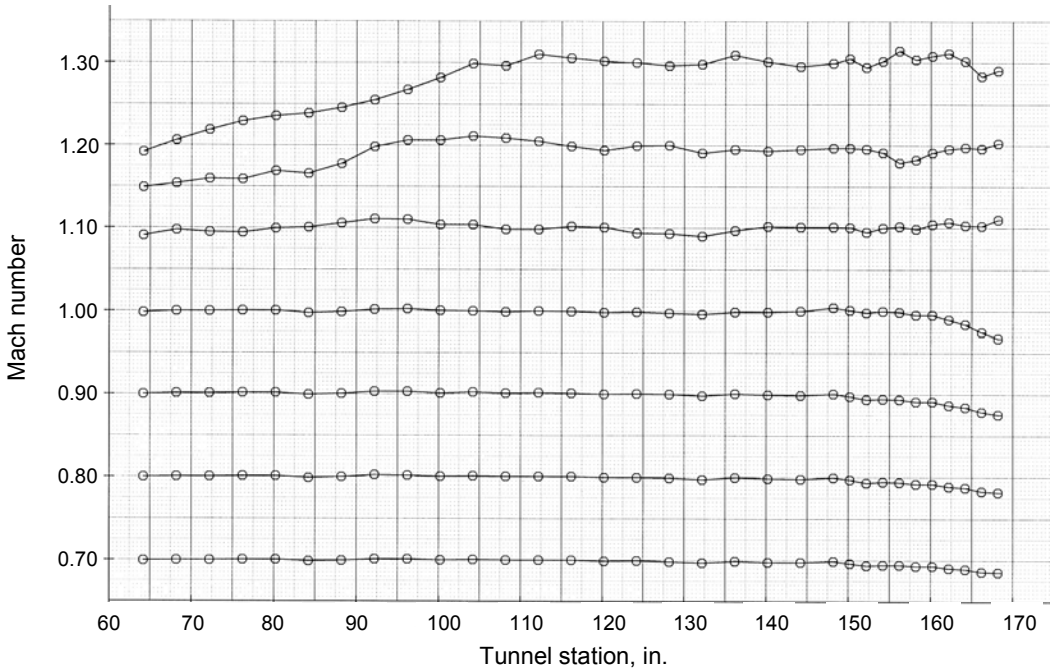



Figure F.12 – Typical Mach number distribution plot from centerline static pipe measurement data. Data shown are for the sting cart with the double-roll mechanism. A test section's longitudinal "sweet spot" can be determined from this plot.

# Annex G—Mach number calibration of the Arnold Engineering Development Center PWT 16-ft Transonic Tunnel (16T) with the High-Angle Automated Sting (HAAS) test section

## G.1 Introduction

The procedure described in this annex was used to calibrate the Arnold Engineering Development Center's (AEDC) 16-ft transonic wind tunnel (16T) with the High-Angle Automated Sting (HAAS) test section installed. The primary objectives were to obtain centerline Mach number distributions, to define the Mach number calibration for use in test conditions and tunnel control algorithms, and to significantly reduce Mach number uncertainty to the level required for the proposed National Wind Tunnel Complex (NWTC) in 1995. The NWTC Mach number uncertainty requirements were based on the customer performance requirements established for drag uncertainty. The allowable drag uncertainty established for NWTC was one drag count independent of the drag coefficient, with no more than one-fourth of the drag uncertainty contribution allowable from Mach number uncertainty. The allowable Mach number uncertainties were 0.0005 and 0.0008 for Mach 0.8 and 1.5, respectively. As a result of the calibration discussed herein, the requirements for supersonic Mach numbers were met, and that for Mach 0.8 was only slightly exceeded, at ±0.0006. These uncertainties require testing at Reynolds numbers of 5 million per ft or greater. We accomplished the low uncertainties by using accurate pressure transducers and by maintaining tight control of tunnel conditions while using a data approximation technique with small residuals.

## G.2 Description of facility

Tunnel 16T is a closed-loop, continuous-flow, variable-density tunnel with a Mach number capability of 0.06 to 1.60 and a stagnation pressure range from 120 to 4000 psfa. The maximum attainable Mach number can vary slightly, depending on the tunnel pressure ratio requirements of a particular test installation. The maximum stagnation pressure attainable is a function of the Mach number and available electrical power. The tunnel stagnation temperature can be varied from approximately 60 to 140 °F, depending on the available cooling water temperature and test condition. The tunnel is equipped with a scavenging system, which removes combustion products during the testing of rocket motors or turbine engines.

Supersonic velocities are obtained with a flexible-wall, Laval-type nozzle. The contour of each sidewall of the nozzle is adjusted by 15 pairs of electric-motor-driven actuators. Automatic control of the actuators can vary the Mach number from 1.00 to 1.60.

The HAAS test cart was installed during the calibration. It provides a test section 16 ft square by 40 ft long enclosed by porous walls. The wall porosity is fixed at 6 percent and is provided by regularly spaced 0.75-in.-diameter holes, which are inclined upstream at a 60° angle. The test section is completely enclosed in a plenum chamber from which air is evacuated at transonic and supersonic conditions, thus removing part of the tunnel airflow boundary layer through the porous walls of the test section. The HAAS test section has a sidewall angle variation capability from −2.0° (convergence) to 0.8° (divergence). The sidewall angle was fixed for this calibration at 0.0°. To compensate for HAAS strut blockage, the HAAS cart sidewalls have a variable-position bulge section that can be varied manually in depth from 5.5 to 7.25 in. For the test reported herein, the bulge was set at the typical 6.0-in. depth. The general arrangement of the pipe installation in Tunnel 16T is shown in Figure G.1.

## G.3 Calibration hardware

Primary pressure data, used to determine the Tunnel 16T calibration, were acquired using a 6.5-in.-diameter centerline static pipe installed in the HAAS support strut roll mechanism. The pipe consists of seven segments that, when assembled, extended the pipe upstream 75 ft from the HAAS strut.

The ogive nose of the pipe was always upstream of the nozzle throat. Two rows of 0.020-in.-diameter static pressure orifices (total of 206) were used to acquire centerline pressure distributions. (The orifices were drilled into brass fittings pressed into the pipe surface.) The static pressure orifices extended from tunnel stations (TS) −31.5 to 24.0 ft, with 6-in. spacing in two rows oriented 45° and 225° from top center looking upstream. The pipe has a 6-in. translation capability that is used to identify orifice effects. A photograph of the centerline pipe installation is shown in Figure G.2.

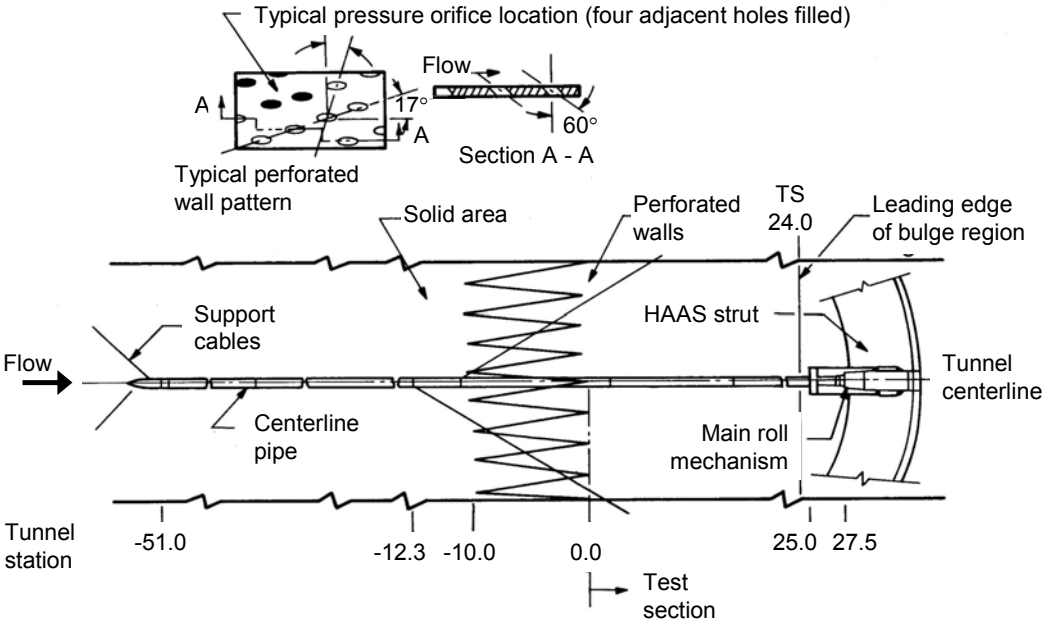



Figure G.1 – General arrangement of the HAAS test section with centerline pipe installed. Hole diameter, 0.75 in.; plate thickness, 0.75 in.; 6-percent open area. All dimensions given in feet unless marked otherwise.



Figure G.2 – Centerline pipe installation in the 16T test section.

In the test section where models are typically installed, the pipe is within 1/16 in. of the test section centerline. The centerline pipe was leveled to within 1 in. of the nozzle/test section centerline as shown in Figure G.3. To accomplish this, moments and tension were imparted to the pipe via hydraulic cylinders attached to the HAAS strut and five cables. Two cables, attached to the top and

bottom of the pipe, near its midsection, were swept downstream. The midsection cables were swept back at 30° to avoid shock formation at supersonic Mach numbers. Three cables attached to the ogive nose were swept upstream (Figure G.1). The nose of the pipe was always in subsonic flow.

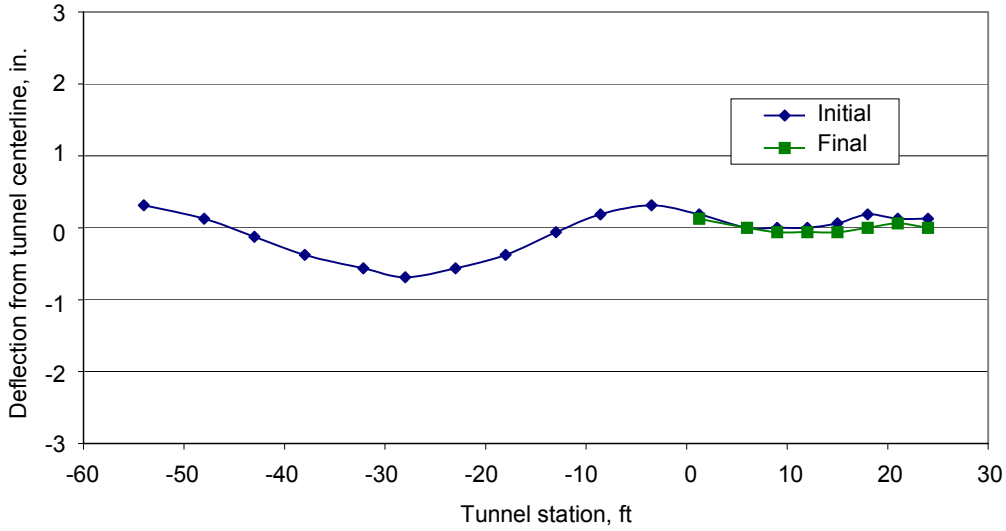



Figure G.3 – Centerline pipe deflection.

The test section walls were also instrumented with static pressure orifices. Bottom wall instrumentation consisted of twenty 0.096-in.-diameter orifices in a row 1 ft west of the test section centerline extending from TS 1 ft to 20 ft. A 2-ft-wide solid section containing a row of 0.040-in.-diameter orifices extending from TS 1 ft to TS 19 ft was installed for the calibration. The solid plate orifices were 3 ft west of the test section centerline. The solid floor section was installed as a backup to the centerline pipe and to obtain baseline data for future calibration verification entries that could be accomplished quickly, without installing the centerline pipe. Top wall instrumentation consisted of twenty 0.060-in.-diameter orifices in a row 1 ft west of the test section centerline extending from TS 1 ft to TS 20 ft. For diagnostic purposes, various other static pressure measurements were obtained in the nozzle and in the bulge region adjacent to the HAAS strut.

## G.4 Calibration instrumentation

Calibration instrumentation consists of 11 ESP transducer modules. The ESP modules are ±15-psid, 64-port, high-density, digitally temperature-compensated modules (ESP-64HD/DTC) manufactured by Pressure Systems, Inc. The modules, which were down ranged to ±5 psid for the calibration, have a quoted manufacturing uncertainty of ±0.05 percent of the down-ranged full scale. The centerline pipe ESP modules were housed inside the pipe in seven individual compartments along the pipe's length. This design minimized the pneumatic tubing lengths between the pressure orifices and the modules, thus decreasing pressure lag time. The floor, ceiling, and bulge ESP modules were housed in a compartment underneath the test section. The nozzle ESP modules were housed in the plenum.

## G.5 Test free-stream conditions

The calibration was conducted over the majority of the Tunnel 16T performance envelope. Test section wall angle was set to 0° for all Mach numbers. The calibration data were obtained for Mach numbers from 0.2 to 1.6 at stagnation pressures ranging from 200 to 3200 psfa, with the range obtained at each Mach number depending on tunnel capability and other constraints encountered during the calibration. Total temperature varied from 95 to 110 °F. Calibration data were obtained within the test condition tolerances listed in Table G.1.

Table G.1 — Tolerances on calibration data

| | |
|---|---|
| Mach number, $M$ | ±0.0005 subsonic; ±0.001 supersonic |
| Total pressure, $P_T$ | ±1 psfa |
| Specific humidity<br>Mach > 1.0 and < 1.5<br>Mach ≥ 1.5 | <br>Less than 0.0015 lbm of water/lbm of dry air<br>Less than 0.0010 lbm of water/lbm of dry air |
| $\Delta T_{DPS}$ ( at Mach ≤ 1.0) | >10 °F |

## G.6 Test procedures

Prior to the calibration, the position of the 16T flexible-wall nozzle was measured and adjusted as required. Accurate nozzle contour measurements were obtained with an SMX laser tracker measurement system (SMX Corp., Kennett Square, PA).

Prior to acquiring data, Tunnel 16T free-stream conditions were set as described previously. Once test conditions were established, data acquisition was delayed 2 to 3 min to allow instrumentation readings to settle and all systems to stabilize, and to complete data quality verification. (Routine data acquisition does not require the 2- to 3-min delay.) Five repeat data points were then acquired in 3- to 5-sec increments, with the average representing a data point in the data set. Typically, four ESP ports were monitored on each module for transducer zero shifts relative to a fixed standard (Mensor). When the difference ($\Delta P_{ESP}$) indicate that zero shifts exceeded 1 psf, the modules were re-zeroed using a pressure calibration unit. For all ESP transducer module pressures, the plenum chamber pressure was used for the reference pressure.

Baseline calibration data were acquired at Mach numbers from 0.2 to 1.6 at a total pressure of 1200 psfa. Reynolds number effects data were acquired at constant Mach numbers and various tunnel total pressures ranging from 200 to 3200 psfa. Repeat data, not obtained sequentially, were acquired at several identical free-stream conditions to evaluate the repeatability of the data.

## G.7 Data uncertainty

Tunnel condition uncertainties (combinations of systematic and random errors) were estimated from repeat calibrations of the instrumentation and from repeatability of the test section data during the calibration. Uncertainties in the instrumentation systems were estimated from repeat calibrations of the systems using secondary standards having uncertainties traceable to National Institute of Standards and Technology (NIST) calibration equipment. The tunnel parameter and instrumentation uncertainties were estimated in accordance with the AIAA uncertainty standard (Reference 26).

## G.8 Results and discussion

The calibration of Tunnel 16T was based on the differential between the test section centerline average Mach number and the plenum chamber equivalent Mach number at various operating conditions. The isentropic relation was used to calculate an equivalent plenum chamber Mach number from the plenum chamber and tunnel stagnation pressure measurements. The calibration parameter $\Delta M$ is defined as the difference between the centerline and equivalent plenum chamber Mach numbers.

### G.8.1 Centerline Mach number distributions

Typical subsonic and supersonic Mach number distributions for the baseline calibration stagnation pressure of 1200 psfa are shown in Figure G.4. Only data from the 225° row are shown. Small variations in the subsonic Mach number distributions are the result of orifice imperfections. This was demonstrated during a previous calibration by translating the pipe one orifice spacing (6 in.).

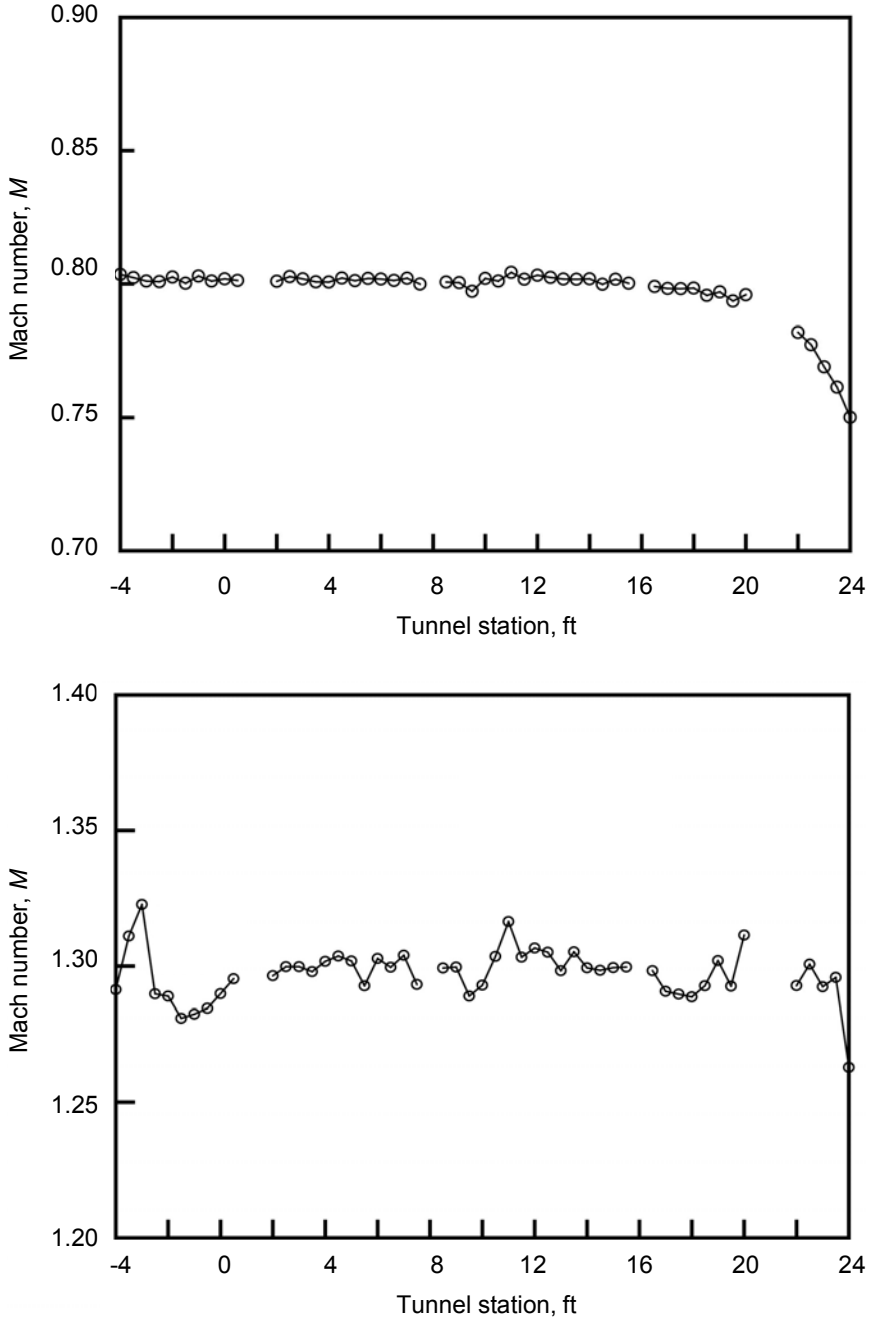



Figure G.4 – Typical centerline Mach distributions along the lower orifice row of static pressure taps; $P_T$, 1200 psia; test section wall angle, 0°.

### G.8.1.1 HAAS strut interference

Upstream propagation of HAAS strut-induced interference is critical to the location of test models in the test section. The extent of the interference was precisely determined during the 1986 calibration by axially translating the centerline pipe and observing the effect on local pressure measurements. This eliminated the influence of orifice imperfections on the data. The criterion established for the 1986 calibration required that aerodynamic test models be installed with the model base upstream of TS 16 ft and that inlet test models be installed with inlets upstream of TS 16 ft.

A slight change in the Mach number deceleration characteristic (tailoff) was noted for data acquired early in the calibration program. This difference, shown in Figure G.5, affected only the flow downstream of TS 18 ft at Mach 0.85 to 0.95. The difference was attributed to the thermocouple rake (Figure G.6) installed on the HAAS support strut leading edge. The thermocouples were installed for only a limited set of runs and then were removed. The Mach number tailoff agreed with the 1986 calibration with the thermocouple rake removed. The calibration parameter $\Delta M$ was not affected by the presence of the rake.

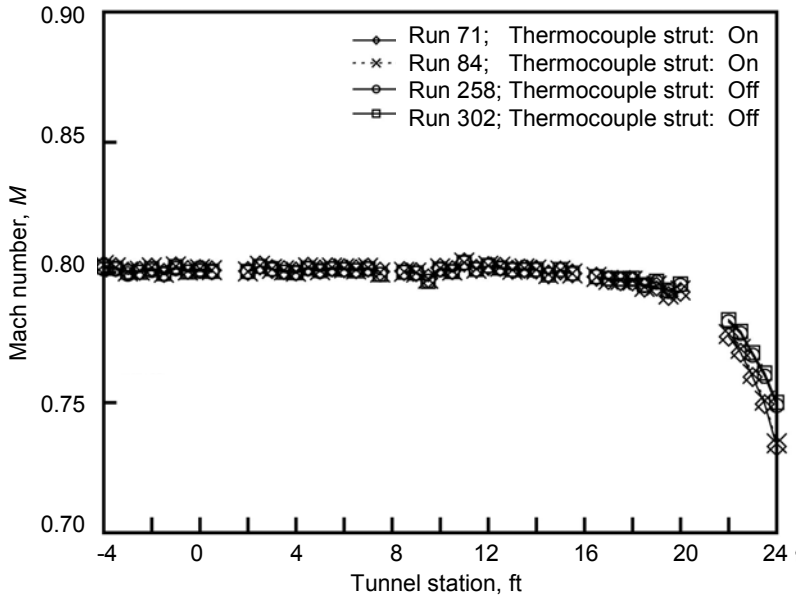



Figure G.5 – Effect of thermocouple rake on the Mach number distribution. Mach numbers measured along the lower orifice row.

The significance of the change in centerline Mach number distribution caused by the HAAS thermocouple rake should be considered when modifications are proposed to the HAAS support strut. Although, in this case, the interference did not propagate into the test region, a larger blockage or different modification may affect the test region. Test programs that have test installations that modify or add equipment near the HAAS support strut should perform analyses to verify that interference effects do not propagate into the test region (TS 6 to 16 ft).

### G.8.1.2 Test region

The test region was selected as a region that provides reasonably uniform flow throughout the tunnel operating range. The test region specified in 1986 again applies to the calibration discussed herein. The upstream boundary of the test region was TS 6 ft because of a wave disturbance emanating from the nozzle/test cart flexures that crossed the test section centerline just upstream of TS 6 ft at Mach 1.6. The downstream boundary of the test region was determined by the upstream propagation of the HAAS strut interference, TS 16 ft, occurring at high subsonic Mach numbers. Although the uniform flow region was a function of the Mach number, the region from TS 6 to 16 ft is the generally recommended test region. Other test regions may be satisfactory for specific test conditions and objectives and can be evaluated further as needed.

### G.8.1.3 Axial Mach number gradients

Mach number streamwise gradients in the test region are shown in Figure G.7. The gradients are the slope term of linear regression approximations of the Mach number distributions in the test region. Included in Figure G.7 is the estimated magnitude of a streamwise linear gradient that will result in 1 count (drag coefficient of 0.0001) of buoyancy drag on a typical fighter model according to a

method suggested in Reference 2. The gradients met this criterion at subsonic and low supersonic Mach numbers, where drag measurement is critical (cruising flight). The proposed NWTC Mach number gradient requirements applied to a fighter configuration are also shown. Again, the Mach number streamwise gradients met this requirement at most Mach numbers. The gradients had not changed significantly in magnitude since the 1986 calibration. The variation in centerline Mach number gradients with Reynolds number (stagnation pressure) is presented in Figure G.8.

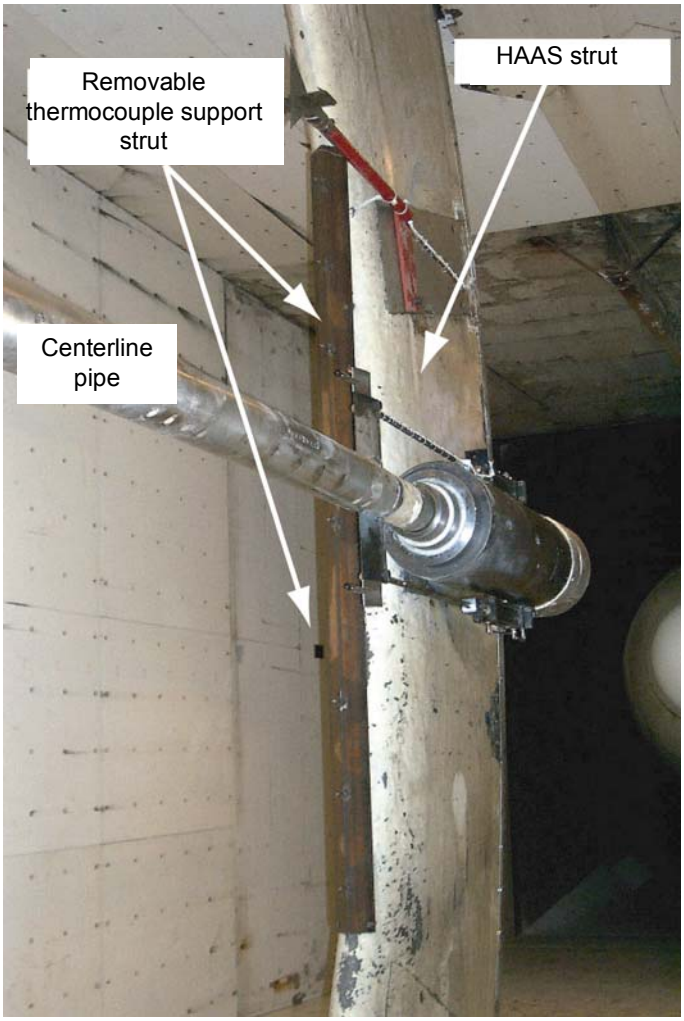



Figure G.6 – Thermocouple support strut.

Comparison of the 1986 data with the current data indicates a long-term stability of the Tunnel 16T Mach number distributions and calibration. Although 15 years between calibrations is not reasonable, this observation supports the notion that annual calibrations are not required. Instead of a full centerline pipe calibration entry, however, some perioidic validation of the calibration should be obtained. Ideally, a short entry with a standard aircraft model should be installed annually or biannually. This would check not only the Mach number calibration, but also the flow uniformity and other parameters. A less desirable alternative would be to repeat only the wall pressure measurements made during the centerline pipe entry to monitor the calibration. A wall pressure validation could be made in one-half to one operating shift. Current thinking at AEDC is to validate tunnel calibrations periodically using a standard model with full calibrations required only after a change is detected by the aforementioned methods or after major modifications are made to the

tunnel or instrumentation. Time between entries has not been determined, but a 1- to 2-year cycle is under consideration.

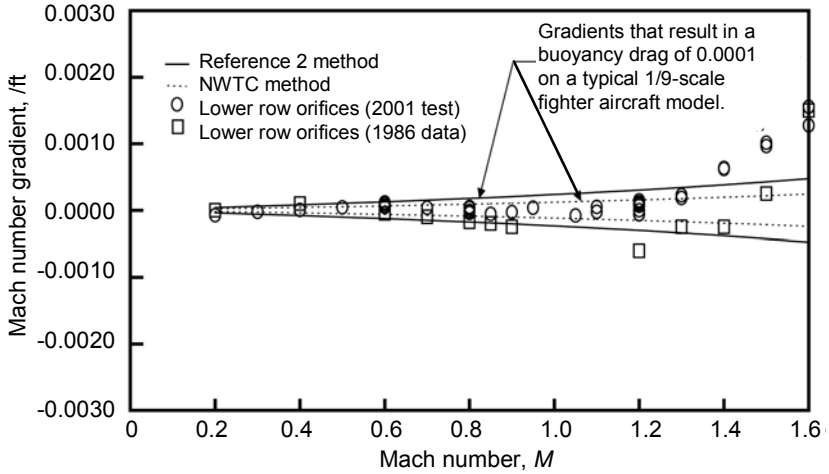



Figure G.7 – Centerline Mach number gradients for tunnel stations 6 to 16 ft.

### G.8.2 Mach number calibration

#### G.8.2.1 Baseline calibration

The baseline Mach number calibration was obtained at $P_T$ = 1200 psfa and wall angle $\theta = 0°$. The Mach number calibration parameter $\Delta M = (M_a - M_{pc})$ versus the equivalent plenum Mach number $M_{pc}$ is shown in Figure G.9. This figure also contains comparisons with the 1986 baseline calibration parameter data. The current and 1986 baseline calibrations are similar and within 0.001 throughout the Mach number range with the exception of Mach numbers 0.20 and 1.60. At Mach 1.60, the current calibration results more closely match the 1984 calibration than the 1986 calibration. The 1984 calibration was obtained just after the initial operating capability of the HAAS mechanism. The cause of difference has not yet been determined and will be investigated further.

#### G.8.2.2 Reynolds number effect

Tunnel 16T is calibrated for the pseudo-Reynolds number effect often noted in the literature. Typical effects of Reynolds number on the Mach number calibration parameter $\Delta M$ for $\theta = 0°$ are shown in Figure G.10. The Reynolds number trend for the current data set is different from the trend noted on previous calibrations. On previous calibrations, the calibration parameter increased with decreasing Reynolds numbers less than 2 million per ft rather than decreasing, as shown in Figure G.10. Also, on the basis of previous calibrations, the trend was deemed to be linear at high Reynolds numbers. The results of this calibration indicate that $\Delta M$ tends to vary as the square root of the Reynolds number.

### G.8.3 Calibration application methodology

The methodology used to apply Mach number calibration data to the Tunnel 16T test condition and control algorithms has been revised as a result of the current calibration. A new data approximation technique is required in order to meet the stringent Mach number uncertainty requirement discussed in the introduction. Previous calibrations used a combination of least-squares polynomial fits of the baseline calibration data ($P_T$ = 1200 psfa) and linear fits of the Reynolds number trends. This method is now unacceptable because of excessive data approximation errors (curve fit residuals). The new data approximation method plots the $\Delta M$ values versus the total pressure $P_T$. Each set of constant Mach number is fitted with a second-order log data fit. These fits will be used in the data reduction and tunnel control algorithms. For Mach numbers off calibrated conditions, a linear interpolation will

be applied to determine the Mach number. Since calibration data were not acquired at some extreme tunnel conditions, data extrapolations were performed such that the surface would extend to all tunnel conditions that could possibly be tested. Reynolds number variation data were not acquired for Mach 0.2 to 0.5; therefore, data for Reynolds number trends were inferred from the Mach 0.6 data and fit through the $P_T$ = 1200 psfa data points. Slightly higher uncertainties are given for tunnel conditions where the calibration parameter is extrapolated or inferred from similar data.

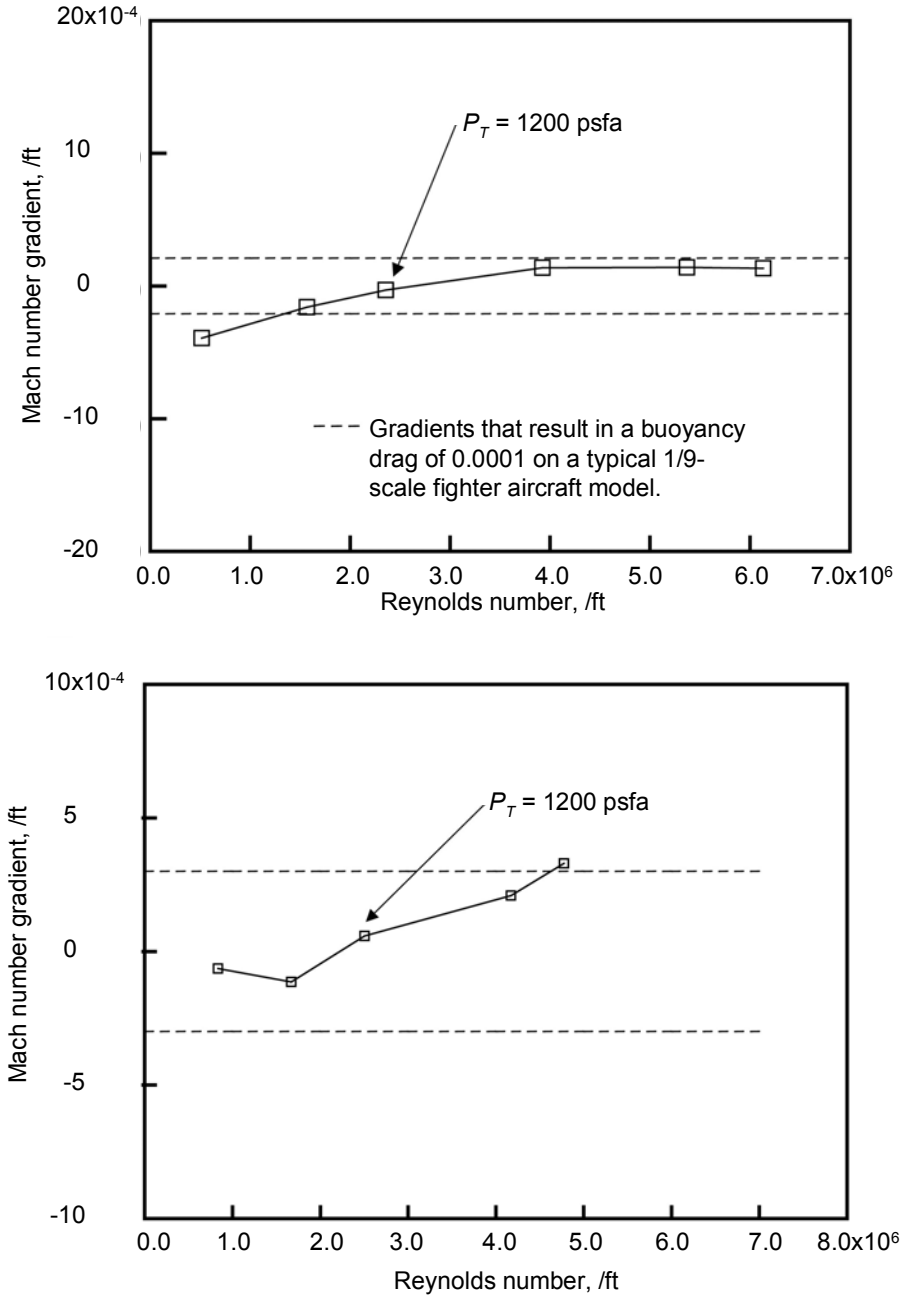



Figure G.8 – Effect of Reynolds number on centerline Mach number gradients. Data from the lower orifice row of the centerline static pipe.

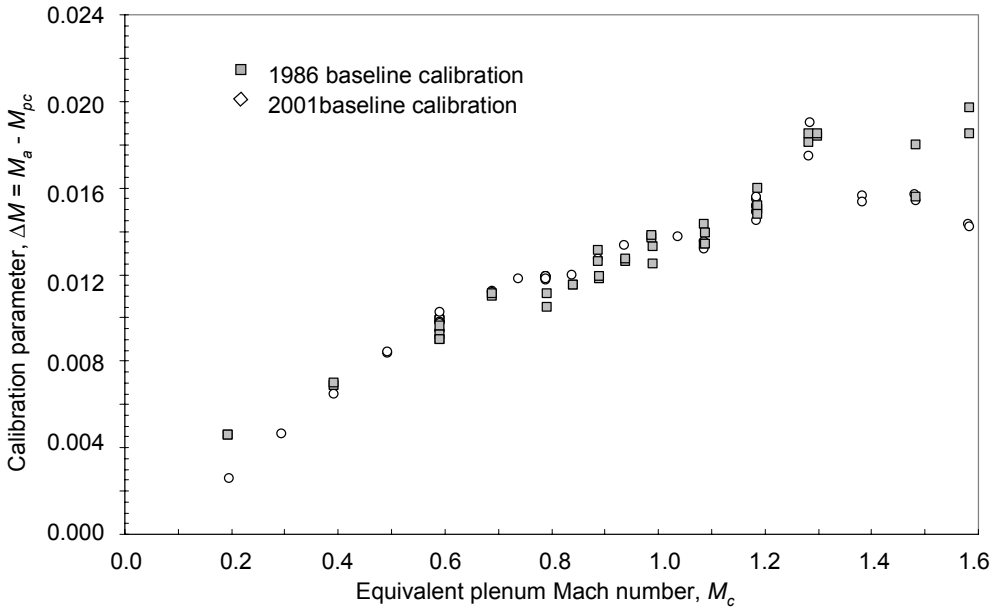



Figure G.9 – Current and prior tunnel 16T baseline calibrations for tunnel stations 6 to 16 ft; data from the lower orifice row. $P_T$ = 1200 psfa.

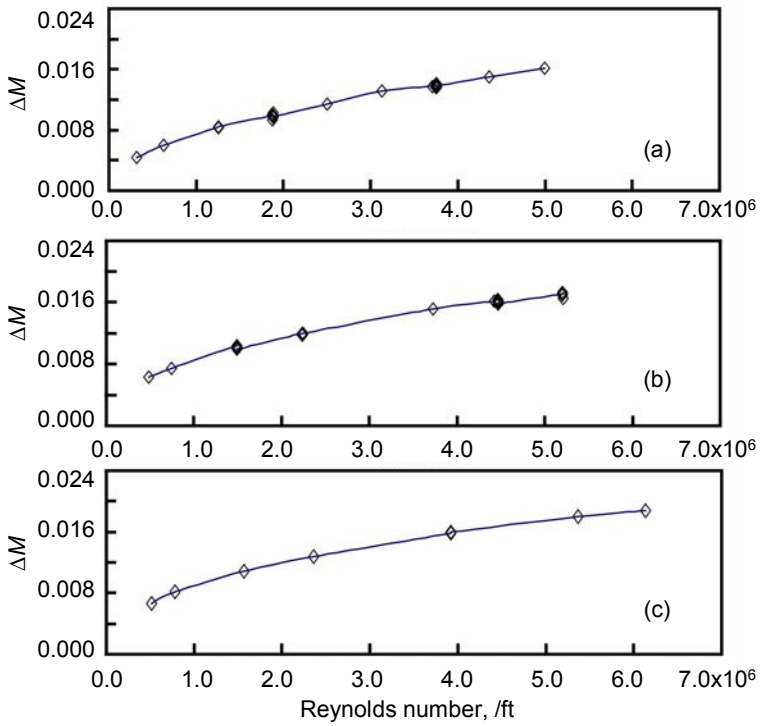



Figure G.10 – Effect of Reynolds number on the tunnel 16T Mach number calibration. (a) Mach 0.60. (b) Mach 0.80. (c) Mach 0.90.

# Annex H—Bibliography of subsonic and transonic tunnel calibration reports

The following reports, along with many listed in the References, document calibration efforts at a range of major facilities, worldwide. The calibrations predate this AIAA Standard and may not reflect all recommended practices therein; however they will provide the reader with further information relating to selection of instrumentation, calibration procedures, achievable accuracy, and other issues.

## Subsonic calibrations

Arnette, S.A.; Porter, C.B.; Meredith, W.S.; Hoffman, J.M.; and Bongsoo Sung: Aerodynamic Commissioning Results for the Korean Aerospace Research Institute Subsonic Wind Tunnel. AIAA Paper 2000–0291, 2000.

Arrington, E.A.; Gonsalez, J.C.; and Curry III, M.R.: Subsonic Calibration of the NASA Glenn Research Center 10-by 10-Foot Supersonic Wind Tunnel (1998 Test). AIAA Paper 2000–2448, 2000.

Eckert, D.: Aerodynamical Calibration of the German-Dutch Wind Tunnel (DNW): A Review of Testing Techniques and Results. DNW–PA–82062, 1983.

Gonsalez, J.C.; and Arrington, E.A.: Aerodynamic Calibration of the NASA Lewis Research Center Icing Research Tunnel (1997 Test). AIAA Paper 98–0633, 1998 (NASA/CR—2001-210809, 2001).

Gonsalez, J.C.; Arrington, E.A.; and Curry III, M.R.: Aero-Thermal Calibration of the NASA Glenn Icing Research Tunnel (2000 Test). AIAA Paper 2001–0233 (NASA/CR—2001-210685), 2001.

Isaacs, D.: Calibration of the RAE Bedford 8ft Times 8ft Wind Tunnel at Subsonic Speeds, Including a Discussion of the Corrections Applied to the Measured Pressure Distribution to Allow for the Direct and Blockage Effects Due to the Calibration Probe Shape. RAE–TR–67038, 1969.

Meredith, W.S.; Martindate, W.; Benetti-Longhini, L.; Boylan, D.; and Chaney, M.: Aerodynamic Commissioning Results for the Korean Air Force Academy Subsonic Wind Tunnel. AIAA Paper 2000–0290, 2000.

Ross, R.; Vannunen, J.W.G.; Young, K.J.; Vanditshuizen, J.C.A.: Aeroacoustic Calibration of the German-Dutch Wind Tunnel (DNW) Open Jet. DNW–TR–82–03, 1983.

Zell, P.T.; and Flack, K.: Performance and Test Section Flow Characteristics of the National Full-Scale Aerodynamic Complex 40-by-80 Foot Wind Tunnel. NASA TM–101065, 1989.

## Transonic Calibrations

Arrington, E.A.; and Gonsalez, J.C.: Low Speed Calibration of the NASA Lewis Research Center 8- by 6-Foot Supersonic Wind Tunnel (1995 Test). NASA CR–198527, 1997.

Arrington, E.A.; Pickett, M.T.; and Soeder, R.H.: Baseline Calibration of the NASA Lewis Research 8- by 6-Foot Supersonic Wind Tunnel (1991 and 1992 Tests). NASA/TM—97-107431, 1997.

Bird, K.D.; and Martin, J.F.: Results of Calibrations and Various Model Configuration Tests in the 4-Foot Transonic Wind Tunnel. Cornell Aeronautical Laboratory, Inc., Report AD–844–W–3, Aug. 1953

Bobbitt, Jr., C.; Everhart, J.; Foster, J.; Hill, J.; McHatton, R.; and Tomek, B.: National Transonic Facility Characterization Status. AIAA Paper 2000–0293, 2000.

Capone, F.J.; Bangert, L.S.; Asbury, S.C.; Mills, C.T..; and Bare, E.A.: The NASA Langley 16-foot Transonic Tunnel—Historical Overview, Facility Description, Calibration, Flow Characteristics, Test Capabilities. NASA TP–3521, 1995.

Czeck, E.A.: 8-Foot Transonic Tunnel Airflow Calibration (Sting Cart Installed—Suction On). Cornell Aeronautical Laboratory, Inc., WTO–401 Report, Dec. 1956.

Czeck, E.A.: 8-Foot Transonic Tunnel Airflow Calibration (Sting Cart Installed—Suction Off). Cornell Aeronautical Laboratory, Inc., WTO–336 Report, 1957.

LaPres, A.J.: Sting Cart Airflow Calibration—Phase III. Cornell Aeronautical Laboratory, Inc., WTO–396 Report, Apr. 1957.

Torngren, L.; Grunnet, J.L.; Nelson, D.M.; Kamis, D.N.: The New FFA T1500 Transonic Wind Tunnel Initial Operation, Calibration and Test Results. AIAA Paper 90–1420, 1990.

## References


1. Pope, A.: Wind Tunnel Calibration Techniques. AGARDograph 54, Apr. 1961.
2. Reed, T.D.; Pope, T.C.; and Cooksey, J.M.: Calibration of Transonic and Supersonic Wind Tunnels; NASA CR–2920, 1977.
3. Henderson, Jr., A.; and McKinney, L.W.: Overview of the 1989 Wind Tunnel Calibration Workshop. NASA TP–3393, 1993.
4. NWTC Final Report. NASA CR–198491, 1996.
5. NWTC Customer Performance Requirements Document Release 11.0. NWT–03–A–9100–05 Volume I and II, Revision A—May 3, 1996.
6. Wheeler, Donald J.; and Chambers, D.S.: Understanding Statistical Process Control. 2nd Edition, SPC Press, 1992.
7. Wheeler, Donald J.: Advanced Topics in Statistical Control. SPC Press, 1995.
8. Eisenhart, Churchill: Realistic Evaluation of the Precision and Accuracy of Instrument Calibration Systems. J. Res. NBS—C. Eng. and Inst., Vol. 67C, No. 2, Apr.-Jun. 1993.
9. Montgomery, Douglas C.: Introduction to Statistical Quality Control. Third Edition, John Wiley and Sons, Inc., 1996.
10. Committee E–11 on Quality and Statistics: Manual on Presentation of Data and Control Chart Analysis. 6th Edition, ASTM Manual Series: MNL 7 Revision of STP 15D, 1990.
11. Hemsch, M.; Grubb, J.; Krieger, W.; and Cler, D.: Langley Wind Tunnel Data Quality Assurance - Check Standard Results. AIAA Paper 2000–2201, 2000.
12. Figliola, R.S.; and Beasley, D.E.: Theory and Design for Mechanical Measurements. 2nd Edition, John Wiley and Sons, 1995.
13. Barlow, J.B.; Rae, W.H.; and Pope, A.: Low-Speed Wind Tunnel Testing. 3rd Edition, John Wiley and Sons, 1999.
14. Pope, A.; and Goin, K.L.: High-Speed Wind Tunnel Testing. John Wiley and Sons, 1965.
15. Goethert, B.H.: Transonic Wind Tunnel Testing. AGARDograph No. 49, Pergamon Press, 1961.
16. Bryer, D.W.; and Pankhurst, R.C.: Pressure-Probe Methods for Determining Wind Speed and Flow Direction. Her Majesties Stationery Office, 1971.
17. Goodyer, M.: The Evolution of Modern High Sensitivity Yawmeters. AIAA Paper 2002–2924, 2002.
18. Clark, E.L.; Henfling, J.F.; and Aeschliman, D.P.: Calibration of Hemispherical-Head Flow Angularity Probes. AIAA Paper 92–4005, 1992.
19. Gonsalez, J.S.: 5-Hole Flow Angle Probe Calibration for the NASA Lewis Icing Research Tunnel. AIAA Paper 96–2201, 1996.
20. Brown, David L.: Predicting Equilibrium Pressures From Transient Pressure Data. Aerospace Research Laboratories, ARL 65–7, Jan. 1965.
21. Sinclair, A.R., and Robins, A.W.: A Method for Determination of the Time Lag in Pressure Measuring Systems Incorporating Capillaries. NACA TN–2793, 1952.
22. Greenblatt, David; Kiedaisch, John; and Nagib, Hassan: Unsteady-Pressure Corrections in Highly Attenuated Measurements at Moderate Mach Numbers. AIAA Paper 2001–2983, 2001.
23. Arrington, E.A.; Spera, D.A.; Blumenthal, P.Z.; and Thompson, J.: Calibration of the NASA Glenn Research Center 10- by 10-ft Supersonic Wind Tunnel (1993 and 1995 Tests). NASA/TM—2000-209799, 2000.
24. Blumenthal, P.Z.: High Response Dew Point Measurement System for a Supersonic Wind Tunnel. NASA CR–198453, 1996.
25. Recommended Practice for Successful Wind Tunnel Testing. AIAA R–092–2003, 2003.
26. Assessment of Experimental Uncertainty with Application to Wind Tunnel Testing. AIAA Standard S–071A–1999, American Institute of Aeronautics and Astronautics, 1999.
27. Guide for Assessing Experimental Uncertainty—Supplement to AIAA S–071A–1999. AIAA G–045–2003, American Institute of Aeronautics and Astronautics, 2003.
28. U.S. Guide to the Expression of Uncertainty in Measurement. ANSII/NCSL Z540–2–1997, 1997.
29. Test uncertainty. ASME PTC 19.1–1998, 1998.
30. Coleman, H.W.; and Steele, Jr., W.G.: Experimentation and Uncertainty Analysis for Engineers. Second Edition, John Wiley & Sons, 1999.
31. Soeder, R.H.: NASA Lewis 9- by 15-Foot Low-Speed Wind Tunnel User Manual. NASA TM–106247, 1993.
32. Yuska, J.A.; Diedrich, J.H.; and Clough, N.: Lewis 9- by 15-Foot V/STOL Wind Tunnel. NASA TM X–2305, 1971.
33. Hughes, C.E.: Flowfield Measurements in the NASA Lewis Research Center 9- by 15-Foot Low-Speed Wind Tunnel. NASA TM–100883, 1989.
34. Arrington, E.A.; Pickett, M.T.; and Soeder, R.H.: Calibration of the NASA Lewis Research Center 9- by 15-Foot Low Speed Wind Tunnel (1992 Test). NASA TM–106860, 1995.
35. Arrington, E.A., and Gonsalez, J.C.: Calibration of the NASA Lewis Research Center 9- by 15-Foot Low-Speed Wind Tunnel (1994 Test). NASA CR–195438, 1995.

36. Arrington, E.A., and Gonsalez, J.C.: Flow Quality Improvements in the NASA Lewis Research Center 9- by 15-Foot Low Speed Wind Tunnel. NASA CR–195439, 1997.
37. Ames Research Staff: Equations, Tables and Charts for Compressible Flow. NACA TR–1135, 1953.
38. Model DAP IFA Thermal Anemometry Software Package Instruction Manual. Rev. A, TSI Inc., St. Paul, MN, Jan. 1993.
39. Hoerner, S.F.: Fluid-Dynamic Drag: Practical Information On Aerodynamic Drag and Hydrodynamic Resistance, 1965.
40. Kmak, F.J.: Modernization and Activation of the NASA Ames 11-by 11-Foot Transonic Wind Tunnel. AIAA Paper 2000–2680, 2000.
41. Kmak, F.; Hudgins, M.; and Hergert, D.: Revalidation of the NASA Ames 11-by 11-Foot Transonic Wind Tunnel With a Commercial Airplane Model. AIAA Paper 2001–0454, 2001.
42. Amaya, M.A.; and Murthy, S.V.: Flow Quality Measurements in the NASA Ames Upgraded 11-by 11-Ft Transonic Wind Tunnel. AIAA Paper 2000–2681, 2000.
43. NASA Ames Research Staff: Equations, Tables and Charts for Compressible Flow. NACA TR–1135, 1953.
44. Increased Reynolds Number for the CAL 8-Foot Transonic Tunnel Through Ejector Augmentation. Cornell Aeronautical Laboratory, Inc., May 1972.
45. Sting Cart Testing in the Calspan 8-ft. Transonic Wind Tunnel. Calspan Corporation, WTO–539 Report, Revised Sep. 1995.
46. Garrell, A.F.; and Paryz, R.W.: Enhanced Weapons Integration Capabilities Using a New Captive Trajectory Simulation Wind Tunnel Model Support System. 2001 Aircraft-Stores Compatibility Symposium, International Test and Evaluation Association, Destin, FL, Mar. 2001.
47. Koscielny, M.G.; Kunecki, A.J.; and Nowakowski, J.R.: Installation and Use of the Paroscientific Digiquartz Intelligent Transmitter Pressure Transducer Model 1000. Calspan Corporation, VTWT Report, Feb. 1995.
48. Paroscientific, Inc.: Digiquartz® Precision Pressure Instruments—Programming and Operation Manual (for Series 1000). Document No. 8107–001 Rev. J, July 1995.
49. System 8400 User's Manual, Version 3.0. Pressure Systems Incorporated, Hampton, VA, May 1990.

American Institute of
Aeronautics and Astronautics

1801 Alexander Bell Drive, Suite 500
Reston, VA 20191-4344

ISBN 1-56347-662-2